

Novel fenofibrate derivatives as cannabinoid receptor ligands

Sarah Jane Spencer B.Sc



School of Pharmacy

The University of Nottingham

Nottingham

UK

**Thesis submitted to the University of Nottingham for the
degree of Doctor of Philosophy**

May 2011

Abstract

Fenofibrate is a PPAR α agonist, used to treat dyslipidemia. Unpublished work that has been previously carried out in our group has identified that fenofibrate also displays affinity for the cannabinoid receptors, CB₁ and CB₂.

A dual receptor ligand, with the PPAR α agonist activity of fenofibrate, combined with antagonist activity at the CB₁ receptor, or agonist activity at the CB₂ receptor, could reduce appetite, decrease plasma triglyceride levels, increase high density lipoprotein (HDL) levels, lower low density lipoprotein (LDL) levels and reduce atherosclerosis. This could enable the multi-symptomatic treatment of obesity with the advantage of avoiding side effects associated with taking multiple medications. However, whilst fenofibrate has affinity for the cannabinoid receptors, only its active metabolite; fenofibric acid (**10b**) activates PPAR α . This project sought to develop novel ligands for the cannabinoid receptors that retain activity at PPAR α .

A series of amide derivatives of fenofibrate were synthesised, and pharmacological testing revealed that the piperidinyl (**48g**) and morpholino (**48h**) derivatives had agonist activity and a higher affinity for the cannabinoid receptors than fenofibrate. However these derivatives failed to bind and activate PPAR α . Although a dual PPAR α / cannabinoid receptor ligand has not been found with these amide derivatives, the compounds synthesised could provide a platform for the further development of cannabinoid receptor ligands of this novel class. This was demonstrated by further modifications to compounds (**48g**) and (**48h**) which indicated that activity at the cannabinoid receptors is tuneable.

Acknowledgements

Firstly I would like to thank my two supervisors Dr Barrie Kellam and Professor David Kendall for their support and guidance throughout this project, Dr Andrew Bennett for help and guidance with the PPAR α pharmacology and also Monika Owen for her instruction in cell culture techniques.

I would like to thank the C-floor chemists, for their help and advice throughout my time working on this project, and also technicians Lee Hibbett and Graeme Parry.

Finally I would like to thank Dr Shailesh Mistry for his support, especially during the writing of this thesis, and my family who have always encouraged and supported me.

This work was funded by the BBSRC.

Abbreviations

Acetyl-CoA	Acetyl Coenzyme A
AIDS	Acquired immunodeficiency syndrome
Apo-AI	Apolipoprotein AI
Apo-AII	Apolipoprotein AII
ATP	Adenosine triphosphate
BSA	Bovine Serum Albumin
CB ₁	Cannabinoid receptor 1
CB ₂	Cannabinoid receptor 2
CBP	CRE binding protein
CDCl ₃	Deuterated Chloroform
cDNA	Complementary DNA
CHO	Chinese Hamster Ovary
Cyclic AMP	Cyclic adenosine monophosphate
DCM	Dichloromethane
DIAD	Diisopropyl azodicarboxylate
Dpm	Disintegrations per minute
<i>E. coli</i>	<i>Escherica coli</i>
EDTA	Ethylenediaminetetraacetic acid
EtOAc	Ethyl Acetate
FBS	Fetal Bovine Serum
TR-FRET	Time resolved fluorescence resonance energy transfer
FT-IR	Fourier Transform Infra-Red
GABA	Gamma aminobutyric acid
GTP γ S	Guanosine 5'-[γ -thio]-triphosphate
HBTU	2-(<i>1H</i> -benzotriazole-1-yl)-1,1,3,3-tetramethyluronium hexafluorophosphate
hCB ₂	human Cannabinoid Receptor 2
HPLC	High Performance Liquid Chromatography
IC ₅₀	Median Inhibition Concentration
IL-6	Interleukin 6
K _i	Equilibrium affinity constant
LB	Luria Bertani
M+	Molecular ion (positively charged)
MAP Kinase	Mitogen Activated Protein Kinase

MeCN	Acetonitrile
MeOH	Methanol
NMR	Nuclear Magnetic Resonance
OSu	Succinimide ester
p300	Binding protein p300
PE	Petroleum ether
PBS	Phosphate Buffered Saline
PEI	Polyethylenimine
ppm	Parts per million
RGS	Regulator of G protein signalling
RLU	Relative light units
SD	Standard Deviation
SE	Standard Error
SRC-1	Steroid Coactivator 1 protein
TBME	tert-Butyl methyl ether
T _H 1	Type 1 helper T cells
THF	Tetrahydrofuran
TLC	Thin Layer Chromatography
TMS	Tetramethylsilane
TOF-ES	Time of Flight-Electrospray
TR-FRET	Time Resolved-Fluorescence Resonance Energy Transfer
UV	Ultra Violet

Table of Contents

Abstract.....	i
Acknowledgements.....	ii
Table of Contents.....	v
1. Introduction	1
1.1. Potential Dual PPAR/ Cannabinoid Receptor Ligands	1
1.2. Peroxisome Proliferator Activated Receptors.....	2
1.2.1. <i>PPAR Structure</i>	2
1.2.2. <i>Activation Mechanism</i>	3
1.2.3. <i>PPARα</i>	4
1.2.4. <i>Ligands for PPARα</i>	5
1.3. G-Protein Coupled Receptors.....	12
1.3.1. <i>GPCR Structure</i>	12
1.4. Cannabinoid Receptors	16
1.4.1. <i>CB₁ Receptor</i>	17
1.4.2. <i>CB₂ Receptor</i>	17
1.4.3. <i>GPR55</i>	18
1.4.4. <i>Ligands for Cannabinoid Receptors</i>	20
1.4.5. <i>CB₁ as a therapeutic target</i>	30
1.4.6. <i>CB₂ as a therapeutic target</i>	33
1.5. Aims	35
1.5.1. <i>Design of fenofibrate analogues</i>	36
2. Amide derivatives of fenofibrate.....	38
2.1. Synthesis	38
2.2. Synthetic Route	38
2.3. Pharmacology results.....	41
2.3.1. <i>Activity at the Cannabinoid Receptors</i>	41
2.3.2. <i>Activity of the analogues at PPARα</i>	48
2.4. Conclusions.....	53
3. Substituted benzyl and phenyl derivatives.....	55
3.1. Synthesis of derivatives	55
3.1.1. <i>Synthetic route</i>	55
3.2. Pharmacology.....	58
3.2.1. <i>Activity at the cannabinoid receptors</i>	58
3.2.2. <i>Activity at PPARα</i>	63
3.3. Conclusions.....	63
4. <i>N</i> -Morpholino-2-(4-(4-chlorobenzoyl)-phenoxy)-2-methylpropanamide (48h) and <i>N</i> -piperidinyl-2-(4-(4-chlorobenzoyl)-phenoxy)-2-methylpropanamide (48g) derivatives	65
4.1. Synthesis of derivatives	65
4.1.1. <i>Synthetic route</i>	66
4.1.2. <i>Pharmacology</i>	69
4.2. Unbranched and Tertiary Amide Derivatives	81
4.2.1. <i>Synthetic routes</i>	81
4.2.2. <i>Pharmacology</i>	84
4.3. Conclusions.....	85
5. Conclusions and future work	88
5.1. Conclusions.....	88
5.1.1. <i>Amide derivatives of fenofibrate</i>	88
5.1.2. <i>Substituted N-benzyl and N-phenyl analogues</i>	91
5.1.3. <i>Substituted benzophenone derivatives</i>	94
5.1.4. <i>Tertiary Amide Derivatives</i>	100

5.2. Future work	100
6. Experimental.....	104
6.1. Pharmacology.....	104
6.1.1. <i>Molecular cloning</i>	104
6.1.2. <i>Cell culture</i>	106
6.1.3. <i>Assays</i>	108
6.1.4. <i>Radioligand binding assays</i>	109
6.2. General Chemistry.....	111
7. References	213

1. Introduction

1.1. Potential Dual PPAR/ Cannabinoid Receptor Ligands

During the past two decades, both Cannabinoid receptors and Peroxisome Proliferator Activated Receptors (PPARs) have been the subject of considerable research efforts.

PPARs are ligand-regulated transcription factors, and have been shown to regulate glucose homeostasis¹, lipid and lipoprotein metabolism², and cellular differentiation¹. They also exhibit inhibitory effects in the inflammation process³.

Cannabinoid receptors, however, belong to the transmembrane G-protein coupled receptor (GPCR) super family, which are modulators of various signalling cascades. The cannabinoid receptor family consists of the CB₁ and CB₂ receptors. The CB₁ receptor is expressed mainly in the brain, whereas the CB₂ receptor is predominantly localised in the cells of the immune system.

There is growing evidence that some cannabinoid ligands will also bind to PPARs^{4, 5}. A compound with antagonist activity at the CB₁ receptor, and agonist activity at both PPAR α and the CB₂ receptors, could reduce appetite, decrease plasma triglyceride levels, increase high density lipoprotein (HDL) levels, lower low density lipoprotein (LDL) levels and reduce atherosclerosis. With this in mind, it would be desirable to develop a ligand with affinity for both of these types of receptor, as there is potential for multi-symptom treatment of certain diseases, such as obesity.

1.2. Peroxisome Proliferator Activated Receptors

PPARs belong to the nuclear receptor family, and were first identified in mice in 1990.⁶ Two years later, three subtypes of PPARs were identified and cloned from a *Xenopus* cDNA library⁷. These three subtypes (α , γ , and δ) share 60 to 70 % sequence identity⁸ and are found in various areas of the body. They have roles in glucose homeostasis, lipid and lipoprotein metabolism, cellular differentiation and inflammation processes¹.

PPAR α is predominantly found in tissues involved in fatty acid catabolism, such as the liver, kidney, heart and skeletal muscle⁹. With the use of fibrates, PPAR α has proven to be an effective target in the treatment of dyslipidemia.

PPAR γ has three further subtypes; PPAR γ 1, PPAR γ 2 and PPAR γ 3. PPAR γ 1 is found in a wide range of tissues such as the kidneys, spleen, heart, and both small and large intestines, whereas PPAR γ 2 is found mainly in adipose tissue. PPAR γ 3 is found in macrophages, adipose tissue and colon epithelium. The PPAR γ receptors are a target for thiazolidinediones, which sensitise tissues to insulin in the treatment of Type 2 *Diabetes mellitus* (T2DM).

The third PPAR subtype, PPAR δ , is less understood and almost ubiquitously expressed. It is thought to be involved in fatty acid metabolism and reproduction¹.

1.2.1. PPAR Structure

PPARs consist of a ligand binding domain (LBD), DNA binding domain (DBD), ligand dependent activating domain (AF-2) and a ligand independent activating domain (AF-1) (**Figure 1-1**).



Figure 1-1-Representation of the different PPAR Domains (adapted from Henke *et al*¹⁰)

The ligand binding domain is formed from 13 α -helices and a small, four stranded β -sheet.

1.2.2. Activation Mechanism

Binding of a ligand (L) to the LBD induces stabilisation of the AF-2 region, and then recruitment of a co-activator (A) such as; CBP, p300 or SRC-1¹. The co-activator binds at a hydrophobic cleft on the surface of the PPAR¹¹, and the PPAR then forms a dimer with retinoid x receptor (RXR). There are three isoforms of RXR (as for PPARs), and they are activated by the endogenous ligand 9-*cis* retinoic acid.

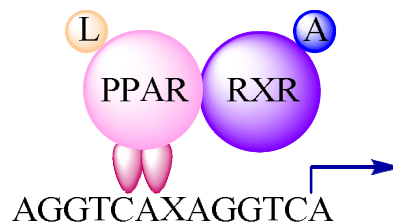


Figure 1-2-Representation of the active complex bound to the PPRE (adapted from Henke *et al*¹⁰)

The PPAR/RXR heterodimer then binds to a Peroxisome Proliferator Response Element (PPRE) via the DBD using two zinc finger motifs (**Figure 1-2**). The PPRE is a sequence of two hexanucleotides, separated by any nucleotide (X) AGGTCAXAGGTCA¹. It is located in the promoter region of genes, and once the activated PPAR/RXR heterodimer is bound, gene transcription can be initiated.

1.2.3. PPAR α

PPAR α is involved in the β -oxidation of fatty acids, and the uptake of fatty acids into cells, by regulating the expression of fatty acid transport protein (FATP) and fatty acid translocatase (FAT)¹². In the liver it regulates enzymes involved in the metabolism of triglycerides, and components that form HDL¹², and in the heart it regulates energy supply by regulating lipoprotein lipase levels, and also fatty acid oxidation¹².

PPAR α also has a role in inflammation and macrophage signalling. In macrophages it stimulates cholesterol efflux via the ABC-A1 (ATP-binding cassette transporter) pathway and also may induce the expression of liver-x-receptor (LXR) which mediates the expression of ABC-A1¹³. PPAR α has been shown to suppress Nuclear Factor κ B (NF- κ B) signalling^{1, 14}. This is significant as many pro-inflammatory genes are under the control of NF- κ B. Inducer of nuclear factor- κ B (I κ B) is an inhibitor of NF- κ B and is also regulated by PPAR α . I κ B levels are increased with PPAR α activation causing retention of NF- κ B in its inactive form. This leads to a decrease in NF- κ B DNA binding and a reduction in the NF- κ B induced inflammatory response¹⁵.

In vivo the role of PPAR α in inflammation has been demonstrated. Patients with atherosclerosis, treated with fenofibrate, demonstrated a decrease in IL-6, (a cytokine released in response to inflammation) and also the acute phase proteins fibrinogen and C-reactive protein (CRP)¹⁴. Another study found that patients with hyperlipidemia, also treated with fenofibrate, had reduced plasma levels of the cytokines interferon- γ (INF γ) and tumour necrosis factor- α (TNF α)¹⁶.

1.2.4. Ligands for PPAR α

The ligand binding pocket in PPAR α is a T-shaped cavity and has a volume of approximately 1300 Å³¹¹. Due to the large size of the binding pocket a wide variety of compounds with widely differing structures can bind. A representation of an hPPAR α LBD in complex with the PPAR α / γ agonist AZ242 is shown in **Figure 1-3**.



Figure 1-3–Representation of a crystal structure of a PPAR α LBD in complex with AZ242 (adapted from Cronet *et al.*¹⁷ 1I7G in protein data bank).

The detergent DBC is shown in cyan and AZ242 in blue.

The ligand binding pocket is in the centre of the ligand binding domain, and is surrounded by helices 3, 5, 7, 11 and 13¹⁷.

1.2.4.1. Agonist Binding in the Ligand Binding Domain

Crystal structures of PPAR LBDs have revealed that the carboxylic head group is important for both natural and synthetic agonist activation^{11, 17, 18}. In the

PPAR α LBD the carboxylic acid forms a hydrogen bond with a tyrosine residue (Tyr⁴⁶⁴) in the AF2 helix, and also hydrogen bonds with Ser²⁸⁰, Tyr³¹⁴, and His⁴⁴⁰ which are part of the coactivator binding site (**Figure 1-4**). Xu *et al* suggested that the interactions with Tyr⁴⁶⁴ and Tyr³¹⁴ stabilise the AF2 helix generating a salt bridge between Glu⁴⁶² and Lys²⁹² which allows a coactivator to bind to the receptor.

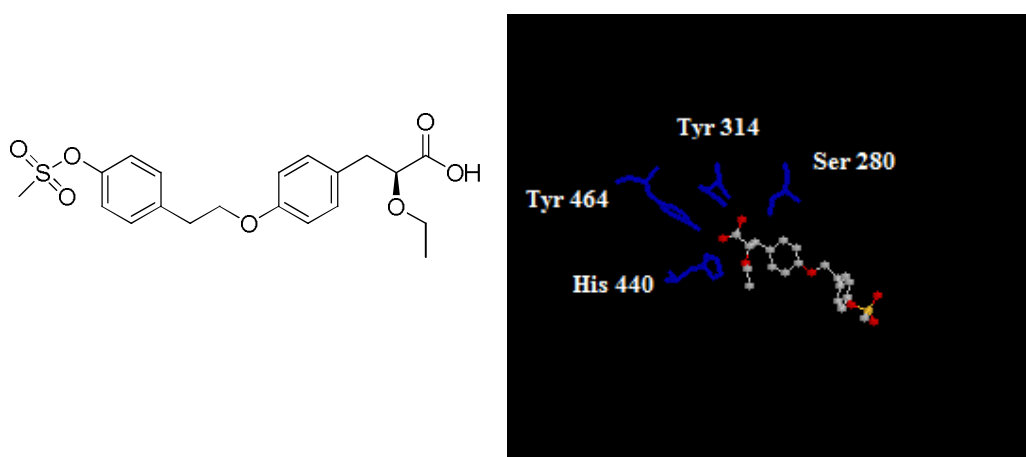


Figure 1-4- Structure of AZ242 and residues involved in hydrogen bonding to the carboxylic acid (protein structure & ligand from the protein data bank 1I7K)

The importance of the acid head group was investigated further by Xu *et al.* and in this next study, the carboxylic acid of the PPAR α agonist GW409544 (**1**) was changed to a large amide group to give an antagonist (GW6471 (**2**)). This alteration reversed the amide and also moved the amide group out by one carbon relative to the carboxylic acid. GW6471 (**2**) was then crystallised with a hPPAR α LBD¹⁹, which showed that hydrogen bonding to Tyr⁴⁶⁴ and also AF-2 stabilisation were prevented. This inhibited activation of the LBD. Xu *et al.* also found that when GW6471 (**2**) binds, a larger pocket is created at the hydrophobic cleft where co-activators and co-repressors bind. This increase in

size could allow co-repressors to bind more easily¹⁹ preventing PPAR activation.

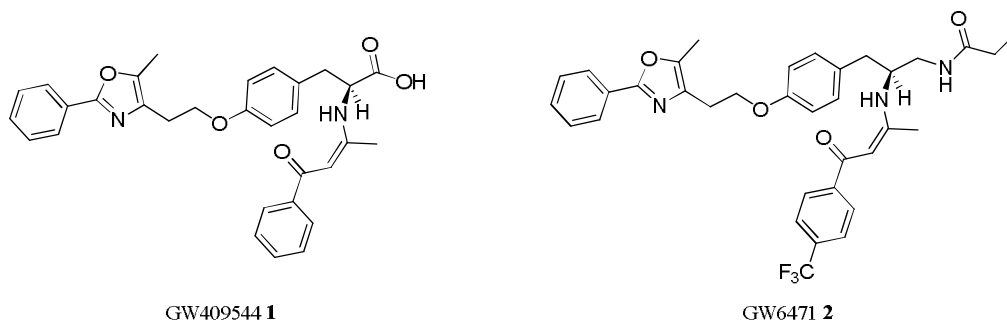


Figure 1-5 Structures of the PPAR α ligands GW409544 and GW6471

1.2.4.2. Natural Ligands

Natural ligands, with agonist activity at PPAR α , consist of fatty acids and eicosanoids such as linoleic acid (**3**) and icosapentanoic acid²⁰. None of the natural ligands have high affinity for PPAR α , so it is thought that the receptor acts as a sensor of fatty acid levels¹⁸.

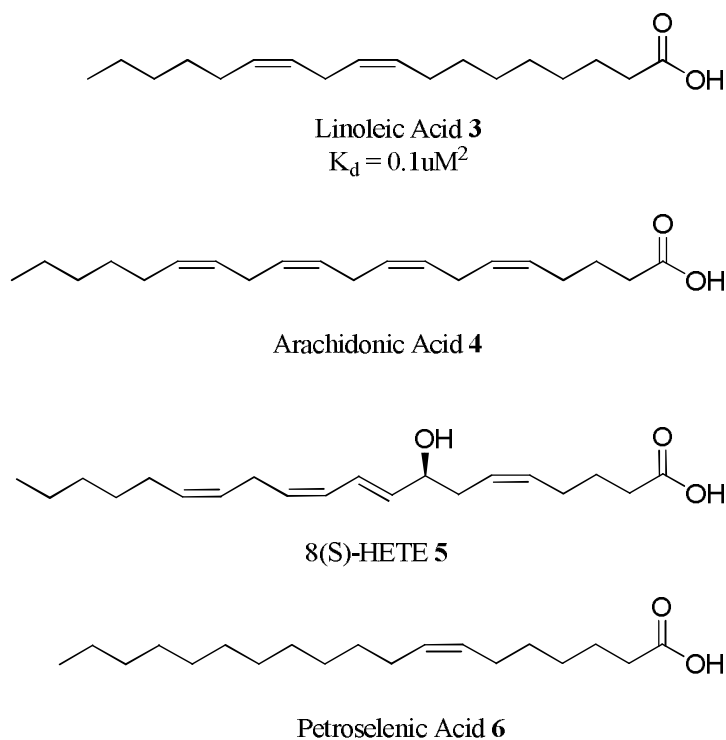


Figure 1-6 Examples of endogenous agonists of PPAR α

1.2.4.3. Synthetic Ligands

1.2.4.3.1. Fibrates

Fibrates are synthetic PPAR α agonists (**Figure 1-7**), and are effective in the treatment of some types of dyslipidemia, such as atherogenic dyslipidemia. This type is found in patients with metabolic syndrome and T2DM, and is associated with high levels of triglycerides, low HDL levels, and small dense LDL particles²¹.

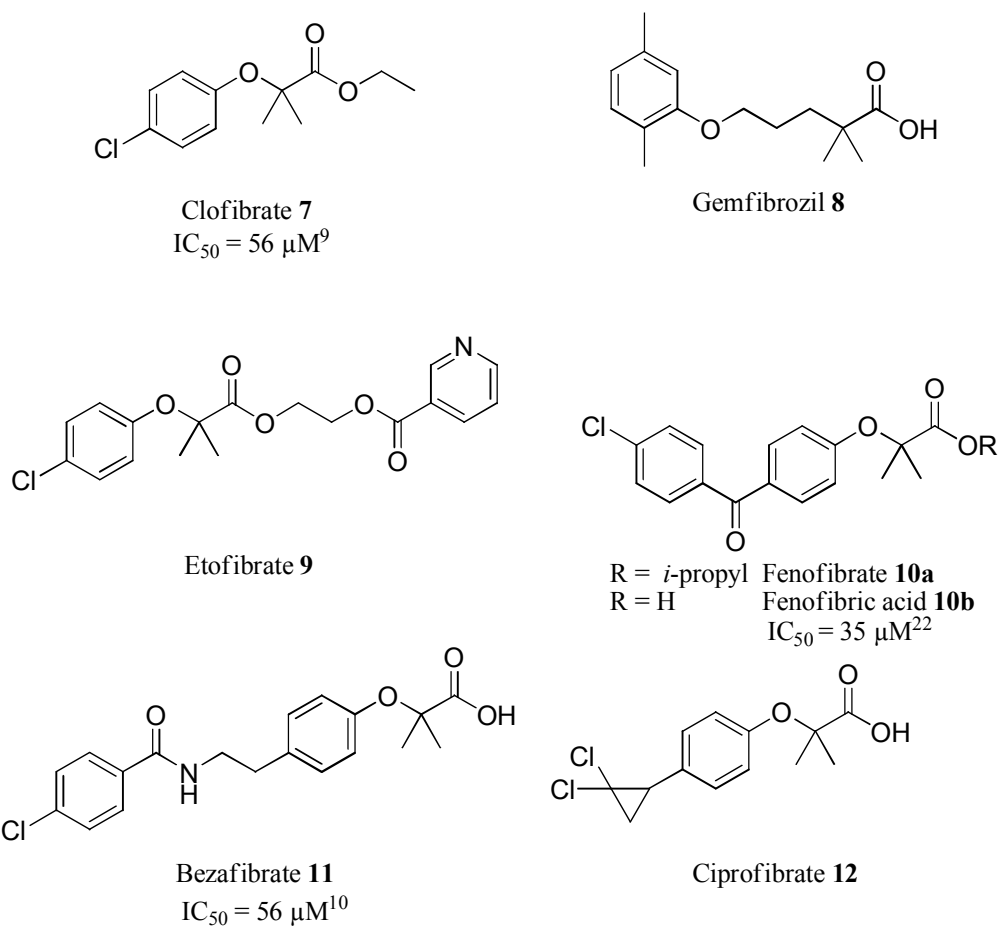


Figure 1-7 Examples of fibrates with agonist activity^{9, 10, 22}

The first fibrate to be reported was clofibrate (**7**) in 1961.²³ In rats, it was observed to reduce lipid and cholesterol levels²⁴ in both the blood and liver; however it caused hepatic peroxisome proliferation, hepatomegaly, and

hepatocarcinogenesis²⁵. None of these toxic effects however are mirrored in humans⁹. Subsequent to the development of clofibrate (7); fenofibrate, gemfibrozil (8), bezafibrate (11) and ciprofibrate (12) were brought to the market.

1.2.4.3.2. Fenofibrate

Fenofibrate (10a) was developed in the 1970s by Groupe Fournier SA²⁶. It is a PPAR α agonist, and is widely used as a hypolipidemic drug. Although fenofibrate (10a) itself has low activity at PPAR α , it is a prodrug and becomes active once the ester is hydrolysed, to give fenofibric acid (10b).

In a randomised controlled trial with 9795 patients with T2DM, the drug was proven to be effective in lowering triglyceride levels and raising HDL levels²⁷ through mechanisms described below in section 1.2.4.4. It was also found to be effective in reducing the number of cardiovascular events, including non-fatal myocardial infarctions and stroke²⁷.

1.2.4.4. Effect of Fibrates on Lipid Metabolism

Fibrates have been utilised in the clinic for over forty years to treat dyslipidemias, and are thought to operate via several mechanisms to alter lipid metabolism. The following mechanisms describe how fibrates affect lipid metabolism:

Firstly, the expression of lipoprotein lipase is increased, and expression of apolipoprotein CIII (an inhibitor of lipoprotein lipase) is decreased, which leads to an increase in triglyceride metabolism, and therefore a lowering of plasma triglyceride levels^{28 21}. Fibrates also inhibit the synthesis of hepatic triglycerides and Very Low Density Lipoproteins (VLDL)²⁸, and increase

hepatic fatty acid uptake. They increase the clearance of LDL and reduce the level of small dense LDL. By increasing the size of LDL, affinity of LDL for the LDL receptor is augmented, and is less likely to be oxidised ²¹. Lastly, fibrates increase the levels of HDL and increase reverse cholesterol transport. The HDL levels are increased by augmenting the expression of the main components of HDL; ApoA-I and ApoA-II ^{21, 29}.

Fibrates have been shown to lower plasma triglyceride levels by 20-50% and raise HDL levels by 10-35%.²⁹

1.2.4.5. Other Synthetic Ligands

Other synthetic PPAR α agonists, developed after the fibrates, include WY14643 (**13**) and BR-931 (**14**). WY14643 (**13**) is a pyrimidine derivative and was first reported in 1974. BR-931 (**14**) is an ethanolamide analogue of WY14643 (**13**). Both of these compounds have shown to be effective hypolipidemic agents^{30, 31}.

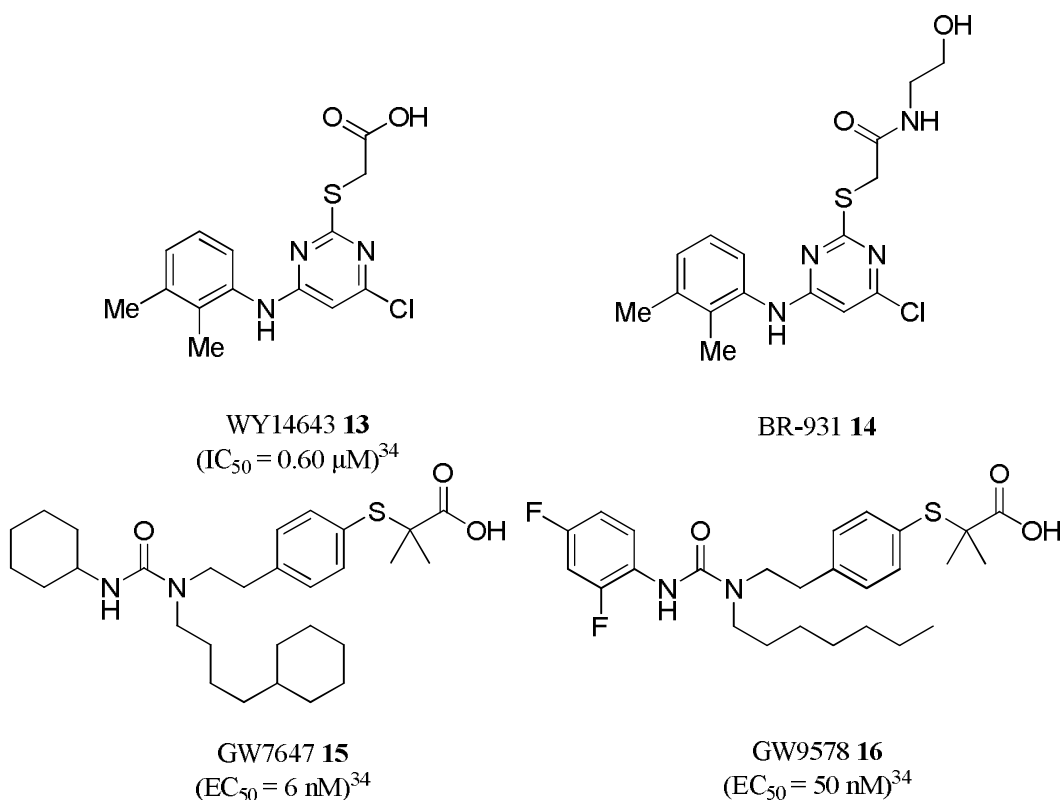


Figure 1-8 Examples of synthetic PPAR α agonists

All of the synthetic PPAR α ligands described so far were developed without the knowledge that they were active at PPARs. Subsequent to the cloning of PPARs and the identification of ligands for these receptors, a new class of ligands was designed. These were urea-substituted thioisobutyric acids, and gave rise to the first selective PPAR α agonists and antagonists. The development of these ligands was initiated with the synthesis of ureido-fibrates. Using combinatorial chemistry a library of 480 compounds was synthesised³², in which 20-50% of the compounds had affinity for PPAR³². However, there was low sub-type selectivity at murine and human PPARs³² so Brown *et al.* substituted the fibrate head group with thioisobutyric acid³³. This led to the synthesis of GW9578 (**16**), which displayed a 300-fold selectivity for

murine PPAR α and 20-fold selectivity for human PPAR α ³³ over other subtypes. To improve the selectivity at PPAR α , two further combinatorial libraries were synthesised by Brown *et al.* Ten compounds were identified as having nanomolar or lower activity at PPAR α , and selectivity of more than 100 fold. GW7647 (**15**) was identified as having the highest activity and being the most selective for hPPAR α ³⁴; it has 200-fold selectivity and also exhibits *in-vivo* lipid lowering activity³⁴.

1.3. G-Protein Coupled Receptors

There are approximately 800 known G-Protein Coupled Receptors (GPCRs), and they are divided into five families based on sequence conservation. The families are; Glutamate (G), Rhodopsin (R), Adhesion (A), Frizzled/Taste (F) and Secretin (S)³⁵. The largest family is the Rhodopsin family which is comprised of 672 receptors³⁵. GPCRs are located in cell membranes, and allow transmission of a low level extracellular signal to the inside of the cell, where the signal is amplified. They are responsible for approximately 80% of signal transduction into cells³⁵.

1.3.1. GPCR Structure

GPCRs are made up of seven transmembrane (7TM) alpha helices, joined by three intracellular and three extracellular loops. The *N*-terminus is on the exoplasmic side of the cell membrane and the *C*-terminus resides on the cytosolic side of the plasma membrane³⁶.

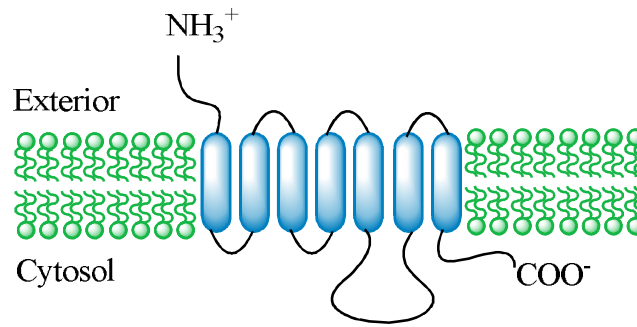


Figure 1-9-Representation of a GPCR structure (adapted from molecular cell biology, 5ed³⁷)

GPCRs are linked to a G-protein, which consists of three subunits G_α , G_β and G_γ , with G_α bound to guanosine 5'-diphosphate (GDP) in the inactive state³⁸. The G-protein is on the interior of the cell, with the G_α and G_γ subunits attached to the cell membrane via lipid anchors³⁹. There are four types of the G_α subunit, which are; G_{ai} , G_{as} , $G_{a12/13}$ and $G_{aq/11}$. $G_{\beta\gamma}$ exists as a dimer and there is only one type³⁹. $G_{ai/o}$ is an inhibitory G-protein which was initially demonstrated to inhibit adenylyl cyclase but was later shown to also interact with other effector enzymes³⁹. G_{as} activates adenylyl cyclase, $G_{aq/11}$ activates phospholipase C- β , and $G_{a12/13}$ may be involved in the regulation of small GTP binding proteins³⁹ such as members of the rho family of GTPases⁴⁰.

1.3.1.1. GPCR Structure Determination

GPCR structures are difficult to elucidate as they are membrane bound receptors, and rely on the cell membrane for their structure. This causes difficulty in isolating, and crystallising them. Early homology models of GPCR structures were based on various studies of bacteriorhodopsin in its inactive state⁴¹⁻⁴³.

The first mammalian GPCR crystal structure was solved in 2000 by Palczewski *et al*⁴⁴. The GPCR studied was bovine rhodopsin, with 11-cis-retinal bound, which maintains the transmembrane region in an inactive conformation. The

2.8Å crystal structure revealed differences from the bacteriorhodopsin structure. One of these is the differing arrangement of helices between the two receptors⁴⁴.

Further advances in GPCR structure determination came in 2007 when two research groups reported the crystal structure of the β_2 -adrenoceptor bound to the partial inverse agonist carazolol^{45, 46}. Rasmussen *et al* crystallised the human β_2 -adrenoceptor in a lipid environment, and with a monoclonal antibody fragment (Fab-5) bound to the third intracellular loop⁴⁶. The antibody fragment helped to stabilise the receptor whilst not affecting ligand binding. They successfully resolved the ends of the transmembrane segments and connecting loops, however the extracellular regions could not be resolved⁴⁶. Similarities and differences between the bovine rhodopsin structure and the human β_2 -adrenoceptor were revealed by overlaying the two crystal structures. The two receptors share a similar overall 7TM structure, but the cytoplasmic ends of the transmembrane segments differ, and the β_2 -adrenoceptor has a more open structure⁴⁶. The two receptors have differing basal activities, as the β_2 -adrenoceptor has a high basal activity, whereas rhodopsin has no detectable basal activity⁴⁶. Even bound with an inverse agonist, the β_2 -adrenoceptor displays 50% activity⁴⁶. The more open structure could explain the high basal activity, as the β_2 -adrenoceptor could be deficient in some of the hydrogen bonds, Van der Waals interactions and ionic interactions present in the inactive rhodopsin structure⁴⁶. Cherezov *et al* modified the β_2 -adrenoceptor (β_2 -AR) structure by inserting a T4 lysozyme sequence in place of the third intracellular loop⁴⁵. This change again stabilised the receptor and was shown not to affect ligand binding. Unlike the 3.4/3.7 Å crystal structure of the β_2 -adrenoceptor

obtained by Rasmussen *et al*, Cherezov *et al*. were able to resolve the extracellular regions, in addition to achieving a resolution of 2.4 Å.

On comparison of the higher resolution β_2 -AR structure, with the bovine rhodopsin structure, several differences were revealed. There is a difference in the transmembrane helices as 2, 5, 6 and 7 have a kink, and the second extracellular loop has an extra helix which is not present in rhodopsin⁴⁵.

The differences in the crystal structures of the β_2 -adrenoceptor, and that of bovine rhodopsin, highlights shortcomings in homology models of various GPCRs that are solely based on rhodopsin.

1.3.1.2. G-protein Activation

The G-protein in its inactive state exists as a heterodimer with GDP bound to the G_α subunit. On G-protein activation, the GDP dissociates and guanosine 5'-triphosphate (GTP) binds to the G_α subunit. This causes the G_α -GTP dimer to dissociate and bind to an effector enzyme such as adenylyl cyclase³⁶.

The GTP is gradually hydrolysed back to GDP by the inherent GTPase activity of the G_α subunit. This GTPase activity can be increased by regulators of G-protein signalling (RGS) proteins³⁸. The G_α unit with GDP is then able to reassociate with $G\beta\gamma$ to form the inactive $G\alpha\beta\gamma$ trimer³⁸ which stops the activity of the G_α subunit on the effector enzyme³⁸.

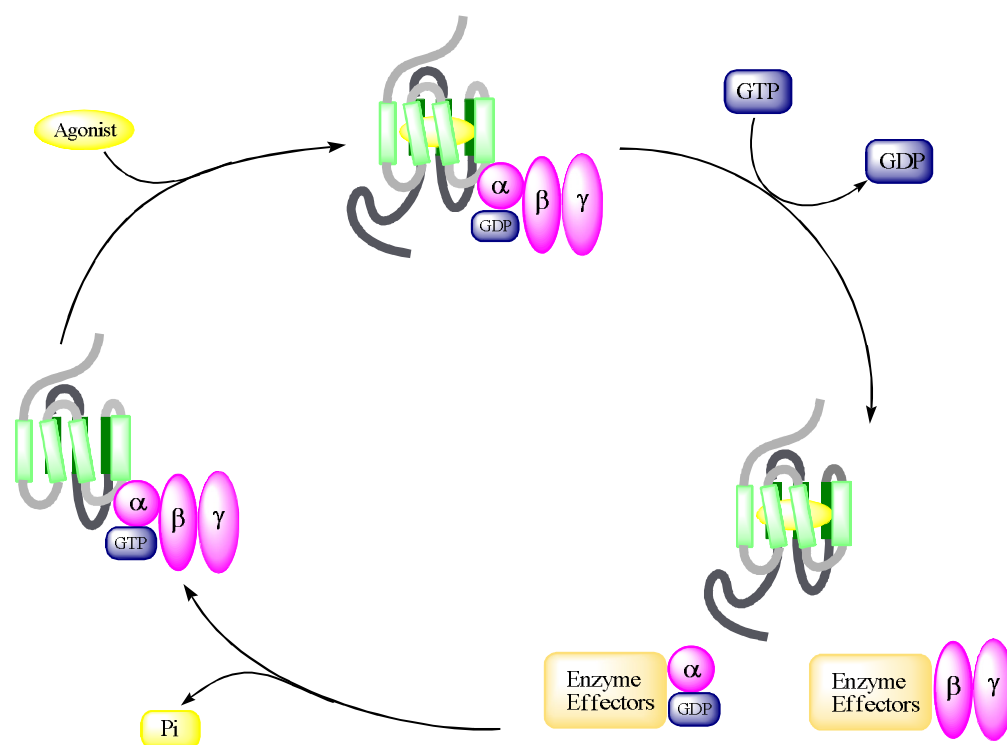


Figure 1-10-Representation of a GPCR activation mechanism (adapted from Barren *et al*³⁸)

1.4. Cannabinoid Receptors

Cannabinoid receptors belong to the Rhodopsin-like family of GPCRs and there are two recognised sub-types; CB₁ and CB₂. The first compounds identified as cannabinoid receptor ligands, were isolated from the plant *Cannabis sativa*. There are approximately 60 cannabinoid compounds present in the Cannabis plant and the first compounds isolated⁴⁷ were cannabinol ($K_i = 211$ nM at CB₁ and 126 nM at CB₂)⁴⁸ and cannabidiol ((**17**) refer to **Figure 1-11**). The compound which gives the plant its psychoactive properties, was identified as Δ^9 -Tetrahydrocannabindiol (Δ^9 -THC (**26**) refer to **Figure 1-14**) by Mechoulam *et al.* in 1964⁴⁹ and is an agonist at both the cannabinoid receptors.

1.4.1. CB₁ Receptor

The CB₁ receptor (CB1R) was identified in 1988 by Devane *et al.* and then cloned in 1990^{50, 51}. It has since been cloned from mouse⁵² and human⁵³ tissues and there is 97-99% sequence identity between them⁵⁴. In humans the CB₁ receptor is found predominantly in the brain in several areas including the hypothalamus, amygdala and the hippocampus⁵⁵. It is found peripherally in adipocytes, liver and on both central and peripheral nerve terminals. Activation of the CB₁ receptor suppresses release of acetylcholine, norepinephrine, dopamine, 5-hydroxytryptamine, GABA, glutamate and aspartate⁵⁴.

The CB₁ receptor is a G_{i/o} coupled receptor, and its activation causes the inhibition of adenylyl cyclase activity and activation of MAP kinase⁵⁴. Adenylyl cyclase is a membrane-bound enzyme that facilitates formation of cyclic AMP from ATP. The CB₁ receptor is also coupled to other effectors such as potassium and calcium channels⁵⁶.

1.4.2. CB₂ Receptor

The CB₂ receptor (CB2R) was the second cannabinoid receptor to be identified and cloned in humans, rats and mice.^{53, 57, 58} The human CB₂ receptor has 81% and 82% sequence identity with mouse and rat CB₂ receptors respectively. It is found in the cells of the immune system, and more recently has been found in low levels in brain stem neuronal cells⁵⁹ and also in microglial cells of the central nervous system⁶⁰.

Like the CB1R, it is G_{i/o} coupled, and activation of the receptor causes inhibition of adenylyl cyclase, and activation of MAP kinase⁵⁴. Unlike the CB₁

receptor, the CB₂ receptor does not couple to calcium Q or inward rectifying potassium channels⁵⁴. The CB₂ receptor has 68% amino acid homology with CB₁ receptors within the transmembrane regions⁵⁴, but only 44% overall⁶¹.

1.4.3. GPR55

For a number of years, evidence grew to suggest the presence of a third cannabinoid receptor, in addition to the CB₁ and CB₂ receptors. Several groups have reported an orphan cannabinoid-like receptor in the brain,^{62, 63} vascular endothelium,^{64, 65} and the immune system⁶⁶. The first suggestion of the existence of a novel third cannabinoid receptor came from studies of the effects of cannabinoids on vasodilation, in which anandamide (**19**) and (*R*)-methanandamide, possessed vasodilatory ability; however Δ^9 -THC ((**26**) refer to **Figure 1-14**) and potent synthetic CB₁ and CB₂ cannabinoids had no effect⁶⁷. The vasodilatory effect was inhibited by the CB₁ antagonist SR141716 (**41**) but a higher concentration of SR141716 (**41**) than necessary to block CB₁ receptors was needed⁶⁴. Parmitoylethanolamine (PEA) has been demonstrated to have potent antinociceptive effects peripherally which were blocked by the CB₂ selective antagonist SR144528 (**42**)⁶⁸. As PEA does not activate the CB₂ receptor, Calignano *et al* suggested that a third cannabinoid receptor may be responsible.

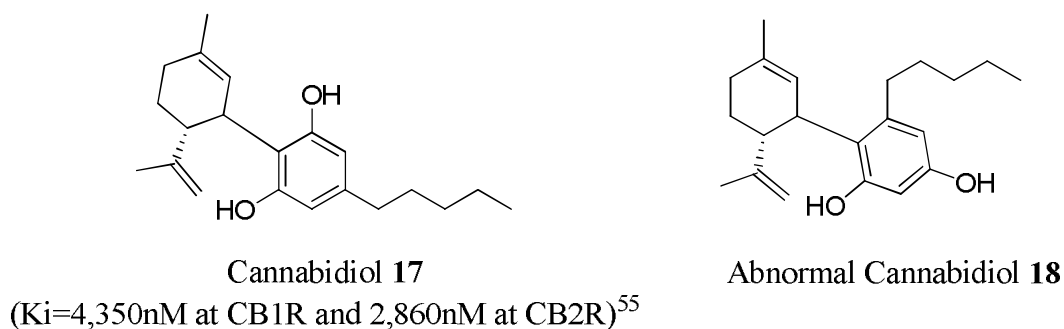


Figure 1-11- Structures of cannabidiol and abnormal cannabidiol

The orphan receptor GPR55 was identified as potentially a novel cannabinoid receptor by Ryberg *et al.* in 1995⁶⁹. Cells transfected with human cDNA for GPR55, were used, and radioligand binding assays showed that the receptor was activated by several endocannabinoids, as well as natural and synthetic cannabinoids. Endogenous ligands active at the receptor include anandamide (**19**), 2-AG (**20**), noladin ether, PEA and virodhamine (**22**). Virodhamine (**22**) had a particularly high efficacy that was double that of anandamide. Other ligands which displayed activity at GPR55 included Δ^9 -THC (**26**), HU210 (**29**), and AM251 (**44**). Cannabidiol (a low affinity CB1R and CB2R ligand (**17**)) and abnormal cannabidiol (**18**), which has no CB₁ or CB₂ activity, are active at GPR55, suggesting that their effects may be mediated by this receptor.

Ryberg *et al*⁶⁹ also reported the pattern of expression of GPR55 in mouse tissues, with the highest levels of GPR55 mRNA were located in the adrenal glands, parts of the gastrointestinal tract and the brain.

GPR55 still remains to be reclassified as a cannabinoid receptor, as more recent evidence has suggested that it may be a receptor for endogenous phospholipids; lysophosphatidylinositols (LPI)⁷⁰, with the arachidonic acid

containing species, 2-arachidonoyl-sn-glycero-3-phosphoinositol, having the highest affinity⁷¹. Several groups have also reported that some cannabinoids, that have been previously described as ligands for GPR55, may not actually have affinity for the receptor^{70, 71}.

1.4.4. Ligands for Cannabinoid Receptors

There are several different classes of ligands for the cannabinoid receptors, including the endocannabinoids, classical THC-like cannabinoids, non-classical cannabinoids and the aminoalkylindoles.

1.4.4.1. Endocannabinoids and the Endocannabinoid System

There have been seven endogenous cannabinoid receptor ligands (endocannabinoids) identified to date, and they are thought to be involved in regulation of food intake,⁷² posture and movement,⁷³ pain perception,⁶⁸ and immune response⁷⁴. At nerve terminals endocannabinoids mediate neurotransmitter release by retrograde signalling across the synapse⁷⁵. Endocannabinoids are synthesised on demand, not stored, and are metabolised in cells by enzymes, including fatty acid amide hydrolase (FAAH) and monoacylglycerol lipase.

The first endocannabinoid identified was anandamide (**19**) (arachidonylethanolamide) in 1992. It is a derivative of arachidonic acid (**4**) and was isolated from pig brain⁷⁶. Anandamide (**19**) has a measureable affinity for both cannabinoid receptors⁵⁴ but only exerts a small agonist effect⁷⁷. During the isolation of anandamide (**19**), two other compounds were found to bind to the CB₁ receptor. These two compounds (homo- γ -linolenylethanolamide (**24**) and docosatetraenylethanolamide (**25**)) were

later identified and synthesised by Hanus *et al*⁷⁸ and were both found to bind to the CB₁ receptor in a competitive binding experiment.

During a study to find peripheral cannabinoid receptor ligands, a third endocannabinoid was reported. It was named 2-arachidonoylglycerol (2-AG) (**20**), and was isolated from canine gut⁷⁹ and rat brain⁸⁰. It is synthesised from diacylglycerol and was shown to bind to CB₁ and CB₂ but demonstrates a higher affinity for CB₁⁷⁹.

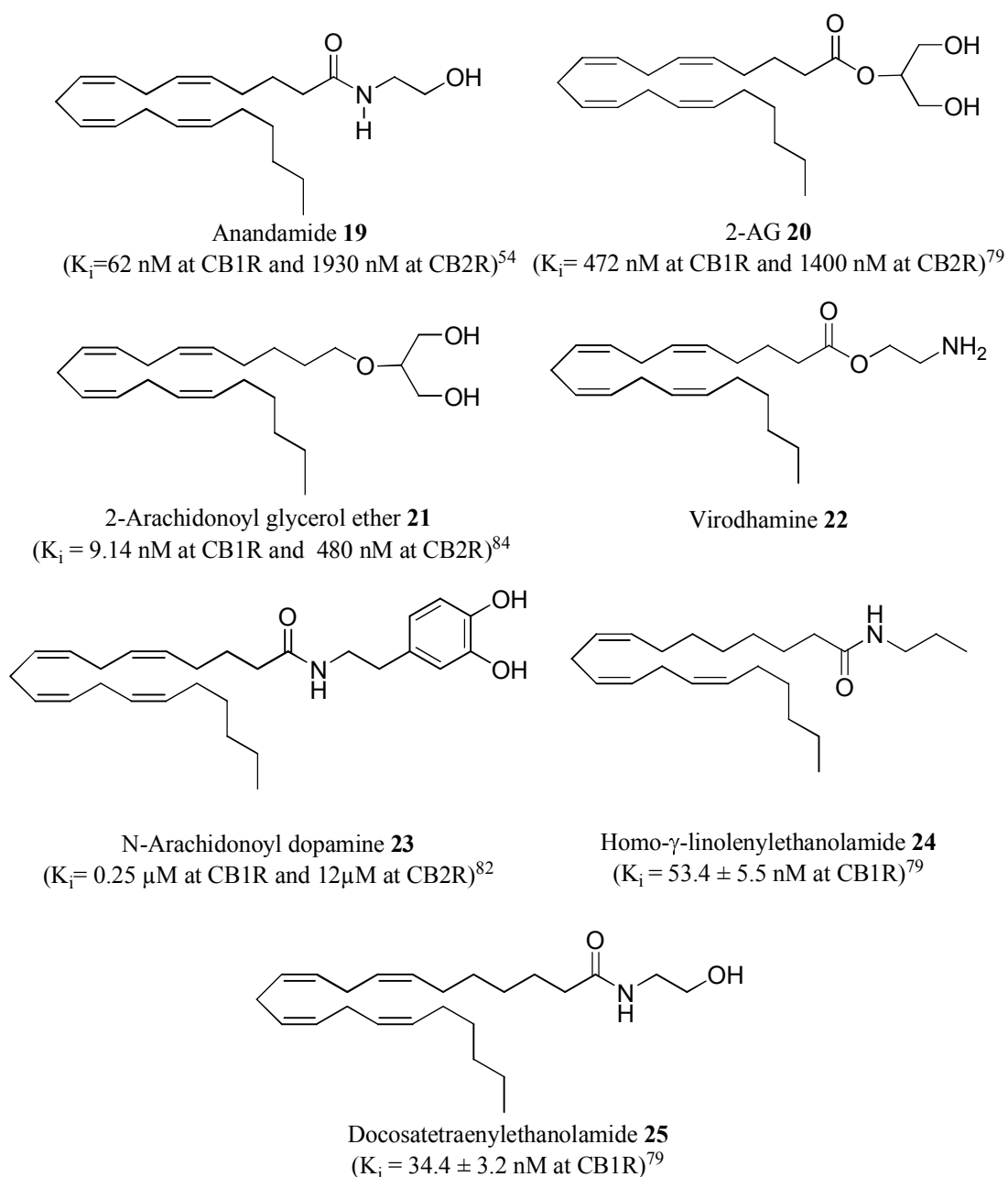


Figure 1-12-Endogenous Cannabinoids

Between 2000 and 2002, three other endocannabinoids were characterised. These were *N*-arachidonoyl dopamine (**23**), noladin ether, and virodhamine (**22**). (**Figure 1-12**).

N-Arachidonoyl dopamine (**23**) (NADA) was isolated from rat brain in 2000⁸¹. It is a selective CB₁ receptor agonist⁸² and also displays agonist activity at the

vanilloid type 1 receptor (TRPV1)⁸¹. In 2001, noladin ether (2-arachidonyl glycerol ether (**21**)) was isolated from porcine brain⁸³. It is an agonist at both CB₁ and CB₂ but displays a higher affinity for the CB₁ receptor⁸⁴. Virodhamine (**22**), an analogue of anandamide (**19**), was the seventh endocannabinoid to be isolated⁸⁵. The ethanolamine moiety is connected *via* the oxygen, instead of the nitrogen, to form an ester. It is an antagonist at the CB₁ receptor and an agonist at the CB₂ receptor.

Two compounds that are structurally related to the endocannabinoids are the PPAR α ligands; palmitoylethanolamine (PEA) and oleoylethanolamine (OEA). OEA has no activity at either cannabinoid receptor, but PEA has slight agonist activity at the CB₂ receptor. Both compounds activate the putative cannabinoid receptor GPR55 at nanomolar concentrations⁶⁹.

It has also been reported that several of the endocannabinoids have activity at PPAR α . In a study by Sun *et al.* they found that anandamide (**19**), noladin ether and virodhamine (**22**) bound to and activated PPAR α ⁵.

1.4.4.2. Classical Cannabinoids

The classical cannabinoids are natural or synthetic analogues of the psychoactive component of *Cannabis sativa*; Δ 9-THC (**26**). They consist of a tricyclic dibenzopyran-type core with a hydroxyl group at C1, and an alkyl group at C3⁵⁴ and varying substituents at C11.

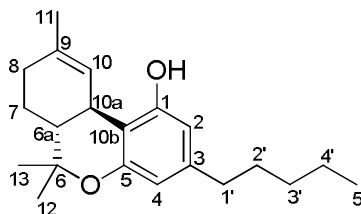


Figure 1-13 - Numbering system of classical cannabinoids

The first synthetic classical cannabinoid was 9-nor-9-hydroxyhexahydrocannabinol (**27**)⁸⁶. It differs in structure from Δ^9 -THC (**26**) at C11 as a hydroxyl group has replaced the methyl group and the double bond between C9 and C10 is absent. The effect of modification of the C3 alkyl substituent on cannabinoid receptor binding was then investigated, leading to the discovery of the high affinity cannabinoid dimethylheptyl-HHC (**28**)⁸⁷ where a dimethylheptyl group replaced the pentyl group.

Later modifications to the Δ^9 -THC (**26**) structure led to HU210 (**29**)⁸⁸. In comparison to Δ^9 -THC (**26**), C11 is hydroxylated, and the C3 alkyl side chain is the dimethylheptyl group from dimethylheptyl-HHC (**28**). HU210 (**29**) is more selective for CB1R than CB2R⁵⁶, and has a 7-fold higher affinity for CB₁ receptors than Δ^9 -THC (**26**). The importance of the stereochemistry of HU210 (**29**), at 6a and 10a, was investigated by Howlett *et al.*⁸⁹, who found that the (6a*R*, 10a*R*) enantiomer had 1500 fold higher affinity for the CB₁ receptor than the (6a*S*, 10a*S*) enantiomer (HU211 (**30**)).

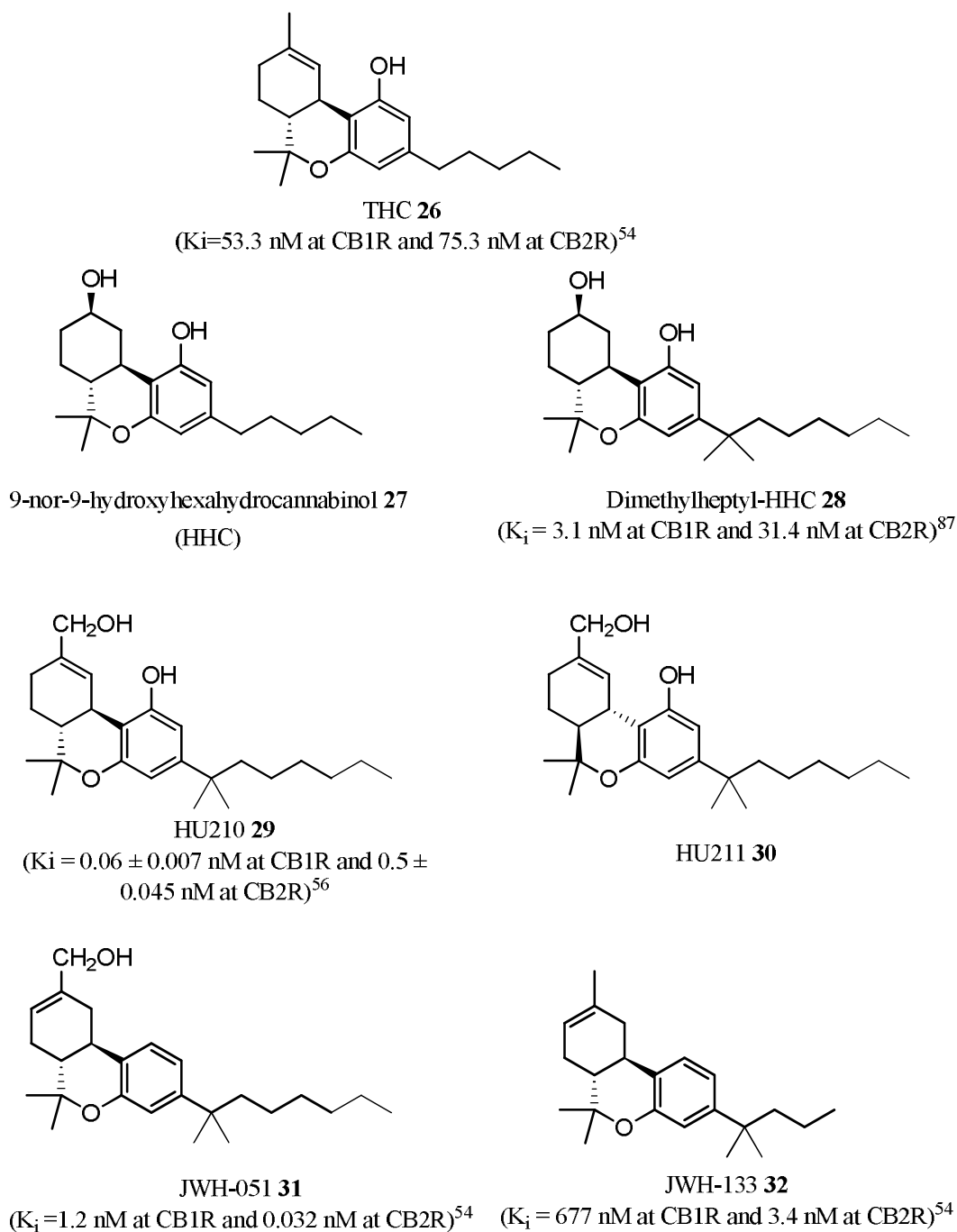


Figure 1-14 Examples of classical cannabinoids

Huffmann *et al* synthesised many synthetic cannabinoids, including the classical cannabinoids JWH-133 (**32**) and JWH-051 (**31**).^{90, 91} JWH-051 (**31**) is structurally related to HU-210, however the hydroxyl on C1 is not present. This change afforded an increased affinity for the CB₂ receptor⁵⁴.

JWH-133 (**32**) also has increased selectivity for the CB₂ receptor. It differs from Δ⁹-THC (**26**) in that it has a double bond between C8 and C9, the hydroxyl on C1 is absent, and a dimethylbutyl group has also been incorporated into the structure⁵⁴.

1.4.4.3. Non Classical Cannabinoids

The first non-classical cannabinoids were first reported by Pfizer in the 1980's⁹². Melvin *et al.* found that when removing the dihydropyran ring present in the classical cannabinoids, cannabinoid activity was retained.⁹² This led to the development of the non-classical cannabinoid CP 47497 (**33**)⁹³.

The non-classical cannabinoids are based on AC bicyclic and ACD tricyclic cores.

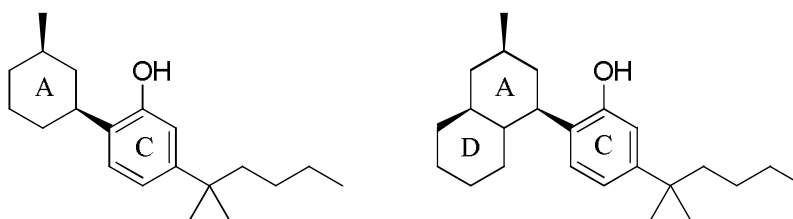


Figure 1-15- Non-classical cannabinoid lettering system

Examples of compounds in this class are shown in **Figure 1-16**.

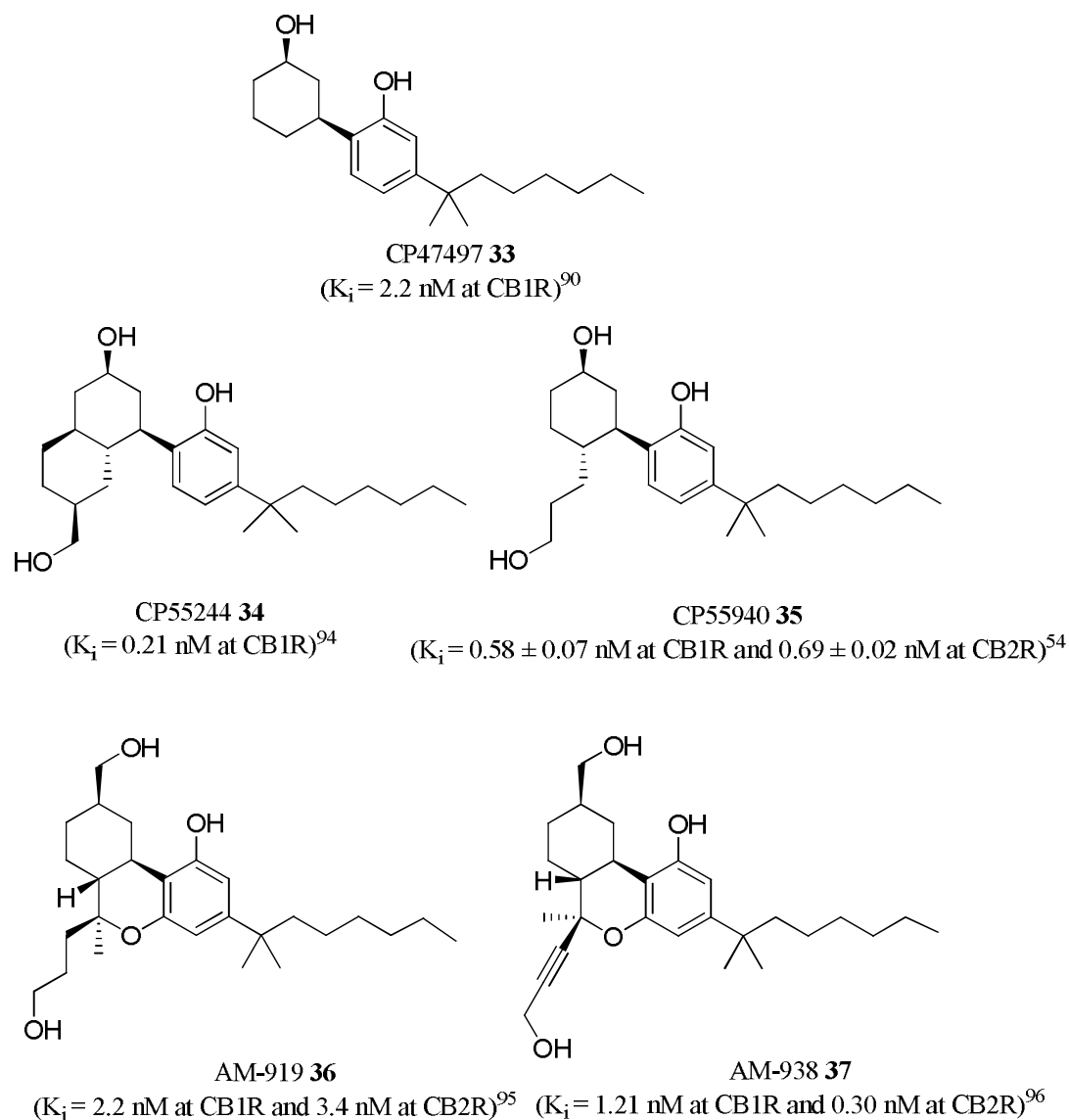


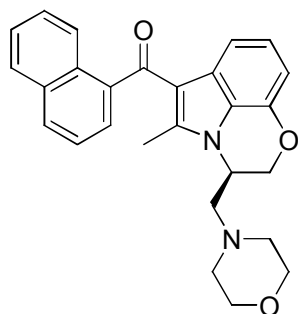
Figure 1-16 Examples of non-classical and classical/non-classical-hybrid cannabinoids

CP55940 (**35**) is a high affinity non-selective cannabinoid receptor agonist, which differs from CP47497 (**33**) by the presence of a propyl alcohol group at C4 of the cyclohexanol ring. The addition of this southern aliphatic hydroxyl (SAH) increased affinity for the CB₁ receptor⁹³. Tritiated CP55940 is an important tool in determining activity of compounds at the cannabinoid receptors, and was used by Devane *et al* in 1988 to characterise the CB₁ receptor⁵⁰.

CP55244 (**34**) is an ACD tricyclic non-classical cannabinoid, where the SAH of CP55940 (**35**) is conformationally restrained. It has a high affinity for the CB₁ receptor and behaves as a full agonist⁹⁴. The restrained SAH of CP55244 (**34**) was incorporated into classical cannabinoids to give non-classical/classical cannabinoid hybrids. Examples of these include AM919 (**36**) and AM938 (**37**) which both have nanomolar affinity for both CB₁R and CB₂R^{95, 96}. AM919 (**36**) is non-selective at the cannabinoid receptors, but AM938 (**37**) has a higher affinity for the CB₂ receptor. Selectivity was increased by rigidification of the SAH with an alkyne.

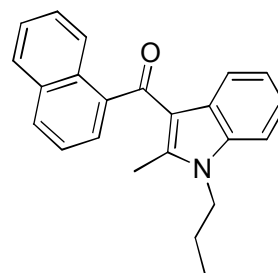
1.4.4.4. Aminoalkylindoles

The aminoalkylindoles were developed by structurally constraining analogues of the non-steroidal anti-inflammatory drug (NSAID) pravadolone. The first compounds in this series displayed reduced prostaglandin synthase inhibitory activity, but retained antinociceptive activity via another mechanism⁹⁷, which later proved to be activity at the cannabinoid receptors⁹⁸.

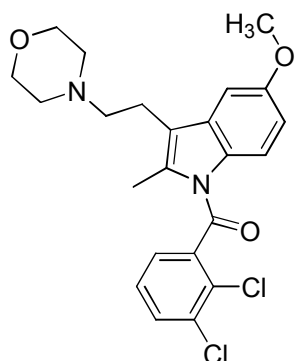


R-(+)-WIN55212 **38**

(K_i at CB₁R=62.3 nM, and 3.3 nM at CB₂R)⁵⁶ (K_i =383 nM at CB₁R and 13.8 nM at CB₂R)⁵⁴



JWH-015 **39**



L-768242 **40**

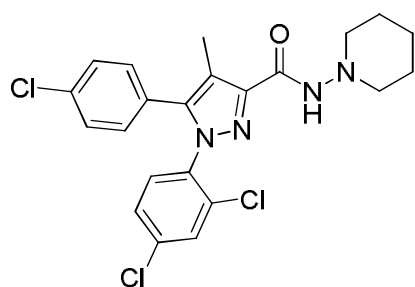
(K_i =1917 ± 381 nM at CB₁R and 12 ± 0.2 nM at CB₂R)⁹⁹

Figure 1-17 Examples of aminoalkylindole cannabinoids

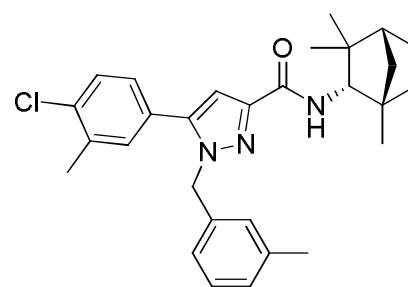
R-(+)-WIN55212 (**38**) is a member of the aminoalkylindole series (**Figure 1-17**), and is a high affinity agonist for both the CB₁ and CB₂ receptors⁵⁶ with a slight selectivity towards the CB₂ receptor. Since the synthesis of these first aminoalkylindoles, several others have been developed, such as the CB₂ selective ligands L-768242 (**40**) (GW405833)⁹⁹ and JWH-015 (**39**)⁵⁴.

1.4.4.5. Diarylpyrazoles

The first 1,5-diarylpyrazole cannabinoid receptor ligands were reported by Sanofi Recherche in the 1990's⁹⁸. They were a structurally novel class of ligands, which provided the first selective high affinity CB₁ and CB₂ receptor antagonists. SR141716 (**41**) (Rimonabant) was reported in 1994 as a CB₁ antagonist¹⁰⁰. It has a high affinity at cloned human CB₁ receptors and has 1000 fold selectivity for CB₁ over CB₂. A high affinity CB₂ antagonist (SR144528 (**42**)) was reported four years later⁹⁹, with 700 fold lower affinity for the CB₁ receptor.



SR141716 **41**
(K_i=5.6 ± 0.5nM at CB₁R, and >1000 nM at CB₂R)¹⁰⁰



SR144528 **42**
(K_i = 0.6 nM at CB₂R, and 400 nM at CB₁R)⁵⁴

Figure 1-18 Examples of diarylpyrazole cannabinoids

1.4.5. CB₁ as a therapeutic target

The CB₁ receptor has potential as a target in several therapeutic areas, including appetite control, pain relief, and multiple sclerosis (MS).

1.4.5.1. Analgesia

Several studies in animal pain models have indicated a role for cannabinoid receptors as analgesics⁹⁷. Richardson *et al.*¹⁰¹ found that anandamide (**19**) administered peripherally in rat paws reduced hyperalgesia and

inflammation¹⁰¹. Reduction of hyperalgesia was prevented by the CB₁ selective inverse agonist SR141716 (**41**)¹⁰¹.

Calignano *et al.*⁶⁸ also found that in mice an analgesic effect was observed when anandamide (**19**), WIN55212 (**38**) or HU210 (**29**) were injected with formalin into paws⁶⁸. The analgesic effect was prevented by SR141716 (**41**) but not the CB₂ selective antagonist SR144528 (**42**)⁶⁸.

In contrast to animal pain models, studies on the effect of cannabinoids on human pain have had varying results. A systematic review of research carried out on human pain trials indicated that cannabinoids had little advantage over traditional pain relief medication in the treatment of post operative pain, with high incidences of adverse effects¹⁰². Buggy *et al.*¹⁰³ also found that 5 mg of Δ^9 -THC (**26**) had no effect on post operative pain¹⁰³. The review however, indicated that cannabinoids may have an application in the treatment of MS, where Δ^9 -THC (**26**) reduced spasticity and neuropathic pain¹⁰².

1.4.5.2. Appetite

The CB₁ receptor was first implicated in appetite control when it was discovered that both anandamide (**19**) and Δ^9 -THC (**26**) induced appetite stimulation.¹⁰⁴

1.4.5.2.1. Appetite Suppression

The CB₁ receptor inverse agonist SR141716 (**41**) (rimonabant) was found to be effective in inducing weight loss, increasing HDL plasma concentrations and decreasing plasma triglycerides in humans¹⁰⁵. It is thought that the initial weight loss is due to the action of SR141716 (**41**) on CB₁ receptors in the brain, by reducing appetite¹⁰⁶. However subsequent weight loss, after the

anorectic effect has diminished, is thought to be due to peripheral CB₁ receptors found in adipocytes¹⁰⁶, which can regulate adiponectin¹⁰⁷ and decrease lipoprotein lipase levels¹⁰⁸.

Rimonabant (**41**) was utilised as an aid to weight loss until 2008, when it was removed from the market, due to evidence of adverse effects in patients, such as depression and suicidal thoughts¹⁰⁹. This in turn led to several pharmaceutical companies abandoning projects researching potential CB₁ antagonists.

1.4.5.2.2. Appetite Stimulation

CB₁ agonists are currently used in patients undergoing chemotherapy treatment and also patients with AIDS. This is due to their ability to increase appetite (orexigenic effect) and relieve nausea (antiemetic effect)⁴⁷. Cannabinoids currently used are nabilone, a synthetic classical cannabinoid, and synthetic Δ^9 -THC (**26**) which is also called dronabinol¹¹⁰.

1.4.5.3. Multiple Sclerosis

Multiple sclerosis (MS) is an auto-immune disease where the myelin sheaths of axons are damaged. This leads to demyelination that causes problems in the transmission of signals in nerve cells. Symptoms include muscle spasticity, spasms, ataxia, tremor and lower urinary tract dysfunction.

Cannabinoid compounds such as Δ^9 -THC (**26**) have shown potential in clinical trials as treatments for MS. In a study carried out in 2003, 630 participants were given a cannabinoid extract, 5 mg of Δ^9 -THC (**26**) a day or placebo.⁷³ In the group treated with 5 mg/day of Δ^9 -THC (**26**), an analgesic effect was

observed and the participants perceived an improvement in spasticity.⁷³ However there was no improvement when measured on the Ashworth scale.⁷³

In a smaller study with participants treated with 2.5 mg Δ^9 -THC (**26**) combined with 0.9 mg cannabidiol (**17**), a lower spasm frequency and increased mobility was observed in comparison to placebo¹¹¹.

Sativex[®] is a cannabinoid treatment that is used to relieve some of the symptoms associated with MS. It was granted full approval for usage as a treatment for MS in the UK in June 2010.¹¹² Sativex[®] is a *Cannabis sativa* extract containing Δ^9 -THC (**26**) and cannabidiol (**17**) and has been shown in clinical trials to reduce spasticity¹¹¹.

1.4.6. CB₂ as a therapeutic target

The therapeutic potential of the CB₂ receptor has attracted less attention, as most studies have focused on the CB₁ receptor. More recently, interest has grown in investigating the ways in which the CB₂ receptor can be exploited.

Various studies have implicated the CB₂ receptor in immune modulation and inflammation, the treatment of chronic pain and neuroprotection.

1.4.6.1. Analgesia

The CB₂ receptor, in addition to the CB₁ receptor, has the potential to be a target in pain relief. Targeting the CB₂ receptor may be advantageous in that central nervous system side effects, mediated by the central CB₁ receptor, could be avoided. Several studies have shown that acute pain induced by a thermal source can be alleviated by some CB₂ agonists¹¹³.

AM1241 has displayed an antinociceptive effect and this effect was blocked by AM630 (**43**), a CB₂ receptor antagonist. The CB₁ receptor antagonist AM251

(**44**) has no effect on AM1241 antinociception suggesting the involvement of the CB₂ receptors¹¹⁴.

CB₂ receptor agonists have also been shown to have an analgesic effect in models of persistent inflammatory pain. Inflammation and pain induced by a carrageenan injection was blocked by the administration of AM1241. This effect was inhibited by the CB₂ receptor antagonist SR144528 (**42**) but not the CB₁ receptor antagonist SR141716 (**41**).¹¹⁴ Antinociception was also observed in the capsaicin and the formalin pain models¹¹⁴.

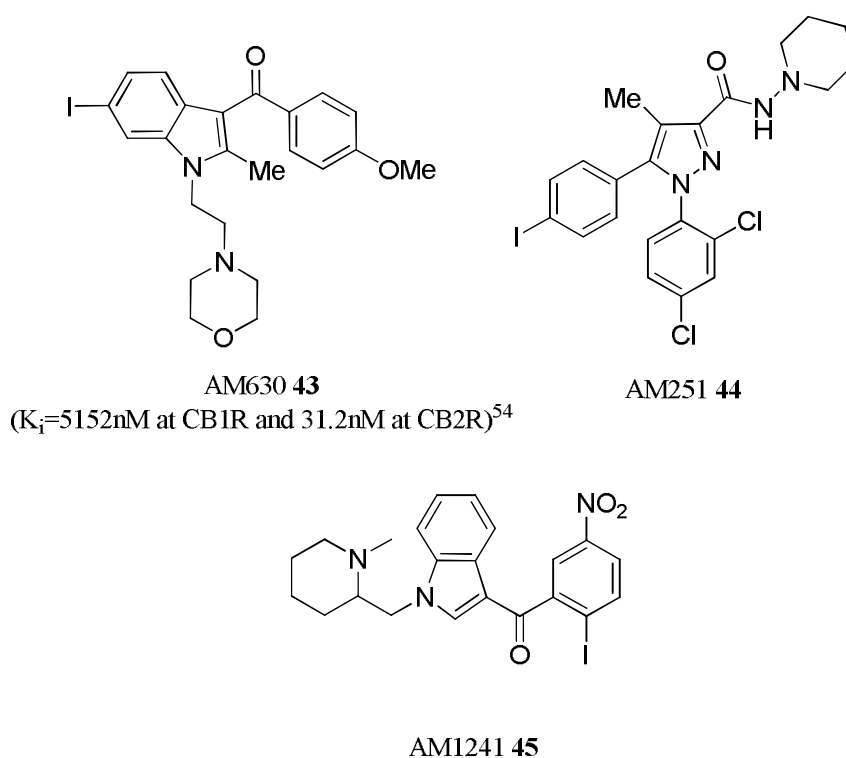


Figure 1-19 Examples of cannabinoids with antinociceptive effects

The CB₂ receptor could also be a target in the relief of neuropathic pain. Several studies have displayed the pain relieving effects of the CB₂ agonists AM1241, JWH-133 (**32**) in behavioural and electrophysiological models¹¹⁴.

1.4.6.2. Immune modulation and inflammation

CB₂ receptors are mainly expressed in cells of the immune system, and could therefore be a target for immune modulation, and in the treatment of inflammatory diseases, such as Crohn's disease, atherosclerosis and arthritis.

It has been found that when tissues expressing CB₂ receptors are stimulated with antigens, CB₂ expression either increases or decreases, depending on the antigens or bioactive substance applied to the cells⁷⁴. Treatment of immune cells also leads to the production and release of endocannabinoids such as anandamide (**19**) and 2-AG (**20**), which can induce migration of various cell types³.

Steffens *et al.*¹¹⁵ found that when mice were treated with a low dose of Δ^9 -THC (**26**) (1 mg Kg⁻¹), the progression of atherosclerosis was reduced¹¹⁵. They concluded that this reduction was mediated by the CB₂ receptor, as it was found in atherosclerotic plaques, and that it exerts its effects by suppressing the T_H1 response and inhibiting the migration of monocytes and macrophages to the site of inflammation¹¹⁵.

1.5. Aims

The aim of this project was to develop a compound with agonist activity at PPAR α combined with antagonist activity at the CB₁ receptor or agonist activity at the CB₂ receptor.

A CB₁ antagonist could reduce appetite, whilst at the same time a PPAR α agonist could decrease plasma triglyceride levels, increase HDL and lower LDL. In addition a CB₂ agonist could reduce inflammation. A dual receptor ligand could offer the benefit of treating multiple symptoms of a disease such as

obesity without the side effects associated with taking multiple medications. To date a high affinity dual PPAR α /cannabinoid receptor ligand has not been developed.

1.5.1. Design of fenofibrate analogues

Recent reports have suggested that some cannabinoids have activity at PPAR α ^{4, 5}. Sun *et al* found that Win55212-2 (**38**), OEA, anandamide (**19**), noladin ether (**21**) and virodhamine (**22**) had micromolar affinity for PPAR α with IC₅₀ values from 10 μ M to 40 μ M. They also found that all of these ligands increased luciferase expression in a reporter gene assay and both noladin ether (**21**) and virodhamine (**22**) doubled luciferase transcription at a concentration of 10 μ M.

From this evidence it was hypothesised that the converse may be possible; that PPAR ligands may have activity at the cannabinoid receptors. From initial screening, by Professor David Kendall, of 13 PPAR ligands, one was found to possess activity at both the cannabinoid receptors. This compound was fenofibrate (**10a**). It binds to the CB₁ receptor with a K_i of 460 nM, and to CB₂ receptor with a K_i of 108 nM. However, fenofibric acid (**10b**), the active metabolite at PPAR α , was inactive at the CB₁ and CB₂ receptors. It was envisaged that the functionalisation of the cannabinoid-inactive fenofibric acid (**10b**), with another group instead of the isopropyl ester, could result in activity at one or both of the cannabinoid receptors, whilst retaining activity at PPAR α .

It was decided to replace the ester with an ethanolamide group. This group was chosen as the addition of an ethanolamide group, to the cannabinoid

receptor inactive compound arachidonic acid (**4**), gives the CB₁ receptor agonist anandamide (**19**).

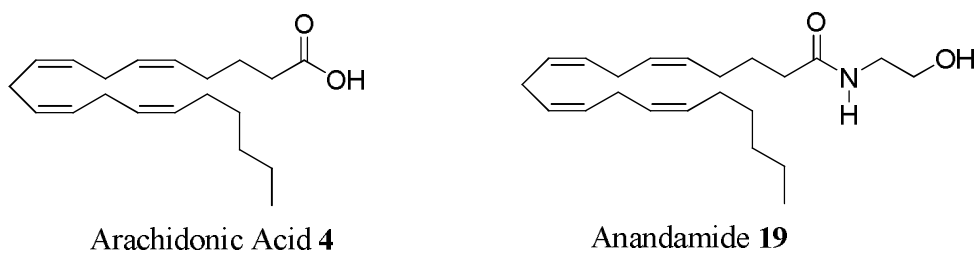


Figure 1-20- Structures of arachidonic acid and anandamide

It was thought that the metabolically more stable amide moiety, would give the fenofibric acid (**10b**) analogue a higher biological stability for interaction at both PPAR α , and the cannabinoid receptors.

Herein is described the synthesis of the fenofibrate (**10a**) derivatives, their pharmacology at PPAR α and the cannabinoid receptors, and any structure activity relationships.

2. Amide derivatives of fenofibrate

This chapter describes the synthesis and pharmacology of the first series of fenofibrate analogues.

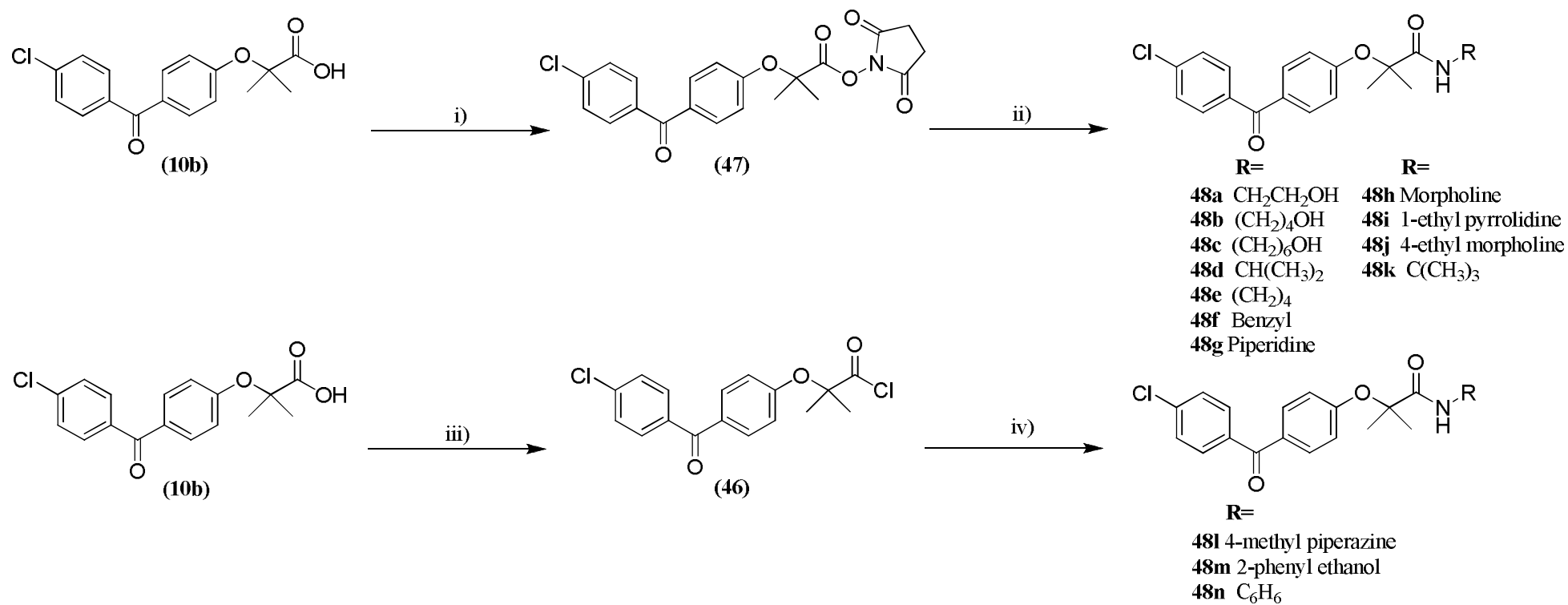
2.1. Synthesis

From the range of PPAR ligands tested, the ability of fenofibrate (**10a**) to activate both cannabinoid receptors resulted in its selection as a lead compound. As fenofibric acid (**10b**) is inactive at the cannabinoid receptors, and esters are rapidly hydrolysed *in-vivo*, potentially more metabolically stable amide derivatives were initially selected for synthesis.

Compounds **48a** to **48e** were aminoalcohol or alkyl derivatives of fenofibrate, with varying chain lengths, based on the aminoethanol group of anandamide. Compounds **48f** to **48n** were aromatic or heterocyclic amine derivatives. The larger aromatic and heterocyclic groups were selected to investigate whether affinity for the receptors could be improved relative to the smaller acyclic substituents.

2.2. Synthetic Route

Compounds **48a** to **48k** were synthesised by initial conversion of fenofibric acid (**10b**) to its corresponding *N*-hydroxysuccinimide (NHS) ester, which then underwent aminolysis with the desired amine to afford the required carboxamides (**48a**) to (**48n**).



Scheme 2-1- Synthesis of compounds **48a** to **48n**

Reagents and conditions, i) *N*-hydroxysuccinimide, EDC, DCM, rt, 23hrs, yield 68% ii) Selected amine, DCM, rt, 5 mins-24hrs, yields 42% - 97% iii) SOCl₂, 60°C 1 h, iv) Selected amine, DCM, Et₃N, rt, 2hrs to overnight, yields 38% -68 % Syntheses of **48a** to **48e** carried out by Dr Barrie Kellam

The activated ester (**47**) of the commercially available fenofibric acid (**10b**) was synthesised using *N*-hydroxysuccinimide and 1-ethyl-3-(3-dimethylaminopropyl) carbodiimide hydrochloride (EDC) in dichloromethane. The advantage of using EDC, rather than other peptide coupling reagents such as DCC, is that the resulting urea by-product is water soluble and therefore easily removed during aqueous work-up. The yellow-white solid afforded from the reaction was triturated with methanol to afford the activated ester (**47**) with a yield of 68%. Displacement of *N*-hydroxysuccinimide from the active ester, using a selection of commercially available amines, gave the target amides.

Formation of **48a** to **48e**, by displacement of *N*-hydroxysuccinimide from **47**, proceeded rapidly, with precipitation of the required product within 10 minutes. Compounds **48f** to **48k** were slower to form using the same method and required stirring from 1 hour to overnight, possibly due to steric hinderance of the amines used.

Subsequent compounds (**48l** to **48n**) were prepared by converting fenofibric acid (**10b**) to its corresponding acid chloride with thionyl chloride, which then underwent direct aminolysis with the required amines in the presence of triethylamine. This method was employed to overcome either the poor nucleophilicity of some of the amines, or possible steric hinderance which compromised amide formation using the NHS ester method.

Structural determination, of the activated ester (**47**) and all the amides prepared, was carried out using NMR, FT-IR and high resolution mass spectrometry (HRMS). With the exception of **48b**, **48g**, **48h**, **48l** and **48m**, the remaining analogues were tested without further purification after work-up.

Compounds **48b**, **48g**, **48h**, **48l** and **48m** were purified by column chromatography or preparative layer chromatography using solvent mixtures of either ethyl acetate and hexane or dichloromethane and methanol.

HPLC analysis confirmed the purity of all analogues (98% or above) for pharmacological testing.

2.3. Pharmacology results

To assess the activity of the analogues synthesised, at PPAR α and the cannabinoid receptors, several assays were employed.

2.3.1. Activity at the Cannabinoid Receptors

Both affinity and efficacy at the cannabinoid receptors were determined in radioligand binding assays. Binding affinity at CB₁ receptors was measured by competitive displacement of ³H-CP55940 from whole rat brain homogenate. Meanwhile, binding at CB₂ receptors was performed using CHO-K1 (Chinese Hamster Ovary) cells stably expressing the human-form of CB₂ receptor. In the absence of a cell line stably expressing the human-form of the CB₁ receptor, tissue containing rat CB₁ receptors can provide a good approximation of activity at human receptors as they have 81% sequence identity⁶¹.

³H-CP55940 has approximately the same affinity for both the cannabinoid receptors ($K_i = 0.58 \pm 0.07$ nM at CB₁R and 0.69 ± 0.02 nM). It is therefore important to use tissue or cells containing only the receptor to be investigated to avoid competitive binding to more than one target.

The compounds were initially screened at a concentration of 10 μ M and the level of binding that a compound displayed is expressed as the percentage of specific binding of the compound at the receptor (specific binding is calculated

by subtracting non-specific binding from total binding). Ligands that displayed a high level of binding were then assayed at six further concentrations, ranging from 10 μ M to 30 nM or 1 μ M to 1 nM, to generate full dose-response curves. From these curves, in combination with the Cheng-Prusoff equation (**Figure 2-1**), the IC_{50} and K_i values were calculated. The IC_{50} is defined as the concentration of a ligand that inhibits the binding of the radioligand by 50 % and is experiment specific. The K_i converts the IC_{50} into a value by which different experiments can be compared as the concentration of radioligand is taken into consideration¹¹⁶.

$$K_i = \frac{IC_{50}}{1 + \frac{[L]}{K_d}}$$

Figure 2-1- Cheng-Prusoff equation

Where IC_{50} is the experimentally determined inhibition constant, $[L]$ is the concentration of radioligand and K_d is the dissociation constant of the radioligand.

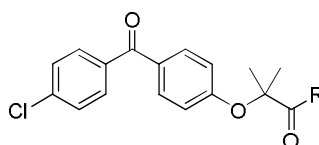
The level of activation of the cannabinoid receptors was measured in a 35 S-GTP γ S binding assay⁵⁸, also using whole rat brain homogenate, or CHO-K1 cells stably expressing human CB₂ receptors. The assay uses a non-hydrolysable radiolabelled analogue of GTP (35 S-GTP γ S) which binds to the G $_{\alpha}$ subunits on receptor activation. As hydrolysis is prevented, the heterotrimer cannot reform, and the G $_{\alpha}$ subunits accumulate. This allows the degree of activation to be calculated. As the assay measures directly the level of activation at the earliest receptor mediated event, which is not subjected to signal amplification, it is a true functional assay and can be used to determine the degree of agonism and efficacy.

At a single concentration of 10 μ M, agonists will increase the nucleotide binding above basal levels, and therefore display percentage activation above 100%. Inverse agonists will decrease nucleotide binding below basal levels and therefore give a percentage below 100%. Finally, neutral antagonists, that do not affect nucleotide binding, display a percentage activation of 100%.

EC₅₀ values were calculated for compounds which displayed a high affinity combined with agonist activity, by measuring the level of receptor activation at six serial concentrations from 10 μ M to 30 nM.

As both of the radioligand binding and activation assays are able to generate a large amount of data, using small quantities of tissue within a short timeframe, they are both suited to high through-put screening.

The affinity and efficacy at both cannabinoid receptors for the first series of analogues is illustrated in **Tables 2-1** and **2-2**.



No.	R	% Specific binding at CB ₁ (1x10 ⁻⁵ M)	K _i (nM)	% Activation at CB ₁ (1x10 ⁻⁵ M)	EC ₅₀ (nM)
48a		*	*	112±7	*
48b		74±1	*	110±29	*
48c		72±1	*	125±8	*
48d		69±2	*	105±19	*
48e		93±2	*	87±13	*
48f		94±4	*	113±11	*
48g		96±4	102±30	137±6	93±2
48h		92±3	150±67	149±7	225±89
48i		81±4	*	101±20	*
48j		80±9	*	123±15	*
48k		81±9	*	108±9	*
48l		57±8	*	94±10	*
48m		67±7	*	101±8	*
48n		88±3	*	87±8	*

Table 2-1 Results from binding and functional assays at the CB₁ receptor for compounds **48a** to **48n**. Binding at the CB₁ receptor was calculated by measuring the displacement of ³H-CP55940 from whole rat brain homogenate. K_i values were determined from binding IC₅₀ values, based on the Cheng-Prusoff equation in which the K_d of ³H-CP55940 is 0.5nM and the concentration of ³H-CP55940 is 0.25nM. Efficacy of compounds **48a** to **n** at the CB₁ receptor was calculated by measuring stimulation of [³⁵S]-GTPγS binding in rat whole brain homogenate. * Not assayed. Results are expressed as the percentage of stimulation of [³⁵S]-GTPγS binding. Basal level of activation is 100%. Data are the mean ± SD mean of three experiments performed in triplicate.

Apart from **48d**, **48l**, and **48m**, the level of binding at the CB₁ receptor of the remaining compounds was high, with percentage values 72% or above.

The hexyl (**48e**), benzyl (**48f**), piperidinyl (**48g**) and morpholino (**48h**) derivatives had the highest level of binding at the CB₁ receptor, with specific binding above 90% at a single concentration of 10 μ M, indicating that an alkyl chain or large substituent may favour CB₁ receptor binding. The piperidinyl (**48g**) and morpholino (**48h**) derivatives also had the highest CB₁ receptor activations of 137 ± 6 nM and 149 ± 7 nM respectively.

Due to time constraints, only compounds with the highest affinities, and agonist activity at 10 μ M were selected for further pharmacological assessment. As **48g** and **48h** showed a high affinity and agonist activity, CB₁ binding and affinity were measured at a series of six concentrations to generate dose-response curves. This allowed determination of K_i and EC₅₀ values. **48g** and **48h** had high nanomolar affinity for the CB₁ receptor with K_i values of 150 ± 67 nM and 102 ± 30 nM respectively. The error in the K_i value for **48g** is quite high as although all the individual K_i values fell within the normal distribution one K_i value was higher than the other two. This compound would need to be re-tested to improve the accuracy of the overall K_i value.

In comparison to fenofibrate (**10a**) (K_i = 460 nM), **48g** and **48h** had a lower affinity for the CB₁ receptor.

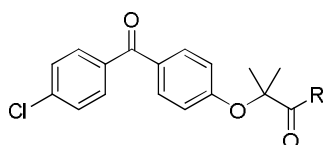
48g (EC₅₀ = 93 ± 2 nM) and **48h** (EC₅₀ = 225 ± 89 nM) are both agonists at the CB₁ receptor and activated it to 37% and 49% above basal levels of activation respectively. In comparison, Fenofibrate acts as a very weak partial agonist and is effectively a functional antagonist.

There is again a high error in the EC₅₀ value for **48h** so this compound would need to be retested in the CB₁ activation assay to confirm the EC₅₀ value.

Interestingly, when an ethylene linker was introduced between the amide and the morpholine moiety, affinity for the CB₁ receptor decreased, as did agonist activity.

The remaining analogues tested, that bound to the CB₁ receptor, were antagonists (retain basal levels of activation), or were partial agonists that did not activate the receptor to maximal levels.

When comparing the 1-hydroxyhexyl and *n*-hexyl derivatives, it appears that a terminal hydroxyl group reduced the level of binding, but resulted in agonist activity. This could indicate that a hydrogen bond acceptor or donor may be important for agonist activation of the CB₁ receptor.



No.	R	% Specific binding at CB ₂ R (1x10 ⁻⁵ M)	K _i (nM)	% Activation at CB ₂ R (1x10 ⁻⁵ M)	EC ₅₀ (μM)
48a		-	>10,000	93±9	*
48b		-	378	144±14	*
48c		-	629	113±6	*
48d		-	440	121±3	*
48e		-	1200	84±2	*
48f		99±4	219±10 ^{***}	84±23	*
48g		98±4 ^{***}	15±4	152±10	*
48h		100±0	16±2	153±2	*
48i		60±2 ^{***}	*	89±15	*
48j		87±7	*	87±8	*
48k		88±1	*	69±10	*
48l		83±4 ^{***}	*	78±10	*
48m		99±1	*	73±7	*
48n		100±0	146±64	104±3	*

Table 2-2 Results from binding and functional assays at the CB₂ receptor for compounds **48a** to **48n**. Binding at the CB₂ receptor was calculated by measuring the displacement of ³H-CP55940 from CHO-K1 cells expressing hCB₂. K_i values were determined from binding IC₅₀ values, based on the Cheng-Prusoff equation in which the K_d of ³H-CP55940 is 0.5 and the concentration of ³H-CP55940 is 0.25nM. Efficacy of compounds 48a to n at the CB₁ receptor was calculated by measuring stimulation of [³⁵S]-GTPγS binding in CHO-K1 cells expressing hCB₂. * Not assayed. Results are expressed as the percentage of stimulation of [³⁵S]-GTPγS binding. Basal level of activation is 100%. Data are the mean ± SD mean of three experiments performed in triplicate. *** n=2. K_i values for **48a** to **48e** were determined by Professor David Kendall.

All of the compounds tested had a high level of binding at the CB₂ receptor, at 10 μM, except for **48i** and **48c**.

The aminoalkyl and aminoalcohol derivatives had higher K_i values for the CB₂ receptor than fenofibrate (K_i = 108 nM); however, as for the CB₁ receptor, **48g** and **48h** both had lower K_i values than fenofibrate at the CB₂ receptor. These two compounds also had agonist activity, with activations 52% and 53% above basal levels at a single concentration of 10 μM respectively. Compounds **48k**, **48l**, **48m**, **48e**, **48f** and **48j** had inverse agonist activity as they had percentage activations that are below basal levels of activation.

As for the CB₁ receptor, introduction of an ethyl linker between the amide and morpholine resulted in a decrease in affinity and agonist activity.

2.3.2. Activity of the analogues at PPARα

After compounds **48a** to **48n** were assessed for activity at the cannabinoid receptors, they were tested in luciferase reporter gene assay and a Time Resolved Fluorescence Energy Transfer (TR-FRET) assay. This was to determine whether PPAR α activity had been retained.

2.3.2.1. PPAR Reporter Gene Assay

The PPARα reporter gene assay employed in this study measures how a ligand affects regulation of the luciferase gene. Cos-7 cells were transfected with two different plasmids, one containing the gene for expression of PPARα, and the other containing a reporter gene for the expression of luciferase. The reporter gene plasmid contains PPARα binding sites that are linked to a promoter which controls luciferase expression.

If a ligand activates PPAR α then the expression of the luciferase gene will increase. The level of activation can be measured by addition of luciferin to the assay. Any luciferase that has been produced will oxidise the luciferin to oxyluciferin, causing measurable light emission.

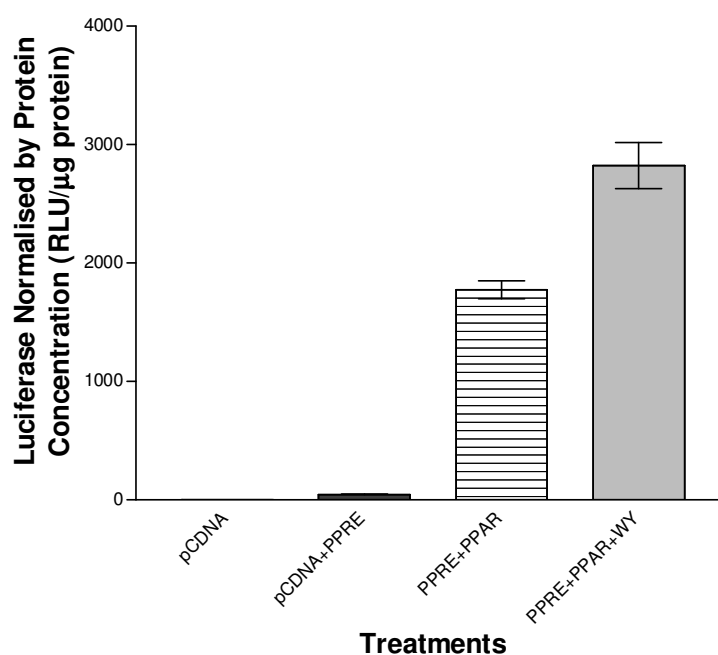


Figure 2-1 Control experiment to establish basal level of luciferase expression and also the level of stimulation by a PPAR α agonist.

COS-7 cells were transiently co-transfected with PPAR α and PPRE reporter gene plasmids. The cells were then exposed to either ligand or no ligand at 10 μ M overnight and the luciferase expression was then measured using luminometry. Data are means \pm SE mean of one experiment carried out in triplicate. WY=WY14643, a PPAR α agonist.

A control experiment was carried out to show the basal level of PPAR α activation, and also to ensure that when PPAR α is stimulated with an agonist, the activation can be observed above basal levels (**Figure 2-1**). The compound used to activate PPAR α was WY14643 (**13**), a high affinity selective PPAR α agonist, which caused a 1.6 fold increase in receptor activation.

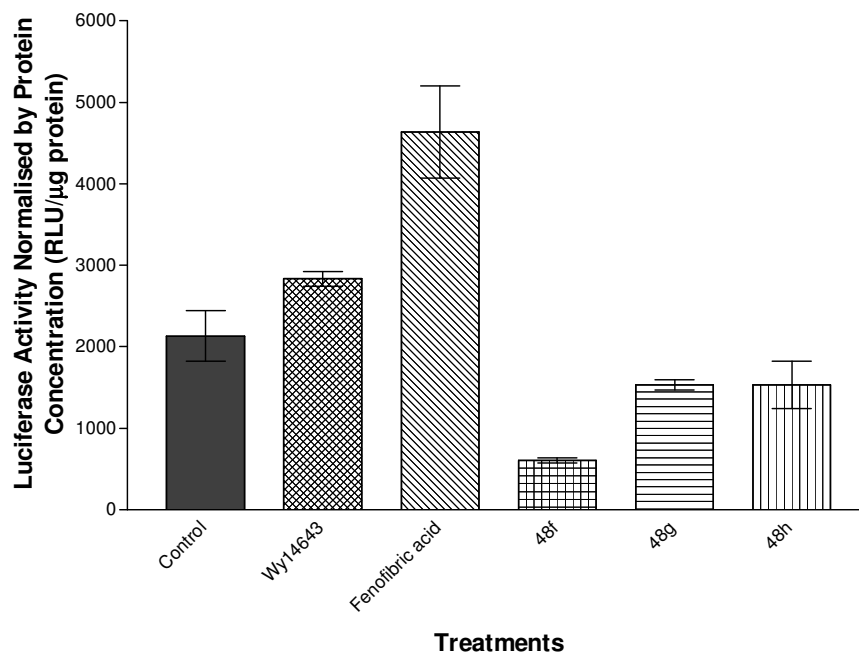


Figure 2-2 - Effects of selected ligands on PPAR α transcriptional activity.

COS-7 cells were transiently co-transfected with PPAR α and PPRE reporter gene plasmids. The cells were then exposed to either ligand or no ligand at 10 μ M overnight and the luciferase expression was then measured using luminometry. Data are means \pm SE mean of one experiment carried out in quadruplicate.

In addition to WY14643, (**13**), fenofibric acid (**10b**) was used as a positive control when testing the fenofibrate analogues, and induced a 2 fold increase, in receptor activation, over basal levels.

Compounds **48g**, **48h**, **48j** and **48l** had no affect on PPAR α activation. A binding assay was conducted to determine whether the lack of activation is due to the compounds binding and having no activity or whether they have no affinity for PPAR α . **48k** and **48m** and **48f** appeared to inhibit luciferase expression, however from this assay alone it is not evident whether this occurs by PPAR α inhibition or not.

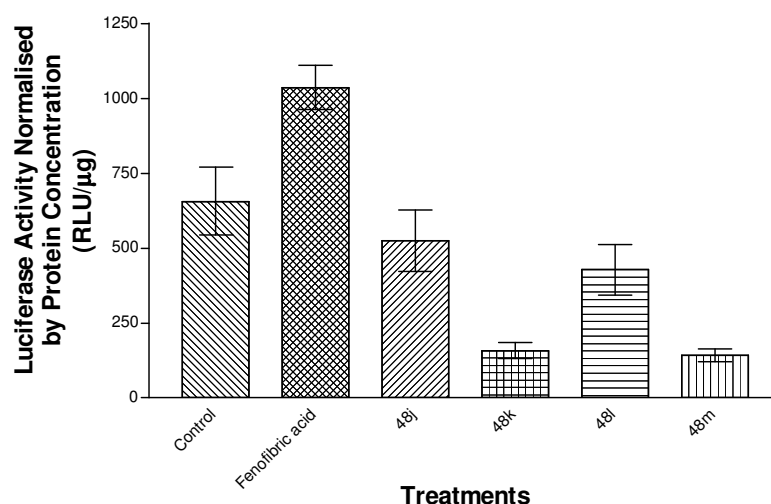


Figure 2-3 - Effects of selected ligands on PPAR α transcriptional activity.

COS-7 cells were transiently co-transfected with PPAR α and PPRE reporter gene plasmids. The cells were then exposed to either ligand or no ligand at 10 μ M overnight and the luciferase expression was then measured using luminometry. Data are means \pm SE mean of one experiment carried out in triplicate. Data are means \pm S E mean of one experiment carried out in quadruplicate.

2.3.2.2. TR-FRET Assay

As the results from the reporter gene assay are downstream of the ligand binding event, the experiment did not indicate whether compounds **48a** to **48n** were binding to PPAR α or exerting their effect in an alternative way in the signalling cascade. Therefore, whilst the functional assay provided some information about our novel compounds, a ligand binding experiment was undertaken.

The assay used was a commercially available competitive binding assay kit which uses a human PPAR α LBD, tagged with glutathione S-transferase (GST), a terbium-labelled anti-GST antibody, and a fluorescent ligand.

When the fluorescent ligand binds there is energy transfer from the Terbium to the ligand and a high FRET ratio is observed. If the fluorescent ligand is displaced by a competing compound then the FRET signal is lost.

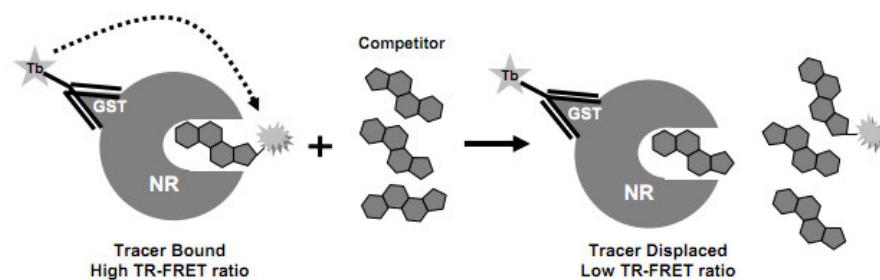


Figure 2-4 - Schematic of the TR-FRET assay

Image from Invitrogen Lanthascreen® Terbium Instrument Control Application Note

By plotting the TR-FRET ratio versus a series of test compound concentrations, and in conjunction with the Cheng-Prusoff equation, the K_i can be calculated.

GW7647 (**15**), a PPAR α selective agonist, and fenofibric acid (**10b**) were used as positive controls in the assay. They displayed affinities of 1.67 nM and 1.16 μ M respectively.

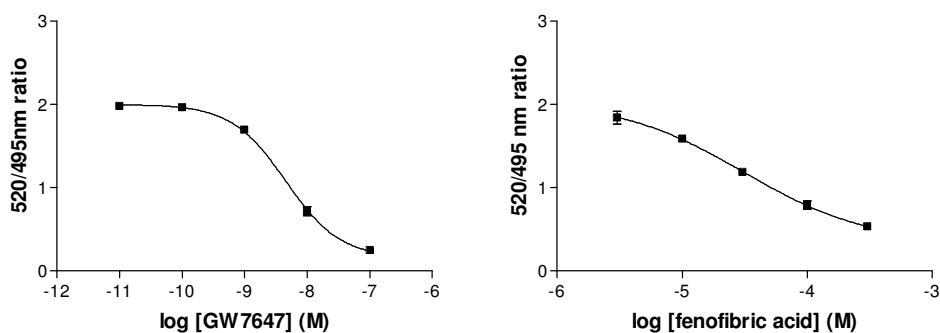


Figure 2-5 - Dose response curves for the positive controls fenofibric acid (**10b**) and GW7647.

K_i values were determined from binding IC_{50} values, based on the Cheng-Prusoff equation in which the K_d of Fluormone Pan-PPAR Green is 12nM and the concentration of Fluormone Pan-PPAR Green is 20nM. Data are means \pm SE mean of one experiment carried out in duplicate and were analysed using Graphpad prism 3.

Of the 14 compounds tested (**48a** to **48n**) none displayed any measurable affinity for PPAR α . Example graphs are shown below in **Figure 2-6**.

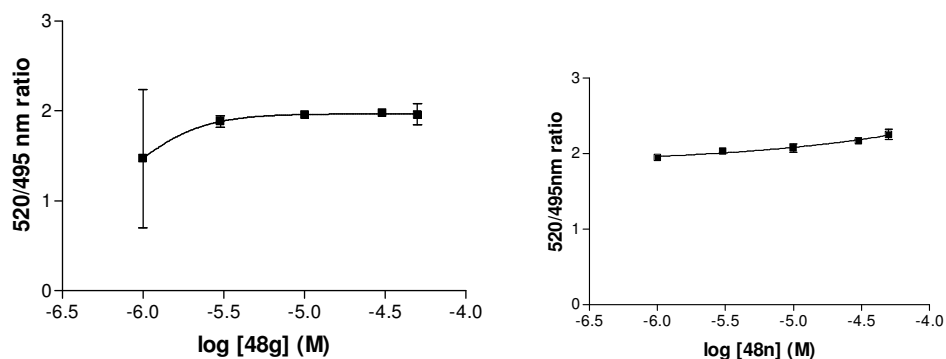


Figure 2-6 - Example dose-response curves from TR-FRET PPAR α competitive binding assay. Data are means \pm SE mean of one experiment carried out in duplicate and were analysed using Graphpad prism 3.

2.4. Conclusions

All the compounds described in this chapter have affinity at one or both of the cannabinoid receptors. However, none of these compounds displayed affinity for PPAR α . The lack of binding to PPAR α for analogues **48a** to **48n** could be due to the loss of the carboxylic head group of fenofibric acid (**10b**) which is known to interact with residues in the ligand binding domain¹⁹. However, this functional group is not critical since anandamide ((**19**), which also contains amide functionality) has been shown to possess agonist activity at PPAR α . It was therefore disappointing that analogue **48a** did not exhibit any activity at PPAR α . However, the structural differences between anandamide (**19**) and fenofibric acid (**10b**) could mean that the two compounds display very different binding poses, or even bind at different locations on the receptor. Computer modelling, in combination with x-ray crystal structures of anandamide (**19**) and fenofibric acid (**10b**) in complex with PPAR α , could provide an insight into how both these ligands bind to and activate PPAR α . Although the compounds described in this chapter failed to bind to PPAR α , they do show promise as cannabinoid receptor ligands at both CB₁ and CB₂.

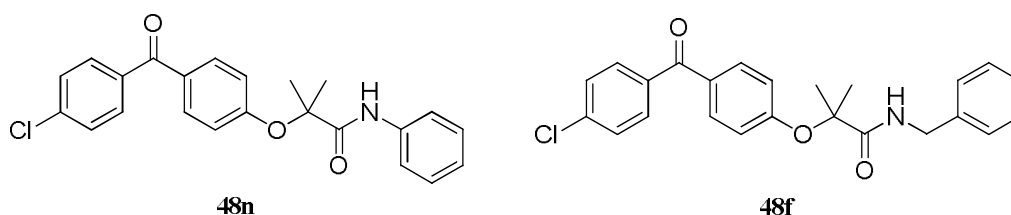
At both of the cannabinoid receptors, the piperidinyl (**48g**) and morpholino (**48h**) analogues have the highest affinity and agonist activity. Compounds **48g** and **48h** have micromolar affinity for the CB₁ receptor (102 ± 30 nM (**48g**) and 150 ± 67 nM (**48h**)) and low micromolar EC₅₀ values (0.92 ± 0.02 μ M (**48g**) and 2.25 ± 0.88 μ M (**48h**)). At the CB₂ receptor they have nanomolar K_i values (15 ± 4 nM (**48g**) and 16 ± 2 nM (**48h**)). Although compounds **48g** and **48h** have shown agonist activity at 10 μ M, EC₅₀ values for the CB₂ receptor still remain to be determined.

Due to the lack of binding of **48a** to **48n** at PPAR α , it was decided to focus on improving affinity for the cannabinoid receptors. The compounds selected for development were the benzyl (**48f**), phenyl (**48n**), piperidinyl (**48g**) and morpholino (**48h**) derivatives. The benzyl (**48f**) and phenyl (**48n**) derivatives were selected as they bind well to the CB₂ receptor, and the benzyl and phenyl groups are also easily substituted. The piperidine (**48g**) and morpholine (**48h**) derivatives were selected, as they have the highest affinities for both the cannabinoid receptors, as well as the highest agonist activities.

The synthesis and pharmacological activity of derivatives of these four lead structures is described in the following two chapters.

3. Substituted benzyl and phenyl derivatives

As described in **Chapter 2** benzyl (**48f**) and phenyl (**48n**) analogues of fenofibric acid (**10b**) were selected for further development. The following chapter describes the synthesis and pharmacology of these substituted compounds.



3.1. Synthesis of derivatives

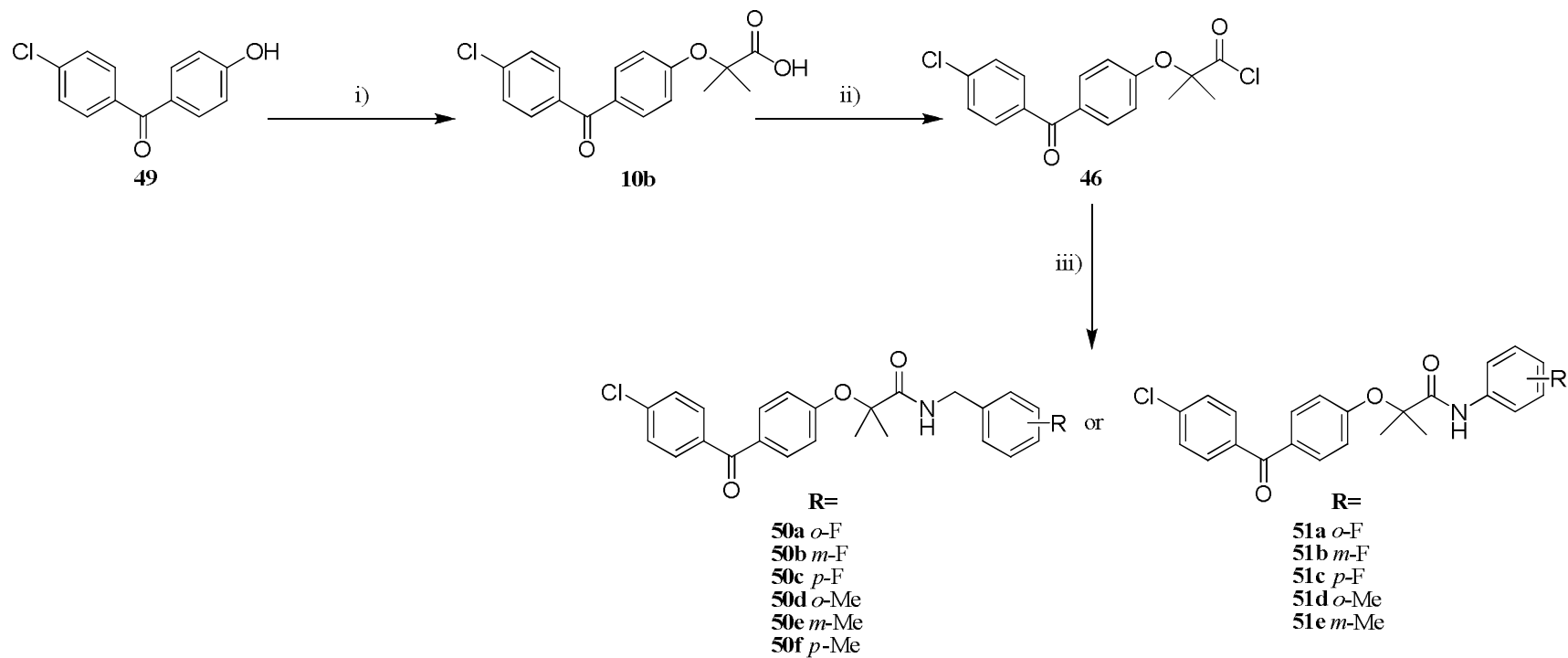
Taking **48f** and **48n** as lead compounds, *N*-benzyl and *N*-phenyl analogues were synthesised, to investigate steric, positional, and electronic effects of substitution. The analogues comprised of *ortho*-, *meta*-, and *para*- fluoro and methyl substituted benzylamines and anilines. A fluoro substituent was selected as it is small, with a similar size to hydrogen, but allows the investigation of electronic effects of substitution and also hydrogen bonding as it is a hydrogen bond acceptor. A methyl substituent was also selected to investigate how a bulky, electron donating substituent affects cannabinoid receptor binding and activation.

3.1.1. Synthetic route

The synthetic route employed, required 2-[4-(4'-chlorobenzoyl)-2-methyl propanoic acid (fenofibric acid (**10b**)) (**Scheme 1**) as a starting material. This was synthesised using a method developed at GlaxoSmithKline by Fitzgerald

*et al.*¹¹⁷, where 4-chloro-4'-hydroxybenzophenone was alkylated with α -bromoisobutyric acid. The yield afforded from this reaction was 68% after purification.

The fenofibric acid (**10b**) was converted to the acid chloride (**46**) by heating in thionyl chloride. Acid chloride (**46**) was then condensed with selected commercially available amines, in the presence of triethylamine to afford the corresponding amides. The formation of the analogues proceeded with reaction times of 1 hour (analogues **51a** to **51d**) or overnight (analogues **50a** to **50f** and **51e**) and with yields between 26% and 59%. All of the analogues were purified by preparative layer chromatography (PLC) and characterised using NMR, FT-IR and HRMS. The purity of all analogues was confirmed by HPLC at 98% or above.



Scheme 3-1 - Synthesis of compounds **50a to **51c****

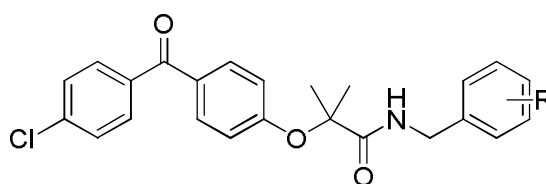
Reagents and conditions: i) α -bromoisobutyric acid, NaOH, butan-2-one, 60°C, 68% ii) Thionyl chloride, 60°C, 1hr. iii) Selected amine, anhydrous dichloromethane, 0°C to room temperature, 1 hr or overnight, yields 26% - 59%.

3.2. Pharmacology

3.2.1. Activity at the cannabinoid receptors

The affinity and efficacy of the analogues at the cannabinoid receptors, was assessed using the ^3H -CP55940 and ^{35}S -GTP γ S radioligand binding assays, with whole rat brain homogenate and CHO cells expressing CB₂ receptors.

3.2.1.1. Substituted benzyl derivatives



No	R	% Specific binding at CB ₁ (1x10 ⁻⁵ M)	% Activation at CB ₁ (1x10 ⁻⁵ M)
48f	H	94±4	104±18
50a	<i>o</i> -F	89±10	83±21
50b	<i>m</i> -F	96±5	87±11
50c	<i>p</i> -F	89±7	100±17
50d	<i>o</i> -Me	79±5	61±18
50e	<i>m</i> -Me	55±3	85±14
50f	<i>p</i> -Me	59±12	76±15

Table 3-1 - Affinity and efficacy of the unsubstituted and substituted benzyl analogues at CB₁R

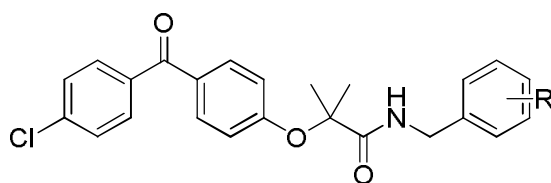
Binding and affinity were evaluated using whole rat brain homogenate, and ^3H -CP55940 or [^{35}S]-GTP γ S. K_i values were determined from binding IC_{50} values, based on the Cheng-Prussoff equation in which the K_d of ^3H -CP55940 is 0.5nM and the concentration of ^3H -CP55940 is 0.25nM. Results are expressed as the percentage of stimulation of binding. Basal level of activation is 100%. Data are the mean \pm SD mean of three experiments performed in triplicate ($n=3$) and were analysed using Graphpad prism 3.

Compounds **50a** to **50c** with a fluoro substituent, at either the *ortho*, *meta* or *para* position, have a high a level of binding at the CB₁ receptor; however compounds with a methyl substituent have a lower level of binding. This could

indicate that smaller substituents are preferred for binding, or that electron withdrawing substituents are preferred over electron donating substituents. More analogues, with various electron donating and withdrawing substituents of differing sizes, would need to be synthesised to establish whether the size or electronic property of a substituent has the greater effect.

Between the positions of the substituents there is not a large difference in the level of binding at the CB₁ receptor, apart from the *ortho*-methyl analogue, which has a higher level of binding than the *meta*- or *para*- analogues.

The unsubstituted and the 4-fluoro substituted analogues are antagonists at CB₁; whereas the other fluoro and methyl substituted analogues appear to have a degree of inverse agonist activity. The analogues with activations around 85% could probably be considered as antagonists as the level of activation probably returns to basal levels (100%) very quickly as the concentration of ligand is decreased.



No	R	% Specific binding at CB ₂ (1x10 ⁻⁵ M)	K _i (nM)	% Activation at CB ₂ (1x10 ⁻⁵ M)
48f	H	99±2	2190±1010	84±23
50a	<i>o</i> -F	99±3	583±170	75±6
50b	<i>m</i> -F	94±10	428±89	69±10
50c	<i>p</i> -F	100±0	242±32	80±2
50d	<i>o</i> -Me	99±2	1140±110	68±9
50e	<i>m</i> -Me	90*	2340±689	39±5
50f	<i>p</i> -Me	93±12	1320±482	40±2

Table 3-2 - Affinity and efficacy of the unsubstituted and substituted benzyl analogues at the CB₂R

*Binding and affinity were evaluated using CHO cells expressing CB₂ receptors and ³H-CP55940 or [³⁵S]-GTPγS. K_i values were determined from binding IC₅₀ values, based on the Cheng-Prussoff equation in which the K_d of ³H-CP55940 is 0.5nM and the concentration of ³H-CP55940 is 0.25nM. * n=1. Results are expressed as the percentage of stimulation of [³⁵S]-GTPγS binding. Basal level of activation is 100%. Data are the mean ± SD mean of three experiments performed in triplicate (n=3) and were analysed using Graphpad prism 3.*

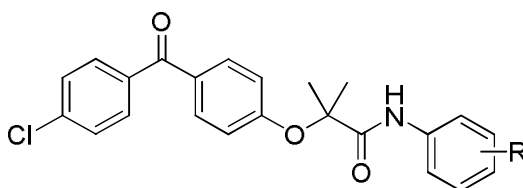
All of the substituted benzylamine analogues have a high level of specific binding at the CB₂ receptor (90-100%), at 1x10⁻⁵ M. This is in contrast to the affinities at the CB₁ receptor where the methyl substituted analogues have lower affinities than the unsubstituted and fluoro substituted compounds.

On comparing the K_i values for the benzylamine analogues, there is an increase in affinity for the CB₂ receptor, when the substituent is fluorine and no improvement when the substituent is a methyl group. Additionally the unsubstituted analogue (**48f**) has a lower affinity for the CB₂ receptor than the fluorine analogues. Taking this into account, the electronic properties of the substituent may be more important for CB₂ receptor affinity than the size of the substituent. The position of the substituent may also influence affinity at the

CB₂ receptor, as there is a slight increase in affinity in the order *para* > *meta* > *ortho*, for the fluorine substituted analogues. For the methyl substituted analogues, there is little difference in the K_i values when the position of the methyl group on the ring is changed. This indicates that the position of the substituent probably has little effect.

In the ³⁵S-GTPγS assay, all the analogues tested displayed inverse agonism. The *meta*- and *para*- methyl substituents exhibit a high level of binding and good inverse agonism, in comparison to the other analogues, which may indicate that this area of the compound may be important for CB₂ receptor activity.

3.2.1.2. Substituted phenyl compounds

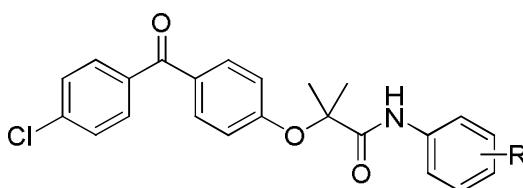


No	R	% Specific binding at CB ₁ (1x10 ⁻⁵ M)	% Activation at CB ₁ (1x10 ⁻⁵ M)
48n	H	88±3	87±8
51a	<i>o</i> -F	82±1	69±16
51b	<i>m</i> -F	71±8	111±11
51c	<i>p</i> -F	76±19	91±2
51d	<i>o</i> -Me	42±25	100±8
51e	<i>m</i> -Me	59±5	114±8

Table 3-3 Affinity and efficacy of the unsubstituted and substituted phenyl analogues at the CB₁R

Binding and affinity were evaluated using whole rat brain homogenate and ³H-CP55940 or [³⁵S]-GTPγS K_i values were determined from binding IC₅₀ values, based on the Cheng-Prusoff equation in which the K_d of ³H-CP55940 is 0.5nM and the concentration of ³H-CP55940 is 0.25nM. Results are expressed as the percentage of stimulation of [³⁵S]-GTPγS binding. Basal level of activation is 100%. Data are the mean ± SD mean of three experiments performed in triplicate (n=3) and were analysed using Graphpad prism 3.

All of the substituted phenyl analogues have a high level of specific binding at the at CB₁ receptor, apart from *ortho* and *meta*-methyl substituted compounds. They also display antagonist activity, except **51a**; which has inverse agonist activity and **51d** and **51e**; which considering their low affinity for the CB₁ receptor, probably have little effect. Further testing is needed to confirm the inverse agonist activity of **51a**.



No	R	% Specific binding at CB ₂ (1x10 ⁻⁵ M)	K _i (nM)	% Activation at CB ₂ (1x10 ⁻⁵ M)
48n	H	99±2	395±191	86±17
51a	<i>o</i> -F	99±3	1160±566	90±4
51b	<i>m</i> -F	100±0	3340±80	97±10
51c	<i>p</i> -F	96±4	1350±485	89±6
51d	<i>o</i> -Me	95±16	1560±113	89±15
51e	<i>m</i> -Me	97±5	762±294	87±4

Table 3-4 - Affinity and efficacy of the unsubstituted and substituted phenyl analogues at the CB₂R

Binding and affinity were evaluated using CHO cells expressing CB₂ receptors and ³H-CP55940 or [³⁵S]-GTPγS K_i values were determined from binding IC₅₀ values, based on the Cheng-Prussoff equation in which the K_d of ³H-CP55940 is 0.5nM and the concentration of ³H-CP55940 is 0.25nM. Results are expressed as the percentage of stimulation of [³⁵S]-GTPγS binding. Basal level of activation is 100%. Data are the mean ± SD mean of three experiments performed in triplicate (n=3) and were analysed using Graphpad prism 3.

All of the compounds tested display a high specific binding at the CB₂ receptor, with binding above 95% for all compounds. The analogues had K_i values in the micromolar range and they all had antagonist activity. When comparing the substituted phenyl compounds with the unsubstituted phenyl analogue there is an obvious reduction in affinity at the CB₂ receptor.

3.2.2. Activity at PPAR α

The compounds were screened for activity at PPAR α using the TR-FRET assay previously described in **Chapter 2**.

As for the compounds described in **Chapter 2**, the substituted benzylamine analogues had no activity at PPAR α . The substituted phenyl analogues also do not display activity at PPAR α .

3.3. Conclusions

Early exploration, of the effects of substitution at the phenyl and benzylamine moieties, has been described in this chapter. The analogues were assessed in three different assays to determine their affinity for PPAR α and both their affinity and efficacy at the cannabinoid receptors.

The phenyl analogues (**51a** to **51e**) were found to be antagonists, or inverse agonists, at the CB₁ receptor, and antagonists at the CB₂ receptor. Meanwhile, the benzylamine (**50a** to **50f**) analogues displayed antagonist or inverse agonist activity at CB₁, and inverse agonist activity at CB₂. Again, both phenyl and benzyl analogues display no activity at PPAR α .

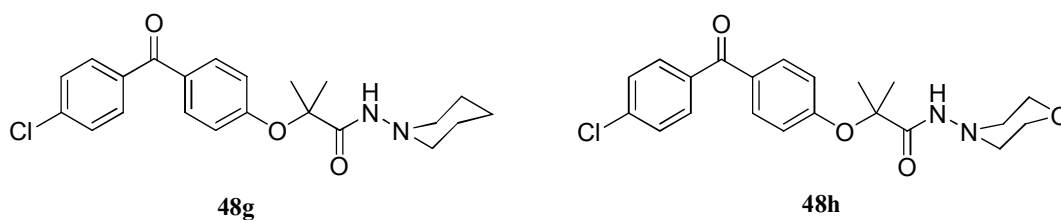
At the CB₁ receptor, when comparing corresponding benzyl and phenyl analogues, the methyl substituted phenyl (**50a** to **50c**) and benzyl analogues (**51d** and **51e**) all have a low level of specific binding at the CB₁ receptor, indicating that the benzylic CH₂ has little effect on binding of these analogues at 10 μ M. However for the unsubstituted (**48f** and **48n**) and fluoro-substituted (**50a** to **50c** and **51a** to **51c**) analogues, the benzyl derivatives appear to have a slightly higher level of binding. When compared directly to their corresponding phenyl derivatives, the benzylic methylene was shown to have a positive influence on the affinity of fluoro substituted benzyl analogues at the

CB₂ receptor. Conversely it has a negative effect on the unsubstituted benzyl derivative (**48f**). When comparing the effect of the benzylic methylene on CB₂ receptor activation, it was observed that the benzyl (**51a** to **51e**) analogues are inverse agonists whereas the phenyl (**50a** to **50f**) derivatives are antagonists. This effect on activation of the receptor could be due to the shift in position of the substituent in the receptor binding site, or perhaps the ability of the benzyl derivatives to form a greater number of conformers, due to the extra rotatable bond.

Although there was little or no improvement in affinity or efficacy at the cannabinoid receptors, with the range of substituted *N*-phenyl or *N*-benzyl compounds synthesised so far, some structure activity relationships have been explored. These relationships indicate that the synthesis of a wider range of substituted benzyl or phenyl analogues may offer the opportunity to tune activity at the cannabinoid receptors.

4. *N*-Morpholino-2-(4-(4-chlorobenzoyl)-phenoxy)-2-methylpropanamide (48h) and *N*-piperidinyl-2-(4-(4-chlorobenzoyl)-phenoxy)-2-methylpropanamide (48g) derivatives

The morpholino (**48h**) and piperidinyl (**48g**) derivatives described in **Chapter 2** displayed a high affinity, in comparison to fenofibrate and analogues displayed in **Table 2-1** and **Table 2-2**, at both cannabinoid receptors. They also display a high level of CB₁ and CB₂ receptor activation indicating that both **48g** and **48h** are agonists at both receptors. They were therefore selected as lead compounds and a library of derivatives were synthesised.



4.1. Synthesis of derivatives

In an attempt to explore the steric, electronic and positional effects of substituents on the lead molecules (**48g** and **48h**), a library comprising of derivatives bearing various electron donating and withdrawing groups in the *ortho*-, *meta*-, or *para* positions on the left hand side of the pharmacophore were synthesised.

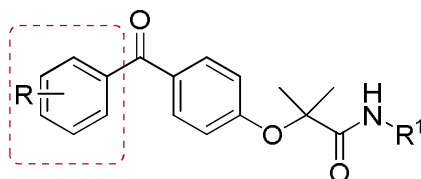


Figure 4-1- Basic benzophenone pharmacophore
(*R* = *o*-, *m*- or *p* CH₃, CN, NO₂, F or Cl, *R*¹ = 1-aminopiperidine or 4-aminomorpholine)

4.1.1. Synthetic route

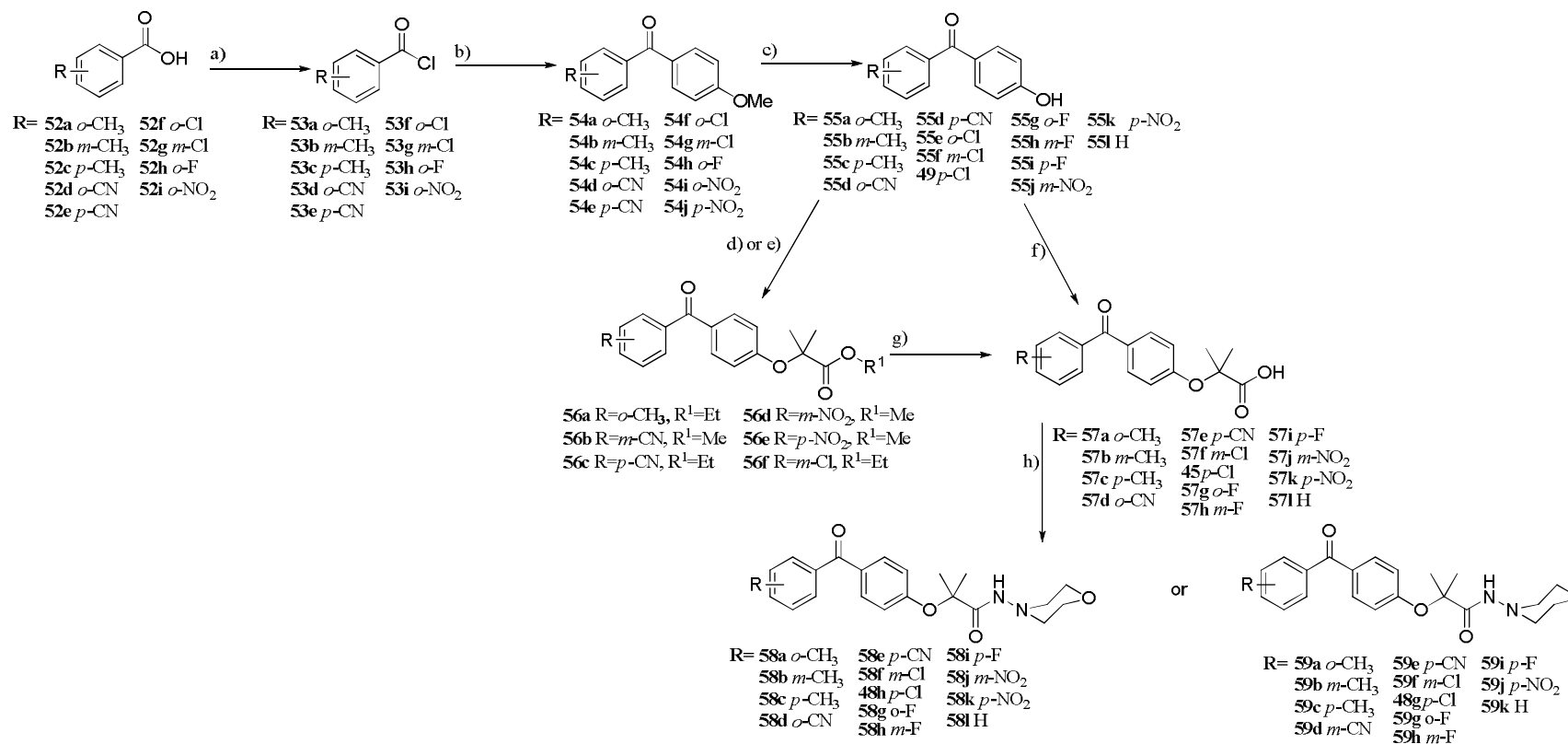
Since the majority of the substituted 4-hydroxybenzophenones were not commercially available, they required synthesis. The first step of the synthesis involved conversion of the substituted benzoic acids (**52a to 52i**) to their corresponding acid chlorides (**53a to 53i**). The acid chlorides (**53a to 53i**) were then condensed with anisole, under Friedel-Crafts conditions, in the presence of AlCl_3 , affording substituted 4-methoxybenzophenones (**54a to 54i**), (**Scheme 1**). As the methoxy group of anisole is *ortho/para* directing, a mixture of 2-methoxy and 4-methoxy isomers were obtained. Separation of these two products was achieved by column chromatography using a mixture of either TBME and PE 40-60 or EtOAc and PE 40-60, with yields ranging from 15% to 71% of the desired isomer.

The next step of the synthesis required *O*-demethylation of the aromatic methyl ether to relinquish the free phenol for subsequent alkylation. Established conditions (BBr_3 in DCM) proved unsuccessful, so a method developed by Kulkarni *et al*¹¹⁸ using pyridine hydrochloride with microwave heating, was attempted. This proved successful as the substituted 4-hydroxybenzophenones (**55a to 55i**) were prepared in yields between 8 and 99%.

For compound **55a** where R is an *ortho*-methyl group the *O*-demethylation occurred simultaneously during the Friedel-Crafts acylation with anisole. This may be due to the ability of aluminium chloride to coordinate to the methoxy group, which then allows removal of the *O*-methyl group by a chloride ion from the aluminium chloride. The aluminate ester formed is then broken down on aqueous work up.

Alkylation of these phenols was possible *via* either Williamson ether synthesis or Mitsunobu chemistry. The Williamson ether synthesis, described previously in **Chapter 3**, utilised butan-2-one as the solvent. The reaction mixture became difficult to stir when butan-2-one was used, in the synthesis of fenofibric acid (**10b**), so the solvent was changed to acetonitrile for the syntheses described in this chapter.

In situations where the Williamson ether synthesis proved unsuccessful I reverted to standard Mitsunobu chemistry (DIAD and triphenyl phosphine) to effect the required phenolic alkylation. Compounds synthesised in this manner were **56b**, **56d** and **56e** in yields of 51%, 42% and 64% respectively after purification by column chromatography. It could be argued that in the case of the compounds that failed to react under Williamson ether conditions, the electron withdrawing groups present within the molecules may have reduced the nucleophilicity of the respective phenolate anions. In the cases where alkylations were carried out with methyl-2-bromo-2-methylpropanoate (**56a**, **56c** and **56f**), the methyl esters obtained were subsequently saponified to their corresponding carboxylic acids, using lithium hydroxide in a mixture of THF and water in yields from 50% to 92%. They were deemed to be pure enough, by ^1H and ^{13}C NMR, to be used directly in the next step after work-up, and were therefore coupled to 1-aminopiperidine or 4-aminomorpholine using HBTU in the presence of triethylamine. This afforded the desired amides (**58a** to **58l** and **59a** to **59h**), which were purified by preparative layer chromatography (PLC) or column chromatography, in yields from 8% to 89%. The analogues were characterised using NMR, FT-IR and HRMS, and purity was confirmed by HPLC at 98% or above.



Scheme 4-1. Synthesis of analogues **58a** to **58l** and **59a** to **59j**

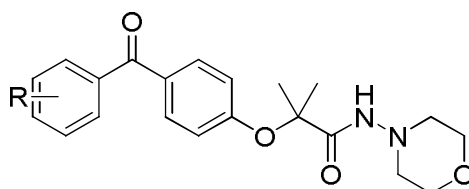
Reagents and conditions: a) SOCl₂, 60°C, N₂ 1 h, b) Anisole, DCM, AlCl₃, N₂, overnight, 15-71% c) Py.HCl, microwave irradiation, 215W, 2-20 mins, 8%-99% d) methyl-2-hydroxyisobutyrate, DIAD, triphenylphosphine, toluene, 80°C, 2 h, 42% -62% e) ethyl-2-bromo-2-methylpropanoate, K₂CO₃, MeCN, reflux, 43%-84% f) α-bromoisobutyric acid, MeCN, NaOH, 2.5 h, 11%-76% g) LiOH.H₂O, THF/water (1:1), N₂, 2 h, 50%-92% h) 4-aminomorpholine or 1-aminopiperidine, HBTU, dichloromethane, Et₃N, 2-18 h, 8%-89%.

4.1.2. Pharmacology

The affinity of compounds at the cannabinoid receptors was assessed by competitive displacement of ^3H -CP55940, from CHO cells expressing hCB₂ receptors, and whole rat brain homogenate. The efficacies of the analogues at both receptors were examined in the ^{35}S -GTP γ S radioligand binding assays, again utilising CHO cells expressing hCB₂ receptors, and whole rat brain homogenate. EC₅₀ values at the CB₂ receptor were not obtained as when a test assay was carried out there was no displacement of radioligand. When the problem was investigated further by PCR, no CB₂ receptor transcript was found. This indicated that the batch of cells had failed to express the CB₂ receptors.

4.1.2.1. *N*-Morpholino-2-(4-(4-chlorobenzoyl)phenoxy)-2-methylpropanamide (48h) derivatives

4.1.2.1.1. Affinity and efficacy at the CB₁ receptor



No.	R	% Specific binding at CB ₁ (1x10 ⁻⁵ M)	K _i (nM)	% Activation at CB ₁ (1x10 ⁻⁵ M)**	EC ₅₀ (μM)
58a	<i>o</i> -CH ₃	95±4	*	99±10	*
58b	<i>m</i> -CH ₃	94±2	*	99±7	*
58c	<i>p</i> -CH ₃	93±3	*	103±18	*
58d	<i>m</i> -CN	39±1	*	107±11	*
58e	<i>p</i> -CN	*	*	*	*
58f	<i>m</i> -Cl	94±1	*	101±6	*
48h	<i>p</i> -Cl	92±3	150±67	149±7	2.25±0.89
58g	<i>o</i> -F	92±4	92±14	130±19	1.24±0.97
58h	<i>m</i> -F	89±7	*	89±9	*
58i	<i>p</i> -F	89±12	*	89±7	*
58j	<i>m</i> -NO ₂	79±6	*	92±14	*
58k	<i>p</i> -NO ₂	*	*	*	*
58l	H	93±4	*	97±18	*

Table 4-1- Binding and efficacy of **58a** to **58l** at the CB₁ receptor

Binding and affinity were evaluated using whole rat brain homogenate, and ³H-CP55940 or [³⁵S]-GTPγS K_i values were determined from binding IC₅₀ values, based on the Cheng-Prussoff equation in which the K_d of ³H-CP55940 is 0.5 nM and the concentration of ³H-CP55940 is 0.25 nM. * Not assayed **Results are expressed as the percentage of stimulation of [³⁵S]-GTPγS binding. Basal level of activation is 100%. Data are the mean ± SD mean of three experiments performed in triplicate.

All of the analogues assayed displayed good levels of specific binding at the CB₁ receptor at a 10 μM concentration apart from the *meta*-cyano **58d** and

meta-nitro **58j** substituted analogues. This could indicate that electron withdrawing groups are unfavourable for CB₁ binding; however the *ortho*- and *para*- nitro and cyano derivatives would need to be assayed to confirm that it is an electronic rather than a positional effect.

The results from the ³⁵S-GTPγS binding assay demonstrated that two of the analogues (**48h** and **58g**) are agonists at the CB₁ receptor, with activations of 49 ± 7% and 30 ± 19% above basal levels. The rest of the analogues were neutral antagonists or displayed slight inverse agonist activity, as they showed high level of binding at the CB₁ receptor, but the level of receptor activation remains at basal levels (approximately 100%) or just below.

Since compounds **58g** and **48h** had a high affinity and a good efficacy, they were further tested at six serial concentrations, in both the binding and activation assays, to give full dose-response curves. This allowed the determination of K_i and EC₅₀ values. The K_i values were in the nanomolar range at 150 ± 67 nM and 92 ± 14 nM respectively, and the EC₅₀ values for both compounds were in the micromolar range at 2.25 ± 0.89 μM and 1.24 ± 0.97 μM respectively.

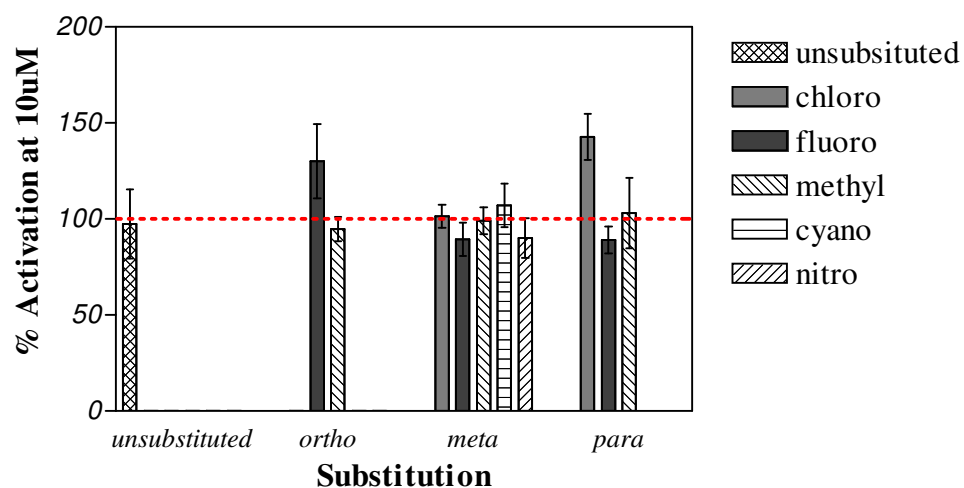
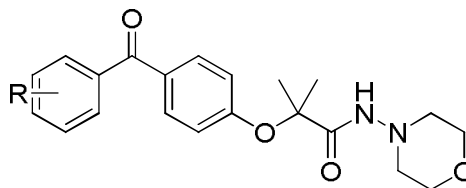


Figure 4-1 – Percentage activation of the CB₁ receptor by compounds **58a** to **58l**.

Results are expressed as the percentages of stimulation of [³⁵S]-GTPγS binding. Data are the mean ± SD mean of three experiments performed in triplicate. Dotted line indicates basal level of receptor activation.

4.1.2.1.2. Affinity and efficacy at the CB₂ receptor



No.	R	% Specific binding at CB ₂ (1x10 ⁻⁵ M)	K _i (nM)	% Activation at CB ₂ (1x10 ⁻⁵ M)
58a	<i>o</i> -CH ₃	92±3	56.8±16.8	148±24
58b	<i>m</i> -CH ₃	90±5	*	104±5
58c	<i>p</i> -CH ₃	96±6	310±16.5	160±9
58d	<i>m</i> -CN	42±10	*	98±1
58e	<i>p</i> -CN	*	*	*
58f	<i>m</i> -Cl	94±5	*	82±4
48h	<i>p</i> -Cl	100±0	12.8±3.5	153±2
58g	<i>o</i> -F	100±0	146±25.2	119±19
58h	<i>m</i> -F	89±6	*	116±5
58i	<i>p</i> -F	99±3	231±90.2	135±7
58j	<i>m</i> -NO ₂	80±5	*	106±14
58k	<i>p</i> -NO ₂	*	*	*
58l	H	96±9	299±3.5	137±8

Table 4-2 - Binding and efficacy of **58a** to **58l** at the CB₂ receptor

Binding and affinity were evaluated using CHO-K1 cells expressing hCB₂, and [³H]-CP55940 or [³⁵S]-GTPγS. K_i values were determined from binding IC₅₀ values, based on the Cheng-Prusoff equation in which the K_d of [³H]-CP55940 is 0.5 nM and the concentration of [³H]-CP55940 is 0.25nM. * Not assayed **Results are expressed as the percentage of stimulation of [³⁵S]-GTPγS binding. Basal level of activation is 100%. Data are the mean ± SD mean of three experiments performed in triplicate.

Analogous with the results at the CB₁ receptor, compounds **58l** to **58k** displayed a high level of specific binding at the CB₂ receptor at a 10 μM concentration, with the exception of the *meta*-nitro (**58j**) and *meta*-cyano (**58d**) substituted analogues, which display less than maximal binding at this concentration (42 ± 10% and 80 ± 5% respectively).

The *meta*- substituted analogues mostly demonstrated antagonist or slight inverse agonist activity at the CB₂ receptor. The exception was the *ortho*-fluoro-substituted analogue (**58g**), which possibly displayed partial agonist activity. Compound **58f**, which displayed inverse agonist activity at 10 μM, can possibly be considered as an antagonist, but further testing is needed to confirm this.

These results could indicate that steric, rather than electronic, factors play a role in activation of the CB₂ receptor, as the fluorine substituent is only slightly larger than hydrogen whereas the other substituents are considerably larger.

The *para*- substituted analogues all display agonist activity, with percentage activations between $35 \pm 7\%$ and $60 \pm 9\%$ above basal levels of receptor activation.

Compounds **58g** and **58a** with *ortho* substituents are possibly partial agonists, although they have large standard deviations, so further testing needs to be carried out to determine whether this is actually the case.

K_i values were determined only for compounds that have a high level of binding, combined with a good efficacy at the CB₂ receptor. All the analogues tested have a range of nanomolar K_i values. The *para*-chloro analogue has the highest affinity at 12.8 nM. The apparent agonist activity imparted by *para*-substituents and the deleterious effect of *meta* substitution may indicate that substituents in the *meta* position may interact unfavourably with residues in the binding pocket. As the results for the *ortho* substituted compounds are mixed, a larger range of *ortho* substituted compounds needs to be synthesised.

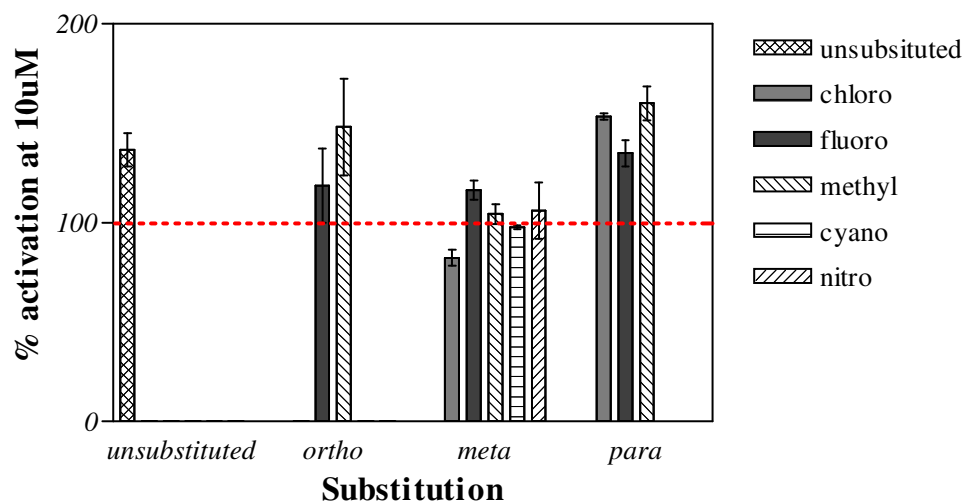
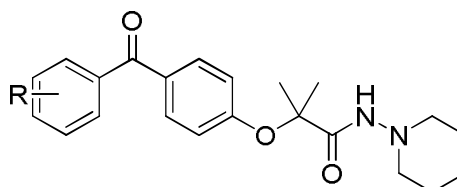


Figure 4-2 - Percentage activation of the CB₁ receptor by compounds **58a** to **58l**.

Results are expressed as the percentages of stimulation of [³⁵S]-GTPγS binding. Data are the mean ± SD mean of three experiments performed in triplicate. Dotted line indicates basal level of receptor activation.

4.1.2.2. 1-Piperidiny-2-(4-(4-chlorobenzoyl)phenoxy)-2-methylpropanamide (48g) derivatives

4.1.2.2.1. Affinity and efficacy at the CB₁ receptor



No.	R	% Specific binding at CB ₁ (1x10 ⁻⁵ M)	K _i (nM)	% Activation at CB ₁ (1x10 ⁻⁵ M)	EC ₅₀ (nM)
59a	<i>o</i> -CH ₃	92±1	*	105±9	*
59b	<i>m</i> -CH ₃	96±0	*	102±14	*
59c	<i>p</i> -CH ₃	94±3	26±10	174±20	367±193
59d	<i>m</i> -CN	71±3	*	112±12	*
59e	<i>p</i> -CN	94±3	*	104±4	*
59f	<i>m</i> -Cl	94±2	*	97±8	*
48g	<i>p</i> -Cl	96±4	102±30	137±6	92.6±2
59g	<i>o</i> -F	94±4	*	119±13	*
59h	<i>m</i> -F	93±3	*	87±15	*
59i	<i>p</i> -F	82±11	46±19	140±22	362±32
59j	H	96±2	*	127±6	*

Table 4-3 - Binding and efficacy of **59a** to **59j** at the CB₁ receptor

K_i values were determined from binding IC₅₀ values, based on the Cheng-Prusoff equation in which the *K_d* of ³H-CP55940 is 0.5 nM and the concentration of ³H-CP55940 is 0.25nM. * Not assayed **Results are expressed as the percentage of stimulation of [³⁵S]-GTPγS binding. Basal level of activation is 100%. Data are the mean ± SD mean of three experiments performed in triplicate.

All of the compounds display a high level of specific binding at the CB₁ receptor at the tested concentration of 10 μM, except the *meta*-cyano derivative (**59d**) (Table 4-3). The cyano group is polar, and linear in shape, which may cause unfavourable interactions with the receptor and reduce affinity, or the observed pharmacology could be due to the electron withdrawing nature of the

group. The comparison of the *meta*-methyl (**59b**) with the corresponding *meta*-trifluoromethyl analogue could reveal whether it is a steric or electronic effect which reduces affinity.

Table 4-3 and **figure 4-3** show that *para* substituted compounds are once again agonists at the CB₁ receptor, except the cyano derivative which displays antagonist activity. The remaining *meta* and *ortho* substituted derivatives are antagonists with activations between $97 \pm 8\%$ and $112 \pm 12\%$. The only exception is the *ortho*-fluoro (**59g**) analogue which has agonist activity.

Compounds **59i**, **59c** and **48g** displayed the highest affinities at the CB₁ receptor as well as corresponding high activations, so K_i and EC₅₀ values were calculated. All three of these compounds have nanomolar affinities and good efficacies with K_i values at 102 ± 30 nM, 26 ± 10 nM, 46 ± 19 nM and EC₅₀ values at 92.6 ± 1.6 nM and 369 ± 42.4 nM respectively. These results may indicate the importance of both positional and electronic effects in agonist activation of the CB₁ receptor, with *para* electron donating substituents favoured.

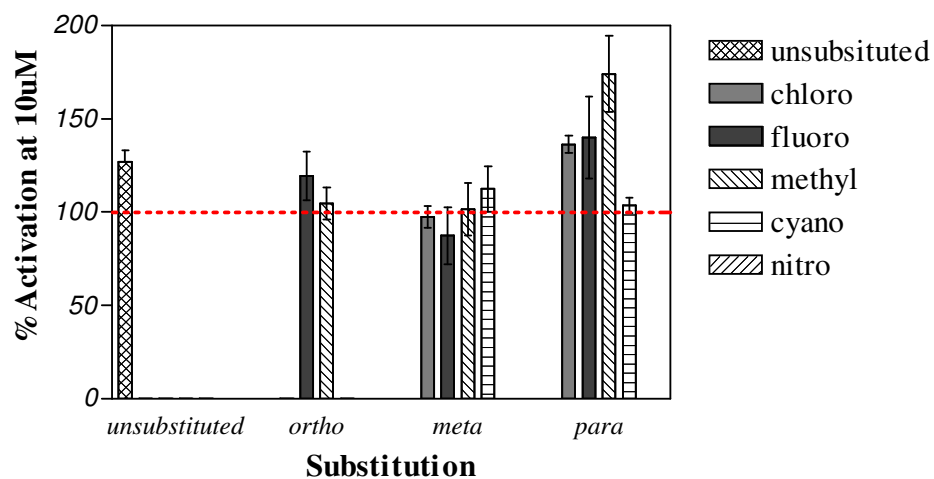
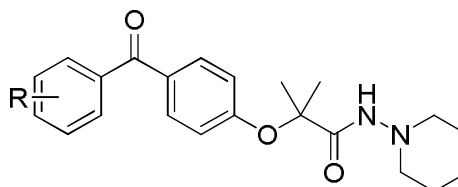


Figure 4-3 - Percentage activation of the CB₁ receptor by compounds **59a** to **59j**. Results are expressed as the percentages of stimulation of [³⁵S]-GTPγS binding. Data are the mean ± SD mean of three experiments performed in triplicate. Dotted line indicates basal level of receptor activation

4.1.2.2.2. Affinity and Efficacy at the CB₂ Receptor



No.	R	% Specific binding at CB ₂ (1x10 ⁻⁵ M)	K _i (nM)	% Activation at CB ₂ (1x10 ⁻⁵ M)
59a	<i>o</i> -CH ₃	91±1	*	102±23
59b	<i>m</i> -CH ₃	90±4	*	77±14
59c	<i>p</i> -CH ₃	93±2	29±11	155±4
59d	<i>m</i> -CN	71±6	*	108±1
59e	<i>p</i> -CN	90±4	*	114±19
59f	<i>m</i> -Cl	91±3	*	82±18
48g	<i>p</i> -Cl	100	15±4	152±10
59g	<i>o</i> -F	91±6	*	134±4
59h	<i>m</i> -F	89±4	*	110±9
59i	<i>p</i> -F	100±0	14±3	129±9
59j	H	94±6	*	124±3

Table 4-4 - Binding and efficacy of **59a** to **59j** at the CB₂ receptor
K_i values were determined from binding IC₅₀ values, based on the Cheng-Prusoff equation in which the *K_d* of ³H-CP55940 is 0.5 nM and the concentration of ³H-CP55940 is 0.25nM. * Not assayed **Results are expressed as the percentage of stimulation of [³⁵S]-GTPγS binding. Basal level of activation is 100%. Data are the mean ± SD mean of three experiments performed in triplicate.

All of the analogues displayed a high level of specific binding at the CB₂ receptor, at the single concentration of 10 μM tested, apart from the *meta*-cyano substituted compound (**59d**) (Table 4-4). The lower level of binding of the *meta*-cyano analogue (**59d**) could be again due to the linearity of the nitrile, or its electron withdrawing properties. Other analogues with electron withdrawing substituents, such as a trifluoromethyl group, would need to be

assayed so that a direct comparison, of the effect of electron withdrawing and electron donating substituents, could be made. The *para*- substituted analogues displayed agonist activity at 10 μ M; however the cyano derivative (**59e**) has a large standard deviation value, so further testing needs to be carried out to determine its efficacy at the receptor. The *meta*-substituted derivatives were antagonists or inverse agonists at the CB₂ receptor, although the *meta*-chloro (**59f**) and methyl (**59b**) analogues could be antagonists as the standard deviations are quite large. Of the two *ortho* substituted analogues tested, the fluoro (**59g**) substituted is an agonist and the methyl (**59a**) substituted is an antagonist, which could indicate that sterics play an important role in activation of the receptor, as the methyl group is larger than the fluoro group. Other possibilities are that it is an electronic effect or that the fluoro substituent is acting as a hydrogen bond acceptor for a residue in the binding pocket.

As compounds **48g**, **59c**, **59i** have a high level of binding and agonist activity, their K_i values were calculated. All of the K_i values are in the nanomolar range indicating high affinity at low concentrations; however (**59c**) has a high standard deviation so further testing is required to confirm this observation.

These results indicate that, for the substituted analogues, substituent position appears to be important for agonist activity at the CB₂ receptor, with *para* substituents favoured. The *ortho* fluoro analogue may also be an agonist due to the fluorine being a similar size to hydrogen, and therefore having less steric bulk which avoids clashes with residues in the binding pocket of the receptor. Conversely an electronic or hydrogen bonding interaction may be occurring.

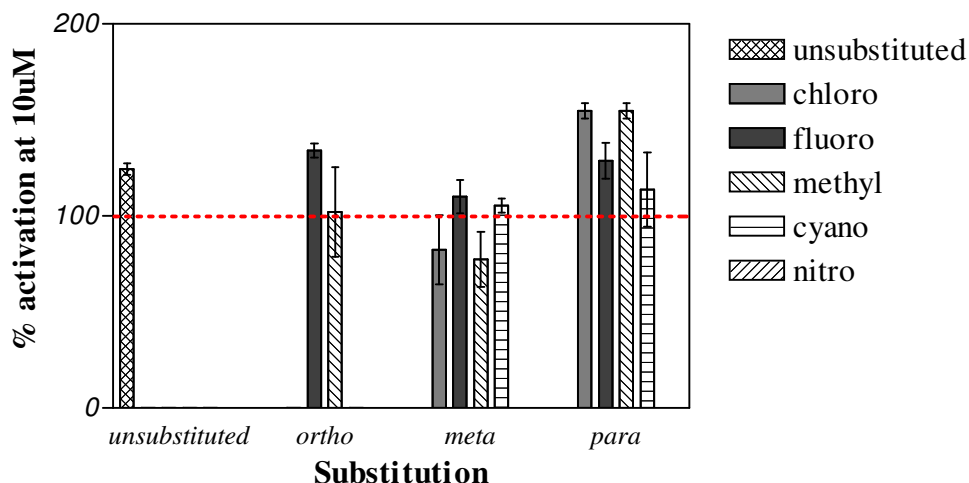


Figure 4-4 - Percentage activation of the CB₂ receptor by compounds **59a** to **59j**. Results are expressed as the percentages of stimulation of [³⁵S]-GTPγS binding. Data are the mean ± SD mean of three experiments performed in triplicate. Dotted line indicates basal level of receptor activation.

4.2. Unbranched and Tertiary Amide Derivatives

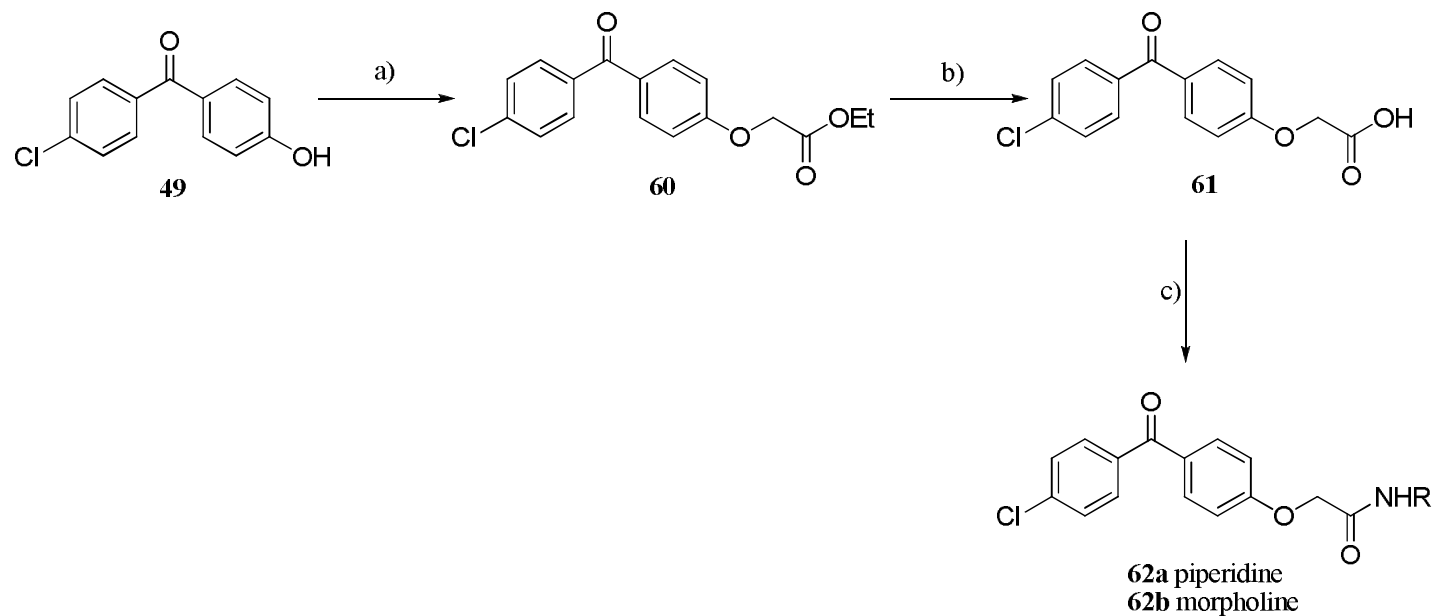
As several of the piperidinyll and morpholino analogues displayed a high affinity at both of the cannabinoid receptors, other alterations were made to the structures of **48g** and **48h** to investigate any further structure activity relationships. Analogues were synthesised omitting the gem-dimethyl groups to investigate their importance. Also, morpholine and piperidine were coupled directly to fenofibric acid (**10b**), affording tertiary amide products, to investigate the relevance of the NH of **48g** and **48h** on receptor binding.

4.2.1. Synthetic routes

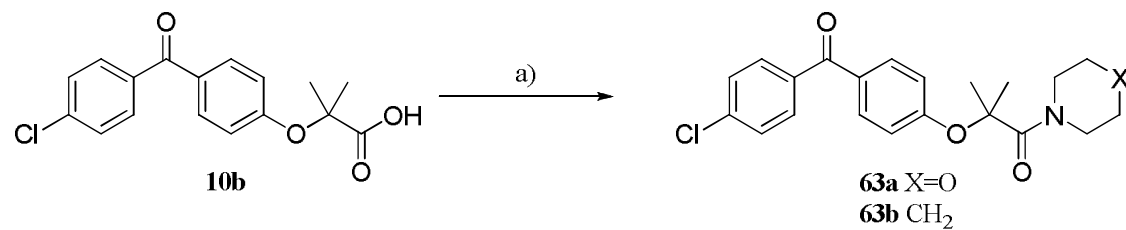
The synthesis of compounds **62a** and **62b** started with alkylation of 4-chloro-(4'-hydroxy)-benzophenone, *via* a Williamson ether synthesis, as described in **Chapter 3**. However ethyl-2-bromoacetate was used instead of α-bromoisobutyric acid. The ethyl ester was saponified using lithium hydroxide in a mixture of THF and water, which afforded the corresponding carboxylic

acid in a yield of 87%. It was deemed pure by ^1H and ^{13}C NMR and mass spectrometry after work-up, and was used without further purification in the coupling to 4-amino morpholine and 1-amino piperidine, using HBTU in the presence of triethylamine. This afforded **62a** and **62b** in crude yields of 25% and 23% respectively. **62a** and **62b** were determined to be a mixture of compounds by NMR, and due to time constraints they were not purified or tested.

Compounds **63a** and **63b** were synthesised by coupling fenofibric acid (**10b**) to piperidine and morpholine using HBTU, in the presence of triethylamine, in yields of 50% and 62% respectively. The analogues were characterised using NMR, FT-IR and HRMS, and purity was confirmed by HPLC at 98% or above.



Scheme 4-2 Reagents and conditions: a) Ethyl bromoacetate, MeCN, NaOH, 3hrs, b) LiOH.H₂O, THF/water (1:1), N₂, 3.75 hrs, 87 % c) 4-aminomorpholine or 1-aminopiperidine, HBTU, dichloromethane, Et₃N, overnight, 23% and 25% crude

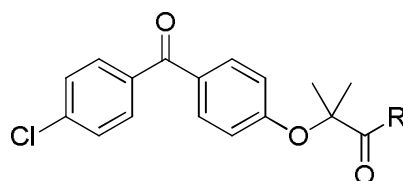


Scheme 4-3 Reagents and conditions: a) 4-aminomorpholine or 1-aminopiperidine, HBTU, dichloromethane, Et₃N, 3hrs, 50% and 62%

4.2.2. Pharmacology

The affinities, and efficacies of **63a** and **63b**, at the cannabinoid receptors, were assessed using the ^3H -CP55940 and ^{35}S -GTP γ S radioligand binding assays. The effect of **62a** and **62b** on cannabinoid receptor binding and activation still remains to be carried out as they were below the necessary purity (approximately 50%) to allow testing.

4.2.2.1. Activity at the cannabinoid receptors

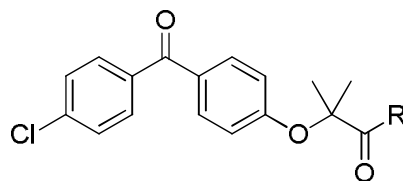


No	R	% Specific binding at CB ₁ (1x10 ⁻⁵ M)	K _i (nM)	% Activation at CB ₁ (1x10 ⁻⁵ M)	EC ₅₀ (μM)
48g	1-aminopiperidine	96±4	102±30	137±6	92.6±1.6
48h	4-aminomorpholine	92±3	150±67	149±7	2.25±0.89
63a	morpholine	65±5	*	94±11	*
63b	piperidine	94±2	*	72±6	*

Table 4-5 - Binding and efficacy of compounds **48g** to **63b** at the CB₁ receptor
*K_i values were determined from binding IC₅₀ values, based on the Cheng-Prusoff equation in which the K_d of ^3H -CP55940 is 0.5 nM and the concentration of ^3H -CP55940 is 0.25nM. * Not assayed **Results are expressed as the percentage of stimulation of [^{35}S]-GTP γ S binding. Basal level of activation is 100%. Data are the mean \pm SD mean of three experiments performed in triplicate.*

On comparing the analogues in **Table 4-5**, **63a** had a lower level of binding at the CB₁ receptor than the other compounds. In contrast to **48g** and **48h**, the piperidine and morpholine analogues had no agonist activity; **63b** had inverse agonist activity and **63a** was an antagonist. This indicates that the NH of the

amide, in **48h** and **48g**, is probably important for binding to the CB₁ receptor, and it appears to be necessary for agonist activity.



No	R	% Specific binding at CB ₂ (1x10 ⁻⁵ M)	K _i (nM)	% Activation at CB ₂ (1x10 ⁻⁵ M)
48g	1-aminopiperidine	100 ± 0	14.8 ± 4.3	152 ± 10
48h	4-aminomorpholine	100 ± 0	12.8 ± 3.5	153 ± 2
63a	morpholine	73 ± 2	*	72 ± 2
63b	piperidine	81 ± 2	*	57 ± 13

Table 4-6 - Binding and efficacy of **48g** to **63b** at the CB₂ receptor

*K_i values were determined from binding IC₅₀ values, based on the Cheng-Prusoff equation in which the K_d of ³H-CP55940 is 0.5 nM and the concentration of ³H-CP55940 is 0.25nM. * Not assayed **Results are expressed as the percentage of stimulation of [³⁵S]-GTPγS binding. Basal level of activation is 100%. Data are the mean ± SD mean of three experiments performed in triplicate.*

Compounds **63a** and **63b** also displayed a lower level of affinity at the CB₂ receptor than **48g** and **48h**. The morpholine and piperidine derivatives also possessed inverse agonist activity. These results indicated that the NH of the amide in both **48g** and **48h** is important for both binding and agonist activation of the CB₂ receptor.

4.3. Conclusions

A series of 24 analogues derived from **48g** and **48h** have been synthesised and their pharmacological activity has been assessed. Several compounds have been identified as having a high affinity and efficacy at the cannabinoid receptors.

Of the **48h** derivatives, **58g** has micromolar agonist activity combined with nanomolar affinity at the CB₁ receptor. The remaining analogues, excluding the *meta*-cyano (**58d**) and *meta*-nitro (**58j**) analogues show a high level of binding and antagonist activity at 10µM. The K_i values of these antagonists still remain to be determined. At the CB₂ receptor the **48h** derivatives have a high level of binding apart from the *meta*-cyano (**58d**) and *meta*-nitro (**58j**) analogues. All of the analogues displayed agonist activity apart from the *meta*-cyano (**59d**), methyl (**59b**) and chloro (**59f**) substituted analogues. The *para* substituted analogues possessed nanomolar affinity combined with nanomolar agonist activity.

The **48g** derived analogues have a high level of binding at the CB₁ receptor except the *meta*-cyano (**59d**) analogue. The unsubstituted (**59j**), *para*-substituted and *ortho*-fluoro (**59g**) analogues displayed agonist profiles whereas the rest of the analogues were antagonists at 10 µM. Compounds **59i**, **59c** and **48g** had both nanomolar agonist activity and affinity. At the CB₂ receptor all of the **48g** derived analogues have a high affinity except the *meta*-cyano analogue. The unsubstituted, *para*-substituted and *ortho*-fluoro analogues had nanomolar agonist activity whereas the rest of the analogues displayed antagonist activity.

The importance of the amide NH on affinity and efficacy at the cannabinoid receptors was investigated by the synthesis and testing of **63a** and **63b** (tertiary amide analogues). These two analogues show that the NH of the amide is important for agonist activity at the CB₁ receptor as **63a** and **63b** have inverse agonist and antagonist activity respectively.

The amide NH is also important for affinity and agonist activity at the CB₂ receptor as both **63a** and **63b** have reduced affinity and inverse agonist activity. In general, all the analogues have a high level of binding at the CB₁ and CB₂ receptors apart from *meta*-substituted analogues with electron withdrawing substituents. Additionally, the stark difference, in both the level of binding and activation, between compounds with and without the amide NH, underline the importance of the NH bond in both receptor binding and activation. *N*-methylated derivatives of **48g** and **48h** could be used to further probe this apparent structure activity relationship. Ideas for the further development of this novel class of cannabinoid receptor ligands are discussed in **Chapter 5**.

5. Conclusions and future work

5.1. Conclusions

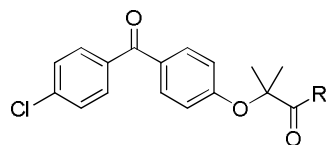
An initial screen, of a library of PPAR α ligands, revealed that one compound (fenofibrate (**10a**)), displayed activity at the cannabinoid receptors.

Considering this, a series of amide derivatives of fenofibrate have been designed, synthesised and evaluated for their activity at PPAR α and both cannabinoid receptors.

5.1.1. Amide derivatives of fenofibrate

The first library of ligands synthesised, was a broad structural exploration into the type of compound which may confer PPAR α and cannabinoid receptor activity. A range of alkyl, alcohol, aromatic, and heterocyclic amide derivatives were synthesised (**Table 5-1**), and two of the heterocyclic analogues (**48g** and **48h**) possessed the highest affinity for the two cannabinoid receptors combined with agonist activity. Unfortunately none of the analogues assayed in the first series had affinity for PPAR α .

The piperidinyl (**48g**) and morpholino (**48h**) derived analogues have micromolar affinity for the CB₁ receptor (150 ± 67 nM (**48h**) and 102 ± 30 nM (**48g**), and low micromolar EC₅₀ values (0.92 ± 0.02 μ M (**48g**) and 2.25 ± 0.88 μ M (**48h**)). At the CB₂ receptor they have nanomolar K_i values (15 ± 4 nM (**48g**) and 16 ± 2 nM (**48h**)). These two derivatives, together with **48f** and **48n**, showed promise as cannabinoid receptor ligands, and therefore were selected for further development, to investigate whether affinity and efficacy at the cannabinoid receptors could be augmented.



No.	R	% Specific Binding at CB ₁ (1x10 ⁻⁵ M)	Ki (nM) at CB ₁	% Activation at CB ₁ (1x10 ⁻⁵ M)	EC ₅₀ at CB ₁	% Specific Binding at CB ₂ (1x10 ⁻⁵ M)	Ki(nM) at CB ₂	% Activation at CB ₂ (1x10 ⁻⁵ M)
48a		*	*	112±7	*	*	>10,000	93±9
48b		74±1	*	110±29	*	*	378	144±14
48c		72±1	*	125±8	*	*	629	113±6
48d		69±2	*	105±19	*	*	440	121±3
48e		93±2	*	87±13	*	*	1200	84±2
48f		94±4	*	113±11	*	99±4	219±10 ^{***}	84±23
48g		96±4	102±30	137±6	93±2	98±4 ^{***}	15±4	152±10
48h		92±3	150±67	149±7	225±89	100±0	16±2	153±2
48i		81±4	*	101±20	*	60±2 ^{***}	*	89±15

No.	R	% Specific Binding at CB ₁ (1x10 ⁻⁵ M)	K _i (nM) at CB ₁	% Activation at CB ₁ (1x10 ⁻⁵ M)	EC ₅₀ at CB ₁	% Specific Binding at CB ₂ (1x10 ⁻⁵ M)	K _i (nM) at CB ₂	% Activation at CB ₂ (1x10 ⁻⁵ M)
48j		80±9	*	123±15	*	87±7	*	87±8
48k		81±9	*	108±9	*	88±1	*	69±10
48l		57±8	*	94±10	*	83±4 ^{***}	*	78±10
48m		67±7	*	101±8	*	99±1	*	73±7
48n		88±3	*	87±8	*	100±0	146±64	104±3

Table 5-1 –Results of all binding and functional assays at CB₁ and CB₂ receptors for compounds **48a** to **48n**

Binding at the CB₁ and CB₂ receptors was calculated by measuring the displacement of ³H-CP55940 from CHO-K1 cells expressing hCB₂ or whole rat brain homogenate. K_i values were determined from binding IC₅₀ values, based on the Cheng-Prussoff equation in which the K_d of ³H-CP55940 is 0.5 and the concentration of ³H-CP55940 is 0.25nM. Efficacy of compounds **48a** to **n** at the CB₁ and CB₂ receptors was calculated by measuring stimulation of [³⁵S]-GTPγS binding in CHO-K1 cells expressing hCB₂ or whole rat brain homogenate. * Not assayed. Results are expressed as the percentage of stimulation of [³⁵S]-GTPγS binding. Basal level of activation is 100%. Data are the mean ±SD mean of three experiments performed in triplicate. *** n=2. K_i values for **48a** to **48e** were determined by Professor David Kendall.

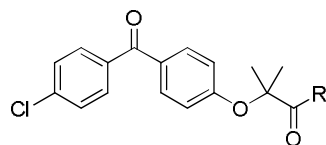
5.1.2. Substituted *N*-benzyl and *N*-phenyl analogues

The second series of compounds were substituted benzyl and phenyl analogues of fenofibrate derived from **48f** and **48n** (Table 5-2). The phenyl and benzyl moieties were substituted with fluoro and methyl groups at the *ortho*, *meta* and *para* positions. These modifications did not offer an increase in affinity at the cannabinoid receptors in comparison to fenofibrate, however; they did provide some structure activity relationship data.

At the CB₁ receptor, the level of binding is lowered, in comparison to **48f** when the benzyl ring bears a methyl substituent. However; the level of binding remains high with the fluoro substituted analogues. This may indicate that the size or electronic properties of a substituent are important for binding at the CB₁ receptor. At the CB₂ receptor the level of binding is high and there is an improvement in affinity when comparing the fluoro substituted analogues with **48f**. However; the affinity of these compounds for the CB₁ receptor is still lower relative to that of fenofibrate (**10a**).

When comparing the substituted phenyl analogues (**51a** to **51e**), they had a lower level of binding compared to the parent compound (**48n**). At the CB₂ receptor the level of binding was high for all of the substituted phenyl analogues; however affinity was lower than for the parent compound (**48n**).

These analogues were not developed any further, as although they are antagonists at the CB₁ receptor they are also antagonists or inverse agonists at the CB₂ receptor (which is undesirable).



No.	R	% Specific Binding at CB ₁ (1x10 ⁻⁵ M)	% Activation at CB ₁ (1x10 ⁻⁵ M)	% Specific Binding at CB ₂ (1x10 ⁻⁵ M)	Ki(nM) at CB ₂	% Activation at CB ₂ (1x10 ⁻⁵ M)
48f		94±4	104±18	99±2	2190±1010	84±23
50a		89±10	83±21	99±3	583±170	75±6
50b		96±5	87±11	94±10	428±89	69±10
50c		89±7	100±17	100±0	242±32	80±2
50d		79±5	61±18	99±2	1140±110	68±9
50e		55±3	85±14	90*	2340±689	39±5
50f		59±12	76±15	93±12	1320±482	40±2
48n		88±3	87±8	99±2	395±191	86±17
51a		82±1	69±16	99±3	1160±566	90±4

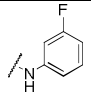
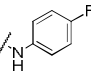
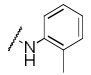
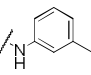
No.	R	% Specific Binding at CB ₁ (1x10 ⁻⁵ M	% Activation at CB ₁ (1x10 ⁻⁵ M)	% Specific Binding at CB ₂ (1x10 ⁻⁵ M	K _i (nM) at CB ₂	% Activation at CB ₂ (1x10 ⁻⁵ M)
51b		71±8	111±11	100±0	3340±80	97±10
51c		76±19	91±2	96±4	1350±485	89±6
51d		42±25	100±8	95±16	1560±113	89±15
51e		59±5	114±8	97±5	762±294	87±4

Table 5-2 - Affinity and efficacy of the unsubstituted and substituted phenyl and benzyl analogues at the CB₁ and CB₂ receptors
Binding and affinity were evaluated using CHO cells expressing CB₂ receptors or whole rat brain homogenate and ³H-CP55940 or [³⁵S]-GTPγS K_i values were determined from binding IC₅₀ values, based on the Cheng-Prusoff equation in which the K_d of ³H-CP55940 is 0.5nM and the concentration of ³H-CP55940 is 0.25nM. Results are expressed as the percentage of stimulation of [³⁵S]-GTPγS binding. Basal level of activation is 100%. Data are the mean ± SD mean of three experiments performed in triplicate (n=3) and were analysed using Graphpad prism 3.

5.1.3. Substituted benzophenone derivatives

The next series of analogues investigated were derivatives of **48g** and **48h** (Table 5-3 and Table 5-4). Substitution of the benzophenone with electron donating and withdrawing groups at the *ortho*, *meta* and *para* positions provided several compounds with high affinity and efficacy at both cannabinoid receptors.

All of the morpholino derived analogues had a high level of binding at the CB₁ receptor apart from analogues with *meta* electron withdrawing substituents.

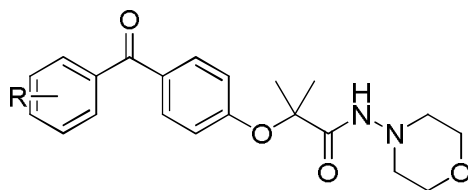
This may indicate that the position of the substituent is important for binding although *ortho*- and *para*- nitro and cyano derivatives would need to be assayed to confirm that it is an electronic rather than a positional effect. The morpholino analogues were all antagonists at the CB₁ receptor apart from the *para* chloro (**48h**) and *ortho* fluoro (**58g**) derivatives which were agonists. This may indicate that positional and electronic effects are not the only factors to affect CB₁ receptor binding.

At the CB₂ receptor the **48h** derivatives had a high level of binding with the exception of the *meta* - nitro and *meta* - cyano derivatives. In general the *para* and *meta* substituted analogues had agonist activity whereas the *ortho* substituted analogues were antagonists. This indicated that position of the substituent is important for agonist activity at the CB₂ receptor. *Ortho* substituents may cause a conformational restriction in the rotation of the benzophenone rings, relative to each other, which may disrupt the interaction required for activation of the receptor.

All the **48g** derivatives displayed a high level of binding at the CB₁ receptor apart from the *meta* cyano analogue (**59d**). In general, *para* electron donating

substituents are favoured for agonist activity, whereas other substituents at the *ortho* and *meta* positions give compounds which are antagonists at the CB₁ receptor. Affinity for the CB₁ receptor was determined for two compounds in the series (**59c** and **59i**), and they displayed a higher affinity than fenofibrate (**10a**) and also the parent compound **48g**.

At the CB₂ receptor, the **48g** analogues displayed a high level of binding apart from the *meta*-cyano substituted analogue (**59d**). The *para* substituted analogues showed agonist activity at the CB₂ receptor and the *meta* substituted analogues were antagonists or inverse agonists. The *ortho* fluoro analogue (**59g**) displayed agonist activity whereas the *ortho* methyl analogue (**59a**) displayed antagonist activity. This may indicate that for *ortho* substituted analogues the size and electronic properties of a substituent are important, and in this case the fluorine atom in **59g** may be acting as a hydrogen bond acceptor. To establish whether this is indeed the case, the corresponding *ortho* OH and OMe analogues could be synthesised. When comparing the **48g** analogues there is no improvement in affinity or efficacy in comparison to **48g**, however they are improved in comparison with fenofibrate (**10a**).



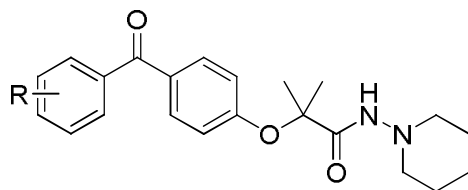
No.	R	% Specific Binding at CB ₁ (1x10 ⁻⁵ M)	Ki (nM) at CB ₁	% Activation at CB ₁ (1x10 ⁻⁵ M)	EC ₅₀ at CB ₁	% Specific Binding at CB ₂ (1x10 ⁻⁵ M)	Ki(nM) at CB ₂	% Activation at CB ₂ (1x10 ⁻⁵ M)
58a	<i>o</i> -CH ₃	95±4	*	99±10	*	92±3	56.8±16.8	148±24
58b	<i>m</i> -CH ₃	94±2	*	99±7	*	90±5	*	104±5
58c	<i>p</i> -CH ₃	93±3	*	103±18	*	96±6	310±16.5	160±9
58d	<i>m</i> -CN	39±1	*	107±11	*	42±10	*	98±1
58e	<i>p</i> -CN	*	*	*	*	*	*	*
58f	<i>m</i> -Cl	94±1	*	101±6	*	94±5	*	82±4
48h	<i>p</i> -Cl	92±3	150±67	149±7	2.25±0.89	100±0	12.8±3.5	153±2
58g	<i>o</i> -F	92±4	92±14	130±19	1.24±0.97	100±0	146±25.2	119±19
58h	<i>m</i> -F	89±7	*	89±9	*	89±6	*	116±5

No.	R	% Specific Binding at CB ₁ (1x10 ⁻⁵ M)	K _i (nM) at CB ₁	% Activation at CB ₁ (1x10 ⁻⁵ M)	EC ₅₀ at CB ₁	% Specific Binding at CB ₂ (1x10 ⁻⁵ M)	K _i (nM) at CB ₂	% Activation at CB ₂ (1x10 ⁻⁵ M)
58i	<i>p</i> -F	89±12	*	89±7	*	99±3	231±90.2	135±7
58j	<i>m</i> -NO ₂	79±6	*	92±14	*	80±5	*	106±14
58k	<i>p</i> -NO ₂	*	*	*	*	*	*	*
58l	H	93±4	*	97±18	*	96±9	299±3.5	137±8

Table 5-3 - Binding and efficacy of **58a** to **58l** at the CB₁ and CB₂ receptors

Binding and affinity were evaluated using CHO-K1 cells expressing hCB₂ or whole rat brain homogenate, and ³H-CP55940 or [³⁵S]-GTPγS. K_i values were determined from binding IC₅₀ values, based on the Cheng-Prusoff equation in which the K_d of ³H-CP55940 is 0.5 nM and the concentration of ³H-CP55940 is 0.25nM. * Not assayed

**Results are expressed as the percentage of stimulation of [³⁵S]-GTPγS binding. Basal level of activation is 100%. Data are the mean ± SD mean of three experiments performed in triplicate.



No.	R	% Specific Binding at CB ₁ (1x10 ⁻⁵ M)	Ki (nM) at CB ₁	% Activation at CB ₁ (1x10 ⁻⁵ M)	EC ₅₀ at CB ₁	% Specific Binding at CB ₂ (1x10 ⁻⁵ M)	Ki(nM) at CB ₂	% Activation at CB ₂ (1x10 ⁻⁵ M)
59a	<i>o</i> -CH ₃	92±1	*	105±9	*	91±1	*	102±23
59b	<i>m</i> -CH ₃	96±0	*	102±14	*	90±4	*	77±14
59c	<i>p</i> -CH ₃	94±3	26±10	174±20	367±193	93±2	29±11	155±4
59d	<i>m</i> -CN	71±3	*	112±12	*	71±6	*	108±1
59e	<i>p</i> -CN	94±3	*	104±4	*	90±4	*	114±19
59f	<i>m</i> -Cl	94±2	*	97±8	*	91±3	*	82±18
48g	<i>p</i> -Cl	96±4	102±30	137±6	92.6±2	100	15±4	152±10
59g	<i>o</i> -F	94±4	*	119±13	*	91±6	*	134±4
59h	<i>m</i> -F	93±3	*	87±15	*	89±4	*	110±9

No.	R	% Specific Binding at CB ₁ (1x10 ⁻⁵ M)	K _i (nM) at CB ₁	% Activation at CB ₁ (1x10 ⁻⁵ M)	EC ₅₀ at CB ₁	% Specific Binding at CB ₂ (1x10 ⁻⁵ M)	K _i (nM) at CB ₂	% Activation at CB ₂ (1x10 ⁻⁵ M)
59i	<i>p</i> -F	82±11	46±19	140±22	362±32	100±0	14±3	129±9
59j	H	96±2	*	127±6	*	94±6	*	124±3

Table 5-4 - Binding and efficacy of **59a** to **59j** at the CB₁ and CB₂ receptors

Binding and affinity were evaluated using CHO-K1 cells expressing hCB₂ or whole rat brain homogenate, and ³H-CP55940 or [³⁵S]-GTPγS. K_i values were determined from binding IC₅₀ values, based on the Cheng-Prusoff equation in which the K_d of ³H-CP55940 is 0.5 nM and the concentration of ³H-CP55940 is 0.25nM. * Not assayed

**Results are expressed as the percentage of stimulation of [³⁵S]-GTPγS binding. Basal level of activation is 100%. Data are the mean ± SD mean of three experiments performed in triplicate.

5.1.4. Tertiary Amide Derivatives

Another modification to the structures of the morpholino and piperidinyl derivatives was to couple morpholine and piperidine directly to fenofibric acid (**10b**) which afforded the tertiary amide products **63a** and **63b**.

The morpholine derivative (**63a**) exhibited a lower level of binding at the CB₁ receptor compared to **48h**, and both **63a** and **63b** lost their agonist activity. This would indicate that the amide NH is important for agonist activity at the CB₁ receptor.

For both **63a** and **63b** the level of binding was quite high at the CB₂ receptor. Additionally, these compounds were inverse agonists. In comparison to **48g** and **48h** the removal of the amide NH diminished the level of binding at the receptor and also switched the activity from agonism to inverse agonism.

5.2. Future work

So far, a series of fenofibrate analogues have been developed that displayed activity at the cannabinoid receptors.

The substituted benzyl and phenyl derivatives showed a high affinity for the CB₂ receptor; however they did not have a higher affinity than fenofibrate (**10a**) or the desirable agonist activity. The fluoro and methyl derivatives synthesised indicated that activity can be tuned by varying the substituent, and potentially affinity and possible efficacy could be altered. A larger library of compounds with differing substituents needs to be synthesised to investigate further whether it is a positional, steric or electronic effect. Some of these substituents could be; hydroxyl, trifluoromethyl, methoxy, nitro and cyano

groups. At the CB₁ receptor, the benzyl and phenyl derivatives had antagonist or inverse agonist activity, and a high level of binding at 10μM apart from the methyl derivatives. Therefore it would be valuable to investigate further whether this is a positional, steric or electronic effect by again synthesising a larger library of compounds as described above.

Considering the pharmacological data obtained to date, the series of 23 morpholino and piperidinyl derivatives, described in **Chapter 4**, appear to be the best candidates to use as leads for further development.

All of the morpholino and piperidinyl analogues displayed a high level of binding at the cannabinoid receptors, apart from *meta* cyano and nitro derivatives. Of these, selected analogues that were assayed, displayed a high affinity. They have displayed varying activities at the cannabinoid receptors, which appears to be substituent dependent, and therefore varying the type of substituent and its position could potentially allow tuning of their activity. As only a few examples of various substituents have been exemplified so far, a wider range may offer this possibility. Examples are shown in **Figure 5-1**.

A larger library of substituted compounds with differing electronic and steric properties could also help clarify whether size, position or electronic effects are responsible for the mixed results at the CB₂ receptor for *ortho*-substituted compounds in the series **58a** to **58l**.

Other alterations to the pharmacophore, to further explore structure activity relationships, could be the rigidification of the benzophenone by tethering the two phenyl rings together to form either an anthracenone or a fluorenone. Morpholino and piperidinyl derivatives (**48g** and **48h**) with the geminal dimethyl groups omitted, may also give an indication of the components of the

pharmacophore that are important for affinity and activity at the cannabinoid receptors. These two compounds have been synthesised but remain to be re-purified and then tested, due to time constraints, as they were below the necessary purity for testing (approximately 50% from NMR).

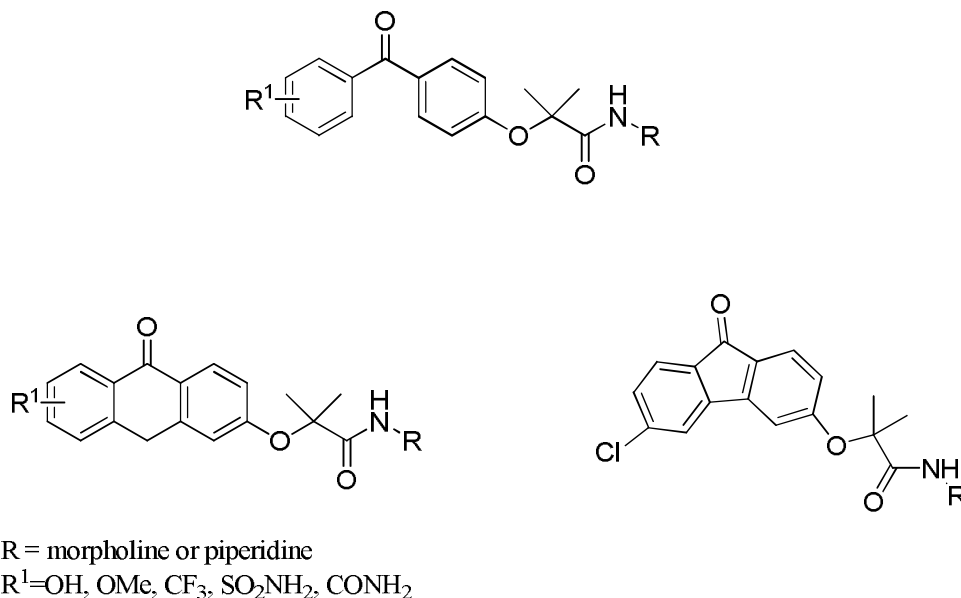


Figure 5-1 Potential pharmacophore modifications

As PPAR α activity of fenofibric acid (**10b**) was lost with substitution of the carboxylic acid with various amides, molecular modelling may indicate which interactions are unfavourable for binding and activation of the receptor. PPAR α has previously been crystallised with both agonists and antagonists^{11, 17, 19}, and so docking studies may indicate the reasons for fenofibric acid (**10b**) and anandamide possessing activity at PPAR α whereas compounds described in this thesis do not.

Although a ligand with dual PPAR α / cannabinoid receptor activity has not been discovered with the amide derivatives synthesised to date, this scaffold could provide a platform for the further development of novel cannabinoid receptor ligands.

The possibility of developing a sub-type selective cannabinoid receptor ligand, or one combining antagonist/inverse-agonist activity at the CB₁ receptor with agonist activity at the CB₂ receptor is still of therapeutic interest. Such an activity profile has the potential to target a variety of disorders, such as pain, MS and obesity.

6. Experimental

6.1. Pharmacology

6.1.1. Molecular cloning

The competent *E.Coli* (xl-blue) was obtained from Promega. The PPAR α pcDNA plasmid was prepared by Yan Sun, the 3xPPRE plasmid was a gift from Walter Wahli at the Université de Lausanne and the RXR plasmid was a gift from David Mangelsdorf at UT Southwestern Medical Centre.

6.1.1.1. Preparation of LB Media

The solutes were added together and either 400 ml or 250 ml deionised water was then added. The mixture was shaken until the solutes dissolved and the pH was adjusted with 1M NaOH. The solution was then autoclaved.

	With Agar (400ml)	Without Agar (250ml)
Tryptone (Oxoid)	4g	2.5g
Yeast Extract (Oxoid)	2g	1.25g
NaCl (Fisher Scientific)	2g	1.25g
1M NaOH (Fisher Scientific)	0.4ml	0.25ml
Agar (MP Biomedicals)	6g	-

6.1.1.2. Preparation of LB plates

LB media with agar was prepared as described above, melted and ampicillin (100 $\mu\text{g ml}^{-1}$) was added. The media was poured onto 10 cm diameter petri dishes and left to set a room temperature. The plates were then stored at 4 °C.

6.1.1.3. Transformation of bacterial cells

The bacterial cells were removed from the freezer and were defrosted on ice over 30 minutes. In three separate vials 50ng of DNA (either PPAR α , PPRE or

RXR) was added 100 μ l of competent cells were then added to each vial. The mixtures were then stored on ice for 30 minutes.

LB medium (800 μ l) was added to each tube and they were incubated at 37°C with shaking for 1 hour. After this time the cells were spread onto LB agar plates containing ampicillin (100 μ g ml⁻¹) and were then incubated at 37°C until the transformed colonies appeared (18 hours).

A single colony of bacteria was inoculated into 10ml of LB medium containing ampicillin (100 μ g ml⁻¹) and was incubated with shaking for 4 hours. After this time 1 ml of each of the plasmid containing competent cells, were transferred into 100 ml each of LB medium containing ampicillin (100 μ g ml⁻¹). The three suspensions were then incubated overnight.

6.1.1.4. Plasmid DNA Preparation

The Maxi-prep of the plasmid DNA was carried out using the Qiagen Plasmid Maxi Kit following the manufacturer's protocol.

6.1.1.4.1. Maxi-preparation

In summary 100 ml of the transformed bacterial culture was pelleted (4000g for 10 minutes). 10 ml of lysis buffer was added, and the lysate was incubated at room temperature for 5 minutes, and then centrifuged at >15,000g for 10 minutes at room temperature. The supernatant was removed and loaded onto the equilibrated column. The solution was allowed to drain by gravity flow and the flow through was discarded. The column was washed once with wash buffer and the solution was allowed to drain by gravity. The flow through was discarded.

15 ml of elution buffer (E4) was added to the column to elute the DNA. The solution in the column was allowed to drain by gravity flow. 150 ml isopropanol was then added to the elution tube to precipitate the plasmid DNA. This was mixed well and was centrifuged at >15000xg for 30 minutes at 4°C. The supernatant was discarded.

5 ml 70 % ethanol was added to the pellet and was centrifuged at >15000xg for 5 minutes at 4°C. The supernatant was removed and the pellet was air dried for 10 minutes. The pellet was then resuspended in 200-500 µl of sterile HPLC water and was stored at -20°C.

6.1.1.4.2. Plasmid DNA Concentration

The plasmid DNA concentrations for PPAR α , RXR and PPRE were determined using a Nanodrop ND1000 spectrophotometer.

6.1.2. Cell culture

All reagents were obtained from Sigma Aldrich unless otherwise stated. All culture flasks and 6-well plates were obtained from Greiner Bio-one GmbH and Nunc respectively. The cells used throughout this study were; COS-7 cells, and were obtained from the American Type Culture Collection (ATCC). *E. Coli* (Promega) was used to carry out the transformation of the three different plasmids for PPAR α , PPRE and RXR. The cells were cultured in Dulbecco's Minimum Essential Medium D6546 (DMEM), which was supplemented with L-glutamine (0.5%), non-essential amino acids (0.5 %), sodium pyruvate (0.5 %) and fetal bovine serum (10 %). The COS-7 cells were incubated at 37°C, 5 % CO₂. All cell culture was carried out in a sterile hood using sterile techniques

6.1.2.1. Passage of cells

The COS-7 cells were passaged when they had reached ~60 % confluence. Firstly the DMEM was aspirated and the cells were then washed with PBS (10 ml) at 37°C. Trypsin/EDTA (4 ml, 37 °C) was added and the cells were incubated at 37 °C, 5 % CO₂ for 2 minutes. After this time the trypsin/EDTA was neutralised with DMEM (15ml) and the cell suspension was centrifuged at 1000 rpm for 5 minutes. The resulting pellet was resuspended in DMEM (3 ml) and 1 ml of the suspension was added to two new 400 ml flasks containing DMEM (35 ml, 37°C).

6.1.2.2. Seeding of cells

COS-7 cells that were at ~70 % confluence were removed from the flask and centrifuged as described above. The cell pellet was resuspended in DMEM (3 ml) and the cells were counted using a haemocytometer. Further DMEM was then added to achieve a density of 1.0×10^5 cells when 1 ml of the suspension was added to 1 well of a six well plate. The plates were then returned to the incubator at 37 °C, 5 % CO₂.

COS-7 cells used for the luciferase assay were seeded into 6-well plates 24 hours before transfection was carried out.

6.1.2.3. Transient transfections

All transfections were carried out in a sterile hood using sterile techniques. The pCDNA 3.1/zeo + and the transfection reagent TransFast was obtained from Promega. All other reagents were from Sigma Aldrich.

6.1.2.3.1. Transfection with TransFast transfection reagent

- All plasmids were diluted to 500 ng / µl.

- 1 ml of combined DNA/TransFast/serum free DMEM mixture was used per well.

Day 1 – COS-7 cells were seeded into 6-well plates, at a density of 5×10^4 cells well⁻¹ in 10% FBS DMEM

Day 2 – To serum free DMEM the DNA, and then TransFast were added. A 1:1 ratio of DNA to TransFast was used (3 µl of TransFast per µg of DNA). The mixture was briefly vortexed and was left to incubate for 15 minutes.

The medium was removed from the cells (~60 % confluent) and 1 ml of the DNA/TransFast mixture was added to each of the wells. The cells were returned to the incubator (37 °C, 5 % CO₂) for 1 hour after which time 1 ml of 1 % FBS DMEM with or without ligands was added. The cells were then returned to the incubator for 24 hours.

6.1.3. Assays

6.1.3.1. Luciferase Assay

24 hours after transfection, the media was aspirated from each of the wells, and the cells were washed with 1ml PBS. The cells were lysed with passive lysis buffer (400 µl, 5x diluted) and the cells were scraped from the plates. The lysates were pipetted into eppendorf vials and were stored at -20 °C for 24 hours. After storage at -20 °C, the lysates were defrosted and centrifuged at 13000 rpm for 2 minutes. 10 µl of each of the samples were tested for luciferase activity by adding 100 µl of luciferase assay buffer (Promega). The light emitted was measured with a luminometer (TD-20/20 luminometer, Turner Designs).

6.1.3.2. TR-FRET assay

The assay was carried out as described in the manufacturer's protocol.

In summary 20 µl of test compound, control competitor, or test compound solvent were pipetted into a 384 well black assay plate. 10 µl of Fluormone Pan-PPAR Green was then added to the plate followed by a 10 µl mixture of PPAR α /Tb-Anti-GST Ab. The plate was gently mixed on an orbital shaker for 30 seconds, covered and then incubated at room temperature. After 2 hours incubation the fluorescent emission signal of each well was measured at 495 nM and 520 nM on a Perkin Elmer EnVision plate reader. The plate was read again after a further 2 hours incubation to ensure that equilibration had been reached.

6.1.4. Radioligand binding assays

6.1.4.1. Preparation of CHO-K1 cells expressing hCB₂ receptors

CHO-K1 cells expressing hCB₂ receptors were grown to confluence, harvested, pelleted and frozen down. This work was kindly carried out by Liaque Latif.

The pellet was defrosted and resuspended in Tris buffer (50 mM Tris, 5 mM MgCl₂, 2 mM EDTA, pH 7.0). The suspension was homogenised and centrifuged (40,000g for 20 minutes) and the supernatant was discarded. This process was repeated twice. The final pellet was resuspended in Tris buffer and divided into 1 ml aliquots to a protein concentration of 5 mg/ml.

6.1.4.2. Preparation of rat brain homogenate

The tissue was weighed and excess fluid was removed. It was then homogenised on ice, in Tris buffer, using a Polytron homogeniser in three, ten second bursts. The tissue was then diluted (1 g in 40mls of Tris buffer) and

centrifuged at 40,000 g for ten minutes, and the supernatant was discarded. This process was repeated twice. The pellet was resuspended in Tris buffer, (1 g of the original tissue in 10mls), and divided into 1 ml aliquots.

6.1.4.2.1. [3H] CP55940 Radioligand Competition Binding Assay

Tubes containing of CHO-K1 membranes expressing human CB₂ receptors or whole rat brain were incubated at 30°C for 1hour 30 minutes in 850 µl assay buffer (50mM Tris.HCl, 2mM EDTA, 5 mM MgCl₂ and 0.2 mg ml⁻¹ bovine serum albumin (BSA) pH 7.0 at 30 °C) with 50 µl ³H CP55940 (Perkin-Elmer Life Sciences Inc.), and 50 µl competing drug (Tris.HCl, 2mM EDTA, 5mM MgCl₂ and 5.0 mg ml⁻¹ bovine serum albumin (BSA) pH 7.0 at 30 °C) giving a final assay volume of 1 ml. Specific binding was calculated by subtracting non specific binding (NSB) from the total binding. The NSB was determined in the presence of 1 µM SR144528. A Brandel cell harvester (Brandel Inc., Gaithersburg, MD, U.S.A) was used to harvest the membranes and separate the bound from unbound radioligand. The membranes were collected on filters pre soaked with assay buffer, and the bound radioligand was quantified using a liquid scintillation counter (Packard, Tri-Carb 2100TR). Nonlinear regression analysis was carried out using GraphPad Prism 3, and K_i values were determined from IC₅₀ values using the Cheng-Prusoff equation where the concentration of [³H] CP 55940 was 0.25 nM and K_D was 0.5 nM. Results are mean values ± SD mean.

6.1.4.2.2. [35S]GTPγS Radioligand Binding Assay

The assay was carried out as described previously by G Griffin et al ⁵⁸.

CHO-K1 cells homogenate expressing human CB₂ membranes, or whole rat brain, was incubated at 30 °C for 20 minutes in 30 ml assay buffer with added GDP (100 µM) and theophylline (1 µM). 0.5 ml of this membrane solution was added to assay tubes containing the desired concentration of drug, and 0.5 ml of [³⁵S]-GTP-γ-S solution (0.05 nM). The tubes were then incubated at 30 °C for 1 hour 30 minutes. The NSB was determined using non-radiolabelled GTP-γ-S (10 µM). The membranes were harvested under vacuum onto filter mats, and the tubes were washed twice with approximately 2 ml of cold wash buffer. The level of bound radioligand was quantified using liquid scintillation spectrophotometry (Packard liquid scintillation analyser, Tri-Carb 2100TR). Nonlinear regression analysis was carried out using GraphPad Prism 3.

The stimulation of the [³⁵S]-GTP γS binding was defined as the percentage increase above basal levels ((dpm (agonist)-dpm (no agonist))/dpm no agonist) x100). Results are mean ± S E mean.

6.2. General Chemistry

Chemicals and solvents were purchased from standard suppliers and used without further purification. Merck Kieselgel 60, 230-400 mesh, for flash column chromatography was supplied by Merck KgaA (Darmstadt, Germany) and deuterated solvents were purchased from Goss International Limited (England) and Sigma-Aldrich Company Ltd (England).

Unless otherwise stated, reactions were carried out at ambient temperature. Reactions were monitored by thin layer chromatography on commercially available precoated aluminium backed plates (Merck Kieselgel 60 F254). Visualisation was by examination under UV light (254 and 366 nm). General

staining carried out with Ninhydrin and potassium permanganate. All organic extracts after aqueous work-up procedures were dried over MgSO_4 or Na_2SO_4 before gravity filtering and then evaporated under reduced pressure at $\leq 40^\circ\text{C}$ (water bath temperature). Purification using preparative layer chromatography was carried out using Fluka silica gel 60 PF254 containing gypsum (200 mm x 200 mm x 1 mm). Flash chromatography was performed using Merck Kieselgel 60 (0.040-0.063 mm) on either a Flashmaster 2 or Isolera 4.

Melting points were recorded on a Reichert 7905 apparatus. FT-IR spectra were recorded as thin films or KBr discs in the range of 4000 – 500 cm^{-1} using and Avatar 360 Nicolet FT-IR spectrophotometer.

Mass spectra (TOF ES +/- or API) were recorded on a Waters 2795 separation module/micromass LCT platform, or Applied Biosystems API2000.

^1H NMR spectra were recorded on a Bruker-AV 400 at 400.13 MHz. ^{13}C NMR spectra were recorded at 101.62 MHz. Chemical shifts (δ) are recorded in ppm with reference to the chemical shift of the deuterated solvent/an internal TMS standard. Coupling constants (J) are recorded in Hz and the significant multiplicities described by singlet (s), doublet (d), triplet (t), quadruplet (q), broad (br), multiplet (m), doublet of doublets (d of d), doublet of doublet of doublets (ddd), doublet of doublet of doublet of doublets (dddd), or doublet of triplets (d of t). Unless otherwise stated all spectra were recorded in CDCl_3 .

Microwave synthesis was carried out in a CEM Explorer series microwave reactor.

Analytical HPLC was performed using **systems 1 to 4** to confirm purity. All retention times are quoted in minutes.

System 1: Waters millennium 995 LC system. Phenomenex Onyx Monolithic reverse phase C18 column (100 x 4.6 mm).

Flow rate: 3.00 mL/min and UV detection at 254 nm.

Gradient 5% - 95% solvent B over 10 minutes.

Solvent A: 0.1% formic acid in water; solvent B: 0.1% formic acid in MeCN.

System 2: Waters millennium 995 LC system. Waters symmetry reverse phase C18 column (75 x 4.6 mm).

Flow rate: 1.00 mL/min. UV detection at 254 and 220 nm.

Gradient: 5% - 95% solvent B over 20 minutes.

Solvent A: 0.1% formic acid in water; solvent B: 0.1% formic acid in MeOH.

System 3: Shimadzu UFLCXR system coupled to an Applied Biosystems API2000. Gemini-NX 3u-110A, 50x2mm column which was thermostated at 40°C.

Flow rate: 0.5ml/min. UV detection at 220 and 254nm.

Gradient: Pre-equilibration run for one min at 10% B, 10 to 98% solvent B in 2min, 98% for 2min, 98 to 10% B in 0.5min then 10% for one min.

Solvent A: 0.1% Formic Acid in water; solvent B: 0.1% Formic Acid in MeCN.

System 4: Shimadzu UFLCXR system coupled to an Applied Biosystems API2000. Luna 3u (PFP2) 110A, 50x2 mm. column which was thermostated at 40°C.

Flow rate: 0.5ml/min. UV detection at 220 and 254 nm.

Gradient: Pre-equilibration run for one min at 10% B, 10 to 98% solvent B in 2min, 98% for 2min, 98 to 10% B in 0.5min then 10% for one min.

Solvent A: 0.1% Formic Acid in water; solvent B: 0.1% Formic Acid in MeCN.

All HPLC and LC-MS traces, of compounds for screening, confirmed purity of 98% or above at both 220 nm and 254 nm.

Compounds were synthesised by the general methods described below unless otherwise stated.

General Method A: To a stirred solution of Fenofibrate-OSu (1.0 eq) in anhydrous dichloromethane (20 ml) the selected amine (1.0 eq) was added. An instantaneous precipitate of *N*-hydroxysuccinimide was formed, and the reaction was stirred for between 5 minutes and 24 hours. Water was added to the reaction, and the organic layer was then washed firstly with potassium hydrogen sulfate, then saturated sodium bicarbonate, water and brine. The organic layer was dried with magnesium sulfate and then filtered. The solvent was evaporated under vacuum.

General Method B: To fenofibric acid (**10b**) (1eq) thionyl chloride was added as the solvent. The mixture was heated at 60°C for between 1 hour and 1 hour 45 minutes. The thionyl chloride was removed under vacuum and the solid or oil afforded was used directly in the next step. The selected amine (1eq) was dissolved in anhydrous dichloromethane and triethylamine (2eq) was added. The mixture was cooled to 0°C and the acid chloride (1eq) was slowly added. After addition the ice bath was removed and the reaction was stirred for

between 1 hour and overnight. The reaction mixture was then washed twice with hydrochloric acid (2M), sodium hydroxide (2M), and then water. The organic phase was dried with sodium sulfate, filtered, and the solvent was removed under vacuum.

General Method C: To the methyl or ethyl ester (1eq), water and THF (1:1) were added. Lithium hydroxide (5eq) was then added under nitrogen. The reaction was stirred between for 2 hours and 24 hours. The THF was removed under vacuum, water was added, and the resulting aqueous solution was acidified to pH 4 with concentrated HCl. The product was then extracted into dichloromethane and the combined organic layers were dried with sodium sulfate. The solvent was then removed under vacuum.

General Method D: To benzoic acid (1eq) thionyl chloride was added as the solvent. The mixture was heated at 60°C for between 1 hour and 2 hours 30 minutes. The thionyl chloride was removed under vacuum and the solid or oil afforded was used directly in the next step. Anisole (1eq) in anhydrous dichloromethane was cooled to 0°C and aluminium chloride (1.5eq) was slowly added. The benzoyl chloride (1eq) was dissolved in dichloromethane and then slowly added to the mixture. After 30 minutes at 0°C, the ice bath was removed and the reaction was stirred at room temperature overnight. The reaction mixture was poured onto a mixture of ice and concentrated HCl and was then extracted with dichloromethane, and the organic were washed with water (x 3) and then brine. The organic layer was dried over magnesium sulfate and the solvent was removed under vacuum.

General Method E: To the 4-hydroxybenzophenone (1eq) dissolved in MeCN, sodium hydroxide or potassium carbonate was added (5.5eq). The mixture was

heated to 50°C and stirred for 1 hour. α -Bromoisobutyric acid (1.5eq) dissolved in acetonitrile was then added and the mixture was heated for a further 2 hours 30 minutes. The solvent was removed under vacuum and the resulting solid was dissolved in dichloromethane. This was then washed with HCl (2M) and water. The organic layer was dried with sodium sulfate and the solvent was removed under vacuum.

General Method F: A mixture of the 4-methoxybenzophenone (1eq) and pyridine hydrochloride (5eq) were placed in a microwave vial and irradiated at 215 W and 150°C, 200°C or 250°C and for between 2 and 14 minutes. Ice water was then added to quench the reaction and it was extracted with ethyl acetate. The organic layer was washed with sodium hydroxide (1M), and then discarded. The aqueous layer was acidified to ~pH5 with concentrated HCl and the resulting precipitate was extracted into ethyl acetate. The organic layer was dried with magnesium sulfate and the solvent was removed under vacuum.

General Method G: To the carboxylic acid in dichloromethane (1eq), triethylamine was added. HBTU was then added and the mixture was stirred for 5 minutes. The selected amine was then added and the reaction was stirred for 1 hour 15 minutes to overnight. The reaction was then diluted with dichloromethane and was washed with HCl (1M), NaOH (1M), and water. The organic layer was dried over sodium sulfate and the solvent was removed under vacuum.

General Method H: To the benzophenone (1eq), and PPh₃ (1.2) in toluene at 80°C, a solution of DIAD (1.2) and methyl-2-hydroxyisobutyrate (1.1eq) and toluene were slowly added via a dropping funnel. The reaction was stirred for 2 hours to 3 hours and was then diluted with toluene. The mixture was washed

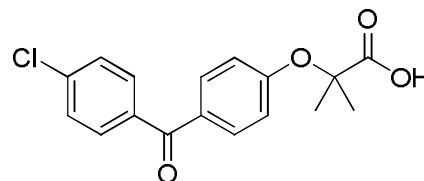
with NaOH (1M), and water and then dried over magnesium sulfate. The solvent was then removed under vacuum.

2-(4-(4-Chlorobenzoyl)phenoxy)-2-methylpropanoic acid (10b)

To 4-chloro-4'-hydroxybenzophenone

(6.917 g, 2.97 mmol), butan-2-one (40ml)

and then NaOH (6.397 g, 0.15 mol) were



added. The mixture was heated at 50°C for 1 hour 45 minutes, and α -bromoisobutyric acid (7.520 g, 4.50 mmol) dissolved in butan-2-one (10 ml) was added. A further 300 ml of butan-2-one was then added to the suspension and was stirred at 50°C for 21 hours. Water (100 ml) was added to the reaction and the organic layer was collected. Ethyl acetate was added to the organic layer and was then washed with HCl (300 ml, 0.5 M) and water (300 ml). The organic layer was reduced in volume under vacuum and petroleum ether 40-60°C was added to precipitate the product. This was collected by vacuum filtration and then recrystallised from toluene.

Yield: 68 %

Appearance: White needle-like crystals

Purification: Recrystallised from toluene

^1H NMR (CDCl_3): 1.59 (s, 6H, $\text{C}(\text{CH}_3)_2$), 6.93 (d, $^3J = 8.8$ Hz, 2H, phenoxy 2-H and 6-H), 7.61 (d, $^3J = 8.6$ Hz, 2H, benzoyl 3-H and 5-H), 7.68-7.74 (m, 4H, phenoxy 3-H and 5-H and benzoyl 2-H and 6-H), 13.08 (broad s, OH, 1H).

^{13}C NMR (CDCl_3): 25.11 ($\text{C}(\text{CH}_3)_2$), 78.93 ($\text{C}(\text{CH}_3)_2$), 117.08 (phenoxy 2-C and 6-C), 128.60 (benzoyl 3-C and 5-C), 129.32 (phenoxy 3-C and 5-C), 131.19 (phenoxy 4-C), 136.30 (benzoyl 1-C), 137.02 (benzoyl 4-C), 159.54 (phenoxy 1-C), 174.42 (carboxylic acid $\text{C}=\text{O}$), 193.26 (ketone $\text{C}=\text{O}$).

Melting point: 181 - 183 °C

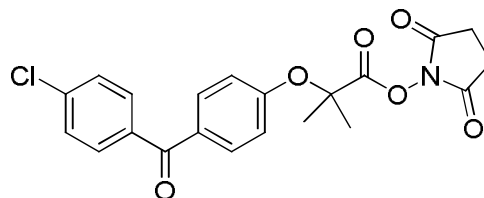
m/z : HRMS (ES-TOF) $\text{C}_{17}\text{H}_{14}\text{ClO}_4$ $[\text{MH}]^-$ calculated 317.0586; found 317.0593.

FT-IR (KBr): 2948 (amide NH), 2608, 2495 (CH₃ stretch), 1742 (carboxylic acid C=O), 1632 (ketone C=O), 1598 (aryl CH stretch), 893, 834 (*para* disubstituted aromatic ring).)

2,5-Dioxopyrrolidin-1-yl
methylpropanoate (47)

2-(4-(4-chlorobenzoyl)phenoxy)-2-

2-(4-(4-Chlorobenzoyl)phenoxy)-2-methylpropanoic acid (**10b**) (1.142 g, 3.58 mmol), was dissolved in anhydrous dichloromethane (50 ml).



N-Hydroxysuccinimide (1.031 g, 8.95 mmol) followed by EDC (1.03 g, 5.37 mmol) were then added to the flask. The reaction was stirred for 12 hours, and saturated sodium bicarbonate (30 ml) was then added to the reaction flask. The aqueous layer was extracted with ether (50 ml), and the organic layer was washed with water (50 ml) and brine (50 ml), and then dried with magnesium sulphate. The solvent was removed under reduced pressure, and the white solid dried under high vacuum for 1 hr to give 2,5-dioxopyrrolidin-1-yl 2-(4-(4-chlorobenzoyl)phenoxy)-2-methylpropanoate (Fenofibrate-OSu).

Yield: 68%

Appearance: White Solid

Purification: Used without further purification

Melting Point: 100 - 101 °C

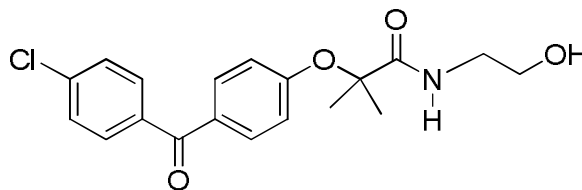
¹H NMR (CDCl₃): 1.81 (s, 6H, C(CH₃)₂), 2.86 (m, ³*J* = 4.1 Hz, 2H, succinimide CH₂), 7.07 (d, ³*J* = 8.6 Hz, 2H, phenoxy 2-H and 6-H), 7.45 (d, ³*J* = 8.6 Hz, 2H, benzoyl 3-H and 5-H) 7.71 (d, ³*J* = 8.6 Hz, 2H, phenoxy 3-H and 5-H), 7.78 (d, ³*J* = 8.9 Hz, 2H, benzoyl 2-H and 6-H).

^{13}C NMR (CDCl_3): 25.63 ($\text{C}(\text{CH}_3)_2$), 30.95 (succinimidyl CH_2), 78.56 ($\text{C}(\text{CH}_3)_2$), 118.52 (phenoxy 2-C and 6-C), 128.58 (benzoyl 3-C and 5-C), 131.24 (phenoxy 3-C and 5-C), 131.42 (phenoxy C-4), 132.06 (benzoyl 2-C and 6-C), 136.28 (benzoyl C-1), 138.51 (benzoyl C-4), 158.48 (phenoxy C-1), 168.74 (succinimidyl $\text{C}=\text{O}$), 169.38 (ester $\text{C}=\text{O}$), 194.50 (ketone $\text{C}=\text{O}$).

m/z : HRMS (ES-TOF $^+$) $\text{C}_{21}\text{H}_{18}\text{ClNO}_6$ $[\text{MH}]^+$ calculated 416.0895; found 416.1038.

N*-(2-Hydroxyethyl)-2-(4-(4-chlorobenzoyl)phenoxy)-2-methylpropanamide (48a)

Following General Method A, Fenofibrate-OSu (0.416 g, 1 mmol), and ethanolamine (0.060 ml, 1.000 mmol) in DCM (20 ml) were reacted for 5 minutes to afford **48a** (0.350 g, 0.967 mmol).



Yield: 97%

Appearance: Colourless Oil

Purification: Used without further purification

^1H NMR (CDCl_3): 1.56 (s, 6H, $\text{C}(\text{CH}_3)_2$), 3.17 (broad s, OH, 1H), 3.42 (d of t, $^3J = 5.8$ Hz, $^3J = 4.8$ Hz 2H, CH_2 next to OH), 3.64 (t, $^3J = 5.0$ Hz, 2H, CH_2 next to NH), 6.93 (d, $^3J = 8.9$ Hz, 2H, phenoxy 2H and 6H), 7.08 (t, $^3J = 6.1$ Hz, 1H, NH), 7.41 (d, $^3J = 8.6$ Hz, 2H, benzoyl 3-H and 5-H), 7.65 (d, $^3J = 8.6$ Hz, 2H, phenoxy 3-H and 5-H), 7.68 (d, $^3J = 8.6$ Hz, 2H, benzoyl 2-H and 6-H).

^{13}C NMR (CDCl_3): 25.22 ($\text{C}(\text{CH}_3)_2$), 42.18 (CH_2NH), 61.75 (CH_2OH), 81.89 ($\text{C}(\text{CH}_3)_2$), 119.62 (phenoxy 2-C and 6-C), 128.62 (benzoyl 3-C and 5-C), 131.23 (phenoxy 3-C and 5-C), 131.50 (phenoxy C-4), 131.87 (benzoyl 2-C

and 6-C), 135.99 (benzoyl C-1) 138.71 (benzoyl C-4), 158.57 (phenoxy C-1), 175.06 (ester C=O), 194.40 (ketone C=O).

m/z: HRMS (ES-TOF⁺) C₁₉H₂₀ClNO₄ [MH]⁺ calculated 362.1154; found 362.1143.

HPLC: System 3, R_t = 2.65 minutes

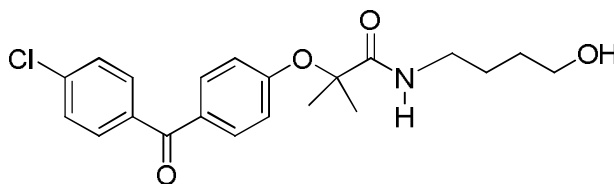
System 4, R_t = 2.67 minutes

*Synthesised by Dr Barrie Kellam

N*-(2-Hydroxybutyl)-2-(4-(4-chlorobenzoyl)phenoxy)-2-methylpropanamide (48b)

Following General Method A, Fenofibrate-OSu (0.208 g, 0.5 mmol), and 4-amino-1-butanol (0.055 ml, 0.600 mmol) in DCM (20 ml) were reacted for 5 minutes to afford **48b**

(0.175g, 0.449 mmol).



Yield: 90%

Appearance: Colourless Oil.

Purification: Used without further purification.

¹H NMR (CDCl₃): 1.47-1.63 (m, 4H, CH₂CH₂NH, CH₂CH₂OH), 1.61 (s, 6H, C(CH₃)₂), 2.19 (broad s, 1H, OH), 3.33 (d of t, ³J = 5.9 Hz, ³J = 5.9 Hz, 2H, CH₂NH) 3.61 (t, 2H, CH₂OH ³J = 5.9 Hz), 6.75 (t, ³J = 5.9 Hz, 1H, NH) 6.96 (d, ³J = 9.0 Hz, 2H, phenoxy 2-H and 6-H), 7.45 (d, ³J = 9.1 Hz, 2H, benzoyl 3-H and 5-H), 7.72 (d, ³J = 9.1 Hz, 2H, phenoxy 3-H and 5-H), 7.74 (d, ³J = 9.1 Hz, 2H, benzoyl 2-H and 6-H).

¹³C NMR (CDCl₃): 25.30 (C(CH₃)₂), 26.09 (CH₂CH₂OH), 29.74 (CH₂CH₂NH), 39.26 (CH₂NH), 62.20 (CH₂OH), 81.88 (C(CH₃)₂), 119.31 (phenoxy 2-C and 6-C), 131.23 (phenoxy 3-C and 5-C) 131.40 (phenoxy C-4),

131.88 (benzoyl 2-C and 6-C), 136.04 (benzoyl C-1), 138.66 (benzoyl C-4), 158.63 (phenoxy C-1), 174.03 (amide C=O), 194.32 (ketone C=O).

m/z: HRMS (ES-TOF⁺) C₂₁H₂₄ClNO₄ [MH]⁺ calculated 390.1467; found 390.150

HPLC: System 3, R_t = 2.70 minutes

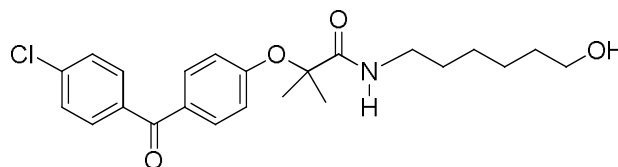
System 4, R_t = 2.73 minutes

*Synthesised by Dr Barrie Kellam

N*-(2-Hydroxyhexyl)-2-(4-(4-chlorobenzoyl)phenoxy)-2-methylpropanamide (48c)

Following General Method A,

Fenofibrate-OSu (0.208 g, 0.5 mmol), and 6-amino-1-hexanol



(0.070 g, 0.600 mmol) in DCM (20 ml) were reacted for 5 minutes to afford **48c** (0.167 g, 0.400 mmol).

Yield: 80%

Appearance: Colourless Oil.

Purification: Used without further purification.

¹H NMR (CDCl₃) 1.20-1.31 (m, 2H, CH₂-(CH₂)₂-NH). 1.32-1.41 (m, 2H, CH₂-(CH₂)₂-OH) 1.44-1.57 (m, 4H, CH₂-(CH₂)₂CH₂-OH), 1.63 (s, 6H, C(CH₃)₂), 3.31 (d of t, ³J = 6.8 Hz, ³J = 6.2 Hz, 2H, CH₂-NH) 3.61 (t, ³J = 6.2 Hz, 2H, CH₂OH,), 6.50 (t, ³J = 5.6 Hz 1H, NH,), 6.95 (d, ³J = 9.0 Hz, 2H, phenoxy 2H and 6H), 7.48 (d, ³J = 8.5 Hz, 2H, benzoyl 3H and 5H), 7.74 (d, ³J = 8.5 Hz, 2H, phenoxy 3H and 5H), 7.76 (d, ³J = 9.0Hz, 2H, benzoyl 2H and 6H).

¹³C NMR (CDCl₃): 25.44 (C(CH₃)₂), 25.47 (CH₂CH₂CH₂OH), 26.71 (CH₂CH₂CH₂NH), 29.61 (CH₂CH₂NH) 32.76 (CH₂CH₂NH), 39.48 (CH₂NH), 62.83 (CH₂OH), 82.06 (C(CH₃)₂), 119.44 (phenoxy 2-C and 6-C), 128.85 (benzoyl 3-C and 5-C), 131.43 (phenoxy 3-C and 5-C), 131.58 (phenoxy C-4), 132.07 (benzoyl 2-C and 6-C), 136.23 (benzoyl C-1), 138.88 (benzoyl C-4), 158.79 (phenoxy C-1), 174.05 (amide C=O), 194.53 (ketone C=O).

***m/z*:** HRMS (ES-TOF⁺) C₂₃H₂₈ClNO₄ [MH]⁺ calculated 418.1780; found 418.1783.

HPLC: System 3, R_t = 2.84 minutes

System 4, R_t = 2.83 minutes

*Synthesised by Dr Barrie Kellam

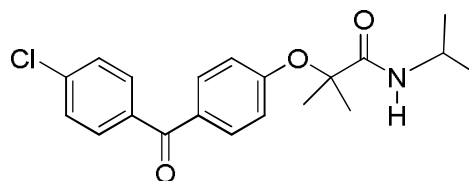
N*-Isopropyl-2-(4-(4-chlorobenzoyl)phenoxy-2-methylpropanamide (48d)

Following General Method A, Fenofibrate-OSu (0.208 g, 0.5 mmol) and Isopropylamine (0.086 ml, 1.0 mmol) in DCM (20 ml) were reacted for 5 minutes to afford **48d** (0.171 g, 0.475 mmol).

Yield: 95%

Appearance: Colourless Oil

¹H NMR (CDCl₃): 1.09 (d, ³J = 6.3 Hz, 6H, isopropyl 2 x CH₃), 1.56 (s, 6H, C(CH₃)₂),



4.01-4.14 (m, 1H, isopropyl CH), 6.21 (d, ³J = 7.2 Hz, 1H, NH), 6.93 (d, ³J = 8.8 Hz, 2H, phenoxy 2-H and 6-H), 7.44 (d, ³J = 8.8 Hz, 2H, benzoyl 3-H and 5-H), 7.68 (d, ³J = 8.8 Hz, 2H, phenoxy 3-H and 5-H), 7.71 (d, ³J = 8.8 Hz, 2H, benzoyl 2-H and 6-H).

¹³C NMR (CDCl₃): 22.72 (isopropyl 2xCH₃), 25.40 (C(CH₃)₂), 41.61 (isopropyl CH), 82.01 (C(CH₃)₂), 119.53 (phenoxy 2-C and 6-C), 128.81

(benzoyl 3-C and 5-C), 131.40 (phenoxy 3-C and 5-C), 131.59 (phenoxy C-4), 132.05 (benzoyl 2-C and 6-C), 136.33 (benzoyl C-1), 138.79 (benzoyl C-4), 158.80 (phenoxy C-1), 173.12 (amide C=O), 194.43 (ketone C=O).

m/z: HRMS (ES-TOF⁺) C₂₀H₂₂ClNO₃ [MH]⁺ calculated 360.1361; found 360.1398.

HPLC: System 3, R_t = 3.00 minutes

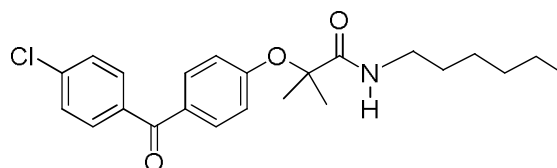
System 4, R_t = 2.99 minutes

*Synthesised by Dr Barrie Kellam

N*-Hexyl-2-(4-(4-chlorobenzoyl)phenoxy)-2-methylpropanamide (48e)

Following General Method A, Fenofibrate-OSu (0.208 g, 0.500 mmol) and hexylamine (0.132 ml, 1.0 mmol) in DCM (20 ml) were reacted for 5 minutes to afford **48e**.

Appearance: White Solid



¹H NMR (CDCl₃) 0.81 (t, ³*J* =

6.3 Hz, 3H, CH₃-(CH₂)₅-NH), 1.21 (m, 6H, CH₃-(CH₂)₃-(CH₂)₂-NH), 1.39-1.49 (m, 2H, CH₂-CH₂-NH), 1.57 (s, 6H, C(CH₃)₂), 3.25 (d of t, ³*J* = 6.4 Hz, ³*J* = 7.1 Hz, 2H, CH₂-NH), 6.47 (t, ³*J* = 7.1 Hz, 1H, NH), 6.93 (d, ³*J* = 8.7 Hz, 2H, phenoxy 2-H and 6-H), 7.41 (d, 2H, ³*J* = 8.6 Hz, benzoyl 3H and 5H), 7.67 (d, ³*J* = 8.4 Hz, 2H, phenoxy 3-H and 5-H), 7.71 (d, ³*J* = 8.7 Hz, 2H, benzoyl 2-H and 6-H).

¹³C NMR (CDCl₃): 13.99 (hexyl CH₃), 22.51 (CH₂CH₃), 25.28 (C(CH₃)₂), 26.50 (CH₂CH₂CH₂NH), 29.38 (CH₂CH₂NH), 31.39 (CH₂CH₂CH₃), 39.49 (CH₂NH), 82.05 (C(CH₃)₂), 119.29 (phenoxy 2-C and 6-C), 128.60 (benzoyl 3-C and 5-C), 131.18 (phenoxy 3-C and 5-C), 131.36 (phenoxy C-4), 131.86

(benzoyl 2-C and 6-C), 136.12 (benzoyl C-1), 138.59 (benzoyl 4-C), 158.65 (phenoxy 1-C), 173.77 (amide C=O), 194.16 (ketone C=O).

HPLC: System 3, R_t = 3.23 minutes

System 4, R_t = 3.16 minutes

m/z: MS (API) $C_{23}H_{29}O_3NCl$ $[MH]^+$ calculated 402.2, found 402.5

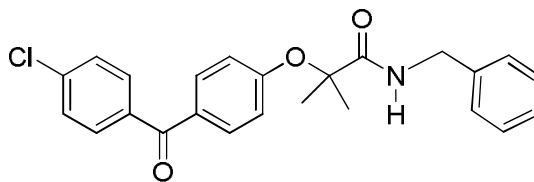
*Synthesised by Dr Barrie Kellam

***N*-Benzyl-2-[4-(4-chloro-benzoyl)-phenoxy]-2-methyl-propionamide (48f)**

Following General Method A, Fenofibrate-OSu (0.201 g, 0.483 mmol) and benzylamine (0.104 ml, 0.967 mmol) in DCM (20 ml) were reacted for 1 hour to afford **48f** (0.138 g, 0.339 mmol).

Yield: 70%

Appearance: White Solid



1H NMR ($CDCl_3$) 1.63 (s, 6H,

$C(CH_3)_2$), 4.48 (d, $^3J = 5.9$ Hz, 2H, benzyl CH_2), 6.77 (t, $^3J = 5.9$ Hz, 1H, NH), 6.92 (d, $^3J = 8.7$ Hz, 2H, phenoxy 2-H and 6-H), 7.21-7.24 (m, 3H, benzyl 2-H, 6-H and 4-H), 7.26-7.32 (m, 2H, benzyl 2-H and 6-H and benzyl 4-H), 7.45 (d, $^3J = 8.5$ Hz, 2H, benzoyl 3-H and 5-H), 7.68-7.72 (m, 4H, phenoxy 2-H and 6-H, and benzoyl 3-H and 5-H).

^{13}C NMR ($CDCl_3$) 25.47 ($C(CH_3)_2$), 43.74 (benzyl CH_2), 82.14 ($C(CH_3)_2$), 119.66 (phenoxy 2-C and 6-C), 127.8 (benzyl 6-C), 127.96 (benzyl 2-C and 6-C), 128.82 (benzyl 3-C and 5-C), 128.92 (benzoyl 3-C and 5-C), 131.41 (phenoxy 3-C and 5-C), 131.72 (phenoxy C-4), 132.05 (benzoyl 2-C and 6-C), 136.28 (benzoyl 1-C), 138.05 (benzyl 1-C), 138.85 (benzoyl 4-C), 158.62 (phenoxy 1-C), 174.06 (amide C=O), 194.39 (ketone C=O).

Melting point: 131.2 - 132.9°C

HPLC: System 1, $R_t = 7.15$ minutes.

System 2, $R_t = 19.08$ minutes.

m/z : HRMS (ES-TOF⁺) $C_{24}H_{22}O_3NCl$ $[MH]^+$ calculated 408.1361; found 408.1647.

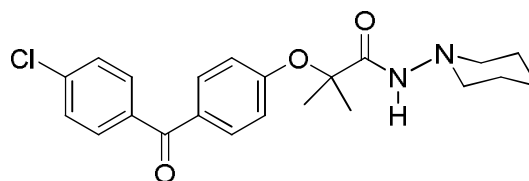
FT-IR (KBr): 1503 (Arene), 1599 (Arene), 1658 C=O (amide), 2938 alkane, 3359 N-H (amide).

1-Piperidinyl-2-(4-(4-chlorobenzoyl)phenoxy)-2-methylpropanamide (48g)

Following General Method A, Fenofibrate-OSu (0.200 g, 0.481 mmol) and 1-aminopiperidine (0.130 ml, 1.202 mmol) in DCM (10 ml) were reacted for 2 hours 45 minutes to afford **48g** (0.082 g, 0.204 mmol).

Yield: 42%

Appearance: Yellow-white solid



1H NMR ($CDCl_3$): 1.23-1.27 (m, 2H

piperidinyl 4- CH_2), 1.61 (s, 6H, $C(CH_3)_2$), 1.66-1.71 (m, 4H, piperidinyl 3- CH_2 and 5- CH_2), 2.68-2.70 (m, 4H, piperidinyl 2- CH_2 and 6- CH_2), 6.97 (d, $^3J = 8.8$ Hz, 2H, phenoxy 2-H and 6-H) 7.11 (s, NH , 1H), 7.45 (d, $^3J = 8.6$ Hz, 2H, benzoyl 3-H and 5-H), 7.71 (d, $^3J = 8.6$ Hz, 2H, phenoxy 2-H and 6-H), 7.75 (d, $^3J = 8.6$ Hz, 2H, benzoyl 2-H and 6-H).

^{13}C NMR ($CDCl_3$): 23.22 ($C(CH_3)_2$), 25.28 (CH_2 , piperidinyl C-4), 25.39 (CH_2 , piperidinyl 3-C and 5-C), 56.82 (CH_2 , piperidinyl C-2 and C-6), 81.64 ($C(CH_3)_2$), 119.16 (phenoxy 2-C and 6-C), 128.68 (benzoyl 3-C and 5-C), 131.26 (phenoxy 3-C and 5-C), 131.50 (phenoxy C-4), 131.93 (benzoyl 2-C

and 6-C), 136.13 (benzoyl C-1), 138.71 (benzoyl C-4), 158.48 (phenoxy C-1), 170.74 (amide C=O), 194.27 (ketone C=O).

Melting point: 152.9 - 153.8°C

HPLC: System 1, R_t = 5.97 minutes.

System 2, R_t = 18.22 minutes

m/z : HRMS (ES-TOF⁺) $C_{22}H_{25}ClN_2O_3$ [MH]⁺ calculated 401.1626; found 401.1643.

FT-IR (KBr): 1504 (Arene), 1598 (Arene), 1684 C=O (amide), 2856 (alkane), 2941 (alkane), 3278 N-H (amide).

***N*-Morpholino-2-(4-(4-chlorobenzoyl)phenoxy)-2-methylpropanamide (48h)**

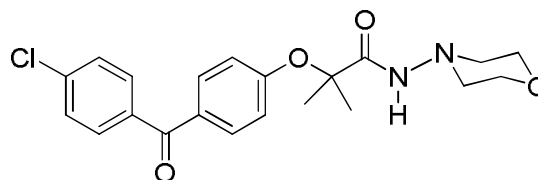
Following General Method A, Fenofibrate-OSu (0.208 g, 0.499 mmol) and 4-aminomorpholine (0.097 ml, 0.998 mmol) in DCM (10 ml) were reacted for 31 hours and 25 minutes to afford **48h** (0.091 g, 0.227 mmol).

Yield: 45%

Appearance: White solid

Purification:

Column



chromatography using 80 % EtOAc / 20 % hexane, and by preparative HPLC.

¹H NMR (CDCl₃) 1.61 (s, 6H, C(CH₃)₂), 2.80 (t, ³*J* = 4.6 Hz, 4H, morpholino 3-CH₂ and 5-CH₂), 3.80 (t, ³*J* = 4.6 Hz, 4H, morpholino 2-CH₂ and 6-CH₂), 6.98 (d, ³*J* = 8.6 Hz, 2H, phenoxy 2-H and 6-H) 7.21 (s, NH, 1H), 7.46 (d, ³*J* = 8.6 Hz, 2H, benzoyl 3-H and 5-H), 7.71 (d, ³*J* = 8.6 Hz, 2H, phenoxy 3-H and 5-H), 7.75 (d, ³*J* = 8.8 Hz, 2H, benzoyl 2-H and 6-H)

¹³C NMR (CDCl₃) 25.32 (C(CH₃)₂), 55.71 (morpholino 3-C and 5-C), 66.38 (morpholino 2-C and 6-C) 81.72 (C(CH₃)₂), 119.39 (phenoxy 2-C and 6-C)

128.70 (benzoyl 3-C and 5-C), 131.25 (phenoxy 3-C and 5-C), 131.76 (phenoxy C-4), 131.95 (benzoyl 2-C and 6-C), 136.06 (benzoyl C-1), 138.77 (benzoyl C-4), 158.26 (phenoxy C-1), 171.22 (amide C=O) 194.21 (ketone C=O).

Melting point: 145.6 - 146.1°C

HPLC: System 1, R_t = 5.27 minutes.

System 2, R_t = 17.03 minutes

m/z : HRMS (ES-TOF⁺) $C_{21}H_{23}ClN_2O_4$ [MH]⁺ calculated 403.1419; found 403.1430.

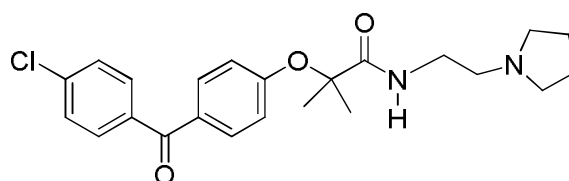
FT-IR (KBr): 1504 (Arene), 1598 (Arene), 1659 C=O (amide), 1681 (aryl ketone), 2844 alkane, 3207 N-H (amide), 3359 N-H (amide).

***N*-(2-Pyrrolidino)ethyl-2-(4-(4-chlorobenzoyl)phenoxy)-2-methylpropanamide (48i)**

Following General Method A, Fenofibrate-OSu (0.214 g, 0.516 mmol) and 1-(2-aminoethyl) pyrrolidine (0.130 ml, 1.029 mmol) in DCM (10 ml) were reacted for 24 hours to afford **48h** (0.091 g, 0.227 mmol).

Yield: 75%

Appearance: Yellow-white solid.



Purification: Used without further purification.

¹H NMR (CDCl₃) 1.62 (s, 6H, dimethyl CH₃), 1.68 (broad s, 4H, pyrrolidine CH₂), 2.42 (broad s, 2H, pyrrolidine CH₂), 2.58 (broad s, 2H, ethylene CH₂), 3.39-3.40 (m, 2H, ethylene CH₂), 6.97(d, ³*J* = 8.5 Hz, 2H, phenoxy 2H and 6H), 7.46 (d, ³*J* = 8.5 Hz 2H, benzoyl 3H and 5H), 7.71 (d, ³*J* = 8.5 Hz, 2H, phenoxy 2H and 6H), 7.73 (d, ³*J* = 8.5 Hz, 2H, benzoyl 2H and 6H).

^{13}C NMR (CDCl_3) 23.76 (pyrrolidine C-3 and C-4), 25.64 ($\text{C}(\text{CH}_3)_2$), 38.11 (ethyl CH_2NH), 54.09 (pyrrolidine C-2 and C-5), 54.61 (ethyl $\text{CH}_2\text{-N}$), 82.05 ($\text{C}(\text{CH}_3)_2$), 119.32 (phenoxy 2-C and 6-C), 128.92 (benzoyl 3-C and 5-C), 131.46 (phenoxy 3-C and 5-C) 131.50 (phenoxy C-4), 132.15 (benzoyl C-2 and C-6), 136.49 (benzoyl C-1) 138.89 (benzoyl C-4) 159.22 (phenoxy C-1) 174.41 (amide C=O) 194.53 (ketone C=O).

Melting point: 100.2-101.5°C

HPLC: System 1, R_t = 4.03 minutes

System 2, R_t = 12.00 minutes

m/z : HRMS (ES-TOF^+) $\text{C}_{23}\text{H}_{27}\text{ClN}_2\text{O}_3$ $[\text{MH}]^+$ calculated 415.1783; found 415.1762.

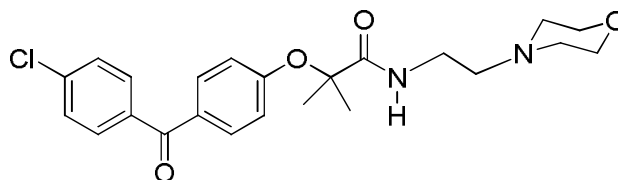
FT-IR (KBr): 1511 (Arene), 1599 (Arene), 1679 C=O (amide), 2803 (alkane), 2828 (alkane), 2873 (alkane), 2931 (alkane), 2961 (alkane), 2978 (alkane), 3389 N-H (amide).

***N*-(2-Morpholino)-ethyl-2-(4-(4-chlorobenzoyl)phenoxy)-2-methylpropanamide (48j)**

Following General Method A, Fenofibrate-OSu (0.1019 g, 0.245 mmol) and 4-(2-aminoethyl)-morpholine (0.064 ml, 0.490 mmol) in DCM (10 ml) were reacted for 2 hours and 40 minutes to afford **48j** (0.064 g, 0.147 mmol).

Yield: 60%

Appearance: Yellow-white solid.



Purification: Used without further purification.

^1H NMR (CDCl_3) 1.63 (s, 6H, dimethyl CH_3), 2.36-2.48 (m, 4H, morpholino CH_2), 3.41-3.54 (m, 4H, morpholino CH_2), 6.97 (d, 3J = 8.5 Hz, 2H, phenoxy

2-H and 6-H), 7.46 (d, $^3J = 8.5$ Hz, 2H, benzoyl 3-H and 5-H), 7.70 (d, $^3J = 8.5$ Hz, 2H, phenoxy 2-H and 6-H), 7.74 (d, $^3J = 8.5$ Hz, 2H, benzoyl 2-H and 6-H).

^{13}C NMR (CDCl_3) 25.58 ($\text{C}(\text{CH}_3)_2$), 35.56 (ethyl CH_2NH), 53.34 (morpholino 3-C and 5-C) 57.05 (ethyl CH_2NH) 66.50 (morpholino 2-C and 6-C) 81.98 ($\text{C}(\text{CH}_3)_2$) 119.17 (phenoxy 2-C and 6-C), 128.94 (benzoyl 3-C and 5-C) 131.47 (phenoxy 3-C and 5-C), 132.15 (benzoyl 2-C and 6-C) 136.36 (benzoyl 1-C) 138.95 (benzoyl 4-C), 159.15 (phenoxy 1-C), 174.42 (amide $\text{C}=\text{O}$), 194.42 (ketone $\text{C}=\text{O}$).

Melting point: 93.8-94.7°C

HPLC: System 1, $R_t = 3.93$ minutes

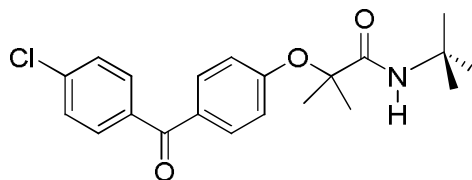
System 2, $R_t = 12.03$ minutes

m/z : HRMS (ES-TOF^+) $\text{C}_{23}\text{H}_{27}\text{ClN}_2\text{O}_4$ $[\text{MH}]^+$ calculated 431.1732; found 431.1778.

FT-IR (KBr): 1511 (Arene), 1600 (Arene), 1677 $\text{C}=\text{O}$ (amide), 2815 (alkane), 2854 (alkane), 2937 (alkane), 2952 (alkane), 2968 (alkane), 2978 (alkane), 3397 N-H (amide).

***N-tert*-Butyl-2-(4-(chlorobenzoyl)phenoxy)-methylpropanamide (48k)**

Following General Method A, Fenofibrate-OSu (0.127 g, 0.304 mmol) and *tert*-butylamine (0.045 ml, 0.608 mmol) in DCM (10 ml) were reacted for 22 hours 40 minutes to afford **48k** (0.089 g, 0.238 mmol).



Yield: 78%

Appearance: Pale orange-yellow solid.

Purification: Used without further purification.

¹H NMR (CDCl₃) 1.34 (s, 9H, tert-butyl CH₃), 1.57 (s, 6H, dimethyl CH₃), 6.96 (d, ³J = 8.8 Hz, 2H, phenoxy 2H and 6H), 7.46 (d, ³J = 8.8 Hz, 2H, benzoyl 3-H and 5H), 7.72 (d, ³J = 8.8 Hz, 2H, phenoxy 2H and 6H) 7.76 (d, ³J = 8.8 Hz, 2H, benzoyl 2H and 6H).

¹³C NMR (CDCl₃) 25.10 (C(CH₃)₂), 28.45 (C(CH₃)₃), 51.04 (C(CH₃)₃) 81.95 (C(CH₃)₂), 119.06 (phenoxy 2-C and 6-C) 128.56 (benzoyl 3-C and 5-C) 131.14 (phenoxy 3-C and 5-C), 131.26 (phenoxy C-4), 131.80 (benzoyl 2-C and 6-C) 136.13 (benzoyl 1-C) 138.54 (benzoyl 4-C), 158.64 (phenoxy 1-C), 173.01 (amide C=O), 194.18 (ketone C=O).

Melting point: 128.1 - 129.0 °C

HPLC: System 1, R_t = 7.20 minutes

System 2, R_t = 19.49 minutes

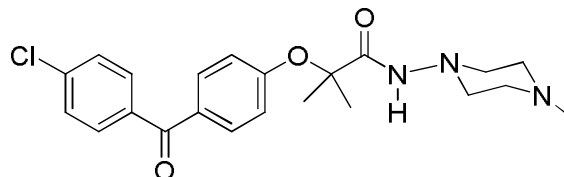
m/z: HRMS (ES-TOF⁺) [MH]⁺ C₂₃H₂₇ClN₂O₄ calculated 374.1517; found 374.1512.

FT-IR (KBr): 1503 (Arene), 1599 (Arene), 1672 C=O (amide), 2933 (alkane), 2976 (alkane), 3371 N-H (amide), 3359 N-H (amide).

***N*-(4-Methylpiperazinyl)-2-(4-(4-chlorobenzoyl)phenoxy)-2-methylpropanamide (48l)**

To a suspension of fenofibric

acid (10b) (0.0507g, 0.157mmol) in toluene (7ml),



thionyl chloride (0.037g, 0.314mmol) was added. The mixture was heated to 95°C for 1 hour 15 minutes. The solvent and excess thionyl chloride were

removed under high vacuum which gave an off white solid. This was used directly in the next step to form the amide. The acid chloride was redissolved in dry dichloromethane (7ml) and 1-amino-4-methyl-piperazine was added. The flask was covered in foil to prevent light entering and the reaction was left stirring for 1 hour 25 minutes. The solvent was then removed under vacuum.

Yield: 64%

Appearance: Yellow-white solid

Purification: Column chromatography 95 % DCM / 5 % MeOH to 80 % DCM / 20 % MeOH over 25 minutes.

¹H NMR (CDCl₃): 1.61 (s, 6H, C(CH₃)₂), 2.29 (s, 3H, 4-methylpiperazine CH₃), 2.57 (broad s, 4H, 4-methylpiperazine CH₂), 2.79 (broad s, 4H, 4-methylpiperazine CH₂), 6.98 (d, ³J = 8.8 Hz, 2H, phenoxy 2-H and 6-H), 7.11 (s, 1H, NH), 7.46 (d, ³J = 8.8 Hz, 2H, benzoyl 3-H and 5-H), 7.71 (d, ³J = 8.8 Hz, 2H, phenoxy 3-H and 5-H), 7.75 (d, ³J = 8.8 Hz, 2H, 2-H and 6-H).

¹³C NMR (CDCl₃): 25.64 (C(CH₃)₂), 46.00 (piperazine CH₃), 54.50 (piperazine 2-C and 6-C), 55.50 (piperazine 3-C and 5-C), 81.99 (C(CH₃)₂), 119.62 (phenoxy 2-C- and 6-C), 128.97 (benzoyl 3-C and 5-C), 131.54 (phenoxy 3-C and 5-C), 131.95 (phenoxy 4-C), 132.23 (benzoyl 2-C and 6-C), 136.39 (benzoyl 1-C), 139.01 (benzoyl 1-C), 158.64 (phenoxy 4-C), 171.34 (amide C=O) 194.18 (ketone C=O).

Melting point: 149.7-150.8 °C

HPLC: System 1, R_t = 3.82 minutes.

System 2, R_t = 11.92 minutes.

m/z: HRMS (ES-TOF⁺) C₂₂H₂₆ClN₃O₃ [MH]⁺ calculated 416.1735; found 416.1759.

FT-IR (KBr): 1505 (Arene), 1597 (Arene), 1692 C=O (amide), 2767 (alkane), 2794 (alkane), 2842 (alkane), 2874 (alkane) 2938 (alkane), 3359 N-H (amide).

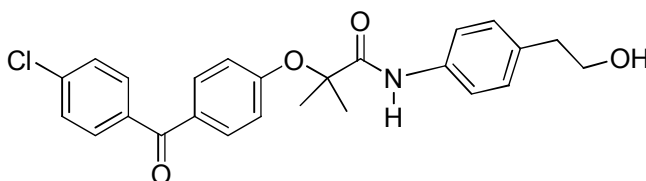
***N*-(4-(2-Hydroxyethyl)phenyl)-2-(4-(4-chlorobenzoyl)phenoxy)-2-methylpropanamide (48m)**

To a suspension of fenofibric acid (**10b**) (0.0507, 0.162mmol) an excess of thionyl chloride (5ml) was

added. The mixture was

heated at 60°C for 1 hour

15 minutes. The thionyl



chloride was removed under high vacuum which gave an off white solid (0.0413g, 0.122mmol). This was used directly in the next step to form the amide. The acid chloride was redissolved in dry dichloromethane (3ml), and cooled to 0°C. 2-(4-aminophenyl)ethanol and triethylamine (0.016ml) were dissolved in dichloromethane (4ml) and DMF (0.2ml) was added as the amine was insoluble. The mixture of 2-(4-aminophenyl)ethanol and triethylamine was then slowly added to the acid chloride and the mixture was stirred for 1 hour 15 minutes. The reaction mixture was washed with 2M HCl (5ml) and the solvent was removed under vacuum.

Yield: 38%

Appearance: Yellow-white solid

Purification: Column chromatography 10 % MeOH : 90 % DCM

¹H NMR (CDCl₃): 1.62 (s, 6H, C(CH₃)₂), 2.84 (t, ³J = 6.7 Hz, 2H, ethylene CH₂ next to phenyl), 3.50 (s, 1H, OH) 3.86 (d of t, ³J = 5.2 Hz, ³J = 6.6 Hz, 2H, ethylene CH₂ next to NH), 7.04 (d, ³J = 8.2 Hz, phenoxy 2-H and 6-H), 7.21 (d, ³J = 8.2 Hz, phenyl 2-H and 6-H), 7.46 (d, ³J = 8.2 Hz, benzoyl 3-H

and 5-H), 7.48 (d, $^3J = 8.2$ Hz, phenyl 3-H and 5-H), 7.71 (d, $^3J = 8.2$ Hz, phenoxy 3-H and 5-H), 7.77 (d, $^3J = 8.2$ Hz, benzoyl 2-H and 6-H), 8.25 (s, 1H, NH).

^{13}C NMR (CDCl_3): 25.11($\text{C}(\text{CH}_3)_2$), 38.59 ($\text{CH}_2\text{CH}_2\text{OH}$), 63.61 ($\text{CH}_2\text{CH}_2\text{OH}$), 82.37 ($\text{C}(\text{CH}_3)_2$), 119.93 (phenoxy 2-C and 6-C), 120.20 (phenyl 3-C and 5-C), 128.65 (benzoyl 3-C and 5-C), 129.64 (phenyl 2-C and 6-C), 131.22 (phenoxy 3-C and 5-C), 132.00 (phenoxy 4-C), 132.07 (benzoyl 2-C and 6-C), 135.07 (phenyl 1-C), 135.67 (phenyl 4-C), 136.00 (benzoyl 1-C), 138.72 (benzoyl 4-C), 158.72 (phenoxy 1-C), 172.16 (amide $\text{C}=\text{O}$), 194.18 (ketone $\text{C}=\text{O}$).

Melting point: 61.0 - 62.3 °C

HPLC: System 1, $R_t = 6.24$ minutes.

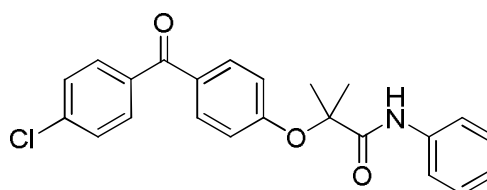
System 2, $R_t = 18.02$ minutes.

m/z : HRMS (ES-TOF $^+$) $\text{C}_{25}\text{H}_{24}\text{ClNO}_4$ $[\text{MH}]^+$ calculated 438.1467; found 438.1483.

FT-IR (KBr): 1505 (Arene), 1598 (Arene), 1669 $\text{C}=\text{O}$ (amide), 2936 (alkane), 3395 N-H (amide).

***N*-(Phenyl)-2-(4-(4-chlorobenzoyl) phenoxy)-2-methylpropanamide (48n)**

Following General Method B, Fenofibric acid (0.200 g, 0.627 mmol) and an excess of thionyl chloride (7ml) were reacted for 1 hours and 30 minutes to afford the corresponding acid chloride (0.211 g, 0.625 mmol). The acid chloride was then reacted directly with aniline (0.117g, 0.625 mmol) and triethylamine (0.118 ml, 0.625 mmol) in DCM (10 ml) to afford **49n**.



Yield: 66%

Appearance: Yellow-orange solid

¹H NMR (CDCl₃): 1.69 (s, 6H, C(CH₃)₂), 7.05 (d, ³J = 8.8 Hz, 2H, phenoxy 2-H and 6-H), 7.14 (dd, ³J = 7.4 Hz, ⁴J = 7.4 Hz, 1H, phenyl 4-H), 7.34 (dd, ³J = 7.4 Hz and ⁴J = 7.4 Hz, 2H, phenyl 3-H and 5-H), 7.45 (d, ³J = 8.6 Hz, 2H, benzoyl 3-H and 5-H), 7.52-7.56 (m, 2H, phenyl 2-H and 6-H), 7.72 (d, ³J = 8.6 Hz, 2H, phenoxy 3-H and 5-H), 7.77 (d, ³J = 8.8 Hz, 2H, benzoyl 2-H and 6-H), 8.28 (s, 1H, NH).

¹³C NMR (CDCl₃): 25.45 (C(CH₃)₂), 82.75 (C(CH₃)₂), 120.22 (phenoxy 2-C and 6-C), 120.36 (phenyl 2-C and 6-C), 125.07 (phenyl 4-C), 128.99 (benzoyl 3-C and 5-C), 129.46 (phenoxy 3-C and 5-C), 131.57 (phenoxy 4-C), 132.35 (benzoyl 2-C and 6-C), 132.45 (phenoxy 4-C), 136.32 (benzoyl 1-C), 137.56 (benzoyl 4-C), 139.06 (phenyl 1-C), 158.51 (phenoxy 1-C), 172.51 (amide C=O), 194.52 (ketone C=O).

Melting point: 144 – 146 °C

HPLC: System 1, R_t = 7.15 minutes

System 2, R_t = 19.30 minutes

System 3, R_t = 3.12 minutes

System 4, R_t = 3.11 minutes

m/z: HRMS (ES-TOF⁺) C₂₃H₂₀ClNO₃ [MH]⁺ calculated 394.1204; found 394.1299.

N-(2-Fluorobenzyl)-2-(4-(4-chlorobenzoyl)phenoxy)-2-methylpropanamide (50a)

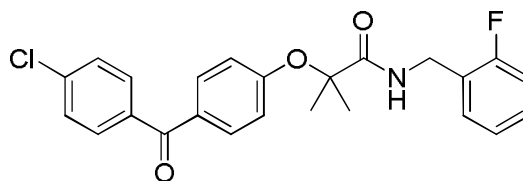
Following General Method B, Fenofibric acid (0.112 g, 0.350 mmol) and an excess of thionyl chloride (5ml) were refluxed for 1 hours and 30 minutes to afford the corresponding acid chloride (0.118 g, 0.350 mmol). The acid

chloride was then reacted directly with 2-fluorobenzylamine (0.04 ml, 0.350 mmol) and triethylamine (0.054 ml, 0.385 mmol) in DCM (6 ml) to afford **50a**.

Yield: 47%

Appearance: Yellow-white solid

Purification: PLC, 3% EtOH/ 97%



DCM

¹H NMR (CDCl₃): 1.60 (s, C(CH₃)₂, 6H), 4.51 (d, ³J = 6.1 Hz, 2H, benzylic CH₂), 6.83 (t, ³J = 5.9 Hz, 1H, NH), 6.88 (d, ³J = 8.8 Hz, 2H, phenoxy 2-H and 6-H), 6.97 (ddd, ³J = 9.9 Hz, ³J = 8.5 Hz, 1H, 2-fluorobenzyl 5-H), 7.08 (ddd, ³J = 7.5 Hz, ³J_{HF} = 7.5 Hz, ⁴J = 1.1 Hz, 2-fluorobenzyl 6-H), 7.21 – 7.28 (m, 1H, 2-fluorobenzyl 3-H), 7.30 (ddd, 1H ³J = 7.5 Hz, ³J = 7.5 Hz, ⁴J_{HF} = 1.7 Hz, 2-fluorobenzyl 4-H), 7.45 (d, ³J = 8.6 Hz, 2H, benzoyl 3-H and 5-H), 7.67 (d, ³J = 8.8 Hz 2H, phenoxy 3-H and 5-H) 7.69 (d, ³J = 8.6 Hz, 2H, benzoyl 2-H and 6-H).

¹³C NMR (CDCl₃): 25.22 (C(CH₃)₂), 37.70 (benzyl CH₂), 81.86 (C(CH₃)₂), 115.42 (d, ²J_{CF} = 21Hz, 2-fluorobenzyl 3-C), 119.27 (phenoxy 2-C and 6-C), 124.29 (d, ⁴J_{CF} = 4Hz, 2-fluorobenzyl 5-C), 124.78 (d, ²J_{CF}=15 Hz, 2-fluorobenzyl 4-C), 128.61 (benzoyl 3-C and 5-C), 129.48 (d, ³J_{CF}=8 Hz, 2-fluorobenzyl 5-C), 130.35 (d, ⁴J_{CF} = 4 Hz, 2-fluorobenzyl), 131.22 (phenoxy 3-C and 5-C), 131.33 (d, ²J_{CF} = 22 Hz, 2-fluorobenzyl 1-C), 131.82 (benzoyl 2-C and 6-C), 136.12 (benzoyl 1-C), 138.63 (benzoyl 4-C), 158.42 (phenoxy 1-C), 161.03 (d, ¹J_{CF} = 246Hz, 2-fluorobenzyl 2-C), 173.95 (amide C=O), 194.18 (ketone C=O).

Melting point: 110-112 °C

HPLC: System 1, R_t = 7.00 minutes.

System 2, R_t = 19.15 minutes.

m/z : HRMS (ES-TOF⁺) $C_{24}H_{21}ClFNO_3$ $[MH]^+$ calculated 426.1261; found 426.1318.

FT-IR (KBr): 3367 (amide NH), 2973, 2942 (CH_3 stretch), 1689 (amide C=O), 1645 (ketone C=O), 1534 (aryl CH stretch), 856 (para disubstituted ring).

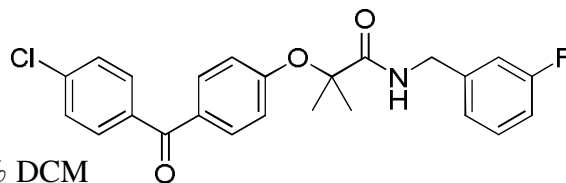
***N*-(3-Fluorobenzyl)-2-(4-(4-chlorobenzoyl)phenoxy)-2methylpropanamide (50b)**

Following General Method B, Fenofibric acid (0.112 g, 0.350 mmol) and an excess of thionyl chloride (5ml) were refluxed for 1 hours and 30 minutes to afford the corresponding acid chloride (0.118 g, 0.350 mmol). The acid chloride was then reacted directly with 3-fluorobenzylamine (0.04 ml, 0.350 mmol) and triethylamine (0.054 ml, 0.350 mmol) in DCM (6 ml) to afford **50b**.

Yield: 47%

Appearance: Yellow-white solid

Purification: PLC 5% EtOH / 95% DCM



1H NMR ($CDCl_3$): 1.64 (s, 6H, $C(CH_3)_2$), 4.48 (d, 3J = 6.0 Hz, 2H, benzylic CH_2), 6.84 (t, NH, 1H, 3J = 5.6 Hz), 6.87-7.13 (m, 5H, phenoxy 2-H and 6-H, 3-fluorobenzyl 2-H/4-H/6-H), 7.22 – 7.29 (m, 1H, 3-fluorobenzyl 5-H), 7.46 (d, 3J = 8.6 Hz, 2H benzoyl 3-H and 5-H), 7.71 (d, 3J = 8.5 Hz, 2H, phenoxy 3-H and 5-H), 7.72 (d, 3J = 8.8 Hz, 2H, benzoyl 2-H and 6-H).

^{13}C NMR ($CDCl_3$): 25.27 ($C(CH_3)_2$), 42.94 (benzyl CH_2), 81.91 ($C(CH_3)_2$), 114.51 (d, 2J = 21.0 Hz, 3-fluorobenzyl 4-C), 119.44 (phenoxy 2-C and 6-C), 123.25 (d, 4J = 2.0 Hz, 3-fluorobenzyl 6-C), 128.64 (benzoyl 3-C and 5-C), 131.76 (d, $^2J_{CF}$ = 26.0 Hz, 3-fluorobenzyl 2-C), 136.06 (benzoyl 1-C), 140.49

(d, $^3J = 8.0$ Hz, 3-fluorobenzyl 5-C), 158.34 (phenoxy 1-C), 162.94 (d, $^1J_{CF} = 246$ Hz, 3-fluorobenzyl 3-C).

Melting point: 99-102 °C

HPLC: System 1, $R_t = 9.99$ minutes.

System 2, $R_t = 19.17$ minutes.

***m/z*:** HRMS (ES-TOF⁺) C₂₄H₂₁ClFNO₃ [MH]⁺ calculated 426.1261; found 426.1345.

FT-IR (KBr): 3377 (amide NH), 2973, 2934 (CH₃ stretch), 1683 (amide C=O), 1650 (ketone C=O), 1535 (aryl CH stretch), 838 (para disubstituted ring).

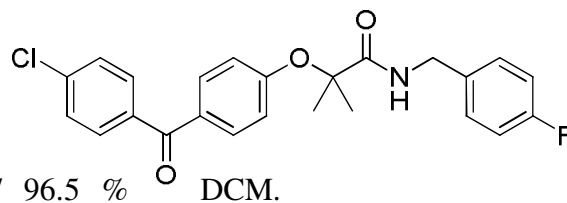
***N*-(4-Fluorobenzyl)-2-(4-(4-chlorobenzoyl)phenoxy)-2-methylpropanamide (50c)**

Following General Method B, Fenofibric acid (0.112 g, 0.350 mmol) and an excess of thionyl chloride (5ml) were refluxed for 1 hours and 30 minutes to afford the corresponding acid chloride (0.118 g, 0.350 mmol). The acid chloride was then reacted directly with 4-fluorobenzylamine (0.04 ml, 0.350 mmol) and triethylamine (0.054 ml, 0.350 mmol) in DCM (6 ml) to afford **50c**.

Yield: 48%

Appearance: Yellow-white solid

Purification: PLC, 3.5% EtOH / 96.5 % DCM.



^1H NMR (CDCl₃): 1.62 (s, 6H, C(CH₃)₂), 4.44 (d, $^3J = 6.0$ Hz, 2H, benzylic CH₂), 6.79 (t, $^3J = 5.8$ Hz, 1H, NH), 6.92 (d, $^3J = 8.8$ Hz, 2H, phenoxy 2-H and 6-H), 6.98 (dd, 2H, $^3J = 8.6$ Hz, $^3J_{\text{HF}} = 8.6$ Hz, 4-fluorobenzyl 3-H and 5-H), 7.19 (dd, 2H, $^3J = 8.8$ Hz, $^4J_{\text{HF}} = 5.3$ Hz, 4-fluorobenzyl 2-H and 6-H), 7.46 (d,

$^3J = 8.6$ Hz, 2H, benzoyl 3-H and 5-H), 7.69 (d, $^3J = 8.6$ Hz, 2H, phenoxy 3-H and 5-H) 7.71 (d, 2H, $^3J = 8.8$ Hz, benzoyl 2-H and 6-H).

^{13}C NMR (CDCl_3): 25.24 ($\text{C}(\text{CH}_3)_2$), 42.80 (benzylic CH_2), 81.93 ($\text{C}(\text{CH}_3)_2$), 115.58 (d, $^2J_{\text{CF}} = 21\text{Hz}$, 4-fluorobenzyl 3-C and 5-C), 119.49 (phenoxy 2-C and 6-C), 128.65 (benzoyl 3-C and 5-C), 129.48 (d, $^3J_{\text{CF}} = 8\text{Hz}$, 4-fluorobenzyl 2-C and 6-C), 131.20 (phenoxy 3-C and 5-C), 131.61 (phenoxy 4-C), 131.85 (benzoyl 2-C and 6-C), 133.76 (d, $^4J_{\text{CF}} = 3\text{Hz}$, 4-fluorobenzyl 1-C), 136.04 (benzoyl 4-C), 138.70 (benzoyl 4-C), 158.36 (amide $\text{C}=\text{O}$), 162.21 (d, $^1J_{\text{CF}} = 246\text{Hz}$, 4-fluorobenzyl 4-C), 194.16 (ketone $\text{C}=\text{O}$).

Melting point: 105-107 °C

HPLC: System 1, $R_t = 6.95$ minutes.

System 2, $R_t = 19.22$ minutes.

m/z : HRMS (ES-TOF^+) $\text{C}_{24}\text{H}_{21}\text{ClFNO}_3$ $[\text{MH}]^+$ calculated 426.1261; found 426.1329.

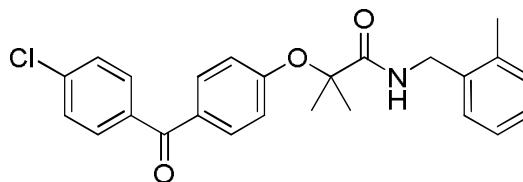
FT-IR (KBr): 3370 (amide NH), 2973, 2926 (CH_3 stretch), 1684 (amide $\text{C}=\text{O}$), 1648 (ketone $\text{C}=\text{O}$), 1536 (aryl CH stretch).

***N*-(2-Methylbenzyl)-2-(4-(4-chlorobenzoyl)phenoxy)-2-methylpropanamide (50d)**

Following General Method B, Fenofibric acid (0.112 g, 0.350 mmol) and an excess of thionyl chloride (5ml) were refluxed for 1 hours and 30 minutes to afford the corresponding acid chloride (0.118 g, 0.350 mmol). The acid chloride was then reacted directly with 2-methylbenzylamine (0.04 ml, 0.350 mmol) and triethylamine (0.054 ml, 0.350 mmol) in DCM (6 ml) to afford **50d**.

Yield: 34%

Appearance: White semi solid



Purification: PLC, 6% EtOH / 94 % DCM.

¹H NMR (CDCl₃): 1.63 (s, 6H, C(CH₃)₂), 2.25 (s, 3H, 2-methylbenzyl CH₃), 4.47 (d, ³J = 5.6 Hz, 2H, benzylic, CH₂), 6.66 (t, ³J = 4.9 Hz, 1H, NH), 6.93 (d, ³J = 8.8 Hz, 2H, phenoxy 2H and 6H), 7.10-7.21 (m, 4H, 2-methylbenzyl 3-H 4-H 5-H and 6-H), 7.45 (d, ³J = 8.6 Hz, 2H, benzoyl 3H and 5H), 7.66-7.71 (m, 4H, phenoxy 3-H and 5-H and benzoyl 2-H and 6-H)

¹³C NMR (CDCl₃): 19.09 (2-methyl benzyl CH₃), 25.43 (C(CH₃)₂), 41.92 (benzylic CH₂), 82.13 (C(CH₃)₂), 119.62 (phenoxy 2-C and 6-C), 126.36 (2-methyl benzyl 6-C), 128.04 (2-methyl benzyl 5-C), 128.74 (2-methyl benzyl 4-C), 128.77 (benzoyl 3-C and 5-C), 130.72 (phenoxy 4-C), 131.36 (phenoxy 3-C and 5-C), 131.71 (2-methyl benzyl 3-C), 132.01 (benzoyl 2-C and 6-C), 135.52 (2-methyl benzyl 2-C), 136.24 (benzoyl 1-C), 136.54 (2-methyl benzyl 1-C), 138.80 (benzoyl 4-C), 158.57 (phenoxy 1-C), 173.85 (amide C=O), 194.33 (ketone C=O).

Melting point: N/A

HPLC: System 1, R_t = 7.22 minutes.

System 2, R_t = 19.75 minutes.

m/z: HRMS (ES-TOF⁺) C₂₅H₂₄ClNO₃ [MH]⁺ calculated 422.1512; found 422.1487.

FT-IR (KBr): 3345 (amide NH), 2980, 2934 (CH₃ stretch), 1665 (amide C=O), 1603 (ketone C=O), 1525 (aryl CH stretch), 854 (para disubstituted aromatic ring).

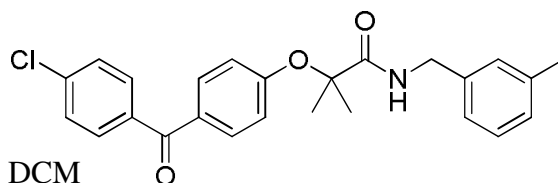
***N*-(3-Methylbenzyl)-2-(4-(4-chlorobenzoyl)phenoxy)-2-methylpropanamide (50e)**

Following General Method B, Fenofibric acid (0.112 g, 0.350 mmol) and an excess of thionyl chloride (5ml) were refluxed for 1 hours and 30 minutes to afford the corresponding acid chloride (0.118 g, 0.350 mmol). The acid chloride was then reacted directly with 3-methylbenzylamine (0.04 ml, 0.350 mmol) and triethylamine (0.054 ml, 0.350 mmol) in DCM (6 ml) to afford **50e**.

Yield: 59%

Appearance: Yellow-white solid

Purification: PLC, 6% EtOH / 94 % DCM



¹H NMR (CDCl₃): 1.63 (s, 6H, C(CH₃)₂), 2.27 (s, 3H, 3-methylbenzyl CH₃), 4.44 (d, ³J = 5.9 Hz, 2H, benzylic CH₂), 6.81 (t, ³J = 5.3 Hz, 1H, NH), 6.93 (d, ³J = 8.8 Hz, 2H, phenoxy 2-H and 6-H), 6.97-7.08 (m, 3H, 3-methylbenzyl 2-H, 4-H and 6-H), 7.17 (dd, ³J = 7.9 Hz, 3-methylbenzyl 5-H), 7.44 (d, ³J = 8.5 Hz, 2H, benzoyl 3-H and 5-H), 7.68 (d, ³J = 8.5 Hz, 2H, phenoxy 3-H and 5-H), 7.70 (d, ³J = 8.8 Hz, 2H, benzoyl 2H and 6H).

¹³C NMR (CDCl₃): 21.41 (3-methylbenzyl CH₃), 25.35 (C(CH₃)₂), 43.58 (benzylic CH₂), 81.96 (C(CH₃)₂), 119.44 (phenoxy 2-C and 6-C), 124.82 (3-methylbenzyl 6-C), 128.37 (3-methylbenzyl 5-C), 128.56 (3-methylbenzyl C-5), 128.67 (benzoyl 3-C and 5-C), 131.25 (), 131.49 (phenoxy 3-C and 5-C), 131.92 (phenoxy C-4), 136.19 (benzoyl 1-C), 137.87 (3-methylbenzyl 1-C), 138.46 (3-methylbenzyl 3-C), 138.67 (benzoyl 4-C), 158.59 (phenoxy 1-C), 194.86 (ketone C=O)

Melting point: 67-70 °C

HPLC: System 1, R_t = 7.22 minutes.

System 2, $R_t = 19.72$ minutes.

m/z : HRMS (ES-TOF⁺) $C_{25}H_{24}ClNO_3$ $[MH]^+$ calculated 422.1512; found 422.1556.

FT-IR (KBr): 3345 (amide NH), 2988, 2926 (CH_3 stretch), 1683 (amide C=O), 1648 (ketone C=O), 855 (para disubstituted aromatic ring).

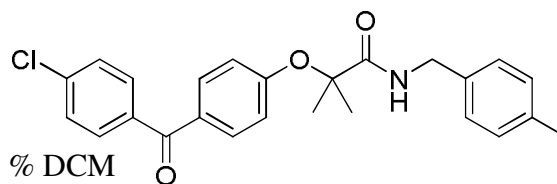
***N*-(4-Methylbenzyl)-2-(4-(4-chlorobenzoyl)phenoxy)-2-methylpropanamide (50f)**

Following General Method B, Fenofibric acid (0.112 g, 0.350 mmol) and an excess of thionyl chloride (5ml) were refluxed for 1 hours and 30 minutes to afford the corresponding acid chloride (0.118 g, 0.350 mmol). The acid chloride was then reacted directly with 4-methylbenzylamine (0.04 ml, 0.350 mmol) and triethylamine (0.054 ml, 0.350 mmol) in DCM (6 ml) to afford **50f**.

Yield: 59%

Appearance: Yellow-white solid

Purification: PLC, 6 % MeOH / 94 % DCM



1H NMR ($CDCl_3$): 1.63 (s, 6H, $C(CH_3)_2$), 2.31 (s, 3H, 4-methylbenzyl CH_3), 4.44 (d, $^3J = 5.8$ Hz, 2H, benzylic CH_2), 6.72 (t, $^3J = 5.4$ Hz, 1H, NH), 6.92 (d, $^3J = 8.8$ Hz, 2H, phenoxy 2-H and 6-H), 7.10 (s, 4H, 4-methylbenzyl aromatic CH), 7.45 (d, $^3J = 8.6$ Hz, 2H, benzoyl 3H and 5H), 7.65-7.75 (m, 4H, phenoxy 3H and 5H and 2H and 6H).

^{13}C NMR ($CDCl_3$): 21.09 (4-methylbenzyl CH_3), 25.28 ($C(CH_3)_2$), 43.33 (benzylic CH_2), 81.94 ($C(CH_3)_2$), 119.46 (phenoxy 2-C and 6-C), 127.77 (4-methylbenzyl 2-C and 6-C), 128.63 (benzoyl 3-C and 5-C), 129.39 (4-methylbenzyl 3-C and 5-C), 131.22 (phenoxy 3-C and 5-C), 131.49 (phenoxy 4-C), 131.86 (benzoyl 2-C and 6-C), 134.81 (4-methylbenzyl 1-C), 136.12

(benzoyl 1-C), 137.36 (4-methylbenzyl 4-C), 138.64 (benzoyl 4-C), 158.48 (phenoxy 1-C), 173.79 (amide C=O), 194.21 (ketone C=O).

Melting point: 115-118 °C

HPLC: System 1, R_t = 7.22 minutes.

System 2, R_t = 19.72 minutes.

***m/z*:** HRMS (ES-TOF⁺) C₂₅H₂₄ClNO₃ [MH]⁺ calculated 422.1512; found 422.1555.

FT-IR (KBr): 3351 (amide NH), 3004, 2919 (CH₃ stretch), 1671 (amide C=O), 1650 (ketone C=O), 1540 (aryl CH stretch), 853, 830 (*para* disubstituted aromatic ring)

***N*-(2-Fluorophenyl)-2-(4-(4-chlorobenzoyl)phenoxy)-2-methylpropanamide (51a)**

Following General Method B, Fenofibric acid (0.1008 g, 0.314 mmol) and an excess of thionyl chloride (5ml) were refluxed for 1 hours and 30 minutes to afford the corresponding acid chloride (0.107 g, 0.317 mmol). The acid chloride was then reacted directly with 2-fluoroaniline (0.03 ml, 0.317 mmol) and triethylamine (0.05 ml, 0.317 mmol) in DCM (6 ml) to afford **51a**.

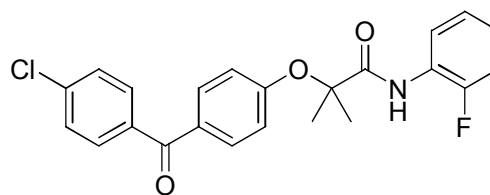
Yield: 50%

Appearance: Yellow-white solid

Purification: PLC, 70 % EtOAc : 30%

hexane.

¹H NMR (CDCl₃): 1.70 (s, 6H, C(CH₃)₂), 7.05-7.12 (m, 4H, phenoxy 2-H and 6-H and 2-fluorophenyl 3-H and 5-H), 7.13-7.20 (m, 1H, 2-fluorophenyl 4-H), 7.45 (d, ³*J* = 8.6 Hz, 2H, benzoyl 3-H and 5-H), 7.72 (d, ³*J* = 8.5 Hz,



2H, phenoxy 3-H and 5-H), 7.77 (d, $^3J = 8.5\text{Hz}$, 2H, benzoyl 2-H and 6-H), 8.34 (m, 1H, 2-fluorophenyl 6-H), 8.61(s, 1H, NH).

^{13}C NMR (CDCl_3): 25.26 ($\text{C}(\text{CH}_3)_2$), 82.66 ($\text{C}(\text{CH}_3)_2$), 115.1277 (d, $^2J_{\text{CF}} = 18.9\text{ Hz}$, 2-fluorophenyl 3-C), 120.30 (phenoxy 2-C and 6-C), 121.76 (2-fluorophenyl 1-C), 124.79 (d, $^4J_{\text{CF}} = 3.7\text{ Hz}$, 2-fluorophenyl 5-C), 125.00 (d, $^3J_{\text{CF}} = 7.6\text{ Hz}$, 2-fluorophenyl 6-C), 125.92 (d, $^3J_{\text{CF}} = 10.2\text{ Hz}$, 2-fluorophenyl 4-C), 128.79 (benzoyl 3-C and 5-C), 131.40 (phenoxy 3-C and 5-C), 132.12 (benzoyl 2-C and 6-C), 132.36 (benzoyl 4-C), 137.52 (d, $^1J_{\text{CF}} = 271.5\text{ Hz}$, 2-fluorophenyl 2-C), 158.27 (phenoxy 1-C), 172.53 (amide $\text{C}=\text{O}$), 194.37 (ketone $\text{C}=\text{O}$).

Melting point: 92-95 °C

HPLC: System 1, $R_t = 7.42$ minutes.

System 2, $R_t = 19.50$ minutes.

m/z : HRMS (ES-TOF^+) $\text{C}_{23}\text{H}_{19}\text{ClFNO}_3$ $[\text{MH}]^+$ calculated 412.1110; found 412.1148.

FT-IR (KBr): 3270 (amide NH), 2991, 2981 (CH_3 stretch), 1704 (amide $\text{C}=\text{O}$), 1634 (ketone $\text{C}=\text{O}$), 1600 (aryl CH stretch), 857 (para disubstituted ring).

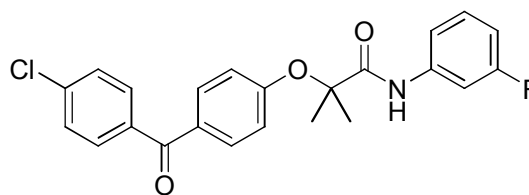
***N*-(3-Fluorophenyl)-2-(4-(4-chlorobenzoyl)phenoxy)-2-methylpropanamide (51b)**

Following General Method B, Fenofibric acid (0.100 g, 0.314 mmol) and an excess of thionyl chloride (5ml) were refluxed for 1 hours and 30 minutes to afford the corresponding acid chloride (0.109 g, 0.323 mmol). The acid chloride was then reacted directly with 3-fluoroaniline (0.03 ml, 0.32 mmol) and triethylamine (0.05 ml, 0.355 mmol) in DCM (6 ml) to afford **51b**.

Yield: 26%

Appearance: Yellow-white solid

Purification: PLC 2.5% ethanol /



97.5% DCM.

¹H NMR (CDCl₃): 1.67 (s, C(CH₃)₂, 6H), 6.84-6.85 (m, 1H, 3-fluorophenyl 4-H), 7.04 (d, ³J = 8.8 Hz, 2H, phenoxy 2-H and 6-H), 7.15-7.17 (m, 1H, 3-fluorophenyl 6-H), 7.24-7.32 (m, 3H, 3-fluorophenyl 5-H), 7.46 (d, ³J = 8.5 Hz, 2H, benzoyl 3-H and 5H), 7.25-7.29 (m, 1H, 3-fluorophenyl 2-H), 7.72 (d, ³J = 8.5 Hz, 2H, phenoxy 3-H and 5-H), 7.78 (d, ³J = 8.8 Hz, 2H, benzoyl 2H and 6H), 8.35 (broad s, NH, 1H).

¹³C NMR (CDCl₃): 25.19 (C(CH₃)₂), 82.62 (C(CH₃)₂), 107.53 (d, ²J_{CF} = 27Hz, 3-fluorophenyl 2-C/4-C), 111.53 (d, ²J_{CF} = 21Hz, 3-fluorophenyl 2-C/4-C), 115.23 (d, ⁴J_{CF} = 2Hz, fluorophenyl 5-C), 120.40 (phenoxy 2-C and 6-C), 128.81 (benzoyl 3-C and 5-C), 130.33 (d, ³J_{CF} = 9Hz, fluorophenyl 4-C), 131.37 (phenoxy 3-C and 5-C), 132.14 (benzoyl 2-C and 6-C), 132.52 (phenoxy C-4), 136.09 (benzoyl 1-C), 138.93 (benzoyl 4-C), 158.09 (phenoxy 1-C), 172.46 (amide C=O), 194.27 (ketone C=O).

Melting point: 100 - 102 °C

HPLC: System 1, R_t = 7.45 minutes.

System 2, R_t = 19.75 minutes.

m/z: HRMS (ES-TOF⁺) C₂₃H₁₉ClFNO₃ [MH]⁺ calculated 412.1110; found 412.1215.

FT-IR (KBr): 3270 (amide NH), 2994, 2983 (para disubstituted), 1686 (amide C=O), 1637 (ketone C=O), 1603 (aryl CH stretch), 853, 840 (para disubstituted aromatic ring).

***N*-(4-Fluorophenyl)-2-(4-(4-chlorobenzoyl)phenoxy)-2-methylpropanamide (51c)**

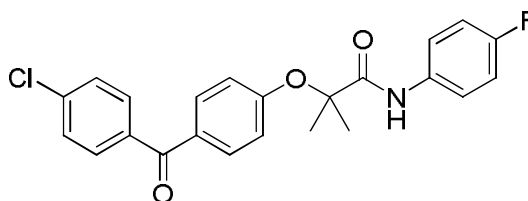
Following General Method B, Fenofibric acid (0.999 g, 0.313 mmol) and an excess of thionyl chloride (5ml) were refluxed for 1 hours and 30 minutes to afford the corresponding acid chloride (0.118 g, 0.350 mmol). The acid chloride was then reacted directly with 4-fluoroaniline (0.03 ml, 0.350 mmol) and triethylamine (0.05 ml, 0.385 mmol) in DCM (6 ml) to afford **51c**.

Yield: 35%

Appearance: Yellow white solid

Purification: PLC 2.5% EtOH/ 97.5

% DCM



¹H NMR (CDCl₃): 1.67 (s, C(CH₃)₂, 6H), 6.99 (m, 4H, phenoxy 2-H and 6-H and 4-fluorophenyl 3-H and 5-H), 7.45 (d, ³*J* = 8.5 Hz, 2H, benzoyl 3-H and 5-H), 7.47-7.53 (m, 2H, 4-fluorophenyl 2-H and 6-H), 7.71 (d, ³*J* = 8.5 Hz, 2H, phenoxy 3-H and 5-H), 7.76 (d, ³*J* = 8.8 Hz, 2H, benzoyl 2H and 6H), 8.31 (broad s, 1H, NH).

¹³C NMR (CDCl₃): 25.23 (C(CH₃)₂), 82.57 (C(CH₃)₂), 115.92 (d, ²*J*_{CF} = 22 Hz, 4-fluorophenyl 3-C and 5-C), 120.29 (phenoxy 2-C and 6-C), 121.97 (d, ³*J*_{CF} = 7.8 Hz, 4-fluorophenyl 2-C and 6-C), 128.81 (benzoyl 3-C and 5-C), 131.37 (benzoyl 2-C and 6-C), 132.14 (phenoxy 2-C and 6-C), 132.38 (phenoxy 4-C), 133.36 (d, ⁴*J*_{CF} = 2.8 Hz, 4-fluorophenyl 1-C), 136.09 (benzoyl 4-C), 138.91 (benzoyl 1-C), 158.21 (phenoxy 1-C), 159.74 (d, ¹*J*_{CF} = 283.9 Hz, 4-fluorophenyl 4-C) 172.32 (amide C=O), 194.30 (ketone C=O).

Melting point: 148-151 °C

HPLC: System 1, R_t = 7.27 minutes.

System 2, R_t = 19.39 minutes.

m/z : HRMS (ES-TOF⁺) $C_{23}H_{19}ClFNO_3$ $[MH]^+$ calculated 412.1110; found 412.1200.

FT-IR (KBr): 3326 (amide NH), 2990, 2976 (CH_3 stretch), 1680 (amide C=O), 1636 (ketone C=O), 1543 (aryl CH stretch), 836 (para- substituted aromatic ring).

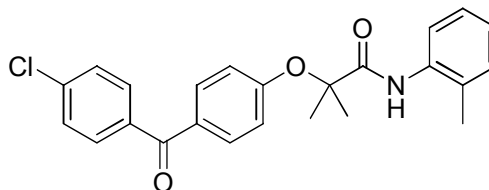
***N*-(2-Methylphenyl)-2-(4-(4-chlorobenzoyl)phenoxy)2-methylpropanamide (51d)**

Following General Method B, Fenofibric acid (0.100 g, 0.314 mmol) and an excess of thionyl chloride (5ml) were refluxed for 1 hours and 30 minutes to afford the corresponding acid chloride (0.119 g, 0.352 mmol). The acid chloride was then reacted directly with 3-methylaniline (0.04 ml, 0.352 mmol) and triethylamine (0.054 ml, 0.387 mmol) in DCM (6 ml) to afford **51d**.

Yield: 53%

Appearance: Yellow-white solid

Purification: 2.5 % EtOH/ 97.5 % PLC



1H NMR ($CDCl_3$): 1.72 (s, 6H, $C(CH_3)_2$), 2.12 (s, 3H, 2-methyl phenyl CH_3), 7.04-7.12 (m, 3H, phenoxy 2-H and 6-H, and 2-methyl phenyl 4-H), 7.15-7.25 (m, CH_{Ar} , 2H, 2-methyl phenyl 5-H and 6-H), 7.46 (d, 3J = 8.6 Hz, 2H, benzoyl 3H and 5H), 7.71 (d, 3J = 8.6 Hz, 2H, phenoxy 3-H and 5-H), 7.78 (d, 3J = 8.6 Hz, 2H, benzoyl 2-H and 6-H) 7.91-7.95 (m, 1H, 2-methyl phenyl 3-H) 8.19 (s, 1H, NH).

^{13}C NMR ($CDCl_3$): 17.54 (2-methyl phenyl CH_3), 25.39 ($C(CH_3)_2$), 82.66 ($C(CH_3)_2$), 119.66 (phenoxy 2-C and 6-C), 122.26 (2-methyl phenyl 6-C), 125.36 (2-methyl phenyl 5-C), 127.07 (2-methyl phenyl 4-C), 128.64 (phenoxy

4-C), 128.79 (benzoyl 3-C and 5-C), 130.67 (2-methyl phenyl 2-C), 131.36 (benzoyl 2-C and 6-C), 132.02 (2-methyl phenyl 3-C), 132.17 (benzoyl 2-C and 6-C), 135.26 (2-methyl phenyl 1-C), 136.16 (benzoyl 1-C), 138.86 (benzoyl 4-C), 158.51 (phenoxy 1-C), 172.11 (amide C=O), 194.29 (ketone C=O).

Melting point: 95-99 °C

HPLC: System 1, R_t = 7.28 minutes.

System 2, R_t = 19.40 minutes.

m/z : HRMS (ES-TOF⁺) $C_{24}H_{22}ClNO_3$ $[MH]^+$ calculated 408.1361; found 408.1368.

FT-IR (KBr): 3355 (amide NH), 2979, 2939 (CH_3 stretch), 1692 (amide C=O), 1647 (ketone C=O), 1566 (aryl CH stretch), 838 (para disubstituted aromatic ring).

***N*-(3-Methylphenyl)-2-(4-(4-chlorobenzoyl)phenoxy)-2-methylpropanamide (51e)**

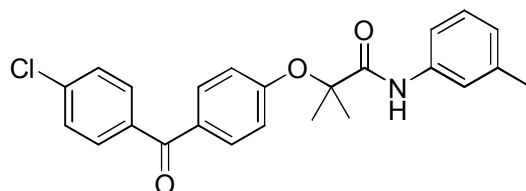
Following General Method B, Fenofibric acid (0.101 g, 0.316 mmol) and an excess of thionyl chloride (5ml) were refluxed for 1 hours and 30 minutes to afford the corresponding acid chloride (0.118 g, 0.350 mmol). The acid chloride was then reacted directly with 3-methylaniline (0.04 ml, 0.350 mmol) and triethylamine (0.054 ml, 0.385 mmol) in DCM (6 ml) to afford **51e**.

Yield: 49%

Appearance: Yellow-white solid

Purification: PLC 2.5 % EtOH/

97.5 % DCM



¹H NMR (CDCl₃): 1.67 (s, C(CH₃)₂, 6H), 2.34 (s, 3H, 3-methyl phenyl CH₃), 6.94 – 6.96 (m, 1H, 3-methyl phenyl 4-H), 7.04 (d, ³J = 8.8 Hz, 2H, phenoxy 2-H and 6-H), 7.22 (dd, ³J = 7.8 Hz, ³J = 7.8 Hz, 1H, 3-methyl phenyl 5-H), 7.29-7.34 (m, 1H, 3-methyl phenyl 6-H), 7.39 – 7.41 (m, 1H, 3-methyl phenyl 2-H), 7.45 (d, ³J = 8.6 Hz, 2H, benzoyl 3-H and 5-H), 7.72 (d, ³J = 8.6 Hz, 2H, phenoxy 2-H and 6-H), 7.77 (d, ³J = 8.8 Hz, 2H, benzoyl 2-H and 6-H) 8.22 (broad s, 1H, NH).

¹³C NMR (CDCl₃): 21.60 (3-fluoro phenyl CH₃), 25.25 (C(CH₃)₂), 82.54 (C(CH₃)₂), 117.05 (3-methyl phenyl 6-C), 120.11 (phenoxy 2-C and 6-C), 120.62 (3-methyl phenyl 2-C), 125.66 (3-methyl phenyl 4-C), 128.79 (benzoyl 3-C and 5-C), 129.07 (phenoxy 4-C), 131.38 (phenoxy 3-C and 5-C), 132.14 (benzoyl 2-C and 6-C), 136.14 (benzoyl 1-C), 137.29 (benzoyl 4-C), 138.86 (3-methyl phenyl 1-C), 139.25 (3-methyl phenyl 3-C), 158.35 (phenoxy 1-C), 172.27 (amide C=O), 194.33 (ketone C=O).

Melting point: 111-113 °C

HPLC: System 1, R_t = 7.52 minutes.

System 2, R_t = 19.95 minutes.

m/z: HRMS (ES-TOF⁺) C₂₄H₂₂ClNO₃ [MH]⁺ calculated 408.1361; found 408.1431.

FT-IR (KBr): 3267 (amide NH), 2996, 2942 (CH₃ stretch), 1689 (amide C=O), 1642 (ketone C=O), 1539 (aryl CH stretch), 853 (para disubstituted ring).

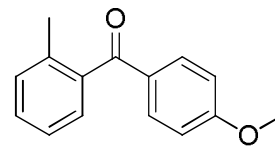
2-Methyl (4'-methoxy)benzophenone (54a)

Following General Method D, 2-methylbenzoic acid (0.500 g, 3.68 mmol) was reacted with an excess of thionyl chloride (5 ml) for 1 hour. The acid chloride

(0.568g, 3.68 mmol) afforded was reacted with anisole (0.398 g, 3.68 mmol) and aluminium chloride (0.753g, 5.51 mmol) in DCM (10 ml) to give **54a**.

Yield: 32%

Appearance: Colourless oil



Purification: 5 % DCM / 95 % PE to 60 % DCM / 40 % PE.

Melting point: N/A

¹H NMR (CDCl₃): 2.30 (s, 3H, 2-CH₃), 3.87 (s, 3H, OCH₃), 6.92 (d, ³J = 8.5 Hz, 2H, 2'-H and 6'-H), 7.20-7.40 (m, 4H, benzoyl CH), 7.78 (d, ³J = 8.5 Hz, 2H, 3'-H and 5'-H).

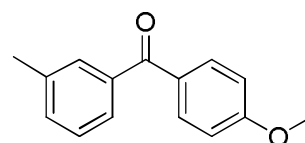
¹³C NMR (CDCl₃): 20.12 (2-CH₃), 55.85 (OCH₃), 114.06 (3'-C and 5'-C), 125.51 (5-C), 128.27 (6-C), 130.12 (1'-C), 130.92 (3-C), 131.16 (2'-C and 6'-C), 132.85 (4-C), 136.51 (2-C), 139.59 (1-C), 164.06 (4'-C), 197.71 (ketone C=O).

m/z: HRMS (ES-TOF⁺) C₁₅H₁₄O₂ [MH]⁺ calculated 227.1067; found 227.9815.

FT-IR (KBr): 2966, 2840 (CH₃ stretch), 1653 (ketone C=O), 1598 (aryl CH stretch), 847 (*para* disubstituted aromatic ring).

3-Methyl(4'-methoxy)benzophenone (**54b**)

Following General Method D, 3-methylbenzoic acid (0.501 g, 3.68 mmol) was reacted with an excess of thionyl chloride for 1 hour. The acid chloride (0.568g, 3.68 mmol) afforded was then reacted with anisole (0.398 g, 3.68 mmol) and aluminium chloride (0.753g, 5.51 mmol) in DCM (10 ml) to give **54b**.



Yield: 51%

Appearance: Colourless oil

Purification: 5 % DCM / 95 % PE, to 60 % DCM / 40 % PE.

Melting point: n/a

¹H NMR (CDCl₃): 2.42 (s, 3H, 3-CH₃), 3.89 (s, 3H, OCH₃), 6.96 (d, ³J = 8.7 Hz, 2H, phenoxy 2'-H and 6'-H), 7.32-7.40 (m, 2H 2-H/6-H), 7.50-7.60 (m, 2H, 4-H/5-H), 7.83 (d, ³J = 8.6 Hz, 2H, 3'-H and 5'-H).

¹³C NMR (CDCl₃): 21.36 (3-CH₃), 55.48 (OCH₃), 113.52 (3'-C and 5'-C), 126.99 (2-C), 127.99 (6-C), 127.99 (5-C), 130.19 (4-C), 130.12 (1'-C), 132.55 (2'-C and 6'-C), 132.66 (3-C), 138.33 (1-C), 163.17 (4'-C), 195.81 (ketone C=O).

m/z: HRMS (ES-TOF⁺) C₁₅H₁₄O₂ [MH]⁺ calculated 227.1067; found 227.0329.

FT-IR (KBr): 2974, 2840 (CH₃ stretch), 1672 (ketone C=O), 1595 (aryl CH stretch), 869, 845 (*para* disubstituted aromatic ring).

4-Methyl-(4'-methoxy)-benzophenone (54c)

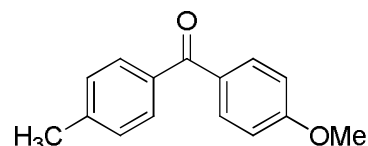
Following General Method D, 4-methylbenzoic acid (0.500 g, 3.67 mmol) was reacted with an excess of thionyl chloride for 1 hour. The acid chloride (0.568 g, 3.68 mmol) afforded was reacted with anisole (0.399 ml, 3.68 mmol) and aluminium chloride (0.735g, 5.51 mmol) in DCM (10 ml) to give **54c**.

Yield: 45 %

Appearance: White needle-like crystals

Purification: Column chromatography 100 %

PE to 20% TBME / 80 % PE.



Melting point: 85 – 87 °C

¹H NMR (DMSO): 2.40 (s, 3H 4-CH₃), 3.86 (s, 3H, OCH₃), 7.08 (d, ³*J* = 8.9 Hz, 2H, phenoxy 3'-H and 5'-H), 7.35 (d, ³*J* = 7.9 Hz, 2H, 3-H and 5-H), 7.60 (d, ³*J* = 8.1 Hz, 2H, 2'-H and 6'-H), 7.73 (d, ³*J* = 8.9 Hz, 2H, 2-H and 6-H).

¹³C NMR (DMSO): 21.59 (CH₃), 56.01 (OCH₃), 114.31 (phenoxy 2-C and 6-C), 129.46 (benzoyl 3-C and 5-C), 130.00 (benzoyl 2-C and 6-C), 130.13 (phenoxy 4-C), 132.49 (phenoxy 3-C and 5-C), 135.47 (benzoyl 1-C), 142.89 (benzoyl 4-C), 163.25 (amide C=O), 194.59 (ketone C=O).

***m/z*:** HRMS (ES-TOF⁺) [MH]⁺ calculated 227.1067; found 226.9554.

FT-IR (KBr): 2918, 2844 (CH₃ stretch), 1644 (ketone C=O), 848, 828 (*p* disubstituted aromatic ring).

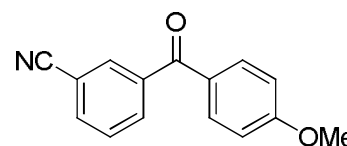
3-Cyano-(4'-methoxy)-benzophenone (54d)

Following General Method D, 3-cyanobenzoic acid (0.501 g, 3.41 mmol) was reacted with an excess of thionyl chloride (5 ml) for 1 hour. The acid chloride (0.565g, 3.41 mmol) afforded was reacted with anisole (0.368 g, 3.41 mmol) and aluminium chloride (0.681 g, 5.11 mmol) in DCM (10 ml) to give **54d**.

Yield: 52%

Appearance: Pale yellow solid

Purification: Column chromatography, 5 %



dichloromethane / 95 % petroleum ether to 100% dichloromethane.

Melting point: 86 – 88 °C

¹H NMR (DMSO): 3.87 (s, 3H, OCH₃), 7.11 (d, ³*J* = 8.9 Hz, 2H, 3'-H and 5'-H), 7.73-7.79 (m, 3H, 2'-H, 6'-H, and 5-H), 7.98 (ddd, ³*J* = 7.9 Hz, ⁴*J* = 1.5 Hz, ⁴*J* = 1.5 Hz, 1H, 6-H), 8.07-8.12 (m, 2H, 2-H and 4-H).

m/z: HRMS (ES-TOF⁺) C₁₅H₁₁NO₂ [MH]⁺ calculated 238.0863; found 238.0865.

FT-IR (KBr): 2938, 2845 (CH₃ stretch), 2232 (CN), 1640 (ketone C=O), 1598 (aryl CH stretch), 850, 811 (*para* disubstituted aromatic ring).

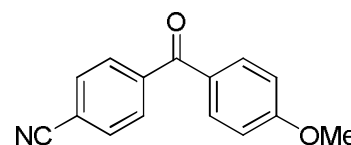
4-Cyano-4'-methoxybenzophenone (54e)

Following General Method D, 4-cyanobenzoic acid (0.500 g, 3.68 mmol) was reacted with an excess of thionyl chloride (5ml) for 1 hour. The acid chloride (0.568g, 3.68 mmol) afforded was reacted with anisole (0.367 g, 3.39 mmol) and aluminium chloride (0.678 g, 5.09 mmol) in DCM (10 ml) to give **54e**.

Yield: 29%

Appearance: White solid

Purification: 2.5 % EtOAc / 97.5 % petroleum ether to 100 % EtOAc



¹H NMR (DMSO): 3.86 (s, 1H, OCH₃), 7.11 (d, ³J = 8.9 Hz, 2H, 3'-H and 5'-H), 7.75 (d, ³J = 8.9 Hz, 2H, 2'-H and 6'-H), 7.82 (d, ³J = 8.6 Hz, 2H, 2-H and 6-H), 8.02 (d, ³J = 8.6 Hz, 2H, 3-H and 5-H).

¹³C NMR (CDCl₃): 55.64 (OMe), 113.99 (4-C), 114.12 (3'-C and 5'-C), 118.21 (CN), 128.45 (1'-C), 129.60 (2-C and 6-C), 132.38 (2'-C and 6'-C), 132.45 (3-C and 5-C), 141.78 (1-C), 163.49 (4'-C), 193.26 (ketone C=O).

Melting point: 133-134 °C

m/z: HRMS (ES-TOF⁺) C₁₅H₁₁NO₂ [MH]⁺ calculated 238.0863; found 238.079.

FT-IR (KBr): 2231 (CN), 1642 (ketone C=O), 1599 (aryl CH stretch), 859, 840 (*para* disubstituted aromatic ring).

2-Chloro (4'-methoxy)benzophenone (54f)

Following General Method D, but using commercially available acid chloride, 3-chlorobenzoyl chloride (5.000 g, 28.6 mmol) was reacted with anisole (3.089 g, 28.6 mmol) and aluminium chloride (5.713 g, 42.9 mmol) in DCM (40 ml) to give **54f**.

Yield: 37 %

Appearance: White solid

Purification: Column chromatography, 1 %

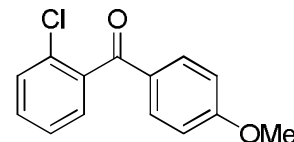
TBME / 99 % PE to 40% TBME / 60% PE. Product then precipitated from EtOAc by addition of PE.

Melting point: 83 – 85 °C

¹H NMR (DMSO): 3.88 (s, 3H, OCH₃), 6.94 (d, ³J = 8.9 Hz, 2H, 3'-H and 5'-H), 7.34-7.37 (m, 2H, 4-H and 5-H), 7.38-7.47 (m, 2H, 3-H and 6-H), 7.79 (d, ³J = 9.0Hz, 2H, 2'-H and 6'-H).

¹³C NMR (CDCl₃): 55.68 (OCH₃), 114.03 (3'-C and 5'-C), 126.78 (5-C), 129.01 (6-C), 129.59 (1'-C), 130.10 (3-C), 130.92 (4-C), 131.24 (1-C), 132.67 (2'-C and 6'-C), 139.17 (2-C), 164.25 (4'-C), 193.99 (ketone C=O).

FT-IR: 1655 (ketone C=O), 1598 (aryl CH stretch).

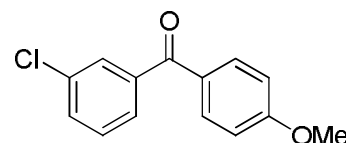


3-Chloro-(4'-methoxy)-benzophenone (54g)

Following General Method D, but using commercially available acid chloride, 2-chlorobenzoyl chloride (5.000 g, 28.6 mmol) was reacted with anisole (3.089 g, 28.6 mmol) and aluminium chloride (5.713 g, 42.9 mmol) in DCM (40 ml) to give **54g**.

Yield: 46 %

Appearance: White solid



Purification: Column chromatography, 1% TBME / 99% PE to 40% TBME / 60% PE. Product then precipitated from EtOAc by addition of PE.

Melting point: 69 – 70 °C

¹H NMR (DMSO): 3.89 (s, 3H, OMe), 6.97 (d, ³J = 8.9 Hz, 2H, 3'-H and 5'-H), 7.41 (dd, ³J = 7.8 Hz, ³J = 7.8 Hz, 2H, 5-H), 7.53 (ddd, ³J = 8.0 Hz, ⁴J = 2.1 Hz, ⁴J = 1.1 Hz, 1H, 6-H) 7.62 (ddd, ³J = 7.6 Hz, ⁴J = 1.3 Hz, ⁴J = 1.3 Hz, 1H, 4-H), 7.72 (dd, ⁴J = 1.8 Hz, ⁴J = 1.8 Hz, 1H, 2-H), 7.81 (d, ³J = 8.9 Hz, 2H, 2'-H and 6'-H).

¹³C NMR (CDCl₃): 55.68 (OCH₃), 114.03 (3'-C and 5'-C), 126.78 (6-C), 129.01 (5-C) 129.59 (1'-C), 130.10 (2'-C and 6-C), 130.92 (2-C), 131.24 (4-C), 132.67 (3-C), 139.17 (1-C), 164.25 (4'-C), 193.99 (ketone C=O).

m/z: HRMS (ES-TOF⁺) [MH]⁺ calculated 247.0520; found 247.0440

FT-IR (KBr): 1648 (ketone C=O), 1596 (aryl CH stretch).

3-Fluoro-(4'-methoxy)-benzophenone (54h)

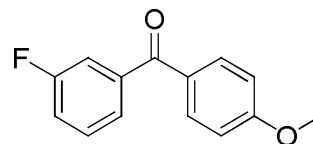
Following General Method D, 3-fluorobenzoic acid (0.502 g, 3.58 mmol) was reacted with an excess of thionyl chloride (5 ml) for 1 hour. The acid chloride (0.568g, 3.58 mmol) afforded was reacted with anisole (0.387 g, 3.58 mmol) and aluminium chloride (0.716 g, 5.37 mmol) in DCM (10 ml) to give **54h**.

Yield: 15%

Appearance: White solid

Purification: Column chromatography, 2%

TBME / 98 % PE to 40 % TBME / 60 % PE.



Melting point: 68 – 70 °C

¹H NMR (CDCl₃): 3.89 (s, 3H, OCH₃), 6.97 (d, ³J = 8.9 Hz, 2H, 2'-H and 6'-H), 7.22-7.29 (m, 1H, 2-H), 7.40-7.55 (m, 3H, 4-H, 5-H and 6-H), 7.82 (d, ³J = 8.9 Hz, 2H, 3'-H and 5'-H).

¹³C NMR (CDCl₃): 55.53 (OCH₃, 113.71 (3'-C and 5'-C), 116.49 (d, ²J_{CF} = 22.4 Hz, 2-C), 118.83 (d, ²J_{CF} = 22.3 Hz, 4-C), 125.41 (d, ⁴J_{CF} = 2.9 Hz, 6-C), 129.41 (1'-C), 129.86 (1'-C), 132.54 (2'-C and 6'-C), 140.41 (d, ³J_{CF} = 6.3 Hz, 1-C), 162.44 (d, ¹J_{CF} = 247.8 Hz, 3-C), 163.51 (4'-C), 194.03 (ketone C=O).

m/z: HRMS (ES-TOF⁺) C₁₄H₁₁FO₂ [MH]⁺ calculated 231.0816; found 230.9698.

3-Nitro-(4'-methoxy)-benzophenone (54i)

Following General Method D, 3-nitrobenzoic acid (0.501 g, 2.99 mmol) was reacted with an excess of thionyl chloride (5 ml) for 1 hour 50 minutes. The acid chloride (0.558g, 2.99 mmol) afforded was reacted with anisole (0.324 g, 2.99 mmol) and aluminium chloride (0.599 g, 4.49 mmol) in DCM (10 ml) to give **54i**.

Yield: 71%

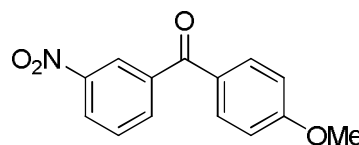
Appearance: Off white solid

Purification: Column chromatography, 5 %

DCM / 95 % PE to 60 % DCM / 40 % PE.

Melting point: 87 – 89 °C

¹H NMR (DMSO): 3.91 (s, 3H, OCH₃), 7.00 (d, ³J = 9.1 Hz, 3'-H and 5'-H), 7.69 (dd, ²J = 7.8 Hz, ²J = 7.8 Hz, 5-H), 7.82 (d, ³J = 8.9 Hz, 2'-C and 6'-C), 8.09 (ddd, ²J = 7.7 Hz, ³J = 1.3 Hz, ³J = 1.3 Hz, 6-C), 8.42 (ddd, ²J = 8.2 Hz, ³J = 1.1 Hz, ³J = 2.3 Hz, 4-C), 5.57 (dd, ⁴J = 1.9 Hz, ⁴J = 1.9 Hz, 1-C).



¹³C NMR (DMSO): 55.57 (OCH₃), 114.18 (3'-C and 5'-C), 124.56 (2-C), 126.37 (4-C), 129.03 (5-C), 130.38 (1'-C), 132.72 (2'-C and 6'-C), 135.32 (6-C), 139.96 (1-C), 148.16 (3-C), 164.09 (4'-C), 192.98 (ketone C=O).

***m/z*:** HRMS (ES-TOF⁺) C₁₄H₁₁NO₄ [MH]⁺ calculated 258.0761; found 258.0762

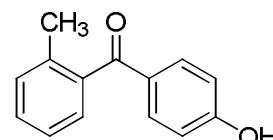
FT-IR (KBr): 1648 (ketone C=O), 1597 (aryl CH stretch).

2-Methyl-(4'-hydroxy)benzophenone (55a)

Following General Method F, 2-methyl-(4'-methoxy)benzophenone (0.253 g, 1.12 mmol) was irradiated in the microwave (300W at 150°C) with pyridine hydrochloride (0.645 g, 5.58 mmol) for 12 minutes to afford **55a**.

Yield: 8 %

Appearance: Orange-brown solid.



Purification: 2 % TBME / 98 % PE to 40 % TBME 60 % PE.

¹H NMR (DMSO): 2.18 (2-CH₃), 6.87 (d, ³*J* = 8.8 Hz, 3'-H and 5'-H), 7.21 – 7.35 (m, 3H, 3-H/5-H/6-H), 7.42 (ddd, ³*J* = 7.3 Hz, ³*J* = 7.3 Hz, ⁴*J* = 1.5 Hz, 1H, 4-H), 7.58 (d, ³*J* = 8.8 Hz, 2H, 2'-H and 6'-H).

¹³C NMR (DMSO): 19.93 (2-CH₃). 115.66 (3'-C and 5'-C), 125.39 (5-C), 128.10 (6-C), 130.11 (1'-C), 130.17 (3-C), 131.02 (2'-C and 6'-C), 133.24 (4-C), 136.25 (2-C), 139.05 (1-C), 161.43 (4'-C), 198.80 (ketone C=O).

***m/z*:** HRMS (ES-TOF⁺) [MH]⁺ calculated 213.0910; found 213.0802

3-Methyl-(4'-hydroxy)-benzophenone (55b)

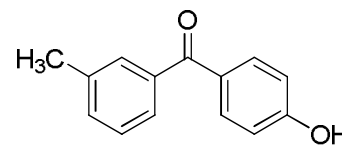
Following General Method F, 3-methyl-(4'-methoxy)benzophenone (0.250 g, 1.11 mmol) was irradiated in the microwave (300W at 150°C) with pyridine hydrochloride (0.639 g, 5.52 mmol) for 10 minutes to give **55b**.

Yield: 91%

Appearance: Off white solid

Purification: Used without further purification

Melting point: 164 – 166 °C



¹H NMR (DMSO): 2.38 (s, 3H, 3-CH₃), 6.89 (d, ³J = 8.8 Hz, 2H, 3'-H and 5'-H), 7.37-7.49 (m, 4H, 2-H, 4-H, 5-H and 6-H), 7.65 (d, ³J = 8.8 Hz, 2H, 2'-H and 6'-H), 10.39 (s, 1H, OH).

¹³C NMR (DMSO): 20.87 (3-CH₃), 115.20 (3'-C and 5'-C), 126.34 (2-C), 128.01 (6-C), 128.17 (5-C), 129.44 (1'-C), 132.37 (4-C), 132.42 (3-C), 137.73 (2'-C and 6'-C), 138.16 (1-C), 161.91 (4'-C), 194.40 (C=O).

m/z: HRMS (ES-TOF⁺) [MH]⁺ calculated 213.0910; found 213.0867.

FT-IR (KBr): 3278 (phenol OH), 1636 (ketone C=O), 1598 (aryl CH stretch), 849 (*p* disubstituted aromatic ring).

4-Hydroxy (4'-methyl)-benzophenone (55c)

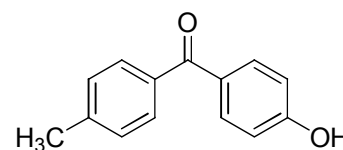
Following General Method F, 4-methyl-(4'-methoxy)benzophenone (0.400 g, 1.77 mmol) was irradiated in the microwave with pyridine hydrochloride (1.021 g, 8.89 mmol) for 2 minutes at 200W and 250°C, and then 2 minutes at 200W and 200°C to give **55c**.

Yield: 66 %

Appearance: Off white crystals

Purification: Recrystallised from EtOAc / PE.

Melting point: 169 -172 °C



¹H NMR (DMSO): 2.39 (s, 3H, phenoxy CH₃), 6.89 (d, ³J = 8.7 Hz, 2H, phenoxy 2-H and 6-H), 7.33 (d, ³J = 7.9 Hz, 2H, benzoyl 3-H and 5-H) 7.58 (d,

$^3J = 8.1$ Hz, 2H, phenoxy 3-H and 5-H), 7.63 (d, $^3J = 8.7$ Hz, 2H, benzoyl 2-H and 6-H), 10.37 (s, 1H, OH).

^{13}C NMR (DMSO): 21.56 (CH_3), 115.64 ($3'\text{-C}$ and $5'\text{-C}$), 128.65 ($1'\text{-C}$), 129.38 (3 and 5), 129.87 (2-C and 6-C), 132.81 ($2'\text{-C}$ and $6'\text{-C}$), 135.7 (1-C), 142.53 (4-C), 162.23 ($4'\text{-C}$), 194.47 (ketone C=O).

m/z : HRMS (ES-TOF $^+$) $[\text{MH}]^+$ calculated 213.0910; found 213.0824.

FT-IR (KBr): 3337 (phenol OH), 1642 (ketone C=O), 1599 (aryl CH stretch).

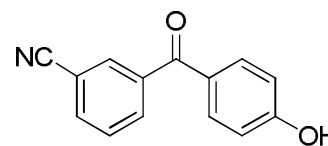
3-Cyano-(4'-hydroxy)-benzophenone (55d)

Following General Method F, 3-cyano-(4'-methoxy)benzophenone (1.007 g, 4.24 mmol) was irradiated in the microwave with pyridine hydrochloride (2.452 g, 21.2 mmol) for 15 minutes at 300W and 150°C to give **55d**.

Yield: 54%

Appearance: Off white solid.

Purification: Product precipitated from EtOAc with addition of PE.



Melting point: 164 – 166 $^\circ\text{C}$

^1H NMR (DMSO): 6.92 (d, $^3J = 8.7$ Hz, 2H, $3'\text{-H}$ and $5'\text{-H}$), 7.68 (d, $^3J = 8.7$ Hz), 2H, $2'\text{-H}$ and $6'\text{-H}$), 7.74 (dd, 1H, $^3J = 7.8$ Hz, $^3J = 7.8$ Hz, 5-H), 7.95 (ddd, $^3J = 1.3$ Hz, $^4J = 1.3$ Hz, $^4J = 7.8$ Hz, 1H, 6-H), 8.04-8.10 (m, 2H, 2-H and 4-H), 10.55 (broad s, 1H, OH).

^{13}C NMR (DMSO): 111.64 (3-C), 115.48 ($3'\text{-C}$ and $5'\text{-C}$), 118.19 (CN), 127.00 ($5'\text{-C}$), 129.72 ($1'\text{-C}$), 132.38 ($2'\text{-C}$ and $6'\text{-C}$), 132.75 (2-C), 133.38 (6-C), 134.97 (4-C), 139.22 (C-1), 162.54 ($4'\text{-C}$), 192.43 (C=O).

m/z : HRMS (ES-TOF) $\text{C}_{14}\text{H}_9\text{NO}_2$ $[\text{MH}]^-$ calculated 222.0561; found 222.0502.

FT-IR (KBr): 3336 (phenol OH), 2230 (CN stretch), 1658 (ketone C=O), 1601 (aryl CH stretch), 850, 818 (*para* disubstituted aromatic ring).

4-Cyano-(4'-hydroxy)benzophenone (**55e**)

Following General Method F, 4-cyano-(4'-methoxy)benzophenone (0.850 g, 3.81 mmol) was irradiated in the microwave with pyridine hydrochloride (1.021 g, 19.0 mmol) for 4 minutes at 100W and 250°C to give **55e**.

Yield: 73 %

Appearance: Yellow – white solid

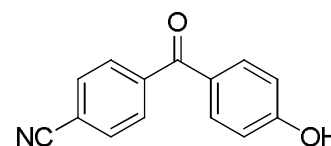
Purification: Product precipitated from EtOAc with addition of PE

Melting point: 179 - 181 °C

¹H NMR (DMSO): 6.91 (d, ³*J* = 8.8 Hz, 2H, 3'-H and 5'-H), 7.67 (d, ³*J* = 8.6 Hz, 2H, 2'-H and 6'-H), 7.79 (d, ³*J* = 8.6 Hz, 2H, 2-H and 6-H), 8.00 (d, ³*J* = 8.3 Hz, 2H, 3-H and 5-H).

¹³C NMR (DMSO): 112.76 (4-C), 144.49 (3'-C and 5'-C), 117.27 (CN), 125.97 (2-C and 6-C), 128.50 (3-C and 5-C), 131.42 (2'-C and 6'-C), 131.74 (3-C and 5-C), 141.20 (1-C), 161.64 (4'-C), 192.08 (ketone C=O).

FT-IR: 3372 (phenol OH), 2238 (CN stretch), 1696 (ketone C=O), 1585 (aryl CH stretch).

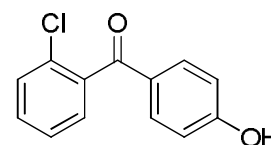


2-Chloro-(4'-hydroxy)benzophenone (**55f**)

Following General Method F, 4-chloro-(4'-methoxy)benzophenone (1.000 g, 4.29 mmol) was irradiated in the microwave with pyridine hydrochloride (2.483 g, 21.5 mmol) for 5 minutes at 200W and 250°C to give **55f**.

Yield: 27 %

Appearance: White Solid



Purification: Column chromatography, 100 % PE to 100 % EtOAc

Melting point: 129 – 131 °C

¹H NMR (DMSO): 6.88 (3'-H and 5'-H), 7.41 – 7.61 (m, 6H, 2'-H/6'H/3-H/4-H/5-H/6-H), 10.62 (s, 1H, OH).

¹³C NMR (DMSO): 115.68 (3'-C and 5'-C), 127.25 (5-C), 127.30 (6-C), 128.63 (3-C), 129.51 (1'-C), 129.67 (4-C), 131.13 (1-C), 132.39 (2'-C and 6'-C), 138.82 (2-C), 163.05 (4'-C), 192.62 (ketone C=O).

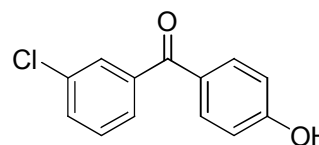
FT-IR: 3296 (phenol OH), 1644 (ketone C=O), 1570 (aryl CH stretch).

3-Chloro-(4'-hydroxy)benzophenone (**55g**)

Following General Method F, 3-chloro-(4'-methoxy)benzophenone (1.000 g, 4.29 mmol) was irradiated in the microwave with pyridine hydrochloride (2.483 g, 21.5 mmol) for 5 minutes at 200W and 250°C to give **55g**.

Yield: 98 %

Appearance: White solid



Purification: Column chromatography, 100 %

PE to 100 % EtOAc

Melting point: 174 – 176 °C

¹H NMR (DMSO): 6.91 (d, ³J = 8.8 Hz, 2H, 3'-H and 5'-H), 7.52 – 7.72 (m, 6H, 2'-H/ 6'-H/ 2-H/ 4-H/5-H/ 6-H), 10.51 (s, 1H, OH).

¹³C NMR (DMSO): 115.39 (3'-C and 5'-C), 127.29 (6-C), 127.69 (5-C), 128.48 (2-C), 130.33 (1'-C), 131.47 (4-C), 131.60 (2'-C and 6-C), 133.23 (3-C), 140.14 (1-C), 162.35 (4'-C), 192.79 (ketone C=O).

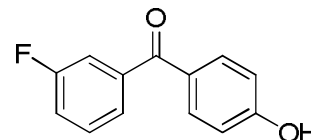
FT-IR: 3298 (phenol OH), 1633 (ketone C=O), 1599 (aryl CH stretch).

3-Fluoro-(4'-hydroxy)benzophenone (**55h**)

Following General Method F, 3-fluoro-(4'-methoxy)benzophenone (0.090 g, 0.19 mmol) was irradiated in the microwave with pyridine hydrochloride (0.226 g, 1.95 mmol) for 4 minutes at 215W and 200°C, to give **55h**.

Yield: 67%

Appearance: Yellow-brown solid.



Purification: Column chromatography, 100 % PE to 100 % EtOAc.

Melting point: 127 – 129 °C

¹H NMR (DMSO): 6.91 (d, ³*J* = 8.6 Hz, 2H, 3'-H and 5'-H), 7.41-7.51 (m, 3H, 4-H, 5-H and 6-H), 7.55-7.62 (m, 1H, 2-H), 7.68 (d, ³*J* = 8.6 Hz, 2H, 2'-H and 6'-H), 10.49 (broad s, 1H, OH).

¹³C NMR (DMSO): 115.35 (3'-C and 5'-C), 115.5 (²*J*_{CF} = 22Hz, 3-C), 118.57 (²*J*_{CF} = 22Hz, 1-C), 125.22 (⁴*J*_{CF} = 5-C), 127.34 (1'-C), 130.54 (³*J*_{CF} = 8Hz, 6-C), 132.57 (2'-C and 6'-C), 140.45 (4-C), 161.77 (C-2, ¹*J*_{CF} = 246 Hz), 194.80 (ketone C=O).

***m/z*:** HRMS (ES-TOF) C₁₃H₉FO₂ [MH]⁻ calculated 215.0514; found 215.0423.

FT-IR (KBr): 3168 (phenol OH), 1602 (ketone C=O), 1560 (aryl CH stretch), 883, 850 (*p* disubstituted aromatic ring).

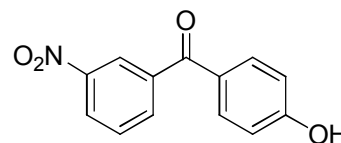
3-Nitro (4'-hydroxy)-benzophenone (**55j**)

Following General Method F, 3-nitro-(4'-methoxy)benzophenone (1.019 g, 3.96 mmol) was irradiated in the microwave with pyridine hydrochloride (2.289 g, 19.8 mmol) for 20 minutes at 300W and 150°C, to give **55j**.

Yield: 32 %

Appearance: Orange-brown solid.

Purification: 100 % PE to 20 % PE / 80 % EtOAc.



Melting point: 169 – 171 °C

¹H NMR (DMSO): 6.93 (d, ³*J* = 7.9 Hz, 2H, 3'-H and 5'-H), 7.71 (d, ³*J* = 7.9 Hz, 2H, 2'-H and 6'-H), 7.83 (dd, ³*J* = 7.9 Hz, ³*J* = 7.9 Hz, 1H, 5-H), 8.10 (ddd, ⁴*J* = 1.3 Hz ⁴*J* = 1.3 Hz, ³*J* = 7.9 Hz, 6-H), 8.37 (dd, ³*J* = 1.8 Hz, ³*J* = 1.8 Hz, 1H, 2-H), 8.46 (ddd, ³*J* = 8.2 Hz, ⁴*J* = 2.4 Hz, ⁴*J* = 1.0 Hz, 1H, 4-H), 10.60 (s, 1H, OH).

¹³C NMR (DMSO): 115.49 (3'-C and 5'-C), 123.48 (2-C), 126.09 (4-C), 126.94 (5-C), 130.21 (1'-C), 132.74 (2'-C and 6'-C), 135.16 (6-C), 139.39 (1-C), 147.61 (3-C), 162.59 (4'-C), 192.12 (ketone C=O).

***m/z*:** HRMS (ES-TOF) C₁₃H₉NO₄ [MH]⁻ calculated 242.0459; found 242.0381.

FT-IR (KBr): 3368 (phenol OH), 1643 (ketone C=O), 1565 (aryl CH stretch), 1346 (NO₂).

4-Nitro-(4'-hydroxy)benzophenone (**55k**)

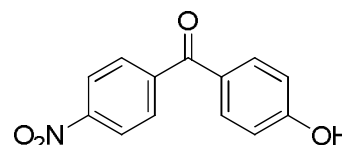
Following General Method F, 4-nitro-(4'-methoxy)benzophenone (3.000 g, 11.2 mmol) was irradiated in the microwave with pyridine hydrochloride (6.738 g, 58.3 mmol) for 18 minutes at 300W and 150°C, to give **55k**.

Yield: 99%

Appearance: Pale yellow solid

Purification: Used without further purification.

Melting point: 196 – 198 °C



¹H NMR (CDCl₃): 6.92 (d, ³*J* = 8.8 Hz, 2H, 3'-H and 5'-H), 7.68 (d, ³*J* = 8.8 Hz, 2H, 2'-H and 6'-H), 7.83 (d, ³*J* = 8.8 Hz, 2H, 2-H and 6-H), 8.27 (d, ³*J* = 8.8 Hz, 2H, 3-H and 5-H), 9.57 (broad s, 1H, OH).

¹³C NMR (CDCl₃): 115.99 (3'-C and 5'-C), 123.66 (3-C and 5-C), 127.99 (2-C and 6-C), 130.50 (1'-C), 133.19 (2-C and 6-C), 144.48 (1-C), 149.64 (4-C), 163.01 (4'-C), 193.83 (C=O).

***m/z*:** HRMS (ES-TOF⁺) [MH]⁺ calculated 244.0604; found 244.0653.

FT-IR (KBr): 3333 (phenol OH), 1638 (ketone C=O), 1599 (aryl CH stretch), 865, 850 (*p* disubstituted aromatic ring).

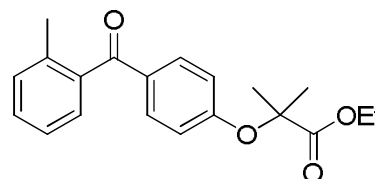
Ethyl 2-methyl-2-(4-(2-methylbenzoyl)phenoxy)propanoate (**56a**)

Following General Method E, 2-methyl-(4'-hydroxy)benzophenone (0.300 g, 1.56 mmol) in MeCN (15 ml) was reacted with K₂CO₃ (0.324 g, 2.33 mmol) and ethyl-2-bromoisobutyric acid (0.364g, 1.87 mmol) for 24 hours to afford **56a**.

Yield: 50 %

Appearance: Colourless oil

Purification: Used without further purification.



Melting point: N/A

¹H NMR (DMSO): 1.22 (t, ³J = 7.1 Hz, CH₂CH₃), 1.66 (s, C(CH₃)₂), 2.23 (s, benzoyl CH₃), 4.22 (quartet, ³J = 7.2 Hz, CH₂CH₃), 6.81 (d, phenoxy 2-H and 6-H), 7.20-7.29 (m, benzoyl 3-H/5-H/6-H) (ddd, ³J = 7.5, ³J = Hz 7.5, ⁴J = 1.6 Hz, benzoyl 4-H), 7.72 (d, ³J = 8.9 Hz, phenoxy 3-H and 5-H).

¹³C NMR (DMSO): 14.16 (CH₂CH₃), 25.53 (C(CH₃)₂), 61.83 (CH₂CH₃), 79.48 (C(CH₃)₂), 117.38 (phenoxy 2-C and 6-C), 125.29 (benzoyl 5-C), 128.15 (benzoyl 6-C), 129.99 (benzoyl 4-C), 130.98 (benzoyl 3-C), 131.15 (benzoyl 4-C), 132.20 (phenoxy 3-C and 5-C), 136.39 (benzoyl 2-C), 139.15 (benzoyl 1-C), 160.12 (phenoxy 1-C), 173.77 (ester C=O), 197.49 (ketone C=O).

m/z: HRMS (ES-TOF⁺) [MH]⁺ calculated 327.1591; found 327.1147.

FT-IR: 2987, 2938 (CH₃ stretch), 1735 (ester C=O), 1659 (ketone C=O), 1597 (aryl CH stretch).

Methyl 2-methyl-2-(4-(2-cyanobenzoyl)phenoxy)propanoate (56b)

Following General Method H, 2-cyano-(4'-hydroxy)benzophenone (0.500 g, 2.22 mmol) was reacted with PPh₃ (0.704 g, 2.68 mmol), DIAD (0.543 g, 2.68 mmol) and methyl-2-hydroxyisobutyrate (0.291 g, 2.46 mmol) in toluene (15 ml) at 80°C for 2 hours 15 minutes to afford **56b**.

Yield: 51 %

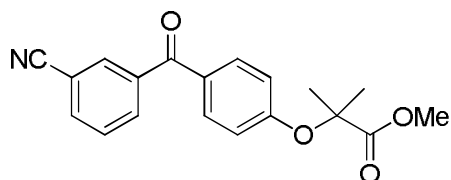
Appearance: Off – white solid.

Purification: Column chromatography,

100% PE to 80 % EtOAc / 20 % PE.

Melting point: 76 – 77 °C

¹H NMR (DMSO): 1.62 (s, C(CH₃)₂, 6H), 3.71 (s, OCH₃, 3H), 6.91 (d, ³J = 8.9Hz, 2H, phenoxy 2-H and 6-H), 7.72-7.78 (m, 3H phenoxy 3-H and 5-H and



benzoyl 5-H), 7.98 (ddd, $^4J = 1.4$ Hz, $^4J = 1.4$ Hz, $^3J = 7.9$ Hz, 1H, benzoyl 6-H), 8.08-8.12 (m, 2H, benzoyl 2-H and 4-H).

^{13}C NMR (DMSO): 25.03 ($\text{C}(\text{CH}_3)_2$), 52.63 (OCH_3), 79.05 ($\text{C}(\text{CH}_3)_2$), 111.70 (benzoyl 3-C), 117.30 (phenoxy 2-C and 6-C), 118.14 (CN), 129.02 (benzoyl 5-C), 129.79 (phenoxy 4-C), 132.19 (phenoxy 3-C and 5-C), 133.50 (benzoyl 2-C), 135.26 (benzoyl 6-C), 138.70 (benzoyl 4-C), 159.47 (phenoxy 1-C), 173.15 (ester $\text{C}=\text{O}$), 192.54 (ketone $\text{C}=\text{O}$).

m/z : HRMS (ES-TOF $^+$) $[\text{MH}]^+$ calculated 324.1230; found 324.1248.

FT-IR (KBr): 2998, 2957 (CH_3 stretch), 2236 (CN stretch), 1736 (amide $\text{C}=\text{O}$), 1662 (ketone $\text{C}=\text{O}$), 1600 (aryl CH stretch), 888, 850 (p disubstituted aromatic ring).

Methyl 2-methyl-2-(4-(4-cyanobenzoyl)phenoxy)propanoate (56c)

Following General Method E, 4-cyano-(4'-hydroxy)benzophenone (0.250 g, 1.12 mmol) in MeCN (15 ml) was reacted with K_2CO_3 (0.232 g, 1.68 mmol) and ethyl-2-bromoisobutyric acid (0.262 g, 1.34 mmol) for 24 hours to afford **56c**.

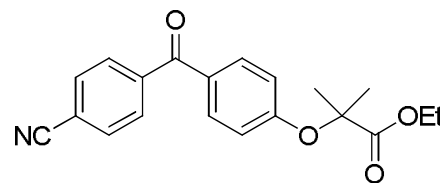
Yield: 43 %

Appearance: Yellow - white solid.

Purification: Used without further purification.

Melting point: 99 – 101 $^{\circ}\text{C}$

^1H NMR (DMSO): 1.23 (t, $^3J = 7.1$ Hz, CH_2CH_3), 1.68 (s, $\text{C}(\text{CH}_3)_2$), 4.24 (quartet $^3J = 7.2$ Hz), 6.87 (d, $^3J = 8.8$ Hz, phenoxy 2-H and 6-H), 7.74 (d, $^3J = 8.9$ Hz, phenoxy 3-H and 5-H), 7.77 (d, $^3J = 7.8$ Hz, benzoyl 2-H and 6-H), 7.81 (d, $^3J = 8.5$ Hz).



^{13}C NMR (DMSO): 14.18 (CH_2CH_3), 25.54 ($\text{C}(\text{CH}_3)_2$), 61.90 (CH_2CH_3), 79.65 ($\text{C}(\text{CH}_3)_2$), 115.38 (benzoyl 4-C), 117.57 (phenoxy 2-C and 6-C), 118.22 (CN), 129.58 (phenoxy 4-C), 130.07 (phenoxy 3-C and 5-C), 132.25 (benzoyl 2-C and 6-C), 132.30 (benzoyl 3-C and 5-C), 142.08 (benzoyl 1-C), 160.37 (phenoxy 1-C), 173.64 (ester $\text{C}=\text{O}$), 193.84 (ketone $\text{C}=\text{O}$).

m/z : HRMS (ES-TOF⁺) [MH]⁺ calculated 338.1387; found 338.1434.

FT-IR: 2983, 2938 (CH_3 stretch), 2233 (CN stretch), 1730 (ester $\text{C}=\text{O}$), 1658 (ketone $\text{C}=\text{O}$), 1595 (aryl CH stretch), 862, 848 (*p* disubstituted aromatic ring).

Methyl 2-methyl-2-(4-(3-nitrobenzoyl)phenoxy)propanoate (56d)

Following General Method H, 3-nitro-(4'-hydroxy)benzophenone (0.160 g, 0.66 mmol) was reacted with PPh_3 (0.207 g, 0.79 mmol), DIAD (0.159 g, 0.79 mmol) and methyl-2-hydroxyisobutyrate (0.086g, 0.72 mmol) in toluene (10 ml) at 80°C for 4 hours 45 minutes to afford **56d**.

Yield: 42 %

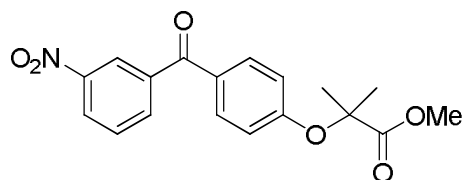
Appearance: White solid

Purification: Column chromatography,

5 % EtOAc / 95 % PE to 40% EtOAc / 60 % PE.

Melting point: 78.8 – 80.5 °C

^1H NMR (CDCl_3): 1.69 (s, 6H, $\text{C}(\text{CH}_3)_2$), 3.78 (s, 3H, CO_2CH_3), 6.89 (d, $^3J = 8.9$ Hz, 2H, phenoxy 2-H and 6-H), 7.69 (dd, $^3J = 7.9$ Hz, $^3J = 7.9$ Hz, 1H, benzoyl 5-H), 7.76 (d, $^3J = 8.9$ Hz, 2H, phenoxy 3-H and 5-H), 8.09 (ddd, $^3J = 7.6$ Hz, $^4J = 1.4$ Hz, $^4J = 1.4$ Hz, 1H, benzoyl 4-H), 8.42 (ddd, 1H, $^3J = 8.3$ Hz, $^4J = 2.3$ Hz, $^4J = 1.0$ Hz, benzoyl 6-H), 8.57 (dd, $^4J = 1.8$ Hz, $^4J = 1.8$ Hz, 1H, benzoyl 2-H).

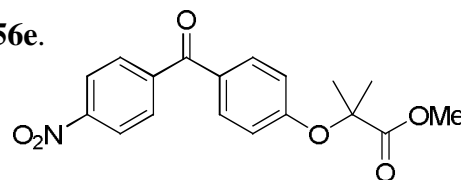


^{13}C NMR (CDCl_3): 25.56 ($\text{C}(\text{CH}_3)_2$), 52.91 (OCH_3), 79.62 ($\text{C}(\text{CH}_3)_2$), 117.58 (phenoxy 2-C and 6-C), 124.56 (benzoyl 2-C), 126.47 (benzoyl 4-C), 129.58 (phenoxy 4-C), 129.71 (benzoyl 5-C), 132.34 (phenoxy 3-C and 5-C), 135.33 (benzoyl 6-C), 139.76 (benzoyl 1-C), 148.16 (benzoyl 3-C), 160.32 (phenoxy 1-C), 174.24 (amide $\text{C}=\text{O}$), 192.96 (ketone $\text{C}=\text{O}$).

2-(4-(4-Nitrobenzoyl)phenoxy)2-methyl propanoate (56e)

Following General Method H, 4-nitro-(4'-hydroxy)benzophenone (1.000 g, 4.11 mmol) was reacted with PPh_3 (1.294 g, 4.93 mmol), DIAD (0.998g, 4.93 mmol) and methyl-2-hydroxyisobutyrate (0.534 g, 4.52 mmol) in toluene (25 ml) at 80°C for 4 hours 15 minutes to afford **56e**.

Yield: 64 %



Appearance: Yellow – white solid

Purification: Used without further purification.

Melting point: $86 - 88^\circ\text{C}$

^1H NMR (DMSO): 1.62 (s, 6H, $\text{C}(\text{CH}_3)_2$), 3.71 (s, 3H, CO_2CH_3), 6.91 (d, $^3J = 8.8$ Hz, 2H, phenoxy 2-H and 6-H), 7.75 (d, $^3J = 8.9$ Hz, 2H, phenoxy 3-H and 5-H), 7.91 (d, $^3J = 8.8$ Hz, 2H, benzoyl 2-H and 6-H), 8.36 (d, $^3J = 8.8$ Hz, 2H, benzoyl 3-H and 5-H).

^{13}C NMR (DMSO): 25.04 ($\text{C}(\text{CH}_3)_2$), 52.67 (OCH_3), 79.09 ($\text{C}(\text{CH}_3)_2$), 117.32 (phenoxy 2-C and 6-C), 123.61 (benzoyl 3-C and 5-C), 128.99 (benzoyl 2-C and 6-C), 130.32 (phenoxy 4-C), 132.22 (phenoxy 3-C and 5-C), 143.25 (benzoyl 1-C), 149.13 (benzoyl 4-C), 159.64 (phenoxy 1-C), 173.15 (ester $\text{C}=\text{O}$), 193.03 (benzoyl $\text{C}=\text{O}$).

m/z : HRMS (ES-TOF $^+$) $[\text{MH}]^+$ calculated 344.1129; found 343.9586.

FT-IR: 2986, 2951 (CH₃ stretch), 1748 (ester), 1652 (ketone C=O), 1596 (aryl CH stretch), 1433 (NO₂), 869, 849 (*p* disubstituted aromatic ring).

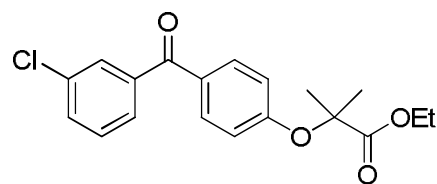
Ethyl-2-(4-(3-chlorobenzoyl)phenoxy)-2-methylpropanoate (56f)

Following General Method E, 3-chloro-(4'-hydroxy)benzophenone (0.250 g, 1.07 mmol) in MeCN (15 ml) was reacted with K₂CO₃ (0.223 g, 1.61 mmol) and ethyl-2-bromoisobutyric acid (0.430 g, 1.52 mmol) for 24 hours to afford **56f**.

Yield: 84 %

Appearance: Off-white solid

Purification: Used without further purification.



Melting point: 84 – 86 °C

¹H NMR (DMSO): 1.15 (t, ³*J* = 7.1 Hz, CH₂CH₃), 1.61 (s, C(CH₃)₂), 4.18 (quartet, ³*J* = 7.2 Hz, CH₂CH₃), 6.91 (d, ³*J* = 8.8 Hz, phenoxy 2-H and 6-H), 7.52-7.76 (m, phenoxy 3-H and 5-H and benzoyl 2-H/4-H/5-H/6-H).

¹³C NMR (DMSO): 13.83 (CH₂CH₃), 25.06 (C(CH₃)₂), 61.34 (CH₂CH₃), 79.06 (C(CH₃)₂), 115.27 (phenoxy 2-C and 6-C), 127.86 (benzoyl 6-C), 128.49 (benzoyl 5-C), 128.60 (phenoxy 4-C), 129.30 (benzoyl 2-C), 130.45 (benzoyl 4-C), 133.32 (benzoyl 3-C), 139.64 (benzoyl 1-C), 159.36 (phenoxy 1-C), 172.62 (ester C=O), 192.93 (ketone C=O).

***m/z*:** HRMS (ES-TOF⁺) [MH]⁺ calculated 347.1045; found 347.0742.

FT-IR: 2992, 2941 (CH₃ stretch), 1726 (ester C=O), 1658 (ketone C=O), 1598 (aryl CH stretch).

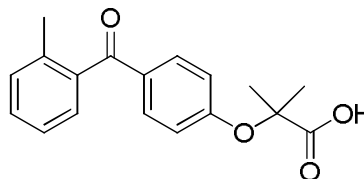
2-(4-(2-Methylbenzoyl)phenoxy)-2-methyl propanoic acid (**57a**)

Following General Method C, ethyl-2-methyl-2-(4-(2-methylbenzoyl)phenoxy)-2-propanoate (0.090g, 0.275 mmol), was reacted with lithium hydroxide (0.058 g, 1.38 mmol) in a mixture of water and THF (1:1, 10 ml) for 22 hours to afford **57a**.

Yield: 85 %

Appearance: Yellow solid

Purification: Used without further purification.



¹H NMR (DMSO): 1.58 (s, 6H, C(CH₃)₂), 2.19 (s, 3H, CH₃), 6.89 (d, ³J = 8.9 Hz, 2H, phenoxy 2-H and 6-H), 7.25-7.36 (m, 3H, benzoyl 3-H/5-H/6-H), 7.44 (ddd, ³J = 7.3 Hz, ³J = 7.3 Hz, ⁴J = 1.6 Hz, 1H, benzoyl 4-H), 7.65 (d, ³J = 8.9 Hz, 2H, phenoxy 3-H and 5-H), 13.23 (s, 1H, OH).

¹³C NMR (DMSO): 19.25 (benzoyl CH₃), 25.09 (C(CH₃)₂), 78.83 (C(CH₃)₂), 117.08 (phenoxy 2-C and 6-C), 125.39 (benzoyl 5-C), 127.49 (benzoyl 6-C), 129.87 (phenoxy 4-C), 130.72 (phenoxy 3-C and 5-C), 131.69 (benzoyl 3-C), 135.22 (benzoyl 2-C), 138.78 (benzoyl 1-C), 159.91 (phenoxy 1-C), 174.32 (carboxylic acid C=O), 196.19 (ketone C=O).

m/z: HRMS (ES-TOF⁺) [MH]⁺ calculated 299.1278; found 299.1268.

2-(4-(3-Methylbenzoyl)phenoxy)-2-methyl propanoic acid (**57b**)

Following General Method E, **55b** (0.1310 g, 0.62 mmol) in MeCN (10 ml) was reacted with NaOH (0.155 g, 0.92 mmol) and α-bromoisobutyric acid (0.136 g, 3.39 mmol) for 3 hours to afford **57b**.

Yield: 61 %

Appearance: Pale yellow solid

Purification: Used without further purification

Melting point: 92 – 94 °C

¹H NMR (CDCl₃): 1.69 (s, C(CH₃)₂, 6H), 2.41 (s, benzoyl CH₃, 3H), 6.94 (d, ³J = 8.8 Hz, 2H, phenoxy 2-H and 6-H), 7.31-7.40 (m, 2H, benzoyl 4-H and 5-H), 7.50-7.59 (m, 2H, 2-H and 6-H), 7.78 (d, ³J = 8.8 Hz, 2H, phenoxy 3-H and 5-H).

¹³C NMR (CDCl₃): 21.49 (benzoyl CH₃), 25.46 (C(CH₃)₂), 79.45 C(CH₃)₂, 118.18 (phenoxy 2-C and 6-C), 127.26 (benzoyl 2-C), 128.18 (benzoyl 6-C), 130.40 (benzoyl 5-C), 131.57 (phenoxy 4-C), 132.30 (phenoxy 3-C and 5-C), 133.07 (benzoyl 4-C), 138.09 (benzoyl 3-C), 138.27 (benzoyl 1-C), 159.09 (phenoxy 1-C), 177.53 (carboxylic acid C=O), 196.21 (ketone C=O).

m/z: HRMS (ES-TOF⁺) [MH]⁺ calculated 299.1278; found 299.1109

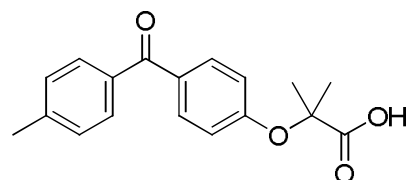
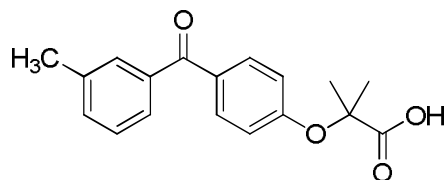
FT-IR (KBr): 2985 (carboxylic acid OH), 1744 (carboxylic acid C=O), 1632 (ketone C=O), 1595 (aryl CH stretch), 847, 811 (*p* disubstituted aromatic ring).

2-(4-(4-Methylbenzoyl)phenoxy)-2-methylpropanoic acid (57c)

Following General Method E, **55c** (0.073 g, 0.34 mmol) in MeCN (5 ml) was reacted with NaOH (0.075 g, 1.87 mmol) and α-bromoisobutyric acid (0.086 g, 1.87 mmol) for 24 hours to afford **57c**.

Yield: 63 %

Appearance: White needle like crystals.



Purification: Recrystallised from toluene.

Melting point: 162 – 164 °C

¹H NMR (CDCl₃): 1.69 (s, 6H, C(CH₃)₂), 2.43 (s, 3H, benzoyl CH₃), 6.94 (d, ³J = 8.8 Hz, 2H, phenoxy 2-H and 6-H), 7.26 (d, ³J = 8.1 Hz, 2H, benzoyl 3-H and 5-H), 7.68 (d, ³J = 8.1 Hz, 2H, phenoxy 3-H and 5-H), 7.76 (d, ³J = 8.8 Hz, 2H, benzoyl 2-H and 6-H).

¹³C NMR (CDCl₃): 21.96 (benzoyl CH₃), 25.64 (C(CH₃)₂), 79.70 (C(CH₃)₂), 118.52 (phenoxy 2-C and 6-C), 129.28 (benzoyl 3-C and 5-C), 130.47 (phenoxy 4-C), 132.07 (benzoyl 2-C and 6-C), 132.39 (phenoxy 3-C and 5-C), 135.48 (benzoyl 1-C), 143.32 (benzoyl 4-C), 159.06 (phenoxy 1-C), 177.69 (carboxylic acid C=O), 195.98 (ketone C=O).

m/z: HRMS (ES-TOF⁺) C₁₉H₁₇O₄ [MH]⁺ calculated 297.1278; found 297.1045.

FT-IR (KBr): 2950 (carboxylic acid OH), 1742 (carboxylic acid C=O), 1625 (ketone C=O), 1591 (aryl CH stretch), 888, 849 (*p* disubstituted aromatic ring).

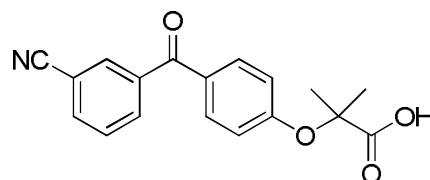
2-(4-(3-Cyanobenzoyl)phenoxy)-2-methyl propanoic acid (57d)

Following General Method C, ethyl-2-methyl-2-(4-(3-cyanobenzoyl)phenoxy)2-propanoate (0.275 g, 0.85 mmol), was reacted with lithium hydroxide (0.102 g, 4.24 mmol) in a mixture of water and THF (1:1, 10 ml) for 3 hours 30 minutes to afford **57d**.

Yield: 71 %

Appearance: Orange brown solid

Purification: Used without further purification.



Melting point: 99 – 101 °C

¹H NMR (CDCl₃): 1.72 (C(CH₃)₂), 6.96 (d, ³J = 8.9 Hz, 2H, phenoxy 2-H and 6-H), 7.62 (dd, ³J = 7.8 Hz, ³J = 7.8 Hz, 1H, benzoyl 5-H), 7.75 (d, ³J = 8.9 Hz, 2H, phenoxy 3-H and 5-H), 7.84 (ddd, ³J = 7.9 Hz, ⁴J = 1.4 Hz, ⁴J = 1.4 Hz, 1H, benzoyl 6-C), 7.97 – 8.03 (m, 2H, benzoyl 2-H and 4-H).

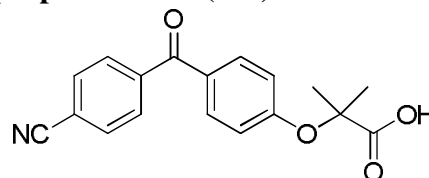
¹³C NMR (CDCl₃): 25.48 (C(CH₃)₂), 79.50 (C(CH₃)₂), 112.86 (benzoyl 3-C), 118.11 (CN), 118.23 (phenoxy 2-C and 6-C), 129.50 (benzoyl 5-C), 129.97 (phenoxy 1-C), 132.31 (phenoxy 3-C and 5-C), 133.32 (benzoyl 6-C), 133.79 (benzoyl 2-C), 135.20 (benzoyl 4-C), 139.18 (benzoyl 1-C), 159.90 (phenoxy 1-C), 177.55 (carboxylic acid C=O), 193.36 (ketone C=O).

m/z: HRMS (ES-TOF⁺) C₁₈H₁₆NO₄ [MH]⁺ calculated 310.1074; found 309.9905.

FT-IR (KBr): 2986 (carboxylic acid OH), 2227 (CN), 1741 (carboxylic acid C=O), 1639 (ketone C=O), 1592 (aryl CH stretch).

2-(4-(4-Cyanobenzoyl)phenoxy)-2-methyl propanoic acid (57e)

Following General Method C, ethyl-2-methyl-2-(4-(4-cyanobenzoyl)phenoxy)2-



propanoate (0.100 g, 0.29 mmol), was reacted with lithium hydroxide (0.036 g, 1.48 mmol) in a mixture of water and THF (1:1, 10 ml) for 21 hours to afford **57e**.

Yield: 92 %

Appearance: White solid

Purification: Used without further purification.

Melting point: 158 – 159 °C

¹H NMR (DMSO): 1.59 (s, 3H, C(CH₃)₂), 6.93 (d, ³J = 8.9 Hz, 2H, phenoxy 2-H and 6-H), 7.73 (d, ³J = 8.8 Hz, 2H, phenoxy 3-H and 5-H), 7.82 (d, ³J = 8.6 Hz, 2H benzoyl 2-H and 6-H), 8.01 (d, ³J = 8.6 Hz, 2H, benzoyl 3-H and 5-H), 8.13 (s, 1H, OH).

m/z: HRMS (ES-TOF⁺) [MH]⁺ calculated 310.1074; found 310.1135.

FT-IR: 2995 (carboxylic acid OH stretch), 2230 (CN stretch), 1743 (ketone C=O), 1596 (aryl CH stretch), 862, 842 (*p* disubstituted aromatic ring).

2-(4-(3-Chlorobenzoyl)phenoxy)-2-methyl propanoic acid (57f)

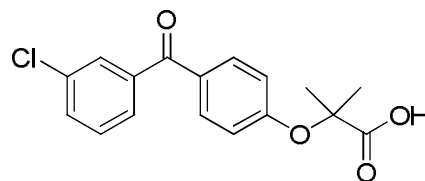
Following General Method C, **56f** (0.150 g, 0.43 mmol), was reacted with lithium hydroxide (0.091 g, 2.16 mmol) in a mixture of water and THF (1:1, 10 ml) for 2 hours 30 minutes to afford **57f**.

Yield: 50 %

Appearance: Yellow solid

Purification: Used without further

purification.



¹H NMR (DMSO): 1.60 (C(CH₃)₂), 6.93 (d, ³J = 8.9 Hz, 2H, phenoxy 2-C and 6-C), 7.55 -7.75 (m, 6H, benzoyl 2-H/4-H/5-H/6-H, phenoxy 3-H and 5-H), 13.27 (carboxylic acid OH).

¹³C NMR (DMSO): 25.09 (C(CH₃)₂), 78.90 (C(CH₃)₂), 117.06 (phenoxy 2-C and 6-C), 127.88 (benzoyl 6-C), 128.59 (benzoyl 5-C), 129.01 (phenoxy 3-C and 5-C), 130.44 (benzoyl C-2), 131.97 (benzoyl 4-C), 133.36 (benzoyl 3-C), 139.68 (benzoyl 1-C), 159.69 (phenoxy 1-C), 174.38 (carboxylic acid C=O), 192.93 (ketone C=O).

2-(4-(2-Fluorobenzoyl)-phenoxy)-2-methylpropanoic acid (57g)

Following General Method E, **55g** (0.501 g, 2.31 mmol) in MeCN (10 ml) was reacted with NaOH (0.509 g, 13.0 mmol) and α -bromoisobutyric acid (0.579 g, 3.46 mmol) for 21 hours to afford **57g**.

Yield: 76%

Appearance: Off – white solid

Purification: Precipitated from EtOAc with

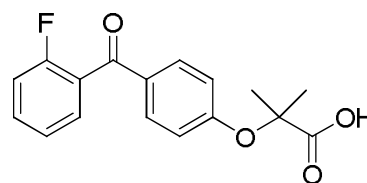
PE. The solid afforded was collected by vacuum filtration.

Melting point: 133 – 135 °C

¹H NMR (DMSO): 1.69 (s, 6H, C(CH₃)₂), 6.91 (d, ³J = 8.9 Hz, 2H, phenoxy 2-H and 6-H), 7.15 (m, 1H, benzoyl CH), 7.23-7.26 (m, 1H, benzoyl CH), 7.48-7.51 (m, 2H, benzoyl CH), 7.52 (d, ³J = 8.8 Hz, 2H, phenoxy 3-H and 5-H).

¹³C NMR (DMSO): 25.45 (C(CH₃)₂), 79.39 (C(CH₃)₂), 116.34 (d, ²J_{CF} = 21.9 Hz, benzoyl 3-C), 118.12 (phenoxy 2-C and 6-C), 124.39 (d, ⁴J_{CF} = 3 Hz, benzoyl 5-C), 127.32 (d, ²J_{CF} = 15.0 Hz, benzoyl 1-C), 130.65 (d, ³J_{CF} = 3 Hz, benzoyl 6-C), 131.25 (phenoxy 4-C), 132.12 (phenoxy 3-C and 5-C), 132.85 (d, ³J_{CF} = 8.0 Hz, benzoyl 4-C), 159.89 (phenoxy 1-C), 159.93 (d, ¹J_{CF} = 251.53 Hz, benzoyl 2-C), 178.68 (carboxylic acid C=O), 192.36 (ketone C=O).
m/z: HRMS (ES-TOF) C₁₇H₁₄FO₄⁻ [MH]⁻ calculated 301.0882; found 301.0907.

FT-IR (KBr): 3089 (carboxylic acid OH), 2603, 2492 (CH₃ stretch), 1745 (carboxylic acid C=O), 1633 (ketone C=O), 1591 (aryl CH stretch), 849, 826 (*para* disubstituted aromatic ring).



2-(4-(3-Fluorobenzoyl)phenoxy)-2-methyl propanoic acid (57h)

Following General Method E, **55h** (0.350 g, 1.62 mmol) in MeCN (10 ml) was reacted with NaOH (0.356 g, 8.90 mmol) and α -bromoisobutyric acid (0.406 g, 2.43 mmol) for 4 hours to afford **57h**.

Yield: 59 %

Appearance: White solid

Purification: Precipitated from EtOAc by addition of PE.

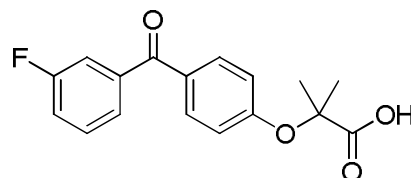
Melting point: 104 – 106 °C

^1H NMR (DMSO): 1.60 (s, 6H, $\text{C}(\text{CH}_3)_2$), 6.93 (d, $^3J = 8.9$ Hz, 2H, phenoxy 2-H and 6-H), 7.44-7.53 (m, 3H, benzoyl 4-H, 5-H, 6-H), 7.56-7.63 (m, 1H, benzoyl 2-H), 7.74 (d, $^3J = 8.9$ Hz, 2H, phenoxy 3-H and 5-H).

^{13}C NMR (DMSO): 25.09 ($\text{C}(\text{CH}_3)_2$), 78.91 ($\text{C}(\text{CH}_3)_2$), 115.64 (d, $^2J_{\text{CF}} = 22.1$ Hz, benzoyl 2-C), 117.07 (phenoxy 2-C and 6-C), 118.94 (d, $^2J_{\text{CF}} = 21.1$ Hz, benzoyl 4-C), 125.43 (d, $^4J_{\text{CF}} = 3.0$ Hz, benzoyl 6-C), 129.08 (phenoxy 4-C), 130.66 (d, $^3J_{\text{CF}} = 8.0$ Hz, benzoyl 5-C), 131.94 (phenoxy 3-C and 5-C), 139.95 (d, $^3J_{\text{CF}} = 7.0$ Hz, benzoyl 1-C), 159.65 (phenoxy 1-C), 161.81 (d, $^1J_{\text{CF}} = 245$ Hz, benzoyl 3-C), 174.38 (carboxylic acid $\text{C}=\text{O}$), 192.97 (ketone $\text{C}=\text{O}$).

m/z : HRMS (ES-TOF $^+$) $[\text{MH}]^+$ calculated 303.1027; found 303.0894.

FT-IR (KBr): 2989 (carboxylic acid OH stretch), 1744 (carboxylic acid $\text{C}=\text{O}$), 1641 (ketone $\text{C}=\text{O}$), 1593 (aryl CH stretch).



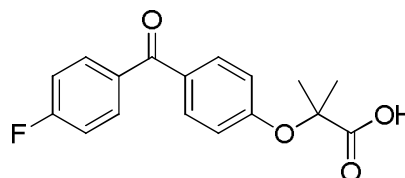
2-(4-(4-Fluorobenzoyl)phenoxy)-2-methylpropanoic acid (**57i**)

Following General Method E, **55i** (0.500 g, 2.31 mmol) in butan-2-one (20 ml) was reacted with NaOH (0.508 g, 12.1 mmol) and α -bromoisobutyric acid (0.579 g, 3.47 mmol) for 24 hours to afford **57i**.

Yield: 11 %

Appearance: White solid

Purification: Column chromatography, 1%



MeOH: 99% DCM to 5% MeOH / 95 % DCM. Then recrystallised from toluene.

Melting point: 159-160 °C

^1H NMR (DMSO): 1.59 (s, 6H, $\text{C}(\text{CH}_3)_2$), 6.92 (d, $^3J = 8.8$ Hz, 2H, phenoxy 2-H and 6-H), 7.37 (dd, 2H, $^3J = 8.8$ Hz, $^3J_{\text{CF}} = 8.8$ Hz, benzoyl 3-H and 5-C), 7.71 (d, $^3J = 8.8$ Hz, 2H, phenoxy 3-H and 5-H), 7.78 (dd, 2H, $^3J = 8.8$ Hz, $^4J_{\text{HF}} = 5.6$ Hz, benzoyl 2-H and 6-H) 13.21 (s, 1H, OH).

^{13}C NMR (DMSO): 25.44 ($\text{C}(\text{CH}_3)_2$), 79.49 ($\text{C}(\text{CH}_3)_2$), 115.57 (d, $^2J_{\text{CF}} = 21.8$ Hz benzoyl 3-C and 5-C), 118.32 (phenoxy 2-C and 6-C), 131.37 (phenoxy 4-C), 132.17 (phenoxy 3-C and 5-C), 132.59 (d, $^3J = 9.5$ Hz, benzoyl 2-C and 6-C), 134.19 (d, $^4J_{\text{CF}} = 2.9$ Hz, benzoyl 1-C), 159.09 (phenoxy 1-C), 165.39 (d, $^1J_{\text{CF}} = 253.9$ Hz, benzoyl 4-C), 177.99 (carboxylic acid $\text{C}=\text{O}$), 194.49 (ketone $\text{C}=\text{O}$).

m/z : HRMS (ES-TOF) $\text{C}_{17}\text{H}_{14}\text{FO}_4$ $[\text{MH}]^-$ calculated 301.0882; found 301.0828.

FT-IR (KBr): 3059 (carboxylic acid OH), 1735 (carboxylic acid $\text{C}=\text{O}$), 1626 (ketone $\text{C}=\text{O}$), 1598 (aryl CH stretch), 864, 852 (*para* disubstituted aromatic ring).

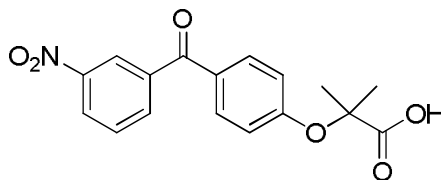
2-(4-(3-Nitrobenzoyl) phenoxy)-2-methyl propanoic acid (57j)

Following General Method C, **56d** (0.090 g, 0.26 mmol), was reacted with lithium hydroxide (0.044 g, 1.83 mmol) in a mixture of water and THF (1:1, 10 ml) for 24 hours 30 minutes to afford **57j**.

Yield: 83 %

Appearance: Brown solid

Purification: Used without further purification



¹H NMR (DMSO): 1.72 (C(CH₃)₂), 6.97 (d, ³J = 8.8 Hz, phenoxy 2-H and 6-H), 7.69 (dd, ³J = 7.9 Hz, ³J = 7.9 Hz, benzoyl 5-H), 7.78 (d, ³J = 8.9 Hz, phenoxy 3-H and 5-H), 8.09 (ddd, ³J = 7.8 Hz, ⁴J = 1.4 Hz, ⁴J = 1.4 Hz, benzoyl 6-H), 8.42 (ddd, ³J = 8.2 Hz, ⁴J = benzoyl 4-H) 8.57 (dd, ⁴J = 1.8 Hz, ⁴J = 1.8 Hz, benzoyl 2-H).

¹³C NMR (DMSO): 25.47 (C(CH₃)₂), 79.55 (C(CH₃)₂), 118.29 (phenoxy 2-C and 6-C), 124.59 (benzoyl 2-C), 126.57 (benzoyl 4-C), 129.75 (benzoyl 5-C), 130.02 (phenoxy 4-C), 132.33 (phenoxy 3-C and 5-C), 135.38 (benzoyl 6-C), 139.62 (benzoyl 1-C), 148.16 (benzoyl 3-C), 159.89 (phenoxy 1-C), 176.69 (carboxylic acid C=O), 193.04 (ketone C=O).

m/z: HRMS (ES-TOF⁺) [MH]⁺ calculated 330.0972; found 330.1026.

FT-IR: 3090 (carboxylic acid OH), 1743 (carboxylic acid C=O), 1638 (ketone C=O), 1596 (aryl CH stretch), 843, 821 (*p* disubstituted aromatic ring).

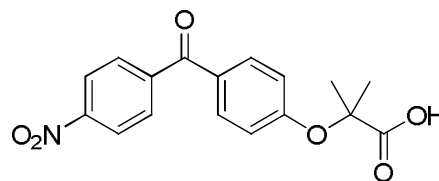
2-(4-(4-Nitrobenzoyl)phenoxy)-2-methyl propanoic acid (57k)

Following General Method C, **56e** (0.600 g, 1.75 mmol), was reacted with lithium hydroxide (0.209 g, 8.73 mmol) in a mixture of water and THF (1:1, 10 ml) for 4 hours to afford **57k**.

Yield: 64 %

Appearance: Yellow solid

Purification: Used without further purification.



Melting point: 170 – 172 °C

¹H NMR (DMSO): 1.60 (s, C(CH₃)₂, 6H), 6.94 (d, ³J = 8.8 Hz, 2H, phenoxy 2-H and 6-H), 7.75 (d, ³J = 8.9 Hz, 2H, phenoxy 3-H and 5-H), 7.91 (d, ³J = 8.8 Hz, 2H, benzoyl 2-H and 6-H), 8.36 (d, ³J = 8.8 Hz, 2H, benzoyl 3H and 5-H).

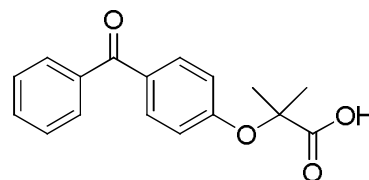
¹³C NMR (DMSO): 25.48 (C(CH₃)₂), 79.47 (C(CH₃)₂), 118.20 (phenoxy 2-C and 6-C), 123.67 (benzoyl 3-C and 5-C), 130.02 (benzoyl 2-C and 6-C), 130.55 (phenoxy 4-C), 132.41 (phenoxy 3-C and 5-C), 143.54 (benzoyl 1-C), 149.78 (benzoyl 4-C), 160.00 (phenoxy 1-C), 177.91 (carboxylic acid C=O), 193.73 (ketone C=O).

m/z: HRMS (ES-TOF⁺) [MH]⁺ calculated 330.0972; found 330.0834.

FT-IR: 3249 (carboxylic acid OH), 1710 (carboxylic acid C=O), 1647 (ketone C=O), 1595 (aryl CH stretch), 1471 (NO₂).

(4-Benzoyl)-phenoxy-2-methylpropanoic acid (57I)

Following General Method E, **55I** (0.500 g, 2.52 mmol) in MeCN (20 ml) was reacted with NaOH (0.555 g, 13.9 mmol) and α-bromoisobutyric acid (0.632 g, 3.78 mmol) for 2 hours 30 minutes to afford **57I**.



Yield: 76%

Appearance: Off – white solid

Purification: Precipitated with petroleum ether. The solid afforded was collected by vacuum filtration.

Melting point: 130 – 132 °C

¹H NMR (CDCl₃): 1.70 (s, 3H, C(CH₃)₂), 6.93 (d, ³J = 8.9 Hz, 2H, phenoxy 2-H and 6-H), 7.46 (dd, ³J = 7.5 Hz, ³J = 7.5 Hz, 2H, benzoyl 3-H and 5-H), 7.57 (t, ³J = 7.4 Hz, 1H, benzoyl 4-H) 7.74-7.79 (m, 4H, phenoxy 3-H and 5-H and benzoyl 2-H and 6-H).

¹³C NMR (CDCl₃): 25.31 (C(CH₃)₂), 79.33 (C(CH₃)₂), 118.15 (phenoxy 2-C and 6-C), 128.24 (benzoyl 3-C and 5-C), 129.83 (benzoyl 2-C and 6-C), 131.35 (phenoxy 4-C), 132.18 (phenoxy 3-C and 5-C), 137.90 (benzoyl 4-C), 158.94 (phenoxy 1-C), 177.76 (carboxylic acid C=O), 194.3 (ketone C=O).

m/z: HRMS (ES-TOF) C₁₇H₁₆O₄ [MH]⁺ calculated 283.0976; found 283.0920.

FT-IR (KBr): 3060 (carboxylic acid OH), 2988 (CH₃ stretch), 1741 (carboxylic acid C=O), 1633 (ketone C=O), 1595 (aryl CH stretch), 848, 823 (*para* disubstituted aromatic ring).

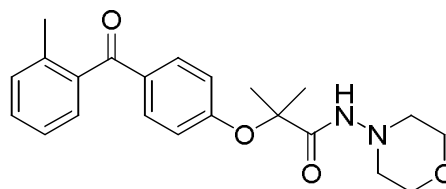
***N*-Morpholino-2-(4-(2-methylbenzoyl)phenoxy)-2-methylpropanamide (58a)**

Following General Method G, **57a** (0.025 g, 0.084 mmol) was reacted with HBTU (0.034 g, 0.092 mmol), 4-aminomorpholine (0.009 g, 0.084 mmol) and triethylamine (17.4 μl, 0.092 mmol) in DCM (3 ml) for 21 hours 30 minutes to afford **58a**.

Yield: 89 %

Appearance: White solid

Purification: Preparative TLC, 3 PE / 7 EtOAc.



Melting point: 111 – 112 °C

¹H NMR (CDCl₃): 1.60 (C(CH₃)₂), 2.77-2.81 (m, 4H, morpholino 2-H and 6-H), 3.78-3.85 (m, 4H, morpholino 3-H and 5-H), 6.93 (d, ³J = 8.8 Hz, 2H, phenoxy 2-H and 6-H), 7.21-7.30 (m, benzoyl 3-H, 4-H, 6-H), 7.38 (ddd, ³J = 7.5 Hz, ³J = 7.5 Hz, ⁴J = 1.8 Hz, 1H, benzoyl 5-H), 7.75 (d, 2H, ³J = 8.8 Hz, phenoxy 3-H and 5-H).

¹³C NMR (CDCl₃): 20.14 (benzoyl CH₃), 25.55 (C(CH₃)₂), 55.89 (morpholino 3-C and 5-C), 66.60 (morpholino 2-C and 6-C), 81.92 (C(CH₃)₂), 119.56 (phenoxy 2-C and 6-C), 125.48 (benzoyl 5-C), 128.42 (benzoyl 6-C), 130.41 (benzoyl 3-C), 131.27 (benzoyl 4-C), 132.26 (phenoxy 3-C and 5-C), 132.62 (phenoxy 4-C), 136.73 (benzoyl 2-C), 138.87 (benzoyl 1-C), 158.83 (phenoxy 1-C), 171.44 (amide C=O), 197.48 (ketone C=O).

HPLC: System 2, R_t = 15.95 minutes

System 3, R_t = 2.64 minutes

System 4, R_t = 2.65 minutes

m/z: HRMS (ES-TOF⁺) C₂₂H₂₇N₂O₄ [MH]⁺ calculated 383.1965; found 383.1958.

FT-IR: 2936, 2861 (CH₃ stretch), 1684 (ketone C=O), 1652 (amide C=O), 1598 (aryl CH stretch).

***N*-Morpholino-2-(4-(3-methylbenzoyl)phenoxy)-2-methylpropanamide
(58b)**

Following General Method G, **57b** (0.059 g, 0.20 mmol) was reacted with HBTU (0.085 g, 0.22 mmol), 4-aminomorpholine (0.020 g, 0.20 mmol) and triethylamine (42 µl, 0.22 mmol) in DCM (3 ml) for 19 hours 30 minutes to afford **58b**.

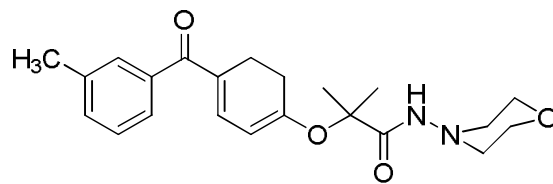
Yield: 31 %

Appearance: White solid

Purification: Precipitated from

EtOAc with addition of PE.

Melting point: 129 – 130 °C



¹H NMR (CDCl₃): 1.61 (s, C(CH₃)₂, 6H), 2.42 (s, 3H, benzoyl CH₃), 2.80 (m, 4H, morpholino 2-CH₂ and 6-CH₂), 3.81 (m, 4H, morpholino 3-CH₂ and 5-CH₂), 6.97 (d, ³J = 8.8 Hz, 2H, phenoxy 2-H and 6-H), 7.24 (broad s, 1H, NH), 7.33-7.42 (m, 2H, benzoyl 3-H and 6-H), 7.50-7.59 (m, 2H, benzoyl 2-H and 6-H), 7.78 (d, ³J = 8.8 Hz, 2H, phenoxy 3-H and 5-H).

¹³C NMR (CDCl₃): 21.51 (benzoyl CH₃), 25.42 (C(CH₃)₂), 55.78 (morpholino 3-C and 5-C), 66.47 (morpholino 2-C and 6-C), 81.74 (C(CH₃)₂), 119.39 (phenoxy 2-C and 6-C), 127.20 (benzoyl 2-C), 128.21 (benzoyl 6-C), 130.34 (benzoyl 5-C), 132.11 (phenoxy 3-C and 5-C), 132.38 (phenoxy 4-C), 133.16 (benzoyl 4-C), 137.91 (3-C), 138.33 (benzoyl 1-C), 158.08 (phenoxy 1-C), 171.39 (amide C=O), 195.77 (ketone C=O).

HPLC: System 2, R_t = 16.30 minutes

System 3, R_t = 2.67 minutes

System 4, R_t = 2.69 minutes

m/z: HRMS (ES-TOF⁺) C₂₂H₂₇N₂O₄ [MH]⁺ calculated 383.1965; found 382.9665

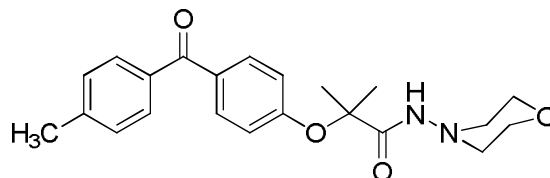
FT-IR (KBr): 3297 (amide NH), 2928, 2850 (CH₃ stretch), 1687 (ketone C=O), 1597 (aryl CH stretch), 882, 858 (*p* disubstituted aromatic ring).

***N*-Morpholino-2-(4-(4-methylbenzoyl)phenoxy)-2-methylpropanamide
(58c)**

Following General Method G, **57c** (0.028 g, 0.094 mmol) was reacted with HBTU (0.039 g, 0.104 mmol), 4-aminomorpholine (0.009 g, 0.094 mmol) and triethylamine (19.0 μ l, 0.104 mmol) in DCM (3 ml) for 2 hours 45 minutes to afford **58c**.

Yield: 59 %

Appearance: White solid



Purification: Column chromatography, 5 % EtOAc / 95 % PE to 100 % EtOAc.

^1H NMR (CDCl_3): 1.61 (s, $\text{C}(\text{CH}_3)_2$, 6H), 2.44 (s, 3H, benzoyl CH_3), 2.81 (m, 4H, morpholino 3- CH_2 and 5- CH_2), 3.81 (m, 4H, morpholino 2- CH_2 and 6- CH_2), 6.97 (d, $^3J = 8.8$ Hz, 2H, phenoxy 2-H and 6-H), 7.24-7.30 (m, 2H, benzoyl 3-H and 5-H), 7.68 (d, $^3J = 8.2$ Hz 2H, phenoxy 3-H and 5-H), 7.77 (d, $^3J = 8.8$ Hz, 2H, benzoyl 2-H and 6-H).

^{13}C NMR (CDCl_3): 21.65 (benzoyl CH_3), 25.29 ($\text{C}(\text{CH}_3)_2$), 55.68 (morpholino 2-C and 6-C), 66.35 (morpholino 3-C and 5-C), 81.62 ($\text{C}(\text{CH}_3)_2$), 119.31 (phenoxy 2-C and 6-C), 128.99 (benzoyl 3-C and 5-C), 130.06 (phenoxy 3-C and 5-C), 131.87 (benzoyl 2-C and 6-C), 135.01 (phenoxy 4-C), 143.09 (benzoyl C-4), 157.79 (phenoxy 1-C), 171.30 (amide $\text{C}=\text{O}$), 195.21 (ketone $\text{C}=\text{O}$).

HPLC: System 2, $R_t = 16.28$ minutes

System 3, $R_t = 2.65$ minutes

System 4, $R_t = 2.69$ minutes

m/z: HRMS (ES-TOF⁺) C₂₂H₂₇N₂O₄ [MH]⁺ calculated 383.1965; found 383.0093.

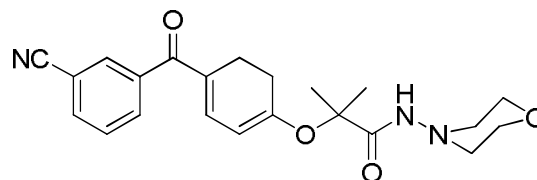
***N*-Morpholino-2-(4-(3-cyanobenzoyl)phenoxy)-2-methylpropanamide
(58d)**

Following General Method G, **57d** (0.044 g, 0.14 mmol) was reacted with HBTU (0.059 g, 0.16 mmol), 4-aminomorpholine (0.014 g, 0.14 mmol) and triethylamine (30.0 µl, 0.092 mmol) in DCM (3 ml) for 21 hours 30 minutes to afford **58d**.

Yield: 46%

Appearance: White solid

Purification: Recrystallised from
PE / EtOAc



Melting point: 89 – 91 °C

¹H NMR (CDCl₃): 1.63 (s, 6H C(CH₃)₂), 2.80 (m, 4H, morpholino CH₂), 3.80 (m, 4H, morpholino CH₂), 7.01 (d, ³J = 8.8 Hz, 2H, phenoxy 2-H and 6-H), 7.19 (broad s, 1H, NH), 7.63 (dd, 1H, ³J = 7.9 Hz, ³J = 7.5 Hz, benzoyl 5-H), 7.75 (d, ³J = 8.8 Hz, 2H, phenoxy 3-H and 5-H), 7.86 (ddd, ³J = 7.7 Hz, ⁴J = 1.3 Hz, ⁴J = 1.3 Hz, 1H, benzoyl 6-H), 7.97-8.03 (m, 2H, benzoyl 2-H and 4-H).

¹³C NMR (CDCl₃): 25.62 (C(CH₃)₂), 55.97 (morpholino 3-C and 5-C), 66.66 (morpholino 2-C and 6-C), 82.13 (C(CH₃)₂), 113.17 (benzoyl 3-C), 118.217 (CN), 119.78 (phenoxy 2-C and 6-C), 129.77 (benzoyl 5-C), 131.08 (phenoxy 4-C), 132.34 (phenoxy 3-C and 5-C), 133.53 (benzoyl 2-C), 133.92 (benzoyl 6-C), 135.53 (benzoyl 4-C), 139.17 (benzoyl 1-C), 159.12 (phenoxy 1-C), 171.38 (amide C=O), 193.36 (ketone C=O).

HPLC: System 2, R_t = 14.20 minutes

System 3, R_t = 2.51 minutes

System 4, R_t = 2.58 minutes

m/z : HRMS (ES-TOF⁺) $C_{22}H_{26}N_3O_4$ $[MH]^+$ calculated 394.1761; found 394.1651

FT-IR (KBr): 3302 (amide NH), 2948, 2851 (CH_3 stretch), 2229 (CN), 1734 (amide C=O), 1646 (ketone C=O), 1572 (aryl CH stretch), 882, 856 (*p* disubstituted aromatic ring).

***N*-Morpholino-2-(4-(4-cyanobenzoyl)phenoxy)-2-methylpropanamide (58e)**

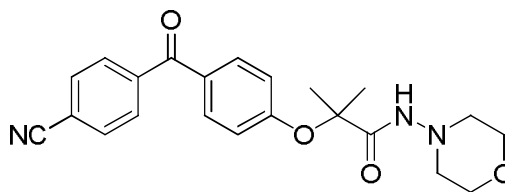
Following General Method G, **57e** (0.020 g, 0.065 mmol) was reacted with HBTU (0.027 g, 0.071 mmol), 4-aminomorpholine (0.007 g, 0.065 mmol) and triethylamine (13.4 μ l, 0.092 mmol) in DCM (3 ml) for 24 hours to afford **58e**.

Yield: 72 %

Appearance: White solid

Purification:

Column



chromatography, 5% EtOAc / 95 % PE to 100 % EtOAc.

Melting point: 145 – 147 °C

1H NMR (DMSO): 1.63 ($C(CH_3)_2$), 2.77- 2.81 (m, 2H, morpholino 3- CH_2 and 5- CH_2), 3.78 – 3.82 (m, 2H, morpholino 2- CH_2 and 6- CH_2), 6.99 (d, 2H, 3J = 8.9 Hz, phenoxy 2-H and 6-H), 7.76 (d, 2H, 3J = 8.8 Hz, phenoxy 3-H and 5-H), 7.79 (d, 2H, 3J = 8.6 Hz, benzoyl 2-H and 6-H), 7.83 (d, 2H, 3J = 8.6 Hz, benzoyl 3-H and 5-H).

^{13}C NMR (DMSO): 25.62 ($C(CH_3)_2$), 55.98 (morpholino 3-C and 5-C), 66.67 (morpholino 2-C and 6-C), 119.72 (phenoxy 2-C and 6-C), 130.32 (phenoxy 3-

C and 5-C), 132.42 (benzoyl 2-C and 6-C), 132.54 (benzoyl 3-C and 5-C), 207.33 (ketone C=O).

m/z: HRMS (ES-TOF⁺) [MH]⁺ calculated 393.1761; found 394.1703.

HPLC: System 2, R_t = 14.37 minutes

System 3, R_t = 2.52 minutes

System 4, R_t = 2.59 minutes

FT-IR: 3367 (amide NH stretch), 2922, 2849 (CH₃ stretch), 2228 (CN stretch), 1683 (ketone C=O), 1644 (amide C=O), 1599 (aryl CH stretch), 878, 861 (*p* disubstituted aromatic ring).

***N*-Morpholino-2-(4-(3-chlorobenzoyl)phenoxy)-2-methylpropanamide (58f)**

Following General Method G, **57f** (0.026 g, 0.080 mmol) was reacted with HBTU (0.033g, 0.089 mmol), 4-aminomorpholine (0.008g, 0.081mmol) and triethylamine (16.8 μl, 0.089 mmol) in DCM (3 ml) for 21 hours 30 minutes to afford **58f**.

Yield: 85 %

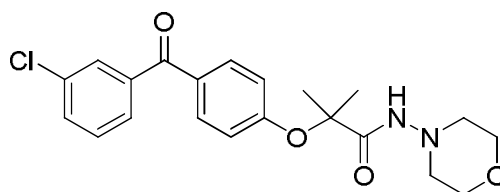
Appearance: White solid

Purification: PLC, 30 % PE / 70 %

EtOAc.

Melting point: 130 – 132 °C

¹H NMR (CDCl₃): 1.62 (s, 6H, C(CH₃)₂), 2.78 – 2.82 (m, 4H, morpholino 3-CH₂ and 5-CH₂), 3.78 – 3.82 (m, 4H, morpholino 2-CH₂ and 6-CH₂), 6.98 (d, ³*J* = 8.8 Hz, 2H, phenoxy 2-H and 6-H), 7.22 (s, 1H, NH), 7.42 (dd, 1H, ³*J* = 7.9 Hz, ³*J* = 8.0 Hz, benzoyl 5-C), 7.55 (ddd, ³*J* = 7.9 Hz, ⁴*J* = 2.0 Hz, ⁴*J* = 1.0 Hz, 1H, benzoyl 6-C), 7.62 (ddd, ³*J* = 7.7 Hz, ⁴*J* = 1.3 Hz, ⁴*J* = 1.3 Hz, 1H,



benzoyl 4-C), 7.72 (dd, $^4J = 1.8$ Hz, $^4J = 1.8$ Hz, 1H, benzoyl 2-C), 7.77 (d, $^3J = 8.8$ Hz, 2H, phenoxy 3-H and 5-H).

^{13}C NMR (CDCl_3): 25.63 ($\text{C}(\text{CH}_3)_2$), 55.99 (morpholino 3-C and 5-C), 66.67 (morpholino 2-C and 6-C), 82.00 ($\text{C}(\text{CH}_3)_2$), 119.65 (phenoxy 2-C and 6-C), 128.14 (benzoyl 6-C), 130.00 (benzoyl 5-C), 131.74 (phenoxy 4-C), 132.34 (phenoxy 3-C and 5-C), 132.53 (benzoyl 2-C), 134.91 (benzoyl 4-C), 139.78 (benzoyl 3-C), 158.75 (phenoxy 1-C), 171.51 (amide $\text{C}=\text{O}$), 194.26 (ketone $\text{C}=\text{O}$).

m/z : HRMS (ES-TOF $^+$) $\text{C}_{21}\text{H}_{24}\text{ClN}_2\text{O}_4$ $[\text{MH}]^+$ calculated 403.1419; found 403.1315.

HPLC: System 2, $R_t = 17.05$ minutes

System 3, $R_t = 2.73$ minutes

System 4, $R_t = 2.74$ minutes

FT-IR: 2846 (CH_3 stretch), 1683 (amide $\text{C}=\text{O}$), 1644 (ketone $\text{C}=\text{O}$), 1597 (aryl CH stretch).

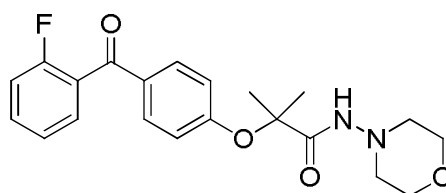
***N*-Morpholino-2-(4-(2-fluorobenzoyl)phenoxy)-2-methylpropanamide (58g)**

Following General Method B, **57g** (0.454 g, 0.501 mmol) and an excess of thionyl chloride (5ml) were reacted for 3 hours and 20 minutes to afford the corresponding acid chloride (0.241 g, 0.750 mmol). The acid chloride was then reacted directly with 4-aminomorpholine (0.115 g, 1.13 mmol) and triethylamine (0.105 ml, 0.750 mmol) in DCM (3 ml) to afford **58g**.

Yield: 27 %

Appearance: Yellow Solid

Purification: PLC, 2% methanol / 98%



DCM

¹H NMR (CDCl₃): 1.63 (s, 6H, C(CH₃)₂), 2.81 (m, 4H, morpholino 2-H and 6-H), 3.82 (m, 4H, morpholino 3-H and 5-H), 6.98 (d, ³J = 8.8 Hz, 2H, phenoxy 2H and 6H), 7.14-7.21 (m, 2H, 2-fluorophenyl 3-H and 5-H), 7.26-7.32 (m, 1H, 2-fluorophenyl 6-H), 7.51-7.57 (m, 2H, 2-fluorophenyl 2-H and 4-H), 7.81 (d, ³J = 8.8 Hz, 2H, phenoxy 3-H and 5-H).

¹³C NMR (DMSO): 25.45 (C(CH₃)₂), 55.76 (morpholino 3-C/5-C), 66.48 (morpholino 2-C/6-C), 81.80 (C(CH₃)₂), 116.37 (d, ²J_{CF} = 22 Hz, benzoyl 3-C), 119.28 (phenoxy 2-C and 6-C), 124.51 (d, ⁴J_{CF} = 3 Hz, benzoyl 5-C), 127.22 (d, ²J_{CF} = benzoyl 1-C), 130.68 (d, ³J_{CF} = 3 Hz, benzoyl 6-C), 131.90 (phenoxy 3-C and 5-C), 132.12 (phenoxy 4-C), 133.07 (d, ³J_{CF} = 8 Hz, benzoyl 4-C), 158.99 (phenoxy 1-C), 159.98 (d, ¹J_{CF} = 251 Hz, benzoyl C-2), 171.27 (amide C=O), 192.06 (benzoyl C=O).

Melting point: 154-155 °C

HPLC: System 2, R_t=14.84 minutes.

System 3, R_t = 2.57 minutes

System 4, R_t = 2.59 minutes

m/z: HRMS (ES-TOF⁺) C₂₁H₂₃FN₂O₄ [MH]⁺ calculated 387.1715; found 386.9297.

FT-IR (KBr): 3288 (amide C=O), 2940, 2830 (CH₃ stretch), 1689 (amide C=O), 1644 (ketone C=O), 1596 (aryl CH stretch), 881, 857 (*para* disubstituted aromatic ring).

***N*-Morpholino-2-(4-(3-fluorobenzoyl)phenoxy)-2-methylpropanamide**

(58h)

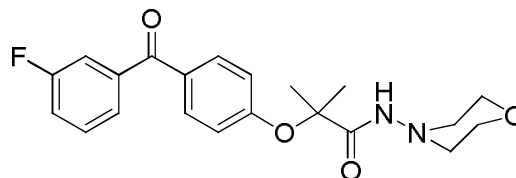
Following General Method G, **57h** (0.100 g, 0.33 mmol) was reacted with HBTU (0.138 g, 0.36 mmol), 4-aminomorpholine (0.034 g, 0.33 mmol) and triethylamine (68.8 μ l, 0.33 mmol) in DCM (5 ml) for 4 hours to afford **58h**.

Yield: 37 %

Appearance: White solid

Purification:

Column



chromatography, 5 % EtOAc / 95 % PE to 100% EtOAc.

Melting point: 152 – 154 °C

¹H NMR (CDCl₃): 1.62 (s, 6H, C(CH₃)₂), 2.80 (m, 4H, morpholino CH₂), 3.80 (m, 4H morpholino CH₂), 6.98 (d, ³*J* = 8.8 Hz, 2H, phenoxy 2-H and 6-H), 7.22 (s, 1H, NH), 7.29 (dddd, ³*J* = 8.3 Hz, ³*J* = 8.3 Hz, ⁴*J* = 2.7 Hz, ⁴*J* = 1.2 Hz, 1H, benzoyl 4-H), 7.43-7.49 (m, 2H, benzoyl 2-H and 5-H), 7.53 (ddd, 1H, ³*J* = 7.7 Hz, ⁴*J* = 1.2 Hz, ⁴*J* = 1.2 Hz, benzoyl 6-H), 7.78 (d, ³*J* = 8.9 Hz, 2H, phenoxy 3-H and 5-H).

¹³C NMR (CDCl₃): 25.42 (C(CH₃)₂), 55.79 (morpholino 3-C and 5-C), 66.47 (morpholino 2-C and 6-C), 81.83 (C(CH₃)₂), 116.7 (d, ²*J*_{CF} = 22.1 Hz, benzoyl 2-C), 119.37 (d, ²*J*_{CF} = 18.1 Hz, benzoyl 4-C), 119.49 (phenoxy 2-C and 6-C), 125.64 (d, ⁴*J*_{CF} = 3.0Hz, benzoyl 6-C), 130.14 (d, ³*J*_{CF} = 8.0 Hz, benzoyl 5-C), 131.63 (phenoxy 4-C), 132.13 (phenoxy 3-C and 5-C), 139.67 (d, ³*J*_{CF} = 7.0Hz, benzoyl 1-C), 158.48 (phenoxy 1-C), 162.59 (d, ¹*J*_{CF} = 247.4 Hz, benzoyl 3-C), 171.30 (amide C=O), 194.09 (ketone C=O).

HPLC: System 2 R_t= 17.60 minutes

System 3, R_t = 2.60 minutes

System 4, $R_t = 2.67$ minutes

m/z: HRMS (ES-TOF⁺) C₂₁H₂₄FN₂O₄ [MH]⁺ calculated 387.1715; found 387.1680.

FT-IR (KBr): 3298 (amide NH), 2929, 2845 (CH₃ stretch), 1686 (amide C=O), 1648 (ketone C=O), 1584 (aryl CH stretch).

***N*-Morpholino-2-(4-(4-fluorobenzoyl)phenoxy)-2-methylpropanamide (58i)**

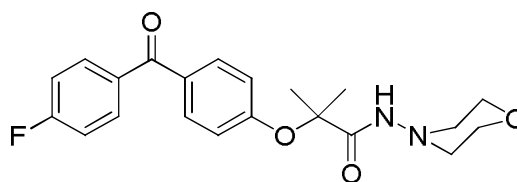
Following General Method B, **57i** (0.214 g, 0.71 mmol) and an excess of thionyl chloride (5ml) were reacted for 3 hours and 30 minutes to afford the corresponding acid chloride (0.227 g, 0.71 mmol). The acid chloride was then reacted directly with 4-aminomorpholine (0.072 g, 1.06 mmol) and triethylamine (0.099 ml, 0.71 mmol) in DCM (3 ml) to afford **58i**.

Yield: 38%

Appearance: White solid

Purification: PLC 20% petroleum

ether/ 80% ethyl acetate



¹H NMR (DMSO): 1.65 (s, 6H, C(CH₃)₂), 2.81 (broad t, ³*J* = 4.5 Hz, 4H, morpholino 3-CH₂ and 5-CH₂), 3.80 (broad t, ³*J* = 4.5 Hz, 4H, morpholino 2-CH₂ and 6-CH₂), 6.98 (d, ³*J* = 8.7 Hz, 2H, phenoxy 2-H and 6-H), 7.16 (dd, ³*J* = 8.6 Hz, ³*J* = 8.6 Hz, 2H, benzoyl 3-H and 5-H), 7.23 (broad s, NH, 1H), 7.75 (d, ³*J* = 8.8 Hz, 2H, phenoxy 3-H and 5-H), 7.80 (dd, ³*J* = 8.6 Hz, ⁴*J* = 5.4 Hz, 2H, benzoyl 2-H and 6-H).

¹³C NMR (DMSO): 25.42 (C(CH₃)₂), 55.78 (morpholino 3-C/5-C), 66.49 (morpholino 2-C/6-C), 81.84 (C(CH₃)₂), 115.62 (d, ²*J*_{CF} = 22 Hz, benzoyl 3-C and 5-C), 119.51 (phenoxy 2-C and 6-C), 131.97 (phenoxy 3-C and 5-C), 132.16 (phenoxy 4-C), 132.52 (d, ³*J*_{CF} = 9 Hz, benzoyl 2-C and 6-C), 134.09

(d, $^4J_{\text{CF}} = 3$ Hz, benzoyl 1-C), 158.23 (phenoxy 1-C), 165.42 (d, $^1J_{\text{CF}} = 254$ Hz, benzoyl 4-C), 171.34 (amide C=O), 194.07 (ketone C=O).

Melting point: 165-167 °C

HPLC: System 2, $R_t = 15.95$ minutes.

System 3, $R_t = 2.60$ minutes

System 4, $R_t = 2.66$ minutes

m/z : HRMS (ES-TOF⁺) $\text{C}_{21}\text{H}_{23}\text{FN}_2\text{O}_4$ $[\text{MH}]^+$ calculated 387.1715; found 386.9297.

FT-IR (KBr): 3273 (amide C=O), 2855, 2824 (CH_3 stretch), 1688 (amide C=O), 1648 (ketone C=O), 1598 (aryl CH stretch), 882, 856 (*para* disubstituted aromatic ring).

***N*-Morpholino-2-(4-(3-nitrobenzoyl)phenoxy)-2-methylpropanamide (58j)**

Following General Method G, **57j** (0.022 g, 0.066 mmol) was reacted with HBTU (0.028 g, 0.074 mmol), 4-aminomorpholine (0.007 g, 0.067 mmol) and triethylamine (13.9 μl , 0.074 mmol) in DCM (3 ml) for 21 hours to afford **58j**.

Yield: 78 %

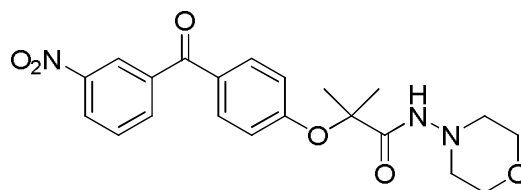
Appearance: White solid

Purification: PLC, 30% PE / 70%

EtOAc.

Melting point: 114 – 115 °C

^1H NMR (DMSO): 1.64 ($\text{C}(\text{CH}_3)_2$), 2.78-2.83 (m, 4H, morpholino 2-H and 6-H), 3.78-3.85 (m, 4H, morpholino 3-H and 5-H), 7.02 (d, $^3J = 8.8$ Hz, 2H, phenoxy 2-H and 6-H), 7.71 (dd, $^3J = 8.0$ Hz, $^3J = 8.0$ Hz, 1H, benzoyl 5-H), 7.78 (d, $^3J = 8.8$ Hz, phenoxy 3-H and 5-H), 8.11 (ddd, $^3J = 7.7$ Hz, $^4J = 1.3$



Hz, $^4J = 1.2$ Hz, 1H, benzoyl 6-C), 8.44 (ddd, $^3J = 8.2$ Hz, $^4J = 2.3$ Hz, $^4J = 1.1$ Hz, 1H, benzoyl 4-C), 8.56 (dd, $^4J = 1.8$ Hz, $^4J = 1.8$ Hz, 1H, benzoyl C-2).

^{13}C NMR (DMSO): 25.64 ($\text{C}(\text{CH}_3)_2$), 56.00 (morpholino 3-C and 5-C), 66.68 (morpholino 2-C and 6-C), 82.10 ($\text{C}(\text{CH}_3)_2$), 119.71 (phenoxy 2-C and 6-C), 124.85 (benzoyl 2-C), 126.93 (benzoyl 4-C), 130.06 (benzoyl 5-C), 130.98 (phenoxy 4-C), 132.37 (phenoxy 3-C and 5-C), 135.54 (benzoyl 6-C), 139.60 (benzoyl 1-C), 148.55 (benzoyl 3-C), 171.36 (amide $\text{C}=\text{O}$), 193.12 (ketone $\text{C}=\text{O}$).

HPLC: System 2, $R_t = 15.34$ minutes

System 1, $R_t = 2.57$ minutes

System 2, $R_t = 2.66$ minutes

m/z : HRMS (ES-TOF $^+$) $\text{C}_{21}\text{H}_{24}\text{N}_3\text{O}_6$ $[\text{MH}]^+$ calculated 414.1660; found 414.1671

FT-IR: 2925, 2860 (CH_3 stretch), 1681 (amide $\text{C}=\text{O}$), 1652 (ketone $\text{C}=\text{O}$), 1598 (aryl CH stretch), 1539 ($\text{C}-\text{NO}_2$).

***N*-Morpholino-2-(4-(4-nitrobenzoyl)phenoxy)-2-methylpropanamide (58k)**

Following General Method G, **57k**

(0.100 g, 0.30 mmol) was reacted

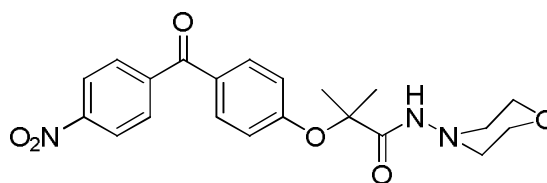
with HBTU (0.127 g, 0.33 mmol),

4-aminomorpholine (0.031 g, 0.30

mmol) and triethylamine (60.0 μl , 0.33 mmol) in DCM (5 ml) for 4 hours 15 minutes to afford **58k**.

Yield: 19 %

Appearance: Yellow – white solid



Purification: Column chromatography, 5 % EtOAc / 95 % PE to 100% EtOAc.

Melting point: 131- 132 °C

¹H NMR (CDCl₃): 1.63 (C(CH₃)₂), 2.77-2.82 (m, 4H, morpholino 3-CH₂ and 5-CH₂), 3.76 – 3.82 (m, 4H, 2-CH₂ and 6-CH₂), 7.00 (d, ³J = 8.8 Hz, 2H, phenoxy 2-H and 6-H), 7.19 (s, 1H, NH), 7.77 (d, ³J = 8.8 Hz, 2H, phenoxy 3-H and 5-H), 7.88 (d, ³J = 8.8 Hz, 2H, benzoyl 2-H and 6-H), 8.33 (d, ³J = 8.8 Hz, 2H, benzoyl 3-H and 5-H).

¹³C NMR (CDCl₃): 25.41 (C(CH₃)₂), 55.76 (morpholino 3-C and 5-C), 66.45 (morpholino 2-C and 6-C), 81.92 (C(CH₃)₂), 119.50 (phenoxy 2-C and 6-C), 123.70 (benzoyl 3-C and 5-C), 130.53 (benzoyl 2-C and 6-C), 130.82 (phenoxy 4-C), 132.23 (phenoxy 3-C and 5-C), 143.29 (benzoyl 1-C), 149.84 (benzoyl 4-C), 159.08 (phenoxy 1-C), 171.14 (amide C=O), 193.50 (ketone C=O).

HPLC: System 3, R_t = 2.61 minutes

System 4, R_t = 2.81 minutes

m/z: HRMS (ES-TOF⁺) [MH]⁺ calculated 414.1660; found 414.1729.

FT-IR (KBr): 3369 (amide NH), 2938, 2857 (CH₃ stretch), 1686 (ketone C=O), 1597 (aryl CH stretch), 1454 (NO₂), 869, 852 (*para* disubstituted aromatic ring).

***N*-Morpholino-2-(4-(benzoyl)phenoxy)-2-methylpropanamide (58l)**

Following General Method B, **57l** (0.487 g, 1.71 mmol) and an excess of thionyl chloride (5ml) were reacted for 3 hours and 45 minutes to afford the corresponding acid chloride (0.517 g, 1.71 mmol). Some of the acid chloride (0.259 g, 0.86 mmol) was then reacted directly with 4-aminomorpholine (0.132

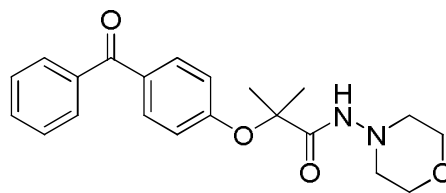
g, 1.29 mmol) and triethylamine (0.119 ml, 0.86 mmol) in DCM (3 ml) to afford **58l**.

Yield: 41%

Appearance: Pale yellow solid

Purification: 5 % EtOAc / 95 PE to 40 %

EtOAc / 60 % PE.



¹H NMR (CDCl₃): 1.62 (s, 6H, (CH₃)₂), 2.81 (m, 4H, morpholino 2-H and 6-H), 3.80 (m, 4H, morpholino 3-H and 5-H), 6.98 (d, ³J = 8.8 Hz, 2H, phenoxy 2-H and 6-H), 7.24 (broad s, 1H, NH), 7.47 (dd, ³J = 7.8 Hz, ³J = 7.8 Hz, 2H, benzoyl 3-H and 5-H), 7.58 (dd, ³J = 7.4 Hz, 1H, benzoyl 4-H), 7.74-7.81 (m, 4H, phenoxy 3-H and 5-H and benzoyl 2H and 6H).

¹³C NMR (DMSO): 25.43 (C(CH₃)₂), 55.79 (morpholino 3-C/5-C), 66.48 (morpholino 2-C/6-C), 81.80 (C(CH₃)₂), 119.46 (phenoxy 2-C and 6-C), 128.45 (benzoyl 3-C and 5-C), 129.93 (benzoyl 2-C and 6-C), 132.13 (phenoxy 3-C and 5-C), 132.28 (phenoxy 4-C), 132.39 (benzoyl 4-C), 137.92 (benzoyl 1-C), 158.18 (phenoxy 1-C), 171.39 (amide C=O), 195.55 (ketone C=O).

Melting point: 106-107 °C

HPLC: System 2, R_t = 17.77 minutes.

System 1, R_t = 3.02 minutes

System 2, R_t = 3.04 minutes

m/z: HRMS (ES-TOF⁺) C₂₁H₂₄N₂O₄ [MH]⁺ calculated 369.1809; found 368.9694.

FT-IR (KBr): 3342 (amide NH), 2986, 2937 (CH₃ stretch), 1634 (amide C=O), 1652 (ketone C=O), 1598 (aryl CH stretch), 875, 850 (*para* disubstituted aromatic ring).

***N*-Piperidinyl-2-(4-(2-methylbenzoyl)phenoxy)-2-methylpropanamide
(59a)**

Following General Method G, **57a** (0.025 g, 0.08 mmol) was reacted with HBTU (0.035 g, 0.09 mmol), 1-aminopiperidine (0.008 g, 0.08 mmol) and triethylamine (17.4 μ l, 0.09 mmol) in DCM (3 ml) for 21 hours 30 minutes to afford **59a**.

Yield: 89 %

Appearance: White solid

Purification: PLC, 50 % PE / 50 %

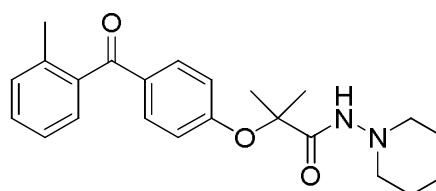
EtOAc.

Melting point: 96 – 97 °C

¹H NMR (CDCl₃): 1.34 – 1.42 (m, 2H, piperidinyl 4-CH₂), 1.59 (s, 6H, C(CH₃)₂), 1.67 (quintet, ³*J* = 5.7 Hz, 4H, piperidinyl 3-CH₂ and 5-CH₂), 2.62 – 2.65 (m, 4H, piperidinyl 2-CH₂ and 6-CH₂), 6.93 (d, ³*J* = 8.9 Hz), 7.09 (s, 1H, NH), 7.21 – 7.30 (m, benzoyl 3-H/5-H/6-H), 7.38 (ddd, ³*J* = 7.5 Hz, ³*J* = 7.5 Hz, ³*J* = 1.8 Hz, 1H, benzoyl 4-H), 7.74 (d, ³*J* = 8.9 Hz, 2H, phenoxy 3-H and 5-H).

¹³C NMR (CDCl₃): 20.20 (C(CH₃)₂), 23.52 (piperidinyl 4-C), 25.68 (piperidinyl 3-C and 5-C), 57.08 (piperidinyl 2-C and 6-C), 81.93 (C(CH₃)₂), 119.43 (phenoxy 2-C and 6-C), 125.54 (benzoyl 5-C), 128.49 (benzoyl 6-C), 130.44 (benzoyl 3-C), 131.31 (phenoxy 3-C and 5-C), 132.45 (phenoxy 4-C), 136.77 (benzoyl 2-C), 139.09 (benzoyl 1-C), 159.12 (phenoxy 1-C), 171.02 (amide C=O).

***m/z*:** HRMS (ES-TOF⁺) C₂₃H₂₉N₂O₃ [MH]⁺ calculated 381.2173; found 381.2076



HPLC: System 2, R_t = 17.32 minutes

System 3, R_t = 2.84 minutes

System 4, R_t = 2.82 minutes

FT-IR: 2940, 2852 (CH_3 stretch), 1698 (amide $\text{C}=\text{O}$), 1646 (ketone $\text{C}=\text{O}$), 1597 (aryl CH stretch),

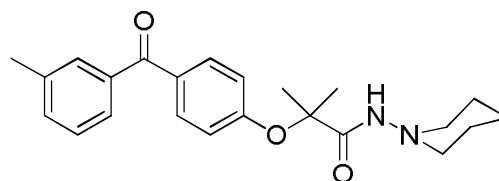
***N*-Piperidinyl-2-(4-(3-methylbenzoyl)phenoxy)-2-methylpropanamide (59b)**

Following General Method G, **57b** (0.100 g, 0.34 mmol) was reacted with HBTU (0.139 g, 0.37 mmol), 1-aminopiperidine (0.034 g, 0.34 mmol) and triethylamine (69.7 μl , 0.37 mmol) in DCM (5 ml) for 24 hours to afford **59b**.

Yield: 21 %

Appearance: Off-White solid

Purification: Column



chromatography, 50 % EtOAc / 50 % PE.

Melting point: 128 – 130 °C

^1H NMR (CDCl_3): 1.35-1.43 (m, 2H, piperidinyl 4- CH_2), 1.61 (s, 6H, $\text{C}(\text{CH}_3)_2$), 1.69 (m, 4H, piperidinyl 3- CH_2 and 5- CH_2), 2.42 (s, 3H, benzoyl CH_3), 2.70 (m, 4H, piperidinyl 2- CH_2 and 6- CH_2), 6.97 (d, 3J = 8.8 Hz, 2H, phenoxy 2-H and 6-H), 7.15 (broad s, NH , 1H), 7.32-7.41 (m, 2H, benzoyl 4-H and 5-H), 7.50-5.59 (m, 2H, benzoyl 2-H and 6-H), 7.77 (d, 3J = 8.8 Hz, 2H, phenoxy 3-H and 5-H).

^{13}C NMR (CDCl_3): 21.52 (CH_3), 23.33 (piperidinyl 4-C), 25.37 ($\text{C}(\text{CH}_3)_2$), 25.49 (piperidinyl 3-C and 5-C), 56.89 (piperidinyl 2-C and 6-C), 81.68 ($\text{C}(\text{CH}_3)_2$), 119.18 (phenoxy 2-C and 6-C), 127.22 (benzoyl 2-C), 128.22 (benzoyl 5-C), 130.37 (phenoxy 4-C), 132.11 (phenoxy 3-C and 5-C), 133.12

(benzoyl 4-C), 138.00 (benzoyl 3-C), 138.31 (benzoyl 1-C), 158.31 (phenoxy 1-C), 170.96 (amide C=O), 195.84 (ketone C=O).

HPLC: System 2, R_t = 17.65 minutes

System 3, R_t = 2.86 minutes

System 4, R_t = 2.84 minutes

m/z : HRMS (ES-TOF⁺) [MH]⁺ calculated 381.2173; found 381.1673

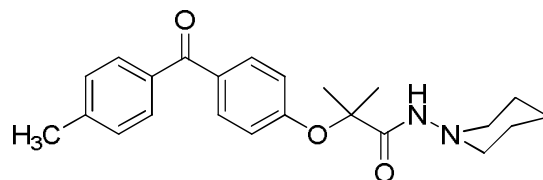
FT-IR (KBr): 3279 (amide NH), 2982, 2861 (CH₃ stretch), 1691 (amide C=O), 1635 (ketone C=O), 1594 (aryl CH stretch).

***N*-Piperidinyl-2-(4-(4-methylbenzoyl)phenoxy)-2-methylpropanamide
(59c)**

Following General Method G, **57c** (0.200 g, 0.67 mmol) was reacted with HBTU (0.293 g, 0.74 mmol), 1-aminopiperidine (0.067 g, 0.67 mmol) and triethylamine (146.0 μ l, 0.74 mmol) in DCM (5 ml) for 2 hours 30 minutes to afford **59c**.

Yield: 29 %

Appearance: White solid



Purification: Column chromatography, 5 % EtOAc / 95 % PE to 100% EtOAc.

Melting point: 160 – 162 °C

¹H NMR (CDCl₃): 1.34-1.44 (m, 2H, piperidinyl CH₂), 1.61 (s, C(CH₃)₂, 6H), 1.69 (m, 4H, piperidinyl 3-CH₂ and 5-CH₂), 2.44 (s, 3H, benzoyl CH₃), 2.69 (m, 4H, piperidinyl 2-CH₂ and 6-CH₂), 6.97 (d, ³J = 8.8 Hz, 2H, phenoxy 2-H and 6-H), 7.13 (s, 1H, NH), 7.28 (d, ³J = 7.9 Hz, 2H, benzoyl 3-H and 5-H), 7.67 (d, ³J = 8.1 Hz, 2H, phenoxy 3-H and 5-H), 7.76 (d, ³J = 8.8 Hz, 2H, 2-H and 6-H).

^{13}C NMR (CDCl_3): 21.78 (benzoyl CH_3), 23.33 (piperidiny 4-C), 25.37 (piperidiny 3-C and 5-C), 25.48 ($\text{C}(\text{CH}_3)_2$), 56.92 (piperidiny 2-C and 6-C), 81.67 ($\text{C}(\text{CH}_3)_2$), 119.21 (phenoxy 2-C and 6-C), 129.10 (benzoyl 3-C and 5-C), 130.20 (benzoyl 2-C and 6-C), 131.99 (phenoxy 3-C and 5-C), 132.36 (phenoxy 4-C), 135.21 (benzoyl 1-C), 143.15 (benzoyl 4-C), 158.15 (phenoxy 1-C), 170.95 (amide $\text{C}=\text{O}$), 195.40 (ketone $\text{C}=\text{O}$).

HPLC: System 2, R_t = 17.60 minutes

System 3, R_t = 2.83 minutes

System 4, R_t = 2.82 minutes

m/z : HRMS (ES-TOF $^+$) $\text{C}_{23}\text{H}_{29}\text{N}_2\text{O}_3$ $[\text{MH}]^+$ calculated 381.2173; found 381.1966.

FT-IR (KBr): 3296 (amide NH), 2941, 2854 (CH_3 stretch), 1677 (amide $\text{C}=\text{O}$), 1636 (ketone $\text{C}=\text{O}$), 1601 (aryl CH stretch), 877, 854 (p disubstituted aromatic ring).

***N*-Piperidiny-2-(4-(3-cyanobenzoyl)phenoxy)-2-methylpropanamide (59d)**

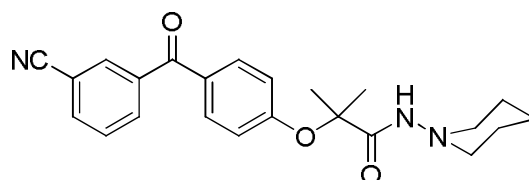
Following General Method G, **57d** (0.044 g, 0.14 mmol) was reacted with HBTU (0.069 g, 0.16 mmol), 1-aminopiperidine (0.014 g, 0.14 mmol) and triethylamine (30.0 μl , 0.16 mmol) in DCM (3 ml) for 28 hours 40 minutes to afford **59d**.

Yield: 8%

Appearance: White solid

Purification: Column

Chromatography, 5 % EtOAc / 95 % PE to 100 % EtOAc.



Melting point: 146 – 148 °C

¹H NMR (CDCl₃): 1.35 – 1.42 (m, 2H, piperidiny 4-CH₂), 1.63 (C(CH₃)₂), 1.69 (quintet, ³J = 5.7 Hz, 4H, piperidiny 3-CH₂ and 5-CH₂), 2.68 – 2.71 (m, 4H, piperidiny 2-CH₂ and 6-CH₂), 7.00 (d, ³J = 8.8 Hz, 2H, phenoxy 2-H and 6-H), 7.07 (s, 1H, NH), 7.63 (dd, ³J = 7.8 Hz, ³J = 7.8 Hz, 1H, benzoyl 5-H), 7.74 (d, ³J = 8.8 Hz, 2H, phenoxy 3-H and 5-H), 7.86 (ddd, ³J = 7.8 Hz, ⁴J = 1.4 Hz, ⁴J = 1.4 Hz, benzoyl 4-H), 7.96 – 8.24 (m, 2H, benzoyl 2-H and 6-H).

¹³C NMR (CDCl₃): 23.32 (piperidiny 4-C), 25.38 (piperidiny 3-C and 5-C), 25.49 (C(CH₃)₂), 56.93 (piperidiny 2-C and 6-C), 81.85 (C(CH₃)₂), 112.96 (benzoyl 3-C), 119.34 (phenoxy 2-C and 6-C), 129.55 (CN), 130.63 (benzoyl 5-C), 132.13 (phenoxy 3-C and 5-C), 133.34 (phenoxy 4-C), 133.73 (benzoyl 6-C), 135.29 (benzoyl 4-C), 139.05 (benzoyl 1-C), 159.13 (phenoxy 1-C), 170.70 (amide C=O).

HPLC: System 2, R_t = 15.67 minutes

System 3, R_t = 2.68 minutes

System 4, R_t = 2.72 minutes

m/z: HRMS (ES-TOF⁺) [MH]⁺ calculated 394.2125; found 394.2108.

FT-IR (KBr): 3285 (amide NH), 2942, 2851 (CH₃ stretch), 2228 (CN), 1691 (amide C=O), 1639 (ketone C=O), 1595 (aryl CH stretch), 885, 851 (*p* disubstituted aromatic ring).

***N*-Piperidiny-2-(4-(4-cyanobenzoyl)phenoxy)-2-methylpropanamide (59e)**

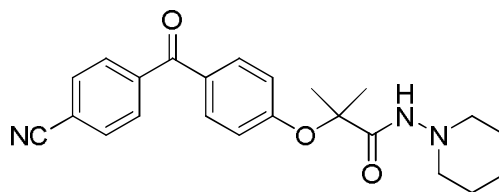
Following General Method G, **57e** (0.020 g, 0.06 mmol) was reacted with HBTU (0.027 g, 0.07 mmol), 1-aminopiperidine (0.006 g, 0.06 mmol) and triethylamine (13.4 µl, 0.07 mmol) in DCM (3 ml) for 24 hours to afford **59e**.

Yield: 85 %

Appearance: White solid

Purification:

Column



chromatography, 5% EtOAc / 95 % PE to 100 % EtOAc.

Melting point: 144 – 146 °C

¹H NMR (DMSO): 1.35 – 1.42 (m, piperidinyl 4-CH₂), 1.62 (s, 6H, (C(CH₃)₂), 1.69 (quintet, 4H, ³J = 5.7 Hz, piperidinyl 3-CH₂ and 5-CH₂), 2.66 – 2.72 (m, 4H, piperidinyl 2-CH₂ and 6-CH₂), 6.99 (d, ³J = 8.8 Hz, 2H, phenoxy 2-H and 6-H), 7.75 (d, ³J = 8.8 Hz, 2H, phenoxy 3-H and 5-H), 7.79 (d, ³J = 8.5 Hz, 2H, benzoyl 2-H and 6-H), 7.83 (d, ³J = 8.6 Hz, 2H, benzoyl 3-H and 5-H).

m/z: HRMS (ES-TOF⁺) [MH]⁺ calculated 392.1969; found 392.1553.

FT-IR: 2935, 2852 (CH₃ stretch), 2229 (CN stretch), 1702 (amide C=O), 1652 (ketone C=O), 1594 (aryl CH stretch), 865, 850 (*p* disubstituted aromatic ring).

***N*-Piperidinyl-2-(4-(3-chlorobenzoyl)phenoxy)-2-methylpropanamide (59f)**

Following General Method G, **57f** (0.027 g, 0.08 mmol) was reacted with HBTU (0.035 g, 0.09 mmol), 1-aminopiperidine (0.009 g, 0.08 mmol) and triethylamine (17.6 μl, 0.09 mmol) in DCM (3 ml) for 21 hours 30 minutes to afford **59f**.

Yield: 80 %

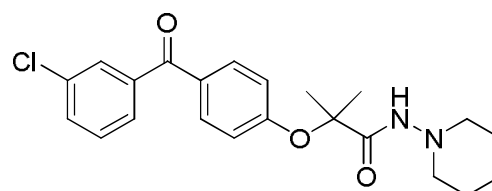
Appearance: White solid

Purification: PLC, 50 % PE / 50 %

EtOAc.

Melting point: 135 – 137 °C

¹H NMR (CDCl₃): 1.35 – 1.45 (piperidinyl 4-CH₂), 1.56 (s, 3H, C(CH₃)₂), 1.62 (s, 3H, C(CH₃)₂), 1.69 (quintet, 4H, piperidinyl 3-CH₂ and 5-CH₂), 2.65 –



2.72 (m, 4H, piperidiny 2-CH₂ and 6-CH₂), 6.98 (d, ³J = 8.8 Hz, 2H, phenoxy 2-H and 6-H), 7.08 (s, 1H, NH), 7.42 (dd, 1H, ³J = 7.9 Hz, ³J = 8.0 Hz, benzoyl 5-C), 7.55 (ddd, ³J = 7.9 Hz, ⁴J = 2.0 Hz, ⁴J = 1.0 Hz, 1H, benzoyl 6-C), 7.62 (ddd, ³J = 7.7 Hz, ⁴J = 1.3 Hz, ⁴J = 1.3 Hz, 1H, benzoyl 4-C), 7.72 (dd, ⁴J = 1.8 Hz, ⁴J = 1.8 Hz, 1H, benzoyl 2-C), 7.77 (d, ³J = 8.8 Hz, 2H, phenoxy 3-H and 5-H).

¹³C NMR (CDCl₃): 25.24 (piperidiny 4-C), 25.35 (C(CH₃)₂), 30.94 (piperidiny 3-C and 5-C), 56.79 (piperidiny 2-C and 6-C), 81.62 (C(CH₃)₂), 119.09 (phenoxy 2-C and 6-C), 127.40 (benzoyl 6-C), 127.81 (benzoyl 5-C), 131.99 (phenoxy 3-C and 5-C), 132.2 (benzoyl 2-C) 139.6 (benzoyl 3-C), 170.6 (amide C=O).

m/z: HRMS (ES-TOF⁺) [MH]⁺ calculated 401.1626; found 401.1545

HPLC: System 2, R_t = 18.35 minutes

System 3, R_t = 2.92 minutes

System 4, R_t = 2.90 minutes

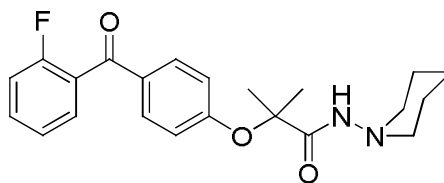
FT-IR 2941, 2858 (CH₃ stretch), 1687 (amide C=O), 1645 (ketone C=O), 1596 (aryl CH stretch).

2-(4-(2-Fluorobenzoyl)phenoxy)-2-methyl-N-(piperidin-1-yl)propanamide (59g)

Following General Method G, **57g** (0.400 g, 1.32 mmol) was reacted with HBTU (0.5524 g, 1.46 mmol), 1-aminopiperidine (0.133 g, 1.32 mmol) and triethylamine (0.275 ml, 1.46 mmol) in DCM (5 ml) for 1 hour 45 minutes to afford **59g**.

Yield: 54%

Appearance: White needle-like crystals



Purification: 5 % EtOAc / 95 % PE to 100% EtOAc, then recrystallised from toluene.

Melting point: 131 – 133 °C

¹H NMR (CDCl₃): 1.32-1.42 (m, 2H, piperidiny 4-CH₂), 1.60 (s, 6H, C(CH₃)₂), 1.68 (quintet, ³J = 5.7 Hz, 4H, piperidiny 3-CH₂ and 4-CH₂), 2.67 (broad t, ³J = 4.9 Hz, 4H, piperidiny 2-CH₂ and 6-CH₂), 6.94 (d, ³J = 8.5 Hz, 2H, phenoxy 2-H and 6-H), 7.06 (s, NH, 1H), 7.15 (dd, ³J = 8.9 Hz, ³J = 8.9 Hz, 1H, benzoyl 5-H), 7.26 (dd, ³J_{CF} = 7.4 Hz, ³J = 7.4 Hz, 1H, benzoyl 3-H), 7.46-7.54 (m, 2H, benzoyl 6-H and 4-H), 7.78 (d, ³J = 7.9 Hz, 2H, phenoxy 3-H and 5-H).

¹³C NMR (CDCl₃): 23.19 (piperidiny 4-C), 25.22 (C(CH₃)₂), 25.36 (piperidiny 3-C and 5-C), 56.75 (piperidiny 2-C and 6-C), 81.59 (C(CH₃)₂), 116.23 (d, ²J_{CF} = 21.9 Hz, benzoyl 3-C), 118.96 (phenoxy 2-C and 6-C), 124.33 (d, ⁴J_{CF}=3.5Hz, benzoyl 5-C), 127.12 (d, ²J_{CF} = 14.6 Hz, benzoyl 1-C), 130.55 (d, ³J_{CF} = 3Hz, benzoyl 5-C), 131.70 (benzoyl 6-C), 131.76 (phenoxy 3-C and 5-C), 132.9 (d, ³J_{CF} = 8.2 Hz, benzoyl 4-C), 159.05 (phenoxy 1-C), 159.83 (d, ¹J_{CF} = 251.7 Hz), 170.62 (amide C=O), 191.98 (ketone C=O).

HPLC: System 2, R_t=16.24 minutes

System 3, R_t=2.77 minutes

System 4, R_t=2.78 minutes

m/z: HRMS (ES-TOF⁺) [MH]⁺ calculated 385.1922; found 385.1414

FT-IR (KBr): 3261 (amide NH), 2945, 2812 (CH₃ stretch), 1685 (amide C=O), 1595 (aryl CH stretch), 885, 848 (*p* disubstituted aromatic ring).

***N*-Piperidiny-2-(4-(3-fluorobenzoyl)phenoxy)-2-methylpropanamide (59h)**

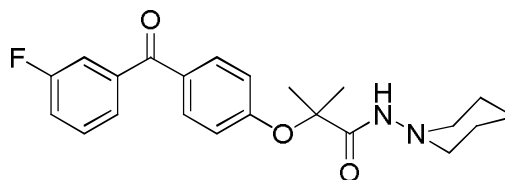
Following General Method G, **57h** (0.100 g, 0.33 mmol) was reacted with HBTU (0.138 g, 0.36 mmol), 1-aminopiperidine (0.033 g, 0.33 mmol) and triethylamine (68.8 μ l, 0.36 mmol) in DCM (5 ml) for 4 hours to afford **59h**.

Yield: 65 %

Appearance: White solid

Purification:

Column



chromatography, 50 % EtOAc / 50 % PE.

Melting point: 117 – 119 °C

¹H NMR (CDCl₃): 1.34-1.43 (m, 2H, piperidiny-CH₂), 1.62 (s, C(CH₃)₂, 6H), 1.69 (m, 4H, piperidiny-3-CH₂ and 5-CH₂), 2.69 (m, 4H, piperidiny-2-CH₂ and 6-CH₂), 6.98 (d, ³J = 8.8 Hz, 2H, phenoxy-2-H and 6-H), 7.09 (s, NH, 1H), 7.24-7.31 (m, 1H, benzoyl-CH), 7.42-7.49 (m, 2H, benzoyl-CH), 7.53 (ddd, ³J = 7.7 Hz, ⁴J = 1.2 Hz, ⁴J = 1.2 Hz, 1H, benzoyl-6-H), 7.77 (d, ³J = 8.8 Hz, 2H, phenoxy-3-H and 5-H).

¹³C NMR (CDCl₃): 23.24 (piperidiny-4-C), 25.38 (C(CH₃)₂), 25.49 (piperidiny-3-C and 5-C), 56.92 (piperidiny-2-C and 6-C), 81.76 (C(CH₃)₂), 116.7 (d, ²J_{CF} = 23.0 Hz, benzoyl-2-C), 119.23 (phenoxy-2-C and 6-C), 119.34 (d, ²J_{CF} = 21.0 Hz, benzoyl-4-C), 125.65 (d, ⁴J_{CF} = 3.0 Hz, benzoyl-6-C), 130.12 (d, ³J_{CF} = 8.0 Hz, benzoyl-5-C), 131.37 (phenoxy-4-C), 132.12 (phenoxy-3-C and 5-C), 140.06 (d, ³J_{CF} = 6.0 Hz, benzoyl-1-C), 158.71 (phenoxy-1-C), 162.61 (d, ¹J_{CF} = 248.5 Hz, benzoyl-3-C), 170.80 (amide C=O), 194.12 (ketone C=O).

HPLC: System 2, R_t = 17.18 minutes

System 3, R_t = 2.79 minutes

System 4, R_t = 2.81 minutes

m/z: HRMS (ES-TOF⁺) C₂₂H₂₆FN₂O₃ [MH]⁺ calculated 385.1922; found 385.1735.

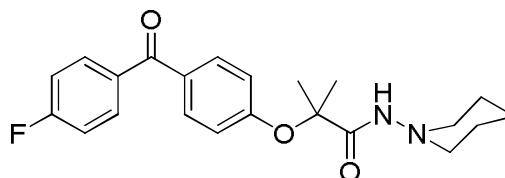
FT-IR (KBr): 3302 (amide NH), 1688 (amide C=O), 1647 (ketone C=O), 1596 (aryl CH stretch).

N-Piperidiny-2-(4-(4-fluorobenzoyl)-phenoxy)-2-methylpropanamide (59i)

Following General Method B, **57i** (0.562 g, 1.85 mmol) and an excess of thionyl chloride (10 ml) were reacted for 2 hours and 30 minutes to afford the corresponding acid chloride (0.596 g, 1.85 mmol). Some of the acid chloride (0.298 g, 0.93 mmol) was then reacted directly with 1-aminopiperidine (0.139 g, 1.39 mmol) in the presence of triethylamine (0.129 ml, 0.93 mmol) to afford **59i**.

Yield: 27%

Appearance: Yellow solid



Purification: Column chromatography, 2% EtOAc / PE, to 100% EtOAc.

¹H NMR (DMSO): 1.29 (m, 2H, piperidiny 4-CH₂), 1.46-1.55 (m, 10H, overlap of piperidiny 3-CH₂ and 5-CH₂ and C(CH₃)₂), 2.64 (m, 4H, piperidiny 3-CH₂ and 5-CH₂), 6.97 (d, ³J = 8.8 Hz, 2H, phenoxy 2-H and 6-H), 7.37 (dd, ³J = 8.8 Hz, ³J_{HF}=8.8 Hz, 2H, benzoyl 3-H and 5-H), 7.71 (d, ³J = 8.8 Hz, 2H, phenoxy 3-H and 5-H), 7.77 (dd, ³J = 8.8 Hz, ³J_{HF} = 5.6 Hz, 2H, benzoyl 2-H and 6-H), 9.04 (broad s, NH, 1H).

¹³C NMR (DMSO): 22.98 (piperidiny 4-C), 25.06 (C(CH₃)₂), 25.26 (piperidiny 3-C/5-C), 54.71 (piperidiny 2-C/6-C), 80.24 (C(CH₃)₂), 115.50 (d, ²J = 22 Hz, benzoyl 3-C and 5-C), 118.03 (phenoxy 2-C and 6-C), 129.86 (phenoxy 4-C), 131.53 (phenoxy 3-C and 5-C), 132.15 (d, ³J = 9.3 Hz, benzoyl 2-C and 6-C), 134.09 (d, ⁴J = 2.8 Hz, benzoyl 1-C), 159.0 (phenoxy 1-C),

164.35 (d, $^1J = 245$ Hz, benzoyl 4-C), 169.67 (amide C=O), 193.04 (ketone C=O).

Melting point: 141-142 °C

HPLC: System 2, $R_t = 16.93$ minutes.

System 3, $R_t = 2.79$ minutes

System 4, $R_t = 2.81$ minutes

***m/z*:** HRMS (ES-TOF⁺) C₂₃H₂₇FNO₃ [MH]⁺ calculated 385.1922; found 384.9540.

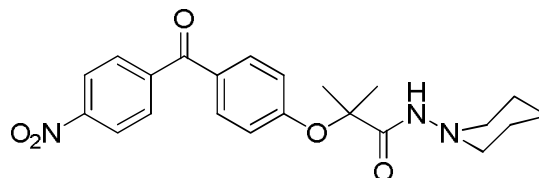
FT-IR (KBr): 2203 (amide NH), 1675 (amide C=O), 1641 (ketone C=O), 1598 (aryl CH stretch), 879, 858 (*para* disubstituted aromatic ring).

***N*-Piperidinyl-2-(4-(4'-nitrobenzoyl)-phenoxy)-2-methylpropanamide (59j)**

Following General Method G, **57k** (0.155 g, 0.47 mmol) was reacted with HBTU (0.196 g, 0.52 mmol), 1-aminopiperidine (0.047 g, 0.47 mmol) and triethylamine (97.8 μ l, 0.52 mmol) in DCM (5 ml) for 2 hours 25 minutes to afford **59j**.

Yield: 28 %

Appearance: Yellow solid



Purification: Column chromatography, 5% EtOAc / 95 % PE to 100% EtOAc.

Melting point: 152 – 153 °C

^1H NMR (CDCl₃): 1.36 – 1.42 (m, 2H, piperidinyl 4-CH₂), 1.62 (C(CH₃)₂), 2.66 - 2.72 (m, 4H, piperidinyl 3-CH₂ and piperidiny; 5-CH₂), 1.69 (quintet, 4H, piperidinyl 3-CH₂ and 5-CH₂), 2.66 (m, 4H, piperidinyl 2-CH₂ and piperidiny; 6-CH₂), 6.99 (d, $^3J = 9.1$ Hz, phenoxy 2-H and 6-H), 7.06 (s, 1H, NH), 7.77 (d, $^3J = 8.9$ Hz, 2H, phenoxy 3-H and 5-H), 7.88 (d, $^3J = 8.8$ Hz, 2H, benzoyl 2-H and 6-H), 8.33 (d, $^3J = 8.8$ Hz, 2H, benzoyl 3-H and 5-H),

^{13}C NMR (CDCl_3): 23.31 (piperidinyl 4-C) 25.37 (piperidinyl 3-C and 5-C), 25.48 ($\text{C}(\text{CH}_3)_2$), 56.89 (piperidinyl 2-C and 6-C), 81.85 ($\text{C}(\text{CH}_3)_2$), 119.29 (phenoxy 2-C and 6-C), 123.70 (benzoyl 3-C and 5-C), 130.54 (benzoyl 2-C and 6-C), 130.57 (phenoxy 4-C), 132.23 (phenoxy 3-C and 5-C), 143.39 (benzoyl 1-C), 149.83 (benzoyl 4-C), 159.31 (phenoxy 1-C), 170.66 (amide $\text{C}=\text{O}$), 193.56 (ketone $\text{C}=\text{O}$).

HPLC: System 1, R_t = 2.79 minutes

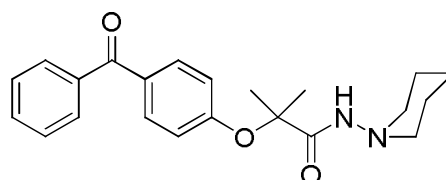
System 2, R_t = 2.81 minutes

FT-IR (KBr): 3319 (amide NH), 2935, 2856 (CH_3 stretch), 1701 (amide $\text{C}=\text{O}$), 1666 (ketone $\text{C}=\text{O}$), 1595 (aryl CH stretch) 1470 (NO_2 stretch), 875, 852 (*p* disubstituted aromatic ring)

2-(4-(Benzoyl)-phenoxy)-2-methyl-N-(piperidin-1-yl)-propanamide (59h)

Following General Method G, **57i** (0.402 g, 1.41 mmol) was reacted with HBTU (0.589 g, 1.55 mmol), 1-aminopiperidine (0.142 g, 1.55 mmol) and triethylamine (0.217 ml, 1.55 mmol) in DCM (5 ml) for 3 hours 25 minutes to afford **59h**.

Yield: 56%



Appearance: White solid

Purification: Column chromatography, 5 % EtOAc / 95 PE to 100% EtOAc.

Melting point: 125 – 127 °C

^1H NMR (CDCl_3): 1.33-1.43 (m, 1H, piperidinyl 4- CH_2), 1.61 (s, 6H, $\text{C}(\text{CH}_3)_2$), 1.69 (quintet, 3J = 5.8 Hz, 4H, piperidinyl 3- CH_2 and 5- CH_2), 2.69 (m, 4H, piperidinyl 2- CH_2 and 6- CH_2), 6.97 (d, 3J = 8.8 Hz, 2H, phenoxy 2-H and 6-H), 7.13 (s, NH, 1H), 7.47 (dd, 3J = 7.6 Hz, 4J = 7.6 Hz, 2H, benzoyl 3-H and 5-H).

and 5-H), 7.58 (t, $^3J = 7.3$ Hz, 1H, benzoyl 4-H), 7.73-7.81 (m, 4H, phenoxy 3-H and 5-H and benzoyl 2-H and 6-H).

^{13}C NMR (CDCl_3): 23.19 (piperidinyl 4-C), 25.24 ($\text{C}(\text{CH}_3)_2$), 25.35 (piperidinyl 3-C and 5-C), 56.76 (piperidinyl 2-C and 6-C), 81.57 ($\text{C}(\text{CH}_3)_2$), 119.08 (phenoxy 2-C and 6-C), 128.28 (benzoyl 3-C and 5-C), 129.81 (benzoyl 2-C and 6-C), 131.85 (phenoxy 4-C), 131.99 (3-C and 5-C), 132.22 (benzoyl 4-C), 137.83 (benzoyl 1-C), 158.23 (phenoxy 1-C), 170.77 (amide $\text{C}=\text{O}$), 195.49 (ketone $\text{C}=\text{O}$).

HPLC: System 2, $R_t = 16.55$ minutes

System 3, $R_t = 2.74$ minutes

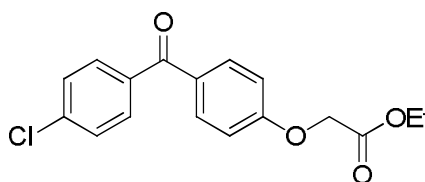
System 4, $R_t = 2.76$ minutes

m/z : HRMS (ES-TOF $^+$) $[\text{MH}]^+$ calculated 367.2016; found 367.1537

FT-IR (KBr): 3302 (amide NH), 2941, 2858 (CH_3 stretch), 1676 (amide $\text{C}=\text{O}$), 1641 (ketone $\text{C}=\text{O}$), 1599 (aryl CH stretch).

Ethyl 2-(4-(4-chlorobenzoyl)phenoxy)ethanoate (60)

Following General Method E, 4-chloro-(4'-hydroxy)benzophenone (1.000 g, 4.29 mmol) in MeCN was reacted with K_2CO_3 (0.891 g, 6.45 mmol) and ethylbromoacetate (0.861 g, 5.16 mmol) for 5 hours 20 minutes to afford **60**.



Appearance: White solid

Purification: Precipitated from ethyl acetate by addition of petroleum ether. Product was isolated by vacuum filtration.

Melting point: 103.9 – 105.2 $^{\circ}\text{C}$

¹H NMR (CDCl₃): 1.31 (t, ³*J* = 7.1 Hz, 3H, CH₃), 4.29 (q, CH₂, 2H, ³*J* = 7.1 Hz), 6.97 (d, ³*J* = 8.9 Hz, 2H, phenoxy 2-H and 6-H), 7.45 (d, ³*J* = 8.6 Hz, 2H, benzoyl 3-H and 5-H), 7.71 (d, ³*J* = 8.6 Hz, 2H, phenoxy 2-H and 6-H), 7.79 (d, ³*J* = 9.0 Hz, 2H, benzoyl 2-H and 6-H).

¹³C NMR (CDCl₃): 14.30 (OCH₂CH₃), 61.78 (OCH₂CH₃), 65.38 (OCH₂C=O), 144.43 (phenoxy 2-C and 6-C), 128.71 (benzoyl 3-C and 5-C), 130.92 (phenoxy 4-C), 131.32 (phenoxy 3-C and 5-C), 132.54 (benzoyl 2-C and 6-C), 136.48 (benzoyl 1-C), 138.59 (benzoyl 4-C), 161.59 (phenoxy 1-C), 168.35 (ester C=O), 194.29 (ketone C=O).

FT-IR (KBr): 2995, 2972 (CH₃ stretch), 1762 (ester C=O), 1647 (ketone C=O), 853, 829 (*p*-disubstituted aromatic ring).

2-(4-(4-Chlorobenzoyl)phenoxy)ethanoic acid (61)

Following General Method C, **60** (0.400g, 1.25 mmol), was reacted with lithium hydroxide (0.150 g, 6.27 mmol) in a mixture of water and THF (15 ml, 1:1) for 3 hours 45 minutes to afford **61**.

Yield: 87 %

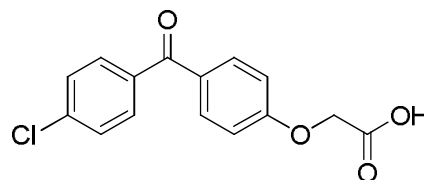
Appearance: White solid

Purification: Used without further purification.

Melting point: 184 – 186 °C

¹H NMR (DMSO): 4.82 (s, 2H, methylene CH₂), 7.07 (d, ³*J* = 8.9 Hz, 2H, phenoxy 2-H and 6-H), 7.61 (d, ³*J* = 8.6 Hz, benzoyl 3-H and 5-H), 7.71 (d, ³*J* = 8.6 Hz, phenoxy 3-H and 5-H), 7.73 (d, ³*J* = 8.6 Hz, benzoyl 2-H and 6-H), 13.13 (s, 1H, CO₂H).

¹³C NMR (DMSO): 64.57 (CH₂), 114.47 (phenoxy 2-C and 6-C), 128.59 (benzoyl 3-C and 5-C), 129.50 (benzoyl 4-C), 131.17 (phenoxy 3-C and 5-C),



132.06 (benzoyl 2-C and 6-C), 136.33 (benzoyl 1-C), 137.01 (benzoyl 4-C), 161.58 (phenoxy 1-C), 169.68 (carboxylic acid C=O), 193.26 (ketone C=O).

m/z: HRMS (ES-TOF⁺) C₁₅H₁₀ClO₄⁻ [MH]⁺ calculated 289.0273; found 289.0269

FT-IR: 2913 (carboxylic acid OH), 1737 (carboxylic acid C=O), 1649 (ketone C=O), 856, 834 (*p* disubstituted aromatic ring)

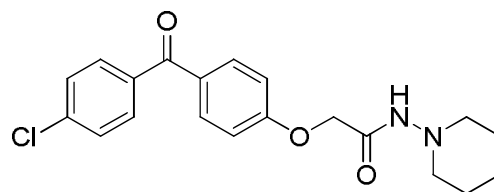
***N*-Piperidinyl-2-(4-(4-chlorobenzoyl)phenoxy)acetamide (62a)**

Following General Method G, **61** (0.100 g, 0.34 mmol) was reacted with HBTU (0.144 g, 0.38 mmol), 1-aminopiperidine (0.03 g, 0.34 mmol) and triethylamine (71.4 µl, 0.38 mmol) in DCM (5 ml) for 23 hours to afford **62a**.

Yield: 25 %

Appearance: White solid

Purification: 2 % MeOH / DCM to 0



% MeOH/ DCM.

Compound was not pure enough for further characterisation.

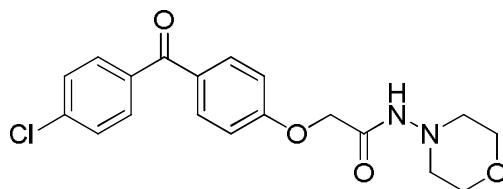
***N*-Morpholino-2-(4-(4-chlorobenzoyl)phenoxy)acetamide (62b)**

Following General Method G, **61** (0.100 g, 0.34 mmol) was reacted with HBTU (0.144 g, 0.70 mmol), 4-aminomorpholine (0.04 g, 0.34 mmol) and triethylamine (71.4 µl, 0.38 mmol) in DCM (5 ml) for 23 hours to afford **62b**.

Yield: 23 %

Appearance: White solid

Purification: 5 % EtOAc / 95 % PE

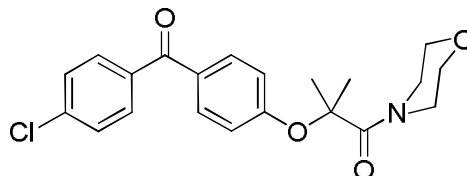


to 100 % EtOAc.

Compound was not pure enough for further characterisation.

**2-(4-(4-Chlorobenzoyl)phenoxy)-2-methyl-1-morpholinopropan-1-one
(63a)**

Following General Method G, **10b** (0.200 g, 0.63 mmol) was reacted with HBTU (0.267 g, 0.70 mmol), morpholine (0.06 g, 0.70 mmol) and triethylamine (98.0 μ l, 0.70 mmol) in DCM (5 ml) for 3 hours to afford **63a**.



Compound prepared as described in General Method G

Yield: 50 %

Appearance: Off – white solid.

Purification: Column chromatography, 5 % EtOAc / 95 % PE to 40 % EtOAc / 60 % PE.

Melting point: 148 – 150 °C

¹H NMR (CDCl₃): 1.70 (s, C(CH₃)₂, 6H), 3.29 (m, 2H, morpholino 3-CH₂ and 5- CH₂), 3.55-3.59 (m, 2H, morpholino 2-CH₂ and 6- CH₂), 3.61-3.66 (m, 2H, morpholino CH₂), 6.91 (d, ³J = 8.8 Hz, 2H, phenoxy 2-H and 6-H), 7.45 (d, ³J = 8.5 Hz, 2H benzoyl 3-H and 5-H), 7.70 (d, ³J = 8.5 Hz, 2H, phenoxy 3-H and 5-H), 7.75 (d, ³J = 8.8 Hz, 2H, benzoyl 2-H and 6-H).

¹³C NMR (CDCl₃): 26.29 (C(CH₃)₂), 43.75 (piperidinyll 2-C/6-C), 47.14 (piperidinyll 2-C/6-C), 66.76 (piperidinyll 3-C/5-C), 67.22 (piperidinyll 2-C/6-C), 81.84 (C(CH₃)₂), 116.70 (phenoxy 2-C and 6-C), 128.93 (benzoyl 3-C and 5-C), 130.81 (phenoxy 4-C), 131.49 (phenoxy 3-C and 5-C), 132.64 (benzoyl 2-C and 6-C), 136.59 (benzoyl 1-C), 138.84 (benzoyl 4-C), 159.55 (phenoxy 1-C), 171.27 (amide C=O), 194.41 (ketone C=O).

HPLC: System 2, R_t =18.07 minutes

System 3, R_t = 2.95 minutes

System 4, R_t = 2.95 minutes

m/z : HRMS (ES-TOF) $C_{21}H_{23}ClNO_4$ $[MH]^-$ calculated 388.1310; found 388.1312.

FT-IR (KBr): 2992, 2858 (CH_3 stretch), 1645 (ketone $C=O$), 1599 (aryl CH stretch), 855, 837 (p disubstituted aromatic ring).

2-(4-(4-Chlorobenzoyl)phenoxy)-2-methyl-1-piperidinypropan-1-one (63b)

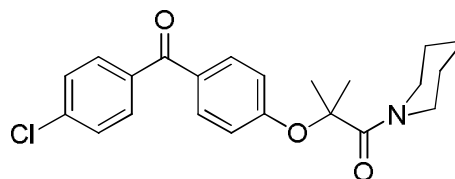
Following General Method G, **10b** (0.250 g, 0.63 mmol) was reacted with HBTU (0.327 g, 0.70 mmol), piperidine (0.07 g, 0.79 mmol) and triethylamine (0.120 ml, 0.86 mmol) in DCM (5 ml) for 3 hours to afford **63b**.

Yield: 62%

Appearance: White solid

Purification: Column chromatography,

5 % EtOAc / 95 % PE to 40 % EtOAc / 60 % PE.



Melting point: 161 – 163 °C

1H NMR ($CDCl_3$): 1.23 (m, 2H, piperidiny CH_2), 1.49 (m, 4H, piperidiny 4- CH_2), 1.69 (s, 6H, $C(CH_3)_2$), 3.56 (m, 2H, piperidiny 3- CH_2 and 5- CH_2), 3.69 (m, 2H, piperidiny 3- CH_2 and 5- CH_2), 6.91 (d, 3J = 8.9 Hz, 2H, phenoxy 2-H and 6-H), 7.44 (d, 3J = 8.6 Hz, 2H, benzoyl 3-H and 5-H), 7.69 (d, 3J = 8.6 Hz, 2H, phenoxy 3-H and 5-H), 7.73 (d, 3J = 8.9 Hz, 2H, benzoyl 2-H and 6-H).

^{13}C NMR ($CDCl_3$): 24.83 ($C(CH_3)_2$), 26.04 (piperidiny CH_2), 26.57 (piperidiny CH_2), 81.99 ($C(CH_3)_2$), 116.82 (phenoxy C-2 and C-6), 128.90 (benzoyl 3-C and 5-C), 130.48 (phenoxy 4-C), 131.50 (phenoxy 3-C and 5-C),

132.53 (benzoyl 2-C and 6-C), 136.74 (benzoyl 1-C), 138.76 (benzoyl 4-C), 160.05 (phenoxy 1-C), 170.89 (amide C=O), 194.52 (ketone C=O).

HPLC: System 2, R_t = 19.80 minutes

System 3, R_t = 3.16 minutes

System 4, R_t = 3.12 minutes

***m/z*:** HRMS (ES-TOF⁻) $C_{22}H_{25}ClNO_3$ $[MH]^-$ calculated 386.1517; found 385.9038.

FT-IR (KBr): 2930, 2852 (CH₃ stretch), 1647 (ketone C=O), 1597 (aryl CH stretch).

7. References

1. Berger, J.; Moller, D. E. The mechanisms of action of ppars. *Annu. Rev. Med.* **2002**, 53, 409-435.
2. Forman, B. M.; Chen, J.; Evans, R. M. Hypolipidemic drugs, polyunsaturated fatty acids, and eicosanoids are ligands for peroxisome proliferator-activated receptors alpha and delta. *Proc. Natl. Acad. Sci. U. S. A.* **1997**, 94, 4312-4317.
3. Klein, T. W. Cannabinoid-based drugs as anti-inflammatory therapeutics. *Nature Reviews Immunology* **2005**, 5, 400-411.
4. O'Sullivan, S. E. Cannabinoids go nuclear: Evidence for activation of peroxisome proliferator-activated receptors. *Br. J. Pharmacol.* **2007**, 152, 576-582.
5. Sun, Y.; Alexander, S. P. H.; Garle, M. J.; Gibson, C. L.; Hewitt, K.; Murphy, S. P.; Kendall, D. A.; Bennett, A. J. Cannabinoid activation of ppar alpha; a novel neuroprotective mechanism. *Br. J. Pharmacol.* **2007**, 152, 734-743.
6. Issemann, I.; Green, S. Activation of a member of the steroid-hormone receptor superfamily by peroxisome proliferators. *Nature* **1990**, 347, 645-650.
7. Dreyer, C.; Krey, G.; Keller, H.; Givel, F.; Helftenbein, G.; Wahli, W. Control of the peroxisomal beta-oxidation pathway by a novel family of nuclear hormone receptors. *Cell* **1992**, 68, 879-887.
8. Willson, T. M.; Moore, J. T. Genomics versus orphan nuclear receptors - a half-time report. *Mol. Endocrinol.* **2002**, 16, 1135-1144.
9. Willson, T. M.; Brown, P. J.; Sternbach, D. D.; Henke, B. R. The ppars: From orphan receptors to drug discovery. *J. Med. Chem.* **2000**, 43, 527-550.
10. Henke, B. R. Peroxisome proliferator-activated receptor alpha/gamma dual agonists for the treatment of type 2 diabetes. *J. Med. Chem.* **2004**, 47, 4118-4127.
11. Xu, H. E.; Lambert, M. H.; Montana, V. G.; Plunket, K. D.; Moore, L. B.; Collins, J. B.; Oplinger, J. A.; Klierer, S. A.; Gampe, R. T.; McKee, D. D.; Moore, J. T.; Willson, T. M. Structural determinants of ligand binding selectivity between the peroxisome proliferator-activated receptors. *Proc. Natl. Acad. Sci. U. S. A.* **2001**, 98, 13919-13924.
12. Kota, B. P.; Huang, T. H. W.; Roufogalis, B. D. An overview on biological mechanisms of ppars. *Pharmacol. Res.* **2005**, 51, 85-94.
13. Chinetti, G.; Lestavel, S.; Bocher, V.; Remaley, A. T.; Neve, B.; Torra, I. P.; Teissier, E.; Minnich, A.; Jaye, M.; Duverger, N.; Brewer, H. B.; Fruchart, J. C.; Clavey, V.; Staels, B. Ppar-alpha and ppar-gamma activators induce cholesterol removal from human macrophage foam cells through stimulation of the abca1 pathway. *Nat. Med.* **2001**, 7, 53-58.
14. Staels, B.; Koenig, W.; Habib, A.; Merval, R.; Lebret, M.; Torra, I. P.; Delerive, P.; Fadel, A.; Chinetti, G.; Fruchart, J. C.; Najib, J.; Macclouf, J.; Tedgui, A. Activation of human aortic smooth-muscle cells is inhibited by ppar alpha but not by ppar gamma activators. *Nature* **1998**, 393, 790-793.

15. Mandard, S.; Muller, M.; Kersten, S. Peroxisome proliferator-activated receptor alpha target genes. *Cell. Mol. Life Sci.* **2004**, 61, 393-416.
16. Delerive, P.; Fruchart, J. C.; Staels, B. Peroxisome proliferator-activated receptors in inflammation control. *J. Endocrinol.* **2001**, 169, 453-459.
17. Cronet, P.; Petersen, J. F. W.; Folmer, R.; Blomberg, N.; Sjoblom, K.; Karlsson, U.; Lindstedt, E. L.; Bamberg, K. Structure of the ppar alpha and -gamma ligand binding domain in complex with az 242; ligand selectivity and agonist activation in the ppar family. *Structure* **2001**, 9, 699-706.
18. Xu, H. E.; Lambert, M. H.; Montana, V. G.; Parks, D. J.; Blanchard, S. G.; Brown, P. J.; Sternbach, D. D.; Lehmann, J. M.; Wisely, G. B.; Willson, T. M.; Kliewer, S. A.; Milburn, M. V. Molecular recognition of fatty acids by peroxisome proliferator-activated receptors. *Mol. Cell* **1999**, 3, 397-403.
19. Xu, H. E.; Stanley, T. B.; Montana, V. G.; Lambert, M. H.; Shearer, B. G.; Cobb, J. E.; McKee, D. D.; Galardi, C. M.; Plunket, K. D.; Nolte, R. T.; Parks, D. J.; Moore, J. T.; Kliewer, S. A.; Willson, T. M.; Stimmel, J. B. Structural basis for antagonist-mediated recruitment of nuclear co-repressors by ppar alpha. *Nature* **2002**, 415, 813-817.
20. Krey, G.; Braissant, O.; L'Horsset, F.; Kalkhoven, E.; Perroud, M.; Parker, M. G.; Wahli, W. Fatty acids, eicosanoids, and hypolipidemic agents identified as ligands of peroxisome proliferator-activated receptors by coactivator-dependent receptor ligand assay. *Mol. Endocrinol.* **1997**, 11, 779-791.
21. Keating, G. M.; Croom, K. F. Fenofibrate - a review of its use in primary dyslipidaemia, the metabolic syndrome and type 2 diabetes mellitus. *Drugs* **2007**, 67, 121-153.
22. Liu, K.; Xu, L.; Berger, J. P.; MacNaul, K. L.; Zhou, G.; Doebber, T. W.; Forrest, M. J.; Moller, D. E.; Jones, A. B. Discovery of a novel series of peroxisome proliferator-activated receptor α/γ dual agonists for the treatment of type 2 diabetes and dyslipidemia. *J. Med. Chem.* **2005**, 48, 2262-2265.
23. Glynne, W. M., J. Thorpe, J.M. Waring, W.S. Pharmaceutical compositions comprising alpha-aryloxy-aliphatic carboxylic acids and/or alpha-arylimino-aliphatic carboxylic acids, their esters and salts. GB860303, 1961.
24. Thorp, J. M.; Waring, W. S. Modification of metabolism and distribution of lipids by ethyl chlorophenoxyisobutyrate. *Nature* **1962**, 194, 948-&.
25. Reddy, J. K.; Azarnoff, D. L.; Hignite, C. E. Hypolipemic hepatic peroxisome proliferators form a novel class of chemical carcinogens. *Nature* **1980**, 283, 397-398.
26. Mieville. Composes hypolipidemiantes. FR2300552, 1976.
27. Keech, A.; Simes, R. J.; Barter, P.; Best, J.; Scott, R.; Taskinen, M. R.; Forder, P.; Pillai, A.; Davis, T.; Glasziou, P.; Drury, P.; Kesaniemi, Y. A.; Sullivan, D.; Hunt, D.; Colman, P.; d'Emden, M.; Whiting, M.; Ehnholm, C.; Laakso, M. Effects of long-term fenofibrate therapy on cardiovascular events in 9795 people with type 2 diabetes mellitus (the field study): Randomised controlled trial. *Lancet* **2005**, 366, 1849-1861.

28. Staels, B.; Dallongeville, J.; Auwerx, J.; Schoonjans, K.; Leitersdorf, E.; Fruchart, J. G. Mechanism of action of fibrates on lipid and lipoprotein metabolism. *Circulation* **1998**, 98, 2088-2093.
29. Backes, J. M.; Gibson, C. A.; Ruisinger, J. E.; Moriarty, P. M. Fibrates: What have we learned in the past 40 years? *Pharmacotherapy* **2007**, 27, 412-424.
30. Tomarelli, R. M.; Bauman, L. M.; Savini, S. Effect of wy-14,643 on cholesterol-metabolism in normal and hypercholesterolemic rats. *Atherosclerosis* **1978**, 30, 301-311.
31. Sirtori, C. R.; Gomasca, P.; Datri, G.; Cerutti, S.; Tronconi, G.; Scolastico, C. Pharmacological profile of br-931, a new hypolipidemic agent that increases high-density lipoproteins. *Atherosclerosis* **1978**, 30, 45-56.
32. Brown, P. J.; Smith-Oliver, T. A.; Charifson, P. S.; Tomkinson, N. C. O.; Fivush, A. M.; Sternbach, D. D.; Wade, L. E.; Orband-Miller, L.; Parks, D. J.; Blanchard, S. G.; Kliewer, S. A.; Lehmann, J. M.; Willson, T. M. Identification of peroxisome proliferator-activated receptor ligands from a biased chemical library. *Chem. Biol.* **1997**, 4, 909-918.
33. Brown, P. J.; Winegar, D. A.; Plunket, K. D.; Moore, L. B.; Lewis, M. C.; Wilson, J. G.; Sundseth, S. S.; Koble, C. S.; Wu, Z. D.; Chapman, J. M.; Lehmann, J. M.; Kliewer, S. A.; Willson, T. M. A ureido-thioisobutyric acid (gw9578) is a subtype-selective ppar alpha agonist with potent lipid-lowering activity. *J. Med. Chem.* **1999**, 42, 3785-3788.
34. Brown, P. J.; Stuart, L. W.; Hurley, K. P.; Lewis, M. C.; Winegar, D. A.; Wilson, J. G.; Wilkinson, W. O.; Ittoop, O. R.; Willson, T. M. Identification of a subtype selective human ppar alpha agonist through parallel-array synthesis. *Bioorg. Med. Chem. Lett.* **2001**, 11, 1225-1227.
35. Millar, R. P.; Newton, C. L. The year in g protein-coupled receptor research. *Mol. Endocrinol.* 24, 261-274.
36. Karnik, S. S.; Gogonea, C.; Patil, S.; Saad, Y.; Takezako, T. Activation of g-protein-coupled receptors: A common molecular mechanism. *Trends Endocrinol. Metab.* **2003**, 14, 431-437.
37. Lodish, H.; Baltimore, D.; Berk, A.; Zipursky, S. L.; Matsudaira, P.; Darnell, J.; Lodish, H.; Baltimore, D.; Berk, A.; Zipursky, S. L.; Matsudaira, P.; Darnell, J. *Molecular cell biology; fifth edition.* 1995.
38. Barren, B.; Artemyev, N. O. Mechanisms of dominant negative g-protein alpha subunits. *J. Neurosci. Res.* **2007**, 85, 3505-3514.
39. Harrison, C.; Traynor, J. R. The [s-35]gtp gamma s binding assay: Approaches and applications in pharmacology. *Life Sci.* **2003**, 74, 489-508.
40. Hart, M. J.; Jiang, X. J.; Kozasa, T.; Roscoe, W.; Singer, W. D.; Gilman, A. G.; Sternweis, P. C.; Bollag, G. Direct stimulation of the guanine nucleotide exchange activity of p115 rhogef by g alpha(13). *Science* **1998**, 280, 2112-2114.
41. Henderson, R.; Baldwin, J. M.; Ceska, T. A.; Zemlin, F.; Beckmann, E.; Downing, K. H. Model for the structure of bacteriorhodopsin based on high-resolution electron cryomicroscopy. *J. Mol. Biol.* **1990**, 213, 899-929.
42. Trumppkallmeyer, S.; Hoflack, J.; Bruinvels, A.; Hibert, M. Modeling of g-protein-coupled receptors - application to dopamine, adrenaline,

- serotonin, acetylcholine, and mammalian opsin receptors. *J. Med. Chem.* **1992**, 35, 3448-3462.
43. Luecke, H.; Schobert, B.; Richter, H. T.; Cartailier, J. P.; Lanyi, J. K. Structure of bacteriorhodopsin at 1.55 angstrom resolution. *J. Mol. Biol.* **1999**, 291, 899-911.
 44. Palczewski, K.; Kumasaka, T.; Hori, T.; Behnke, C. A.; Motoshima, H.; Fox, B. A.; Le Trong, I.; Teller, D. C.; Okada, T.; Stenkamp, R. E.; Yamamoto, M.; Miyano, M. Crystal structure of rhodopsin: A g protein-coupled receptor. *Science* **2000**, 289, 739-745.
 45. Cherezov, V.; Rosenbaum, D. M.; Hanson, M. A.; Rasmussen, S. G. F.; Thian, F. S.; Kobilka, T. S.; Choi, H. J.; Kuhn, P.; Weis, W. I.; Kobilka, B. K.; Stevens, R. C. High-resolution crystal structure of an engineered human beta(2)-adrenergic g protein-coupled receptor. *Science* **2007**, 318, 1258-1265.
 46. Rasmussen, S. G. F.; Choi, H. J.; Rosenbaum, D. M.; Kobilka, T. S.; Thian, F. S.; Edwards, P. C.; Burghammer, M.; Ratnala, V. R. P.; Sanishvili, R.; Fischetti, R. F.; Schertler, G. F. X.; Weis, W. I.; Kobilka, B. K. Crystal structure of the human beta(2) adrenergic g-protein-coupled receptor. *Nature* **2007**, 450, 383-U384.
 47. Di Marzo, V.; De Petrocellis, L. Plant, synthetic, and endogenous cannabinoids in medicine. *Annu. Rev. Med.* **2006**, 57, 553-574.
 48. Rhee, M. H.; Vogel, Z.; Barg, J.; Bayewitch, M.; Levy, R.; Hanus, L.; Breuer, A.; Mechoulam, R. Cannabinol derivatives: Binding to cannabinoid receptors and inhibition of adenylylcyclase. *J. Med. Chem.* **1997**, 40, 3228-3233.
 49. Gaoni, Y.; Mechoulam, R. Isolation, structure and partial synthesis of active constituent of hashish. *J. Am. Chem. Soc.* **1964**, 86, 1646-&.
 50. Devane, W. A.; Dysarz, F. A.; Johnson, M. R.; Melvin, L. S.; Howlett, A. C. Determination and characterization of a cannabinoid receptor in rat-brain. *Mol. Pharmacol.* **1988**, 34, 605-613.
 51. Matsuda, L. A.; Lolait, S. J.; Brownstein, M. J.; Young, A. C.; Bonner, T. I. Structure of a cannabinoid receptor and functional expression of the cloned cDNA. *Nature* **1990**, 346, 561-564.
 52. Chakrabarti, A.; Onaivi, E. S.; Chaudhuri, G. Cloning and sequencing of a cDNA encoding the mouse brain-type cannabinoid receptor protein. *DNA Sequence* **1995**, 5, 385-388.
 53. Gerard, C. M.; Mollereau, C.; Vassart, G.; Parmentier, M. Molecular-cloning of a human cannabinoid receptor which is also expressed in testis. *Biochem. J* **1991**, 279, 129-134.
 54. Howlett, A. C.; Barth, F.; Bonner, T. I.; Cabral, G.; Casellas, P.; Devane, W. A.; Felder, C. C.; Herkenham, M.; Mackie, K.; Martin, B. R.; Mechoulam, R.; Pertwee, R. G. International union of pharmacology. Xxvii. Classification of cannabinoid receptors. *Pharmacol. Rev.* **2002**, 54, 161-202.
 55. Herkenham, M.; Lynn, A. B.; Little, M. D.; Johnson, M. R.; Melvin, L. S.; Decosta, B. R.; Rice, K. C. Cannabinoid receptor localization in brain. *Proc. Natl. Acad. Sci. U. S. A.* **1990**, 87, 1932-1936.
 56. Felder, C. C.; Joyce, K. E.; Briley, E. M.; Mansouri, J.; Mackie, K.; Blond, O.; Lai, Y.; Ma, A. L.; Mitchell, R. L. Comparison of the

- pharmacology and signal-transduction of the human cannabinoid cb1 and cb2 receptors. *Mol. Pharmacol.* **1995**, 48, 443-450.
57. Shire, D.; Calandra, B.; RinaldiCarmona, M.; Oustric, D.; Pessegue, B.; BonninCabanne, O.; LeFur, G.; Caput, D.; Ferrara, P. Molecular cloning, expression and function of the murine cb2 peripheral cannabinoid receptor. *Biochimica Et Biophysica Acta-Gene Structure and Expression* **1996**, 1307, 132-136.
 58. Griffin, G.; Tao, Q.; Abood, M. E. Cloning and pharmacological characterization of the rat cb2 cannabinoid receptor. *J. Pharmacol. Exp. Ther.* **2000**, 292, 886-894.
 59. Van Sickle, M. D.; Duncan, M.; Kingsley, P. J.; Mouihate, A.; Urbani, P.; Mackie, K.; Stella, N.; Makriyannis, A.; Piomelli, D.; Davison, J. S.; Marnett, L. J.; Di Marzo, V.; Pittman, Q. J.; Patel, K. D.; Sharkey, K. A. Identification and functional characterization of brainstem cannabinoid cb2 receptors. *Science* **2005**, 310, 329-332.
 60. Nunez, E.; Benito, C.; Pazos, M. R.; Barbachano, A.; Fajardo, O.; Gonzalez, S.; Tolon, R. M.; Romero, J. Cannabinoid cb2 receptors are expressed by perivascular microglial cells in the human brain: An immunohistochemical study. *Synapse* **2004**, 53, 208-213.
 61. Reggio, P. H. Pharmacophores for ligand recognition and activation/inactivation of the cannabinoid receptors. *Curr. Pharm. Des.* **2003**, 9, 1607-1633.
 62. Di Marzo, V.; Breivogel, C. S.; Tao, Q.; Bridgen, D. T.; Razdan, R. K.; Zimmer, A. M.; Zimmer, A.; Martin, B. R. Levels, metabolism, and pharmacological activity of anandamide in cb1 cannabinoid receptor knockout mice: Evidence for non-cb1, non-cb2 receptor-mediated actions of anandamide in mouse brain. *J. Neurochem.* **2000**, 75, 2434-2444.
 63. Hajos, N.; Ledent, C.; Freund, T. F. Novel cannabinoid-sensitive receptor mediates inhibition of glutamatergic synaptic transmission in the hippocampus. *Neuroscience* **2001**, 106, 1-4.
 64. Jarai, Z.; Wagner, J. A.; Varga, K.; Lake, K. D.; Compton, D. R.; Martin, B. R.; Zimmer, A. M.; Bonner, T. I.; Buckley, N. E.; Mezey, E.; Razdan, R. K.; Zimmer, A.; Kunos, G. Cannabinoid-induced mesenteric vasodilation through an endothelial site distinct from cb1 or cb2 receptors. *Proc. Natl. Acad. Sci. U. S. A.* **1999**, 96, 14136-14141.
 65. Ho, W. S. V.; Hiley, C. R. Vasodilator actions of abnormal-cannabidiol in rat isolated small mesenteric artery. *Br. J. Pharmacol.* **2003**, 138, 1320-1332.
 66. Kaplan, B. L. F.; Rockwell, C. E.; Kaminski, N. E. Evidence for cannabinoid receptor-dependent and -independent mechanisms of action in leukocytes. *J. Pharmacol. Exp. Ther.* **2003**, 306, 1077-1085.
 67. Wagner, J. A.; Varga, K.; Jarai, Z.; Kunos, G. Mesenteric vasodilation mediated by endothelial anandamide receptors. *Hypertension* **1999**, 33, 429-434.
 68. Calignano, A.; La Rana, G.; Giuffrida, A.; Piomelli, D. Control of pain initiation by endogenous cannabinoids. *Nature* **1998**, 394, 277-281.
 69. Ryberg, E.; Larsson, N.; Sjogren, S.; Hjorth, S.; Hermansson, N. O.; Leonova, J.; Elebring, T.; Nilsson, K.; Drmota, T.; Geasley, P. J. The orphan receptor gpr55 is a novel cannabinoid receptor. *Br. J. Pharmacol.* **2007**, 152, 1092-1101.

70. Henstridge, C. M.; Balenga, N. A. B.; Ford, L. A.; Ross, R. A.; Waldhoer, M.; Irving, A. J. The gpr55 ligand 1- α -lysophosphatidylinositol promotes rhoa-dependent ca^{2+} signaling and nfat activation. *FASEB J.* **2009**, 23, 183-193.
71. Oka, S.; Toshida, T.; Maruyama, K.; Nakajima, K.; Yamashita, A.; Sugiura, T. 2-arachidonoyl-sn-glycero-3-phosphoinositol: A possible natural ligand for gpr55. *J. Biochem.* **2009**, 145, 13-20.
72. Di Marzo, V.; Goparaju, S. K.; Wang, L.; Liu, J.; Batkai, S.; Jarai, Z.; Fezza, F.; Miura, G. I.; Palmiter, R. D.; Sugiura, T.; Kunos, G. Leptin-regulated endocannabinoids are involved in maintaining food intake. *Nature* **2001**, 410, 822-825.
73. Zajicek, J.; Fox, P.; Sanders, H.; Wright, D.; Vickery, J.; Nunn, A.; Thompson, A.; Grp, U. M. R. Cannabinoids for treatment of spasticity and other symptoms related to multiple sclerosis (cams study): Multicentre randomised placebo-controlled trial. *Lancet* **2003**, 362, 1517-1526.
74. Klein, T. W.; Newton, C.; Larsen, K.; Lu, L.; Perkins, I.; Nong, L.; Friedman, H. The cannabinoid system and immune modulation. *J. Leukocyte Biol.* **2003**, 74, 486-496.
75. Wilson, R. I.; Nicoll, R. A. Endogenous cannabinoids mediate retrograde signalling at hippocampal synapses. *Nature* **2001**, 410, 588-592.
76. Devane, W. A.; Hanus, L.; Breuer, A.; Pertwee, R. G.; Stevenson, L. A.; Griffin, G.; Gibson, D.; Mandelbaum, A.; Etinger, A.; Mechoulam, R. Isolation and structure of a brain constituent that binds to the cannabinoid receptor. *Science* **1992**, 258, 1946-1949.
77. RinaldiCarmona, M.; Calandra, B.; Shire, D.; Bouaboula, M.; Oustric, D.; Barth, F.; Casellas, P.; Ferrara, P.; LeFur, G. Characterization of two cloned human cb1 cannabinoid receptor isoforms. *J. Pharmacol. Exp. Ther.* **1996**, 278, 871-878.
78. Hanus, L.; Gopher, A.; Almog, S.; Mechoulam, R. 2 new unsaturated fatty-acid ethanolamides in brain that bind to the cannabinoid receptor. *J. Med. Chem.* **1993**, 36, 3032-3034.
79. Mechoulam, R.; Benshabat, S.; Hanus, L.; Ligumsky, M.; Kaminski, N. E.; Schatz, A. R.; Gopher, A.; Almog, S.; Martin, B. R.; Compton, D. R.; Pertwee, R. G.; Griffin, G.; Bayewitch, M.; Barg, J.; Vogel, Z. Identification of an endogenous 2-monoglyceride, present in canine gut, that binds to cannabinoid receptors. *Biochem. Pharmacol.* **1995**, 50, 83-90.
80. Sugiura, T.; Kondo, S.; Sukagawa, A.; Nakane, S.; Shinoda, A.; Itoh, K.; Yamashita, A.; Waku, K. 2-arachidonoylglycerol - a possible endogenous cannabinoid receptor-ligand in brain. *Biochem. Biophys. Res. Commun.* **1995**, 215, 89-97.
81. Huang, S. M.; Bisogno, T.; Trevisani, M.; Al-Hayani, A.; De Petrocellis, L.; Fezza, F.; Tognetto, M.; Petros, T. J.; Krey, J. F.; Chu, C. J.; Miller, J. D.; Davies, S. N.; Geppetti, P.; Walker, J. M.; Di Marzo, V. An endogenous capsaicin-like substance with high potency at recombinant and native vanilloid vr1 receptors. *Proc. Natl. Acad. Sci. U. S. A.* **2002**, 99, 8400-8405.
82. Bisogno, T.; Melck, D.; Bobrov, M. Y.; Gretskaya, N. M.; Bezuglov, V. V.; De Petrocellis, L.; Di Marzo, V. N-acyl-dopamines: Novel synthetic

- cb1 cannabinoid-receptor ligands and inhibitors of anandamide inactivation with cannabimimetic activity in vitro and in vivo. *Biochem. J* **2000**, 351, 817-824.
83. Hanus, L.; Abu-Lafi, S.; Frider, E.; Breuer, A.; Vogel, Z.; Shalev, D. E.; Kustanovich, I.; Mechoulam, R. 2-arachidonyl glyceryl ether, an endogenous agonist of the cannabinoid cb1 receptor. *Proc. Natl. Acad. Sci. U. S. A.* **2001**, 98, 3662-3665.
 84. Shoemaker, J. L.; Joseph, B. K.; Ruckle, M. B.; Mayeux, P. R.; Prather, P. L. The endocannabinoid noladin ether acts as a full agonist at human cb2 cannabinoid receptors. *J. Pharmacol. Exp. Ther.* **2005**, 314, 868-875.
 85. Porter, A. C.; Sauer, J. M.; Knierman, M. D.; Becker, G. W.; Borna, M. J.; Bao, J. Q.; Nomikos, G. G.; Carter, P.; Bymaster, F. P.; Leese, A. B.; Felder, C. C. Characterization of a novel endocannabinoid, virodhamine, with antagonist activity at the cb1 receptor. *J. Pharmacol. Exp. Ther.* **2002**, 301, 1020-1024.
 86. Wilson, R. S.; May, E. L.; Martin, B. R.; Dewey, W. L. "9-nor-9-hydroxyhexahydrocannabinols - synthesis, some behavioral and analgesic properties, and comparison with tetrahydrocannabinols. *J. Med. Chem.* **1976**, 19, 1165-1167.
 87. Palmer, S. L.; Thakur, G. A.; Makriyannis, A. Cannabinergic ligands. *Chem. Phys. Lipids* **2002**, 121, 3-19.
 88. Mechoulam, R.; Lander, N.; Srebnik, M.; Breuer, A.; Segal, M.; Feigenbaum, J. J.; Jarbe, T. U.; Consroe, P. Stereochemical requirements for cannabimimetic activity. *NIDA Res. Monogr.* **1987**, 79, 15-30.
 89. Howlett, A. C.; Champion, T. M.; Wilken, G. H.; Mechoulam, R. Stereochemical effects of 11-oh-delta-8-tetrahydrocannabinol-dimethylheptyl to inhibit adenylate-cyclase and bind to the cannabinoid receptor. *Neuropharmacology* **1990**, 29, 161-165.
 90. Huffman, J. W.; Yu, S.; Showalter, V.; Abood, M. E.; Wiley, J. L.; Compton, D. R.; Martin, B. R.; Bramblett, R. D.; Reggio, P. H. Synthesis and pharmacology of a very potent cannabinoid lacking a phenolic hydroxyl with high affinity for the cb2 receptor. *J. Med. Chem.* **1996**, 39, 3875-3877.
 91. Huffman, J. W.; Liddle, J.; Yu, S.; Aung, M. M.; Abood, M. E.; Wiley, J. L.; Martin, B. R. 3-(1',1'-dimethylbutyl)-1-deoxy-delta(8)-thc and related compounds: Synthesis of selective ligands for the cb2 receptor. *Biorg. Med. Chem.* **1999**, 7, 2905-2914.
 92. Melvin, L. S.; Johnson, M. R.; Harbert, C. A.; Milne, G. M.; Weissman, A. A cannabinoid derived prototypical analgesic. *J. Med. Chem.* **1984**, 27, 67-71.
 93. Huffman, J. W.; Thompson, A. L. S.; Wiley, J. L.; Martin, B. R. Synthesis and pharmacology of 1-deoxy analogs of cp-47,497 and cp-55,940. *Biorg. Med. Chem.* **2008**, 16, 322-335.
 94. Griffin, G.; Wray, E. J.; Martin, B. R.; Abood, M. E. Cannabinoid agonists and antagonists discriminated by receptor binding in rat cerebellum. *Br. J. Pharmacol.* **1999**, 128, 684-688.
 95. Drake, D. J.; Jensen, R. S.; Busch-Petersen, J.; Kawakami, J. K.; Fernandez-Garcia, M. C.; Fan, P. S.; Makriyannis, A.; Tius, M. A. Classical/nonclassical hybrid cannabinoids: Southern aliphatic chain-

- functionalized c-6 beta methyl, ethyl, and propyl analogues. *J. Med. Chem.* **1998**, 41, 3596-3608.
96. Harrington, P. E.; Stergiades, I. A.; Erickson, J.; Makriyannis, A.; Tius, M. A. Synthesis of functionalized cannabinoids. *J. Org. Chem.* **2000**, 65, 6576-6582.
 97. Bell, M. R.; Dambra, T. E.; Kumar, V.; Eissenstat, M. A.; Herrmann, J. L.; Wetzel, J. R.; Rosi, D.; Philion, R. E.; Daum, S. J.; Hlasta, D. J.; Kullnig, R. K.; Ackerman, J. H.; Haubrich, D. R.; Luttinger, D. A.; Baizman, E. R.; Miller, M. S.; Ward, S. J. Antinociceptive (aminoalkyl)indoles. *J. Med. Chem.* **1991**, 34, 1099-1110.
 98. Dambra, T. E.; Estep, K. G.; Bell, M. R.; Eissenstat, M. A.; Josef, K. A.; Ward, S. J.; Haycock, D. A.; Baizman, E. R.; Casiano, F. M.; Beglin, N. C.; Chippari, S. M.; Grego, J. D.; Kullnig, R. K.; Daley, G. T. Conformationally restrained analogs of pravadoline - nanomolar potent, enantioselective, (aminoalkyl)indole agonists of the cannabinoid receptor. *J. Med. Chem.* **1992**, 35, 124-135.
 99. Gallant, M.; Dufresne, C.; Gareau, Y.; Guay, D.; Leblanc, Y.; Prasit, P.; Rochette, C.; Sawyer, N.; Slipetz, D. M.; Tremblay, N.; Metters, K. M.; Labelle, M. New class of potent ligands for the human peripheral cannabinoid receptor. *Bioorg. Med. Chem. Lett.* **1996**, 6, 2263-2268.
 100. Rinaldicarmona, M.; Barth, F.; Heaulme, M.; Shire, D.; Calandra, B.; Congy, C.; Martinez, S.; Maruani, J.; Neliat, G.; Caput, D.; Ferrara, P.; Soubrie, P.; Breliere, J. C.; Lefur, G. Sr141716a, a potent and selective antagonist of the brain cannabinoid receptor. *FEBS Lett.* **1994**, 350, 240-244.
 101. Richardson, J. D.; Kilo, S.; Hargreaves, K. M. Cannabinoids reduce hyperalgesia and inflammation via interaction with peripheral cb1 receptors. *Pain* **1998**, 75, 111-119.
 102. Campbell, F. A.; Tramer, M. R.; Carroll, D.; Reynolds, D. J.; Moore, R. A.; McQuay, H. J. Are cannabinoids an effective and safe treatment option in the management of pain? A qualitative systematic review. *Br. Med. J.* **2001**, 323, 13-16.
 103. Buggy, D. J.; Toogood, L.; Maric, S.; Sharpe, P.; Lambert, D. G.; Rowbotham, D. J. Lack of analgesic efficacy of oral delta-9-tetrahydrocannabinol in postoperative pain. *Pain* **2003**, 106, 169-172.
 104. Williams, C. M.; Kirkham, T. C. Observational analysis of feeding induced by delta(9)-thc and anandamide. *Physiol. Behav.* **2002**, 76, 241-250.
 105. Despres, J. P.; Golay, A.; Sjostrom, L.; Rimonabant Obesity Lipids Study, G. Effects of rimonabant on metabolic risk factors in overweight patients with dyslipidemia. *New Engl. J. Med.* **2005**, 353, 2121-2134.
 106. Pacher, P.; Batkai, S.; Kunos, G. The endocannabinoid system as an emerging target of pharmacotherapy. *Pharmacol. Rev.* **2006**, 58, 389-462.
 107. Bensaid, M.; Gary-Bobo, M.; Esclangon, A.; Maffrand, J. P.; Le Fur, G.; Oury-Donat, F.; Soubrie, P. The cannabinoid cb1 receptor antagonist sr141716 increases acrp30 mrna expression in adipose tissue of obese fa/fa rats and in cultured adipocyte cells. *Mol. Pharmacol.* **2003**, 63, 908-914.
 108. Cota, D.; Marsicano, G.; Tschop, M.; Grubler, Y.; Flachskamm, C.; Schubert, M.; Auer, D.; Yassouridis, A.; Thone-Reineke, C.; Ortmann,

- S.; Tomassoni, F.; Cervino, C.; Nisoli, E.; Linthorst, A. C. E.; Pasquali, R.; Lutz, B.; Stalla, G. K.; Pagotto, U. The endogenous cannabinoid system affects energy balance via central orexigenic drive and peripheral lipogenesis. *J. Clin. Invest.* **2003**, 112, 423-431.
109. Le Foll, B.; Gorelick, D. A.; Goldberg, S. R. The future of endocannabinoid-oriented clinical research after cb1 antagonists. *Psychopharmacology* **2009**, 205, 171-174.
 110. Pertwee, R. G. Emerging strategies for exploiting cannabinoid receptor agonists as medicines. *Br. J. Pharmacol.* **2009**, 156, 397-411.
 111. Wade, D. T.; Makela, P.; Robson, P.; House, H.; Bateman, C. Do cannabis-based medicinal extracts have general or specific effects on symptoms in multiple sclerosis? A double-blind, randomized, placebo-controlled study on 160 patients. *Multiple Sclerosis* **2004**, 10, 434-441.
 112. Pharmaceuticals, G. Gw announces uk launch of worlds first prescription cannabis medicine. In 2010.
 113. Malan, T. P.; Ibrahim, M. M.; Deng, H. F.; Liu, Q.; Mata, H. P.; Vanderah, T.; Porreca, F.; Makriyannis, A. Cb2 cannabinoid receptor-mediated peripheral antinociception. *Pain* **2001**, 93, 239-245.
 114. Guindon, J.; Hohmann, A. G. Cannabinoid cb2 receptors: A therapeutic target for the treatment of inflammatory and neuropathic pain. *Br. J. Pharmacol.* **2008**, 153, 319-334.
 115. Steffens, S.; Veillard, N. R.; Arnaud, C.; Pelli, G.; Burger, F.; Staub, C.; Karsak, M.; Zimmer, A.; Frossard, J. L.; Mach, F. Low dose oral cannabinoid therapy reduces progression of atherosclerosis in mice (vol 434, pg 782, 2005). *Nature* **2005**, 435, 528-528.
 116. Neubig, R. R.; Spedding, M.; Kenakin, T.; Christopoulos, A. International union of pharmacology committee on receptor nomenclature and drug classification. Xxxviii. Update on terms and symbols in quantitative pharmacology. *Pharmacol. Rev.* **2003**, 55, 597-606.
 117. Davis, R. D.; Fitzgerald, R. N.; Guo, J. S. Improved method for the synthesis of 2-methyl-2-aryloxypropanoic acid derivatives. *Synthesis-Stuttgart* **2004**, 1959-1962.
 118. Kulkarni, P. P.; Kadam, A. J.; Mane, R. B.; Desai, U. V.; Wadgaonkar, P. P. Demethylation of methyl aryl ethers using pyridine hydrochloride in solvent-free conditions under microwave irradiation. *Journal of Chemical Research-S* **1999**, 394-395.